Development of Ultra-Fast Modulation for Application in Multi-Dimensional Gas Chromatography

Daniel Bahaghighat

A dissertation

submitted in partial fulfillment of the

requirements for the degree of

Doctor of Philosophy

University of Washington

2018

Reading Committee:

Robert Synovec, Chair

Bo Zhang

Dan Fu

Program Authorized to Offer Degree:

Department of Chemistry

University of Washington

Abstract

Development of Ultra-Fast Modulation for Application in Multi-Dimensional Gas Chromatography

Daniel Bahaghighat

Chair of the Supervisory Committee:
Professor Robert E. Synovec
Department of Chemistry

A combination of four instrumental systems and one chemometric method are presented that improves the efficiency, resolving power (i.e. peak capacity/ peak capacity production), and lessens the typical time of multi-dimensional gas chromatography (MDGC) separation in a straightforward, easily interpretable manner. Application of partial modulation via a commercially available high speed pulse flow valve for two-dimensional gas chromatography (GC×GC) is shown to provide ultra-fast modulation with modulation periods (P_M) as short as 50 ms. This technique performs a combination of vacancy chromatography and frontal analysis by an injection of carrier gas at the union of the first column (^{1}D) and second column (^{2}D). Each pulse disturbance in the analyte concentration profile as it exits the first column (^{1}D) results in vacancy like data that is readily converted into a second separation (^{2}D). A three-step process converts the raw data into

a format equivalent to a traditional GC×GC separation chromatogram: 1. signal differentiation, 2. inversion of data, 3. baseline correction. The first instrumental system (GC×GC-Flame Ionization Detector (FID) with a P_M of 500 ms, separating a 115-component mixture composed of a wide range of boiling points (36–372 °C) compounds with apparent peak widths on the ^{2}D, ^2W_b, ranged from 10 to 40 ms, producing a ^{2}D peak capacity, ^2n_c, of ~ 20, and the total peak capacity, $n_{c,2D}$, was 7200 or a peak capacity production of 1200 peaks/min. For a P_M of 75 ms, separating a low boiling point 15-component mixture isothermally, apparent peak widths on the ^{2}D, ^2W_b, averaged 10 ms producing a ^{2}D peak capacity, ^2n_c, of ~ 7.5, with a peak capacity production of 950 peaks/min. The second system incorporated a high temperature diaphragm valve modulator and a pulse valve flow modulator to create a three-dimensional gas chromatography system (GC^3) with a peak capacity production of 1000 peaks/min which is a ~5 times increase in efficiency compared to other GC^3 systems. The third instrumental design established capability with a time-of-flight mass spectrometer (TOF), a method was developed for GC×GC-TOF separation in which a concentration study was conducted with an 18-component mixture and a P_M of 50 ms. The subsequent data was deconvoluted with multivariate curve resolution-alternating least squares (MCR-ALS) in order to obtain their identification via match values. The resulting MCR-ALS data was converted in a similar manner as before into GC×GC chromatograms.

Lastly, the pulse valve flow modulator was demonstrated to conduct continuous gas sampling of a system via one dimensional (1D) chromatography. The method applies the partial modulation technique to create frontal analysis peaks that are then transformed into a 1D chromatogram of analytes from a dynamic system that present a novel method of continuous sampling.

TABLE OF CONTENTS

LIST OF FIGURES

LIST OF TABLES

ACKNOWLEDGEMENTS

The research for this dissertation was only possible due to many influential individuals, both current and from the past for which I would like to briefly thank.

During the course of the last three years it has been a privilege to study and learn under my advisor, Professor Rob Synovec. I will forever be grateful to him for his leadership and mentoring as I gained a strong understanding of the field of multi-dimensional chromatography. His years of experience and knowledge seems to have no end, and my only regret is that I cannot spend more time under his guidance. To the members of the research group both past and current, your help, conversation and dedication to teamwork was pivotal in my success, I wish only the best for all of you. I would like to also thank my high school algebra teacher, Roger Brown, without his mentorship and encouragement, an advanced education beyond high school would not have been possible.

To the Department of Chemistry and Life Science at the United State Military Academy who has supported my educational endeavors, I will forever be thankful. Why you picked a fella with a southern draw to serve as a chemistry instructor at USMA is beyond me, all I can say is GO Army Beat Navy.

Finally, to my wife and children, I am forever in your debt for understanding that I am so busy studying all week, to ensure we have a safe future. My greatest joy in life is being a husband and father; I love every moment we spend together as a family, and look forward to many more now that my work at the University of Washington is finished.

DEDICATION

To my wife. My life began when we were introduced all those years ago. You always bring out the best in me, thanks for your endless support over the years, both for my work, and for my never ending studies. As we often say to each other, ‘I like us’. I love you, and our four energetic children.

Chapter 1. Fundamentals of Gas Chromatography Separations, Multi-Dimensional Gas Chromatography, Chemometrics, and Modulator Evolution.

Some parts of this chapter have been reproduced from three sources: 1) S.E. Prebihalo, K.L. Berrier, C.E. Freye, H.D. Bahaghighat, N.R. Moore, D.K. Pinkerton, and R.E. Synovec, "Multidimensional Gas Chromatography: Advances in Instrumentation, Chemometrics, and Applications" *Analytical Chemistry* 90 (2018) 505-532, 2) C.E. Freye, H.D. Bahaghighat and R.E. Synovec, "Comprehensive two-dimensional gas chromatography using partial modulation via a pulsed flow valve with a short modulation period" *Talanta* 177 (2018) 142-149, and 3) H.D. Bahaghighat, C.E. Freye, and R.E. Synovec, "Recent Advances in Modulator Technology for Comprehensive Two Dimensional Gas Chromatography" *prepared for submission in TrAC.*

1.1 INTRODUCTION

1.1.1 *Multi-Dimensional Gas Chromatography Background*

The separation, identification, and quantification of analytes contained within complex mixtures is often addressed with chromatographic methods. The goal of analytical separations, such as gas chromatography (GC), is to provide the desired chemical information to meet the goals of the analysis, often with analysis speed being an important factor. This type of situation commonly occurs in the analysis of complex mixtures frequently experienced in the following areas: food, flavors, fragrance [1–3], environmental [4,5], petroleum sciences [6,7], forensic [8,9], biological, metabolomics, and volatile organic compounds [10,11]. While the GC field is dominated by traditional one-dimensional gas chromatography (1D-GC), two-dimensional gas chromatography (2D-GC) has rapidly emerged from a niche technique into a widely used method in industrial, national laboratory and academic research sectors. 2D-GC principally takes on two

forms, either heart-cutting (GC-GC), or comprehensive (GC×GC) [12] experimentally pioneered in 1991 by Liu and Phillips [13]. In the pioneering GC×GC design, analytes eluting from the primary (^{1}D) column were trapped at ambient temperature external to the oven, and then re-injected onto a secondary (^{2}D) column using a resistively heated design, which is a form of thermal modulation. Indeed, the critical component for GC×GC to perform properly is the modulator, which for over a quarter of a century has been under constant development. Numerous useful reviews over the years have been produced covering the development of 2D-GC [14–16], and specifically the development of the modulator [17–19].

1.1.2 *Heart Cutting (GC-GC) versus Comprehensive (GC×GC)*

This introduction is focused on the modulators associated with both forms of 2D-GC, heart-cutting (GC-GC) and comprehensive (GC×GC) but will emphasize the evolution of modulators tailored toward the use with GC×GC. It is important to define the difference between GC-GC and GC×GC, both of which are categorized as multidimensional gas chromatography (MDGC). Heart-cutting predates comprehensive in use [20] and is tailored toward targeted analysis of select regions of the ^{1}D separation. In its most basic form, GC-GC transfers only selected regions of eluate containing targeted compounds from a ^{1}D column to a ^{2}D second column. This method is effective in providing the additional chromatographic benefits associated with MDGC, but for only select regions of the ^{1}D separation. Comparatively, GC×GC applies the benefits of MDGC to the entirety of the separation of analytes injected on the ^{1}D column. In this manner the modulator of GC×GC operates continuously during the entire ^{1}D separation by injecting increments of the ^{1}D eluate onto ^{2}D column with a user defined modulation period (P_M). The practice of GC×GC maintains the integrity of the ^{1}D separation, while providing the additional ^{2}D separations throughout the entire ^{1}D separation in an untargeted fashion [12–14,21].

1.2 PRINCIPLES OF MODULATION

1.2.1 *Modulators: An Overview and Operation Principles*

One can view the modulator as the "heart" of the GC×GC instrument, since it is solely responsible for transferring analyte from the ^{1}D column to the ^{2}D column, facilitating a comprehensive separation. Modulators can be broadly classified into three categories: thermal [13,22–26], valve-based [27–30], and flow [18,20,29,31–34]. Thermal modulators use temperature control to trap and then release the analytes in the eluate during transfer from the ^{1}D column to the ^{2}D column. Valve-based modulators employ a mechanical valve to control and divert aliquots of collected ^{1}D eluate to accomplish transfer of analyte whereby the ^{1}D and ^{2}D column flows are not coupled. Flow modulators in a similar fashion divert gas flow for analyte transfer, but the column flows remain coupled. Each modulator category has distinct advantages and disadvantages, but have a common function of isolating and transferring eluate from the ^{1}D column to the ^{2}D column as quickly and efficiently as possible.

Modulators have four parameters by which their performance may be evaluated: duty cycle, modulation period, injection pulse width, and resulting peak capacity provided by the ^{2}D separation. Duty cycle is defined as the fraction of analyte that is transferred from the ^{1}D column to the ^{2}D column. A modulator that completely transfers all of the ^{1}D eluate to the ^{2}D column has a duty cycle of 1.0. All thermal modulators provide a duty cycle of 1.0, since the columns are serially connected, providing thermal modulators with a fundamental advantage over other forms of modulation due to increased detection sensitivity and signal-to-noise ratio (*S/N*). Most valve-based and flow modulators have a duty cycle < 1.0 since only a portion of the analyte is directed to the ^{2}D column and on to detection. A duty cycle ≤0.5 is referred to as a low duty cycle modulator.

In general, flow and valve-based modulation overcomes, in part, the lower duty cycle through zone compression of the analyte upon injection onto the head of the ^{2}D column.

The modulation period P_M, defined as the amount of time between modulations (i.e., separation run time on ^{2}D), can play a role in modulator performance considerations. Typical modulation periods are in the 1-10 s range [29,30,35–40], with a minimum of 50 ms recently reported, and the focus of this dissertation [34]. The P_M should be selected to complement the width-at-base (W_b) (4σ) of the ^{1}D peaks. Proper P_M selection is driven by the need to provide an acceptable sampling density (ρ_s). The sampling density [41] (also referred to as modulation ratio, M_R) [42], is the ^{1}D peak width divided by the time length of the ^{2}D separation, i.e., the modulation period, P_M.

$$\rho_s = \frac{^{1}W_b}{P_M} \tag{1.1}$$

Generally, the P_M should be chosen to provide a sampling density of $\rho_s \sim 2$ to 4 [41,43]. A $\rho_s < 2$ results in under sampling of the ^{1}D separation, causing loss of analytical information such as a reduction in the ^{1}D resolution and peak capacity, and possibly loss of quantitative precision and accuracy [21,44]. A $\rho_s > 4$ is essentially over sampling the ^{1}D separation which is not detrimental to the ^{1}D resolution and peak capacity. However, there is a reduced peak capacity for the ^{2}D separation [45,46], since the P_M used to produce the $\rho_s > 4$ could be increased to make room for more ^{2}D peaks without adversely impacting the ^{1}D separation.

Indeed, the best practice of GC×GC relies on maximizing peak capacity [47,48]. The peak capacity ($n_{c,1D}$) in a 1D separation at unit resolution, $R_s = 1$, defined as the total time (^{1}t) of the ^{1}D separation divided by the average width-of-base, $^{1}W_b$, is given by,

$$n_c = \frac{^{1}t}{^{1}W_b} \tag{1.2}$$

For GC×GC the ideal peak capacity is given by,

$$n_{c,2D} = {}^{1}n_c \times {}^{2}n_c \quad (1.3)$$

where ${}^{1}n_c$ and ${}^{2}n_c$ are the ^{1}D and ^{2}D peak capacities, respectively. Equation (1.3) can be rewritten to assist in discussions of modulator performance, and the impact on peak capacity optimization,

$$n_{c,2D} = \frac{{}^{1}t}{{}^{1}W_b} \times \frac{{}^{2}t}{{}^{2}W_b} = \frac{{}^{1}t}{{}^{1}W_b} \times \frac{P_M}{{}^{2}W_b} \quad (1.4)$$

where ${}^{1}t$ is the total time of the ^{1}D separation, ${}^{2}t$ is the time of the ^{2}D separation (equivalent to P_M), and ${}^{1}W_b$ and ${}^{2}W_b$ describe the average width-of-base at (4σ) on each separation. To maximize peak capacity, the GC×GC instrument must produce highly efficient separations, characterized by narrow peak widths in both dimensions, ${}^{1}W_b$ and ${}^{2}W_b$. Minimizing the ^{1}D peak widths benefits from a narrow injection pulse onto the ^{1}D column, likewise, minimizing the ^{2}D peak widths relies upon providing a narrow injection pulse from the modulator [49–52]. Hence, $n_{c,2D}$ relies heavily upon the performance of the modulator. Overall, optimally applied GC×GC performance should provide ~10-fold increase in peak capacity over 1D-GC, concurrent with applying a ρ_s ~ 2 to 4 [53,54].

Each modulator, no matter the category, operates on the premise of trapping and/or isolating a portion of the ^{1}D eluate and injecting that portion onto the head of the ^{2}D column. Thermal modulators principally trap analytes in a region of cold (relative to the current separation conditions), with the trapped analytes held until some form of heating is applied to release them onto the head of the ^{2}D column.

Thermal modulation concentrates analyte during the trapping stage. For example, if a P_M = 3 s is applied, and if the injected pulse width produced by the modulator is 30 ms, then the

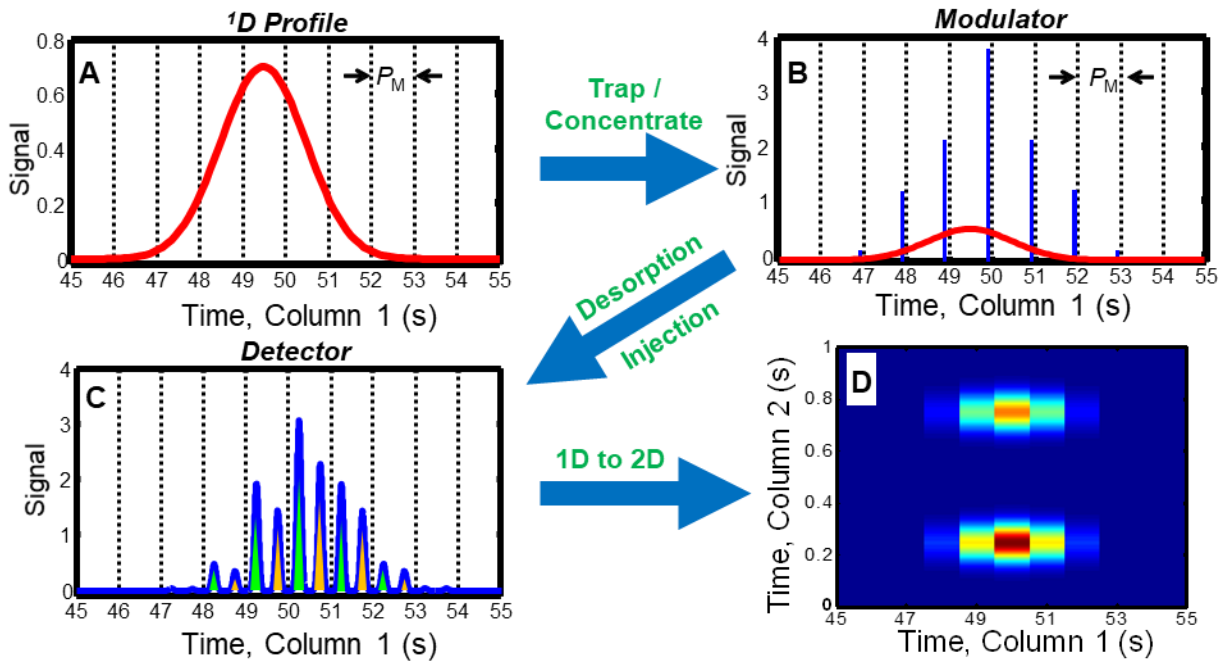

388

Figure 1.1 Illustration of Thermal Modulation for GC×GC

Thermal modulation is graphically shown, demonstrating the process of trapping and releasing of analytes via temperature control. For this demonstration co-eluting analytes on the first dimension are shown. (**A**) Peak profile in red is shown of co-eluting analytes as they enter the thermal modulator. The dashed lines are used to demonstrate the modulation period (P_M) of 1 second used for this demonstration. (**B**) The blue vertical bars represent the collected analyte at the modulator. For each modulation analyte is collected for approximately 1 second, then rapidly released via heating. For this example, one could assume a 950 ms trapping phase, followed by a 50 ms desorption phase. which leads to an approximate 18-fold increase in concentration of analytes for the injection onto head of ^{2}D column. The red Gaussian peak overlaid from (**A**) is meant to illustrate this concept. (**C**) Injection on the ^{2}D separation column results in separation of the co-eluting analytes from the ^{1}D column shown in (**A**). (D) Through the commonly applied practice of folding the data by the modulation period (1 s) a 2D chromatogram is generated for the two respective analytes with the respective ^{1}D and ^{2}D retention times shown.

389 analyte trapped over this P_M cycle has been concentrated 100-fold via the thermal modulation
390 process. For thermal modulation the injection pulse width is dominated by two parameters: the

391 physical dimensions of the region in which trapping occurs, and the time interval required to
392 release the trapped analytes via rapid heating onto the head of ^{2}D column. Ideally, both of these
393 contributors to the modulator pulse width should be negligibly small to minimize ^{2}D band
394 broadening due to the modulation process. Figure 1.1, demonstrates the process of thermal
395 modulation of two overlapped analytes on the ^{1}D separation column. The 1D peak profile of the
396 overlapped analytes is shown in Figure 1.1A, as the analyte peak enters the cooled region of the
397 modulator where the analyte is trapped and concentrated, represented by blue colored bars in
398 Figure 1.1B. At the prescribed modulation period time, the now concentrated analyte is desorbed
399 via rapid heating and injected onto the head of the second column, the resulting separated analyte
400 peaklets at the detector is shown in Figure 1.1C. The resultant data is folded by the modulation
401 period, which is 1 second in this example to form the 2D chromatogram shown in Figure 1.1D.
402 Flow and diaphragm valve-based modulators function by rapid redirection of gas flow, normally
403 where a portion of the ^{1}D eluate is directed into a short sample loop made from either a glass
404 capillary column, or stainless steel. This eluate portion is then redirected onto the head of the ^{2}D
405 column during the modulator injection stage. Depending on the direction of flow within the sample
406 loop, the modulator would be considered a forward flush modulator (FFF), or a reverse flow
407 modulator (RFF). Flow modulators are considered forward flush if the flush (injection) is in the
408 same direction as the original fill stage, and reverse if the injection is performed in the opposite
409 direction of the fill stage [32]. Hence, for valve-based and flow modulators the injection pulse
410 width is often dominated by the amount of time the flow of gas containing the eluate from the ^{1}D
411 column is directed onto the head of the ^{2}D column. Figure 1.2, demonstrates the process of
412 valve/flow modulation of two overlapped analytes on the ^{1}D separation column. The 1D peak
413 profile of the overlapped analytes is shown in Figure 1.2A. As the analyte peak flows through the

414 sample loop/connecting column of the modulator, at prescribed time the valve/flow modulator is

415 activated to inject the analyte present in the connection loop/column, represented by blue colored

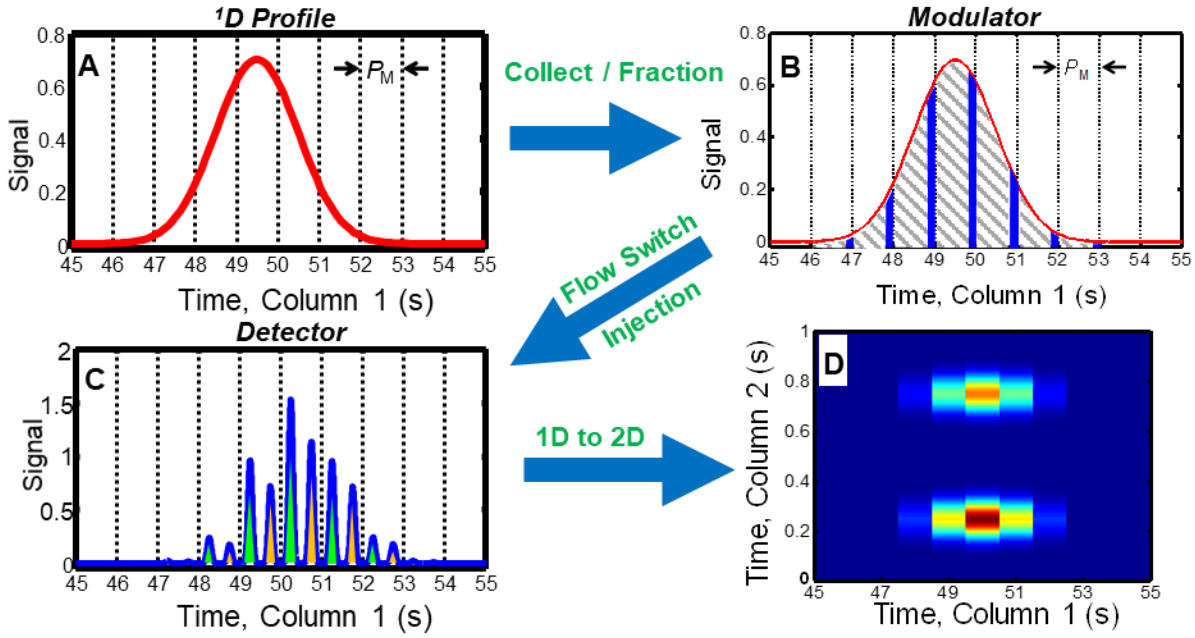

416

417

Figure 1.2. Illustration of Flow/Valve-Based Modulation for GC×GC

Flow and Valve modulation is graphically shown, demonstrating the process of transferring analytes from ^{1}D to ^{2}D columns via gas flow control. Flow and Valve modulators have a few key differences that distinguish the two forms of modulations, which is explained within the body of the paper, for this demonstration the two are treated equal as both transfer via flow switching control. For this demonstration co-eluting analytes on the first dimension are shown. (**A**) Peak profile in red is shown of co-eluting analytes as they enter the modulator collection column/loop. The dashed lines are used to demonstrate the modulation period (P_M) of 1 second used for this demonstration. (**B**) The blue vertical bars represent the analyte from the collection column/loop that is transferred from the modulator to the head of the ^{2}D column. The grey region between the blue bars represents analyte that is either lost through a vent, or directed to a second detector. For this example, one could assume for 900 ms analyte is flowing through the collection column/loop, followed by a 100 ms flow switching phase that flushes the contents (analytes), which leads to the injection of analytes onto head of ^{2}D column. This would be an example of an approximate duty cycle of (0.2). The flush depending on the modulator is either in the direction of the original flow (Forward Flow Flush), or reveres the original flow (Reverse Flow Flush). The red Gaussian peak overlaid from (**A**) is meant to illustrate that the modulator does not concentrate the analyte as with thermal modulation. However due to zonal compression during the flushing phase, analyte concentration within the injection is increased, helping improve *S/N* and reducing the effect of a low duty cycle. (**C**) Injection on the ^{2}D separation column results in separation of the co-eluting analytes from the ^{1}D column shown in (**A**). (**D**) Through the commonly applied practice of folding the data by the modulation period (1 s) a 2D chromatogram is generated for the two respective analytes with the respective ^{1}D and ^{2}D retention times shown.

bars in Figure 1.2B. The greyed out region shown in Figure 1.2B for this example is the portion of the analyte peak lost or directed towards a secondary detector, resulting in a duty cycle of (< 1.0). During the injection phase, which is either a reverse or forward flush of the collection loop/column, the analyte undergoes compression which results in increased *S/N* helping off set analyte lost and improving sensitivity. The resulting separated analyte peaklets seen at the detector are shown in Figure 1.2C. The resultant data is folded by the modulation period, which is 1 second in this example to form the 2D chromatogram shown in Figure 1.2D.

Several published papers group diaphragm valve-based and flow modulators together [16,18,19] since both use gas flow control to transfer ^{1}D eluate onto the ^{2}D column. However, in this text, the two are introduced separately in order to emphasize key differences between these two modulation approaches. An important advantage of diaphragm valve-based modulators is the fully de-coupled flows of the ^{1}D and ^{2}D columns, so the two columns are operated independently. Flow modulators also utilize different ^{1}D and ^{2}D flow rates, however, the two column flows 'communicate' with the other at the modulator union and cannot be operated truly independently. With the flows fully decoupled, method development can be inherently easier with diaphragm valve-based modulation. In general, all three of the modulator category designs have distinct advantages and disadvantages, with the shared mission to transfer eluate from the ^{1}D column to the ^{2}D column as efficiently and quickly as possible.

1.3 Historical Background and Recent Developments of Thermal Modulation

Thermal modulation, initially introduced in 1991 [13], continues to be the most commonly applied technique. It relies on low temperatures to trap and focus analytes as they elute from the ^{1}D column and introduces them to the ^{2}D column through rapid heating. Thermal modulators can

be further broken down into three subcategories: resistively heated trap, heated sweeper, and cryogenic focus, which is often divided into longitude movable trap and jet trap [15]. The first two categories, resistively heated trap and heated sweeper, were the center of developmental focus during the 1990's. However, cryogenic focus has all but replaced both forms [17]. For a thorough history of thermal modulation we direct the reader to previous reviews [15,17,18]. While cryogen-based jet modulators have proven to be highly reliable, recent innovations have been directed toward providing simpler and more cost-effective thermal modulator designs. To that end, a major thrust is the research, development, and commercialization of cryogen-free thermal modulators.

1.3.1 *Cryogen-Free Thermal Modulators*

Two commercially available cryogen-free thermal modulators have recently been introduced. The ZOEX Corporation has introduced the ZX2 thermal modulator which employs a closed cycle refrigerator/heat exchanger to create a two-stage loop modulator capable of modulating C_7+, offering the closest performance to cryogen based systems of C_4+. The two-stage loop modulator uses a continuous cold jet flow with a regularly pulsed hot jet to re-inject trapped analytes. The cold jet can produce temperatures of -90 °C, and the hot jet can produce temperatures of 475 °C, with a minimum P_M of 1 s. Liquid nitrogen based thermal modulators trap with a cold jet in the range of -190 °C, allowing for trapping typically down to C_3. A secondary oven is offered for use with the ^{2}D column that can lead or lag the GC oven up to 40 °C. This design has been used to study petroleum products in several different studies [55–58], although the modulation rating to C_7 did not have an impact on the modulators ability to be used for these applications. The temperature range, and P_M of 1 s may limit the applicability of the ZX2 in the analysis of highly volatile analytes and high speed GC×GC separations, but should be appropriate for a wide variety of analyses.

J&X Technologies recently introduced the Solid State Modulator 1800 (SSM1800), the world's first commercial SSM that uses thermoelectric (TE) cooling, mica-thermic heating, and a movable capillary column. The modulator uses a two stage method to trap and inject analytes, via a "modulation" column. The SSM1800 utilizes two zones of trapping and releasing, so analytes are trapped and released, then trapped and released a second time onto the head of ^{2}D column. Use of this two stage trapping system is meant to minimize breakthrough concerns. Modulation takes place in one of three "modulation" columns that come with the SSM1800, whereby the selected modulation column serves as the union between the ^{1}D and ^{2}D columns. This design places limitations on the analysis, as each modulation column has a specific application range: C_2-C_{12}, C_5-C_{30}, and a third listed for use with mineral oils and organic components analysis of aerosols. An additional, unique feature of the SSM1800 is the augmentation of a gas flow stream which decouples the flows of the ^{1}D and ^{2}D columns allowing for independent optimization of separation conditions on both columns. Luong et. al. were the first to demonstrate the SSM1800 using a test mixture with a volatility range equivalent to C_6 to C_{24}.[59]

One of the more promising thermal modulators under development is a single-stage consumable-free modulator, which uses a coated stainless steel capillary trap [60–62]. Trapping is accomplished using cooled ceramic pads, and the subsequent desorption is completed using a capacitive discharge power supply to resistively heat the trap. Mascalu et. al. compared the modulator to the widely used LECO quad jet LN_2 modulator using a 4 s P_M [60]. The performance of each was judged in the context of applying a routine accredited method of analysis of polychlorinated biphenyls, organochlorine pesticides and chlorobenzenes. Twenty-five analytes were evaluated for their ^{2}D peak widths, ^{1}D and ^{2}D retention times, and concentration limit of detection (LOD). Additionally, tests were performed to confirm robustness. The results from this

modulator were generally consistent with the quad jet system in all figures-of-merit, albeit with a noted 35% increase in average peak widths with the single-stage consumable-free modulator, which would cause a reduction in ^{2}D peak capacity. In a more recent study [62], Ntlhokwe et. al. analyzed the volatile constituents of honeybush tea via SPME extraction to evaluate the performance of their consumable-free modulator. In this study the cryogen-free modulator was demonstrated with a P_M of 5 s and modulated the lightest compound 1-pentanol (b.p. 138 °C, equivalent to C_8 b.p. 125 °C). Breakthrough did occur with a few compounds at high injected concentration, but this was attributed to the high concentration and not the performance of the modulator.

Another approach to cryogen-free modulation that applies the principles of a resistively heated trap similar to the original Liu and Phillips design [13] was developed by Mucédola et.al., termed a "Do-It-Yourself" interface that can be built using two low cost, commercially available components [63]. This design is a segmented loop-based thermal modulator that requires no cryogens. Excellent GC×GC – FID chromatograms of petroleum samples and hop oils were obtained. Trapping was accomplished using a delay loop composed of metallic modulation loop (1 m) with a 0.50 µm stationary phase film thickness located in the oven at ambient temperature. Desorption was accomplished by resistive heating of the metal column with application of a short heat pulse (355-500 ms) provided by a 32-45 W power source. A reproducible minimum P_M of 6 s was reported, restricting applicability to longer GC×GC separations that necessarily produce wider ^{1}D peaks.

A micro thermal modulator (µTM) was first introduced by Kurabayaski et. al. in 2010 to produce an ultra-small 'lab on chip' modulator [64]. The original design had a P_M of 7 s and was able to trap from 250 °C to -20 °C in ~ 0.9 s and then rapidly heated for re-injection in 150 ms.

The µTM was designed to be used with µGC×µGC, employing a solid-state TE cooler to facilitate portability, thus making the power of thermal modulated GC×GC more amenable for remote site analyses [65,66]. An air-gap spacer was added in a subsequent design to enhance the trapping and desorption of the µTM using a TE cooler, which improved the temperature uniformity across the device channels [66]. This improvement resulted in a 25% increase in detection sensitivity. A second key improvement to the performance of a µTM using a TE cooler with temperature programming was the combination of an ionic liquid as the stationary phase to assist in trapping the ^{1}D eluate resulting in narrower ^{2}D peaks at the point of re-injection [65].

Recent improvements in cryogen-free modulators have yielded several key breakthroughs in performance, attaining figures-of-merit similar to that obtained by cryogen-based (either LN_2 or CO_2) modulation, and thus similar peak capacities for ^{2}D separations. However, two key issues for universal application of the cryogen-free thermal modulators remain. First, there is the challenge to properly modulate C_3-C_7, and second, the relatively long modulation periods provided negate the opportunity to apply the cryogen-free modulators for high speed GC×GC applications. The challenge to address these issues will be impetus for future research efforts.

1.3.2 *Cryogen-Based Thermal Modulators*

Due to the well-developed and understood modulation properties, and the excellent modulation performance, the use of cryogens (either LN_2 or CO_2) for thermal modulators remains popular and continues to be further developed. In particular, there is continued development of cryogen-based single-stage jet trap modulators. Unlike the more popular dual-stage cryogen trap modulators that utilize two trap and release stages (often referred to as a quad jet modulator), the single stage concept uses only one cold and one hot jet sequence. The quad jet design is intended to help address breakthrough and desorption concerns while providing a double focusing of analyte

to assist with optimizing *S/N* and the LOD. Jet trap modulators are considered the simplest form of thermal modulation since there are no moving parts.

A single-stage cryogenic modulator was recently reported by Mostafa and Górecki [67]. The use of silica wool inside a trapping column, serves as a restriction at the point of the cold jet to increase trapping efficiency by slowing the gas flow during the trapping and desorption stage to preventing breakthrough and desorption issues [67]. Performance of the modulator was evaluated with a broad range (C_5 to C_{24}) of compounds. Narrow peak widths were achieved, down to ^2W_b of 60 ms, with no breakthrough observed. An experiment was conducted to elucidate that the carrier gas flow rate slows down during the trapping stage, which involved doping the carrier gas with propane. During the trapping stage, a negative peak was produced due to the decrease in carrier gas flow rate, observed as a reduction in propane signal. The reduction in carrier gas flow rate during eluate trapping is instrumental in improving trapping efficiency. Performance of the restricted modulator was similar to a traditional quad jet modulator while significantly reducing the quantity of LN_2 consumed.

Another design using a single jet modulation, does so with a loop-based configuration. One set of jets traps and then desorbs the eluate which travels around the loop where it is trapped again, and then desorbed onto the ^{2}D column. An important parameter for modulation in GC×GC is the carrier gas velocity at the point of re-injection (desorption) [68,69]. For loop-based thermal modulation, similar to other types of thermal modulation, the ^{1}D and ^{2}D columns are serially coupled. This means that the ^{2}D flow rate is directly influenced by the length, diameter, and flow rate of ^{1}D. To optimize the re-injection conditions, a bleed line can be added using a Y connector at the end of ^{1}D between the outlet of the modulator loop and ^{2}D column. Others have used this technique to improve the separation on the ^{2}D column [70,71]. A significant number of research

groups have contributed to thermal modulator development, aiming to perfect cryogen-free and cryogen-based thermal modulators. For a deeper examination of current research efforts, the reader is encouraged to review several methods and modulators developed in the last few years but not discussed here [72–81].

1.4 Historical Background and Recent Developments of Valve Modulation

Diaphragm valve-based modulation was first introduced in 1998 by Bruckner et. al. [27]. The original design utilized a VICI 6 port diaphragm valve, which diverted eluate from the ^{1}D to the ^{2}D column with a P_M of 500 ms using only four of the six ports in the valve. The results of this study produced narrow ^{2}D peak widths with excellent $^{2}t_R$ reproducibility. There were, however, two key limitations, only ~10% (low duty cycle) of the eluate from the ^{1}D separation was transferred to the ^{2}D column, and due to mechanical limitations the valve could not be operated above 175 °C. An early solution to the temperature limit was to have the valve face-mounted external to the oven [30]. This approach extended the useable temperature range of the valve to 250 °C, enabling application to higher boiling point analytes. To address the low duty cycle of the initial demonstration of diaphragm valve-based modulation, Seeley and co-workers improved performance by employing a sampling loop to collect the ^{1}D eluate, which provided a much higher fraction of the ^{1}D column eluate being transferred to the ^{2}D column producing improved detection sensitivity [28]. Also, using the sample loop, flow during the re-injection can be reversed creating a narrow injection pulse to improve $^{2}W_b$ and detection *S/N*.

A unique feature of the diaphragm valve-based modulator that distinguishes it from other forms of flow modulation is that the ^{1}D and ^{2}D columns do not significantly ‘communicate’ at the

valve since they are isolated from each other. This allows independent optimization of each separation dimension. Instead of using thermal zones to trap eluate from the ^{1}D separation, diaphragm valve-based modulators collect the ^{1}D eluate in a short collection loop which is then flushed with an independent carrier gas flow onto the ^{2}D column. The six-port valve operates on a simple principle. In the "collect" mode the eluate from ^{1}D flows through the sample loop and out the waste port. Then, in the "re-inject" mode the valve actuates with the flow in the loop reversed based upon how the capillary connections have been configured, with the collected eluate injected onto the ^{2}D column.

Recent improvements have resulted in a higher temperature limit for commercially available diaphragm valves. The original temperature limit of 175 °C was overcome by replacing the temperature sensitive O-ring with a perfluoroelastomer-based O-ring, allowing reliable function up to 325 °C [29]. Freye et. al investigated the updated modulator, and found that the valve produced narrow, reproducible ^{2}D peak widths and reproducible $^{2}t_{R}$'s. This "high temperature" diaphragm valve modulates compounds across a wide range of boiling points (e.g. C_1 to C_{40}+), requires minimal consumables, and has a relatively simple design. Under the demonstrated conditions, about 30% of the modulated analyte made it to the FID detector, and yet, the detection sensitivity was about 8-fold higher than 1D-GC due to zone compression. In a follow up study, flow rates of 1.0 ml/min on the ^{1}D column and 3 ml/min on the ^{2}D column performed well with TOFMS detection [82]. Under these flow conditions it was demonstrated that a diesel fuel with a boiling point range of 98-450 °C could be separated. A high 2D peak capacity of $n_{c,2D}$ ~ 14,000 was achieved in a ^{1}D run time of 120 min. These high temperature diaphragm valves have also been recently implemented in comprehensive GC^{3} with TOFMS detection (GC×GC×GC – TOFMS) [83].

1.5 Historical Background and Recent Developments of Flow Modulation

Flow switching is a time tested technology that originated with heart-cutting (GC-GC) originally performed with pneumatic valves. The key breakthrough for flow switching came with the development of the Deans' switch in 1968 [20]. In the past 11 years, flow modulation has gained in popularity as a valued modulation approach for GC×GC. Similar to valve-based modulation, flow modulation uses gas pressures to control the transfer of eluate from the ^{1}D column to ^{2}D column. Unlike diaphragm valve-based modulation, the two columns flows are inextricably connected, so the column flows significantly communicate with each other, adding complexity to method development and application. Comprehensive GC×GC flow modulation was pioneered in 2006, by Seeley who introduced a simple design based upon a Deans' switch in which 100% of the ^{1}D eluate was transferred to the ^{2}D column [31,84]. This method has been adapted and modified by many groups at the commercial level and academic research level, in efforts to improve upon the initial concept and demonstration. Indeed, several breakthroughs have been reported for flow modulator designs over the last five years. A comprehensive review was published in 2011 which provides a detailed summary of flow modulation [19].

Currently there are six commercially available flow modulators: Agilent CFT, SepSolve INSIGHT, SGE SilFlow, Perkin Elmer Swafer, Gerstel Multi-Column Switching System, and the Shimadzu Advanced Flow Technology Series. Only the CFT and INSIGHT systems are marketed as capable of being used for both GC×GC and GC-GC separations while the others are only for GC-GC. For a detailed discussion of these systems and the Deans' switch we refer readers to reviews by Marriot and Seeley [15,31,85].

A key issue with flow modulators that has hampered application is the high flow rates on ^{2}D separations, often ~ 20 ml/min, posing compatibility issues for mass spectrometry detection due to the connection to a vacuum system. A typical approach to address this issue is to split the flow exiting the modulator prior to MS detection: either split part of the flow into a bleed column, or split to an additional detector, typically an FID. Performing the latter allows for various combinations of detectors to be used simultaneously with MS that can be tailored to meet specific analytical goals. Armstrong and co-workers have shown that simultaneous detection using FID and quadrupole mass spectrometry (qMS) is very advantageous because the FID readily provides a reliable quantitative analysis, while the qMS spectral scan speed is sufficient to enable more confident analyte identification [86].

In 2007, shortly after Seeley's ground breaking work, Agilent Technologies' introduced their flow modulator, Capillary Flow Technology (CFT), which resulted in the wider adoption of flow modulation. The CFT is an in-oven modulator based upon a Deans' switch, compatible with most forms of MDGC. This simple low-thermal mass modulator has proven to be very reliable with excellent reproducibility of ^2t_R and ^2W_b, which is particularly appealing for industrial applications [87]. SepSolve Analytical recently introduced their own version of a flow modulator based upon a Deans' switch called the INSIGHT that is implemented as a RFF modulator. The INSIGHT has been recently utilized in two studies, one in the study of the volatile organic compounds of human blood [88], and the other study examining the benefits of tandem ionization for analyte identification [89]. In the Dubois study [88], a mixture of 108 compounds was analyzed with a P_M of 2.5 s. The results were favorable with an average ^{2}D width-at-half-height of 340 ms and a tailing factor of 1.16. Minimal breakthrough was observed down to C_4. In the Freye study [89], a P_M of 2 s with a flush time of 80 ms was applied. The study did not focus on the performance

of the modulator but rather focused on a novel chemometric technique applied to the data generated. For more data on the performance of the INSIGHT, SepSolve Analytical provides white papers on their web site. The use of either the CFT or INSIGHT modulators rely upon application of a split flow to reduce the flow rate on the ^{2}D column in order to facilitate MS detector use, which also affords the ability to use dual detectors. In the case of the CFT up to three detectors can be used simultaneously.

Very recently, Seeley has demonstrated two novel developments with a Deans' switch flow modulator. Using a high speed Deans' switch, constructed from commercially available parts, a low duty cycle modulator was demonstrated using a flow rate of 2 ml/min for the ^{2}D separation [90]. Sub 50 ms pulse widths were generated at the low flow rate of 2 ml/min, resulting in narrow ^{2}D peak widths and reproducible $^{2}t_{R}$'s, with a ~ 10% duty cycle of the ^{1}D eluate transfer. In another intriguing study, Seeley applied the same high speed Deans' switch in a new approach to GC×GC modulation. A pattern of primary ^{1}D eluate, referred to as "pattern modulation," is transferred to the ^{2}D column instead of a single pulse per each modulation [91]. The unorthodox appearing raw data is readily transformed into a traditional GC×GC chromatogram using Lucy-Richardson deconvolution. The resulting 2D peaks were 16-36 times more intense, and the ^{2}D peak widths were 40-70% narrower, than ^{2}D peaks obtained by traditional flow modulation. In 2017, Seeley introduced a multi-mode modulator (MMM) that is capable of performing heart cutting (GC–GC), low duty cycle GC×GC, and total transfer GC×GC [33]. In the heart-cutting and low duty cycle mode, the ^{2}D flow rates were sub 1.0 ml/min. However, in the total transfer mode, the flow was 10 ml/min, which may be a challenge to be used on conjunction with MS detection. This work is a noteworthy step toward producing a universal flow interface for all forms of MDGC.

Over the past several years, the Mondello group has made several advancements in flow modulation. In 2011, they developed a flow modulator using a seven port valve with a flexible loop between ports to collect sample, in conjunction with qMS detection [92]. A needle bleed valve connected to a waste line at the head of the ^{2}D column was required to reduce the flow rate to ~2.5 ml/min, resulting in a low duty cycle estimated at ~ 5%. Using the same 7-port modulator coupled with HR-TOFMS detection, a proof-of-principle study was performed [93]. In this study, separation conditions were modified resulting in an initial flow rate of 3.4 ml/min and a duty cycle of ~ 40% at the beginning of the separation. At the end of the separation (310 °C) the flow rate was 2.1 ml/min with slightly lower duty cycle.

In a recent study, the Mondello group purposely used mismatched lengths of deactivated fused silica, to achieve lower carrier gas flow rates (6-8 ml/min) on the ^{2}D column compared to the typically high gas flows (~ 20 ml/min) while still providing efficient re-injection of the ^{1}D eluate. However, a longer flush time (i.e. re-injection time) was required to totally clear the loop [69]. The design and flow conditions were found to be compatible with qMS and TOFMS, with an additional benefit of no loss of analyte or the need to divert flow to another detector [69,93]. Further advancements were demonstrated using the Deans' switch design at a flow rate of 4 ml/min on the ^{2}D separations in conjunction with qMS detection, while providing increased detection sensitivity relative to 1D-GC [94]. A long injection period (700 ms) enabled an efficient accumulation-loop flushing at gas flow rates of 4 ml/min. At this flow rate this modulator is compatible with any MS detector concurrent with optimal duty cycle.

A unique modulation approach was recently introduced that utilizes partial modulation via introduction of pulses of pure carrier gas, i.e., a form of vacancy chromatography. This approach most closely resembles flow modulation, but unlike other flow modulators, no form of flow

diversion into adjoining capillaries occurs. This interesting, yet unconventional, modulation approach, was first introduced by Cai and Stearns in 2004 [95]. In this study, small pulses of carrier gas were repetitively injected at the interface between the ^{1}D and ^{2}D columns, creating either local high (positive) or low (negative) analyte concentration pulses in the eluate departing the ^{1}D column, which are then separated on the ^{2}D column. In the negative concentration pulse mode, the approach is functionally performing vacancy chromatography. A P_M of 1 s was applied and ^{2}D peak widths ~ 60 ms were achieved. This method required additional data processing to produce a conventional appearing 2D chromatogram contour plot.

Very recently and focus of this work, this technique of modulation is revisited using a commercially available pulse flow valve (i.e., pulse flow valve modulation) [34]. This form of modulation and the exploration of this new technique is the basis of this dissertation. Modulation periods as short as 50 ms were reported, which is a 4-fold decrease in modulation period of the fastest thermal modulation study reported [96] and a 20-fold decrease for the typical "fast" flow modulation application [90]. Pulse flow valve modulation is achieved by rapid introduction of a pulse of carrier gas at the union of the ^{1}D and ^{2}D columns. This modulation approach produces a rapid decrease in analyte concentration that produces signals that are (currently) most readily treated as the combination of two methods: vacancy chromatography and frontal analysis (Figure 1.3). A simple three-step process was developed to convert the raw data, into a format analogous to a 2D contour plot chromatogram. The resulting ^{2}D peaks are not traditional and are referred to as 'apparent' ^{2}D peaks, with peak widths-at-base ranging from 12 to 45 ms. A closer look at the three-step process (1: data differentiation, 2: inversion, 3: baseline correction) of data conversion from raw data to 'apparent' 2D peaks is shown in Figure 1.4. In this example it can be seen that the critical data is contained in the sharp negative error function, with the remaining data being of

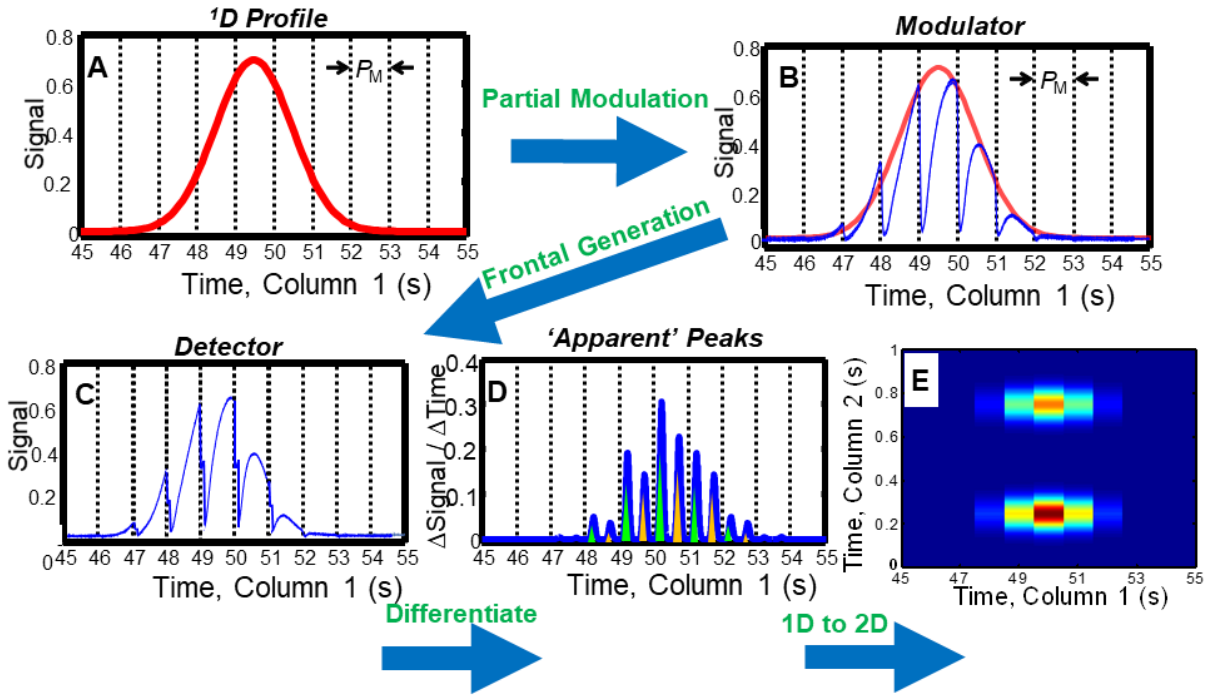

716

Figure 1.3. Illustration of Partial Modulation for GC×GC

Partial modulation via the pulsed flow valve modulator is graphically shown, demonstrating the process of modulation by injection of carrier gas, that is a combination of vacancy chromatography and frontal analysis. For this demonstration co-eluting analytes on the first dimension are shown. (**A**) Peak profile in red is shown of co-eluting analytes as they enter the T-union connection between ^{1}D and ^{2}D columns. The dashed lines are used to demonstrate the modulation period (P_M) of 1 second for this demonstration. (**B**) The blue chromatogram represents the shape of the modulated peak at the modulator. For this example, one could assume modulation occurs every 998 ms by a 2 ms injection of carrier gas. This process is very unique and does not have the added effect of increasing the concentration of analyte injected on the ^{2}D column, however it does have a duty cycle of essentially 1.0, like that of the thermal modulator. The red Gaussian peak overlaid from (**A**) is meant to illustrate this concept. (**C**) Injection on the 2D separation column results in separation of the co-eluting analytes manifest in two separate 'fronts' and not the traditional peaklets generated by all other forms of modulation. (**D**) Through signal differentiation the negative slope of the fronts are converted into 'apparent' peaks. Peak intensity and width-at-base are related to the retention of the analyte on the ^{2}D column. The more retained the analyte, the wider the width-at-base of the peak which is related to the slope of the front generated by the analyte. (**E**) Appling the commonly used practice of folding the data (**D**) by the modulation period (1 s) a 2D chromatogram is generated for the two respective analytes with the respective ^{1}D and ^{2}D retention times shown.

717 lesser importance. A closer look at the key step of

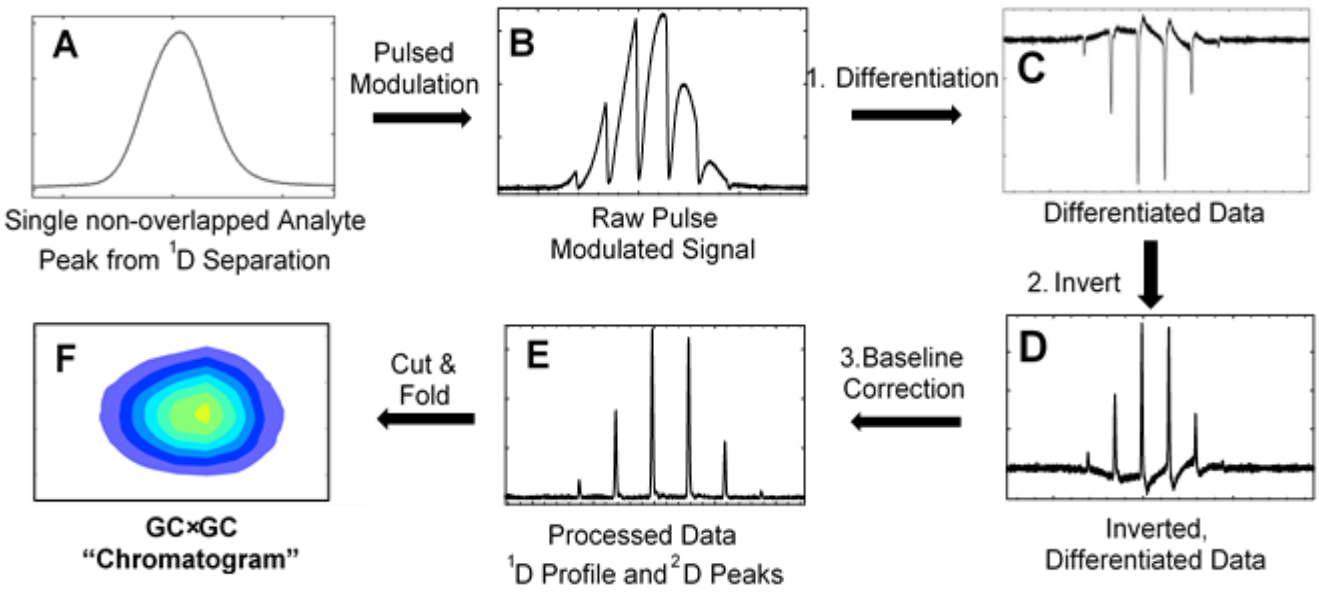

Figure 1.4. Three Step Process to Convert Partial Modulation into Final ^{2}D Peaks.

Represented is the process of partial modulation performed by the pulse valve flow modulator shown in figure 1.4B. Step one differentiation of the signal in figure 1.4B is shown in figure 1.4C, step two inversion generates figure 1.4D. The baseline sag seen in figure 1.4D is removed in step three via an in-house written low frequency filter with the resultant data shown in figure 1.4E. The generation of the GC×GC chromatogram seen in figure 1.4F is produced by cutting the data in figure 1.4E by the modulation period then folding the data which generates the 2D chromatogram.

differentiation is shown in Figure 1.5. As is highlighted in Figure 1.5B, the inflection point of the negative error function becomes the peak apex, shown as the negative peak in Figure 1.5C. The gradual return of the signal to its original intensity following the error function in Figure 1.5B is manifest as a baseline artifact in the data seen in Figure 1.5C and Figure 1.4D. The baseline artifact is removed by an in-house low frequency noise filter with the result shown in Figure 1.4E. This instrumental schematic used for the previous work is shown in Figure 1.6. The pulse valve flow modulator is held external to the GC oven and is connected to the internal 3-way union in which the ^{1}D and ^{2}D columns are connected.

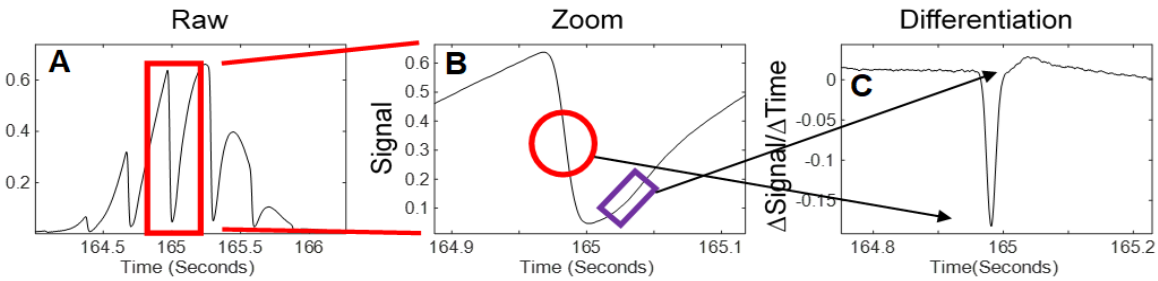

726

Figure 1.6. Close up View of Frontal Analysis Differentiation

A single modulation from non-overlapped peak is shown to demonstrate the conversion of the negative error function into a ^{2}D 'apparent' peak. The inversion point of the negative error function is highlighted in figure 1.5B. This inflection point of the negative error function becomes the apex of the negative Gaussian peak shown in figure 1.5C after the differentiation step. The initial return of the analyte signal to its original intensity following the partial modulation does become manifest in this example as an artifact of the differentiation shown in figure 1.5C. This form of artifacts is removed via an in-house written low frequency filter in step three of data conversion shown in figure 1.4E.

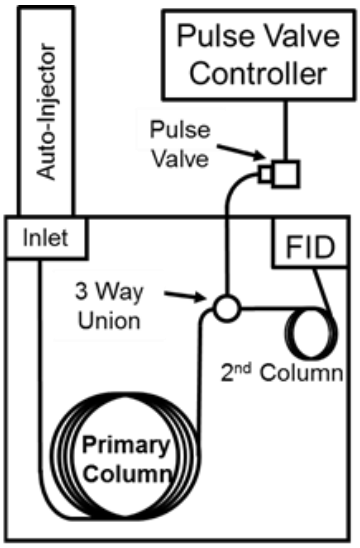

Figure 1.5. GC×GC-FID Pulse Flow Valve Instrumental Schematic.

Instrumental schematic to perform comprehensive 2D gas chromatography (GC × GC) using partial modulation via the pulse flow valve.

Modulation via carrier gas takes place at the 3-way union at a user defined modulation period. This technique of partial modulation and data conversion presented is based on two older techniques, vacancy chromatography and frontal analysis. Vacancy chromatography is an older chromatographic technique first demonstrated by Reilley and co-worker in 1962 [97]. Then termed inverse chromatography, it was demonstrated that in a separation with a steady state concentration of analytes, the removal of an analyte would give the equal but inverted response as an injection of the analyte. In the traditional application of vacancy gas chromatography, the mobile phase contains a small fraction of analyte contained in the carrier gas. An injection of pure carrier gas into the region that contains the analyte cause a region of negative concentration of analyte. This negative concentration of carrier gas will have the same retention time as positive injection of the analyte. This behavior lends vacancy gas chromatography applicable to process monitoring. However, it is not a commonly used technique as most analytical chemist opt to take periodic samples to be separated. Currently most literature on vacancy chromatography is related to liquid chromatography, specifically vacancy ion-exclusion chromatography [98–101]. In process monitoring a mobile phase would contain a solute at a concentration that is continually passed through a column until equilibrium is achieved at both the inlet and outlet. If a pulse of pure carrier gas were to be injected a negative peak profile would be created and pass through the column the same way a positive peak would be expected to pass through. In a similar manner the pulse flow valve modulator injects carrier gas at a user defined time period (modulation period) creating vacancies in the signal. The key difference between traditional vacancy chromatography and the pulse flow valve is that the pulse flow valve is not performed on analytes at equilibrium along the length of the column, but rather on chromatographic peaks resulting from the injection of analytes on the ^{1}D column. The results of partial modulation by carrier gas created by the pulse flow valve

are displayed as error functions. In this technique the error functions contain the critical chromatographic information that is analyzed using a modified frontal analysis technique. Frontal analysis traditionally is a form of chromatography where a continuous flow of analytes passes through a column, each component elutes at a different time depending on its affinity for the

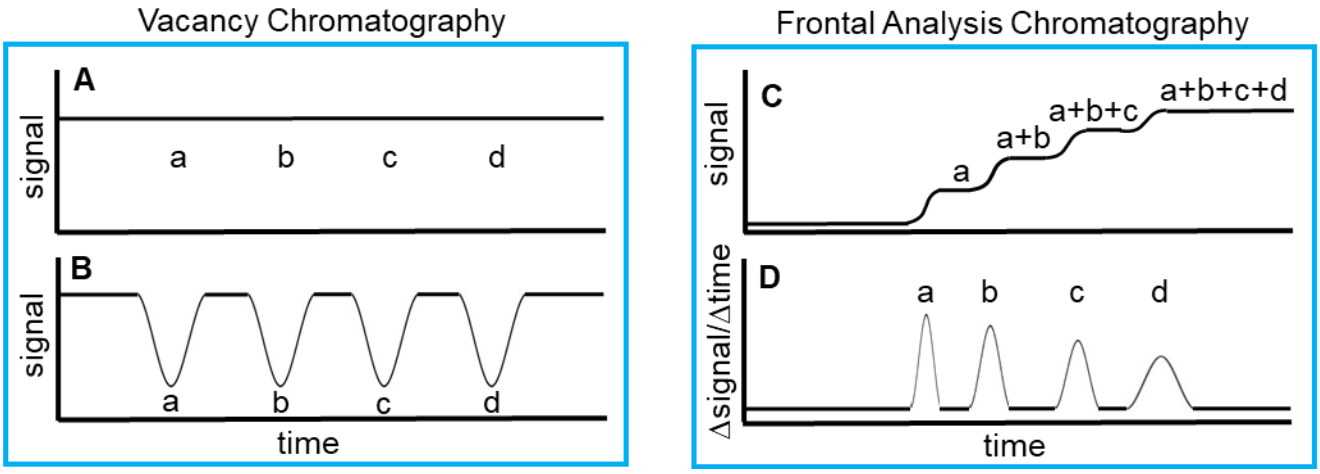

Figure 1.7. Example of Vacancy and Frontal Analysis Chromatography.

(A) An example detector signal of four analytes placed on a column in a continuous injection that has reach equilibrium concentration in the carrier gas. (B) Vacancy chromatography signal of four analytes that were at equilibrium (A), with a segment of their concentration replaced by injection of pure carrier gas. The negative peaks of the analytes matches the retention times exactly as if the analytes had been injected in a one-time discreet injection from an auto-injection system. (C) Frontal response of a continuous injection of an analyte sample mixture onto a capillary column. The region of combined signal of the four analytes shown is exactly the same as (A) when the analytes are at equilibrium. (D) Differentiated signal generated by taking the differential of the error function front produced in (C).

stationary phase of the column [102–104]. This type of analysis traditionally is used for liquid chromatography and the resulting appearance of analytes would only happen once for a separation as the solution elutes from the column. In the current application, the combination of the principles of vacancy chromatography and frontal analysis (Figure 1.7) occurs with each pulse of the valve, with the production of error functions encoded with the critical chromatographic information.

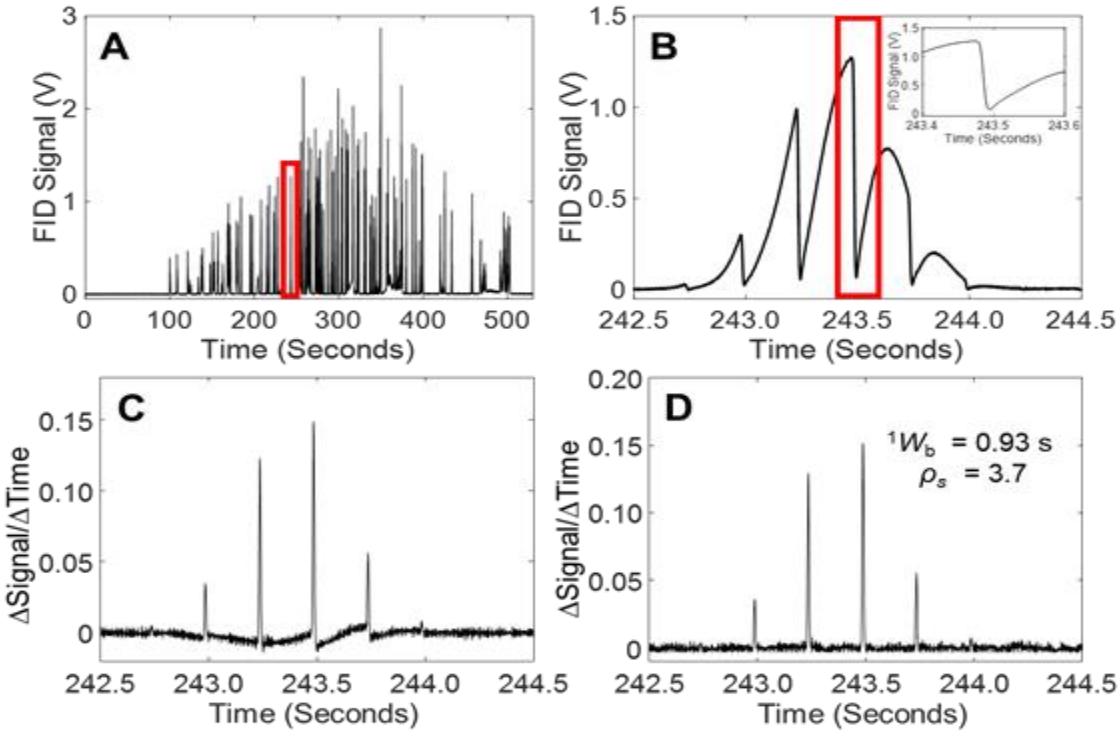

759

Figure 1.8. GC×GC-FID 115-Component Test Mixture Data

(A) Chromatogram (raw data on ^{1}D) of the 115 component test mixture collected using a modulation period P_M of 250 ms. (B) Shown is a mid-elution non-overlapped analyte on ^{1}D. The inset figure shows a zoom of a single "peak" create by pulse modulation. (C) Processed data wherein the raw data in (B) has been differentiated to produce ^{2}D peaks. (D) Data from (C) has been baseline corrected using a rolling minimum. Peaks on the ^{2}D separation are narrow yielding a high peak capacity despite a short modulation period of P_M of 250 ms. Reproduced from C.E. Freye, H.D. Bahaghighat, R.E. Synovec, *Talanta*. 177 (2018) 142-149.

760 Application of this technique of modulation and data processing is seen in Figure 1.8 in which a
761 115-component mix is separated using a P_M of 250 ms. Detail is shown for a single non-overlapped
762 peak, the baseline artifact and removal is shown. Figure 1.9 is a demonstration of two overlapped
763 analytes on the ^{1}D separation. The error functions previously shown are different in this example,
764 as two smaller error functions are seen within the larger error function in Figure 1.9A. These two

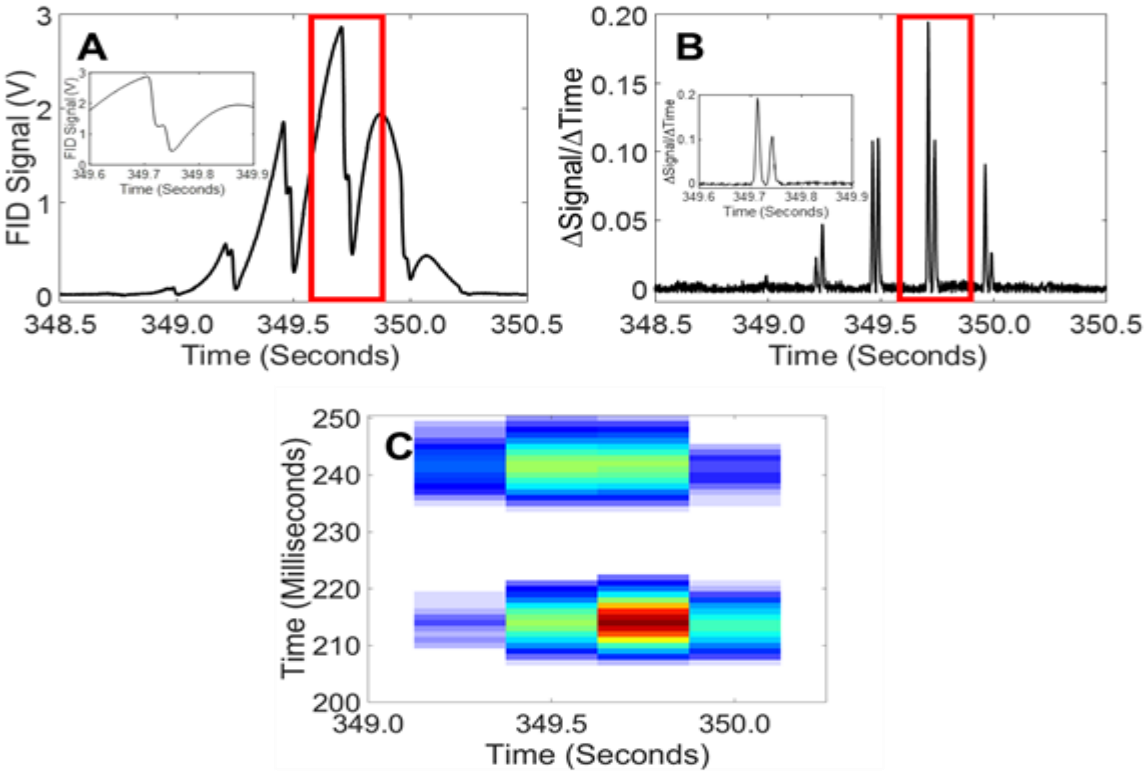

765

Figure 1.9. Close-up View of Overlapped Analytes from GC×GC-FID Data

An example of an overlapped peak on the ^{1}D dimension for a modulation period P_M of 250 ms. (A) Raw data on ^{1}D for two overlapped analytes. The inset shows an enhanced view, for one modulation. Two smaller error functions are shown within the larger error function. (B) After data processing, the two analytes are transformed into apparent peaks which are resolved on the ^{2}D dimension. (C) View of the fully processed data in a GC×GC separation. Reproduced from C.E. Freye, H.D. Bahaghighat, R.E. Synovec, *Talanta*. 177 (2018) 142-149.

766 smaller error functions represent two separate analytes as is seen in the processed data of Figure
767 1.9B and 1.9C. A 2D chromatogram example of the 115-component mixture with the P_M of 250
768 ms (Figure 1.8A) is demonstrated in Figure 1.10. During this work it was determined that ^{2}D peak
769 widths are based on error function slope, which is directly related to the retention of the analyte on
770 the ^{2}D dimension. Data compiled from three different modulation periods is shown in Figure 1.11,
771 demonstrating the relationship between peak widths on the second dimension and their respective
772 retention times. The ultra-fast modulation capabilities of the pulse

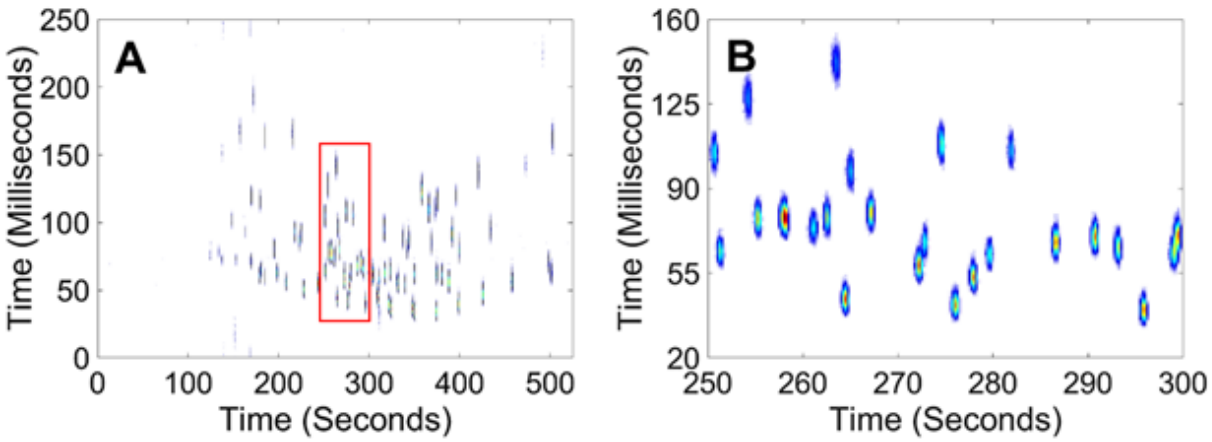

773

Figure 1.10. 2D GC×GC-FID Chromatogram of 115-Component Test Mixture

(A) GC×GC – FID chromatogram of the 115 component test mixture collected using a modulation period P_M of 250 ms. The ^{2}D separation has been reregistered by 680 ms to remove the dead time. (B) Enhanced view of a selected portion of the chromatogram is shown. Reproduced from C.E.

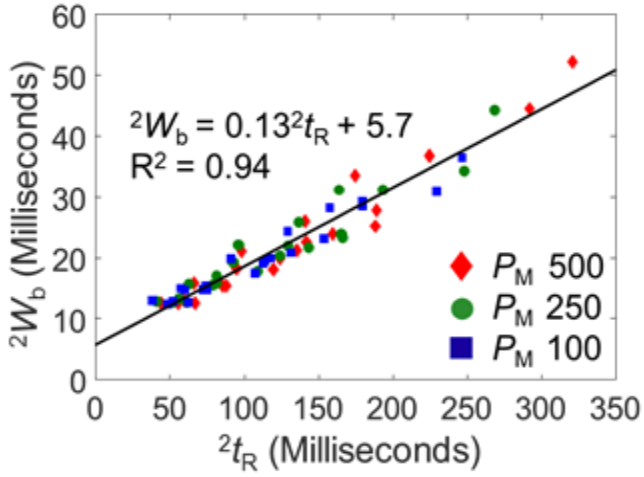

774

Figure 1.11. Plot of ^2W_b versus ^2t_R for three different modulation periods

Plot of apparent ^2W_b versus ^2t_R for a set of selected analytes for three different modulation periods P_M of 500, 250 and 100 ms. Reproduced from C.E. Freye, H.D. Bahaghighat, R.E. Synovec, *Talanta*. 177 (2018) 142-149.

775 valve flow modulator is displayed in Figure 1.12, in which a modulation period of 50 ms is
776 demonstrated. As a result of this rapid modulation the sampling density is extremely high at 17.4.
777 These results are impressive, but the sampling density gives away total peak capacity thus reducing

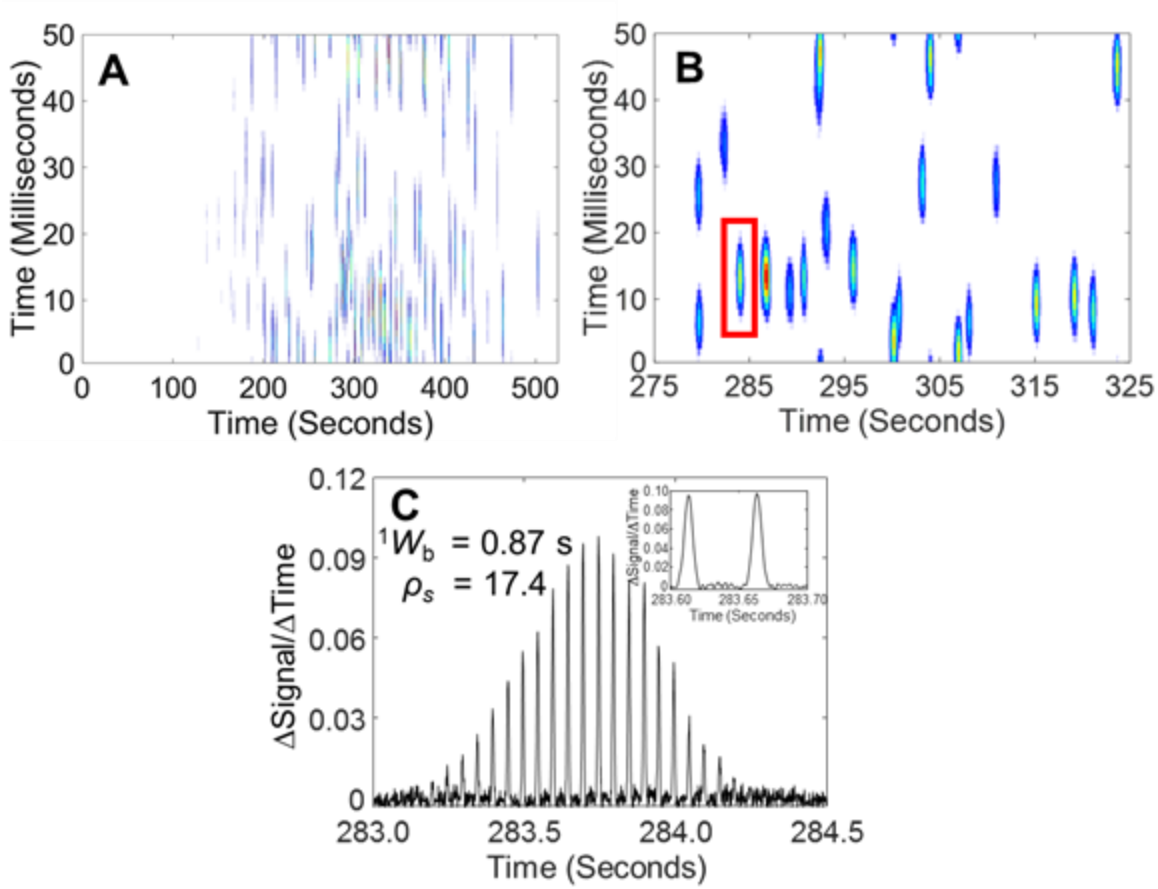

778

Figure 1.12. P_M 50 ms GC×GC-FID 2D Chromatogram

(A) GC×GC – FID chromatogram, using a modulation period P_M of 50 ms instead of 250 ms. (B) Enhanced view of a selected portion of the chromatogram is shown. (C) Raw 1D vector form of the GC × GC – FID data for a single peak, highlighted in (B). Due to the ultra-fast P_M, the peak is highly sampled. The insert shows the peaks for two modulations. Reproduced from C.E. Freye, H.D. Bahaghighat, R.E. Synovec, *Talanta*. 177 (2018) 142-149.

779 this result to purely a display of potential. To determine the quantification capability of overlapped
780 peaks, a controlled study of two overlapped analytes cyclohexane and benzene
781 selected that co-elute on the ^{1}D separation column but were separated on the ^{2}D dimension, as seen
782 in Figure 1.13. The body of the work contained in this dissertation focuses on future developments
783 that utilize pulse flow valve modulation for high speed MDGC separations including application
784 with a time of

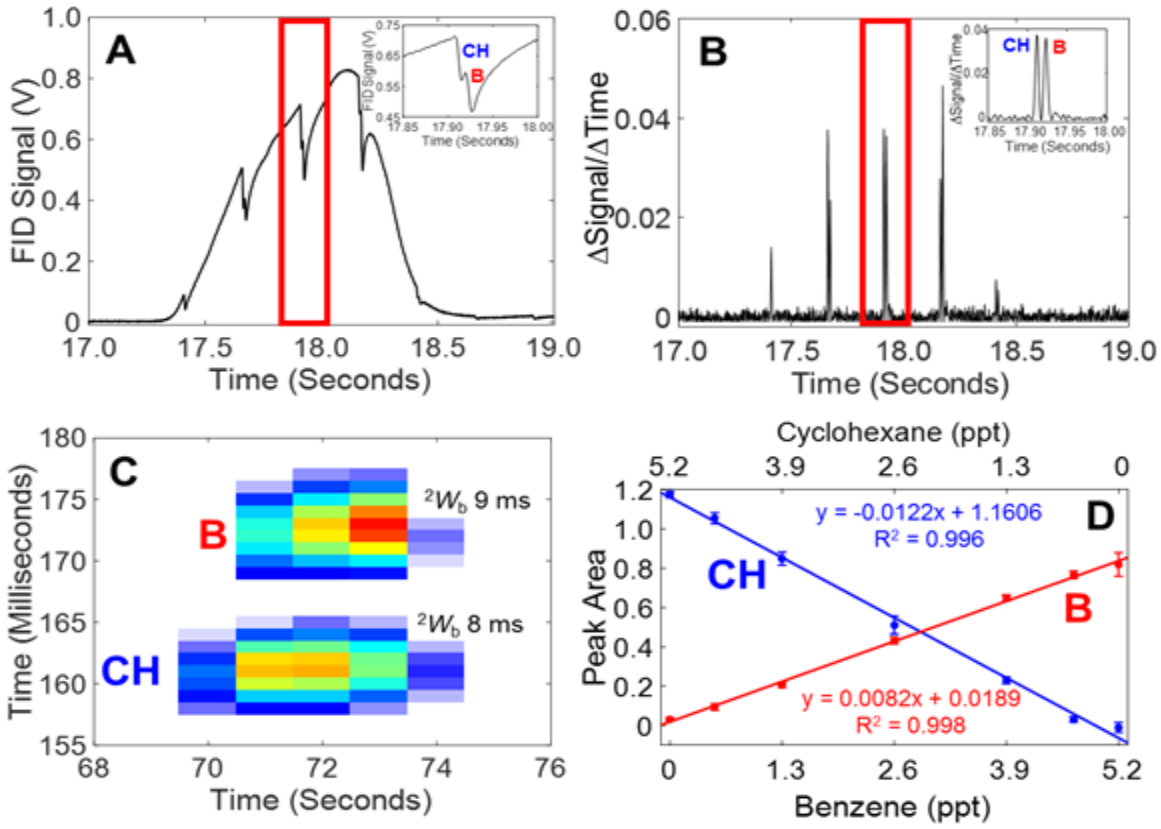

785

Figure 1.13. Quantitative Overlap Study using Pulse Flow Modulator.

Partial modulation using the pulse flow valve was investigated to determine if the data is suitable to perform quantitative analysis, using mixtures of cyclohexane and benzene. (A) Raw vector form of the data for cyclohexane and benzene, labeled CH and B, respectively. (B) Processed data is shown, whereby the ^{2}D peaks are observed to be baseline resolved on the ^{2}D separation. (C) The processed data is shown in the form of a GC×GC separation with the apparent ^2W_b provided. (D) The concentration in ppt (parts per thousand) of cyclohexane and benzene were varied in order to study the quantitative aspects of the technique. Reproduced from C.E. Freye, H.D. Bahaghighat, R.E. Synovec, *Talanta*. 177 (2018) 142-149.

786 flight mass spectrometer, ultrafast GC[3] and using multivariate curve resolution alternating least

787 squares (MCR-ALS) to quickly deconvolute and quantify resultant data.

1.6 DATA ANALYSIS AND CHEMOMETRICS

1.6.1 *Introduction to Chemometrics*

With a properly conducted gas chromatography separation method, the resulting data set could be on the order of several megabytes to gigabytes depending on the collection parameters and scope of the study. The ability to analyze the GC data and isolate pertinent chemical information is required if the separation is to be informative. By comparison, MDGC separations produce data several orders of magnitude larger than that of a 1D separation, especially when coupled with multichannel detectors such as a time-of-flight mass spectrometer (TOFMS). Compounding the demand for data extraction is realized when multiple samples or replicates are analyzed and in many cases compared to one another looking for minute differences in samples composed of 1000's of compounds. Adding to the challenge of working with large and complex data sets, misalignment between multiple runs, low resolution, poor *S/N*, complex and time-consuming computations can lead to issues with confident discovery of chromatographic differences between samples, and isolation of meaningful information. The field of chemometrics itself is the application of mathematically methods to glean meaningful data from in this case gas chromatography separations[27,113–118]. To go from raw data to a dataset that can be evaluated using various applicable chemometric techniques often have specific requirements such as bilinearity or trilinearity within the dataset. Not all methods were meant to be applied to a particular set of data, and thus it becomes incumbent on the researcher to understand the numerous chemometric techniques and apply them accordingly. The common classes of chemometrics include property prediction, pattern recognition, deconvolution, and retention time/index modeling [114,117,118]. For the research covered in this text, deconvolution proved to be most important, a brief overview of deconvolution chemometrics is provided.

1.6.2 *Deconvolution*

Overlapped analytes even in GC×GC separations, are ever-present and require the application of chromatographic peak deconvolution methods, that are often key to confident analyte identification, quantification, and peak purity assessment. By the application of deconvolution methods, such as parallel factor analysis (PARAFAC), and multivariate curve resolution-alternating least squares (MCR-ALS), peaks that are overlapped can be computationally separated in three dimensions; ^{1}D time, ^{2}D time, and spectral. Peak data that has successfully deconvoluted can be identified using the deconvoluted spectra and quantified based on the peak profiles (loadings) obtained, thus allowing for a method to calibrate quantity of a particular analyte present[119,120]. Application is either targeted or non-targeted, depending on whether the analytes are known or unknown prior to the separation.

MCR-ALS, is a tensor rank decomposition method that can be applied to GC×GC-TOFMS data for deconvolution, identification, and quantification. Based on alternating least-squares decomposition, MCR-ALS is best suited for bilinear data. It works well with data that experiences minor shifts in retention time on the ^{2}D dimension. MCR-ALS has been successfully applied to GC×GC-TOFMS separations of petroleum, metabolomics, and environmental samples, providing identification, calibration data[121,122].

1.7 CHALLENGES AND MOTIVATIONS

The goal of MDGC, is to provide the greatest amount of information within the shortest period of time. For this dissertation this requirement will be addressed in two different approaches, instrumentation via the pioneering development of MDGC using pulse flow valve modulation, and the use of chemometrics to glean the most accurate and relevant information from the data. The

first approach is to use a state-of-the-art pulse flow valve modulation system that renders in high peak capacity production and high chemical selectivity in conjunction with a selective detector such as a TOFMS. The second approach is to use chemometrics in order to extract useful and meaning chemical information from the rich datasets.

There are many attributes that one envisages to provide the perfect modulator for MDGC: robust, universal, ultra-fast, high duty cycle, reproducible, narrow injection pulse, mass spectrometry compatible, small footprint, etc. Great strides have been made since 1991 to address many of these characteristics, and yet the "perfect" solution has not been developed. Each modulator category aims to fulfill or meet certain goals. Thermal modulation remains the dominate form of modulation for numerous reasons: the original focus of development (most mature), high duty cycle (1.0), narrow injection pulse, fast modulation period ($P_M \geq 200$ ms) [96] although a $P_M \geq 1$ s is typical, high detection sensitivity, mass spectrometry compatibility, and wide applicability (C_4-C_{40}+), although not fully universal ($\leq C_3$). Thermal modulators commonly have two potential issues to be aware of in operation, breakthrough and incomplete desorption. Breakthrough, occurs when an analyte is not completely trapped and is able to pass through to the head of the ^{2}D column. Incomplete desorption results when the trapped analyte is not quickly and/or is only partially desorbed resulting in wider or tailing peaks on the ^{2}D column. Perhaps the most glaring shortcoming, that is also a primary motivator for improvements to thermal modulation, is elimination of expensive and cumbersome cryogens. Not only is cost a concern, but floor space to support the instrumentation and availability in many locations around the world may serve to hold back wider application of cryogen-based thermal modulation. The primary approach to address this issue is to eliminate the need for cryogens while maintaining all of the benefits associated with thermal modulation, i.e., the development of "cryogen-free" thermal modulators.

Flow-based and valve-based modulators have been a mainstay in the GC field for many years. First used over 50 years ago for GC-GC [20], it was not until the late 1990's that gas flow switching (microfluidics) [27] was developed for use as a GC×GC modulator. Since the late 1990's flow switching (flow and diaphragm valve-based) modulators have made great strides toward becoming a routine, accepted methods of GC×GC modulation. The ideal flow switching modulator design should have many of the same desired traits of a thermal modulator along with addressing a few specific concerns: (a) a high working temperature range, (b) the capability to operate at mass spectrometry compatible gas flows, (c) chemical inertness, (d) low thermal mass, (e) the ability to change flows without disturbing the flow on either separation dimension, and (f) a high duty cycle (>0.5). Flow switching modulators have an advantage in that they can modulate (C1-C40+) without concern of breakthrough or incomplete desorption like that of thermal modulators, and they also do not require cryogens. Flow switching however has its concerns, primarily the high flow rates on the ^{2}D column, and the typically low duty cycle (<0.5) which may limit applicability due to a resulting loss in detection sensitivity. Similar to thermal modulators, much effort has been devoted to development of flow and valve-based modulators that addresses these fundamental issues while preserving all of the benefits.

Within this context, the research reported herein demonstrates my efforts to improve the science of modulation via the use of the pulse flow valve modulator first introduced by C.E. Freye and myself [34]. Chapter 2, uses information building directly from past work [34,83,123] and information learned to substantially improve peak capacity production for a three-dimensional (3D) gas chromatography (GC^3) instrumental platform by application of a P_M of 50 ms with the pulse valve flow modulator to peaks generated from a diaphragm valve modulator. With sufficiently narrow peak generation from the diaphragm valve modulator, the pulse flow valve

modulator is demonstrated herein to be properly used at its fastest modulation period while maintaining a sampling density of 2-4. This research will not only demonstrate the value of the pulse flow valve modulator, but also advance the field of three-dimensional separations. Chapter 3, demonstrates the modulators ability to function with a detector at vacuum (GC×GC-TOFMS) with MCR-ALS chemometrics applied to deconvolute the data. This work is critical to address two concerns, the ability to use the data without the need apply the three step method of converting the data, and to understand if this method of modulation can it be applied to a system at vacuum without excess flow rates that can overwhelm the detectors vacuum system. Finally, Chapter 4, takes the concept of frontal analysis and applies it to continuous monitoring of headspace to demonstrate the potential of the pulse flow valve to be used in a continuous sampling system.

1.8 HYPOTHESES

The following chapters describe the investigative research performed over the past three years, which focus on new modulators for two-dimensional and three-dimensional gas chromatography and MCR-ALS chemometric method for deconvolution and analysis of complex datasets. A brief summary of each chapter is provided below.

1.8.1 *Chapter 2: Investigation of Ultrafast Separations via a Pulse Flow Valve for MDGC (GC×GC, GC^3)*

Ultrafast modulation with a modulation period $P_M \geq 50$ ms via a pulse flow valve is demonstrated for comprehensive two-dimensional gas chromatography (GC×GC) and comprehensive three-dimensional (3D) gas chromatography (GC^3). Significant increases in peak capacity and peak capacity production are achieved relative to previous studies using pulse flow valve modulation.

Due to the nature of the "partial" modulation process, the separation dimension following pulse flow valve modulation is not a traditional chromatogram, rather requires data processing to convert the data to expose the encoded chromatographic information, producing "apparent" chromatographic peaks. In the GC×GC mode, a 115-component test mixture was evaluated using a P_M of 500 ms, creating an apparent ^{2}D peak width-at-base ^2W with an average of 25 ms, producing a ^2n_c of 20. Based on the average ^1W of 1.0 s for the 6 min first dimension ^{1}D separation, an ideal peak capacity $n_{c,2D}$ of 7,200 is achieved (1,200/min peak production). For a high-speed GC×GC separation (30 s run), a P_M of 75 ms produced apparent ^2W of 8 ms, ideal for the third dimension of a GC^3 instrument. Using the knowledge gained from this high-speed GC×GC experiment, the pulse flow valve was implemented as the second modulator in GC^3. Three samples were evaluated in the GC^3 mode: a simple mixture containing 18 compounds (to illustrate basic concepts), the 115-component test mixture (to determine peak capacity figures-of-merit), and a diesel spiked with 8 polar compounds (to illustrate chemical selectivity benefits of GC^3). For the 115-component test mixture with a ^1P_M of 1.2 s and a ^2P_M of 60 ms, average ^1W of 3.2 s, ^2W of 130 ms, and apparent ^3W 13 ms were produced, resulting in a ^1n_c of 220, ^2n_c of 9.5, and ^3n_c of 5, respectively. Hence, an ideal peak capacity, $n_{c,3D}$ of 12,000 was achieved for the 12 min separation of the 115-component test mixture (1,000 peaks/min).

1.8.2 *Chapter 3: A Study of Ultra-Fast Modulation for Comprehensive (GC×GC) gas chromatography with Multivariate Curve Resolution-Alternating Least Squares*

A new form of ultrafast flow modulation ($P_M \geq 50$ ms) for GC×GC-TOFMS is demonstrated, producing narrow peak widths, ^2W_b, combined with shortest known modulation periods, P_M, yielding the potential for ultrafast separation with high two-dimensional GC×GC peak capacity. The modulator is a pulse flow valve that injects a narrow (2 ms) pulses of carrier gas at a user

defined P_M, at the union between the primary, ^{1}D, column and the secondary ^{2}D column. This pulse is detected in the data as a sudden decrease in signal intensity combining the properties of vacancy chromatography and frontal analysis, which then rapidly returns to the primary signal concentration. The resultant distinctive data was deconvoluted using unconstrained MCR-ALS to identify and quantify analytes. In a straightforward three-step process, the MCR-ALS loadings were converted via differentiation into traditional GC×GC data through a process commonly used during frontal analysis. An 18-component test mixture at seven different concentrations is demonstrated using a modulation period of P_M = 50 ms. The resultant ^{2}D peaks generated using a P_M of 50, are symmetrical with and average ^2W_b of 16 ms and an average RSD of 3.75 %. At an injected concentration of 14 ng per analyte, an average match value of 822 was achieved using in-house spectra for comparison, with an average RSD of 7.12 %. Quantification of analytes was achieved by use of the MCR-ALS loading areas of the analytes, with R^2 values of 0.999 achieved for three of the overlapped analytes demonstrated. The advancement in modulation demonstrated represents a four-fold decrease in modulation period of the fastest documented modulator, while maintaining the benefits of a duty cycle of 1.0, with no need for large cumbersome equipment, and no limits to the modulation range (C1-C40+) of analytes associated with thermal modulators while being compatible with the vacuum requirements of the TOF detector.

1.8.3 *Chapter 4: Continuous Monitoring with One-Dimensional Gas Chromatography (1D-GC) via Injection by Pulse Flow Valve.*

The following document is a brief review of limited research into using the pulse valve flow modulator as the instrumental platform to conduct continuous monitoring via one dimensional gas chromatography (1D-GC) of a chemical system. This idea was born from observing the behavior and performance of the pulse flow valve over the course of nearly a year of research.

This work discussed in this chapter required development of a simple test vessel that that affords the ability to slowly release volatile analytes in a continuous manner. A brief introduction will be presented discussing the concept, along with a detailed instrument setup and experimental conditions. The discussion will be limited to lessons learned and the qualitative data that resulted from various experimental conditions applied. The experimental setup did not allow for a quantitative evaluation of the system. It is of note that this design utilizes only one separation column (1D-GC) unlike previous 2D-GC and GC3 research discussed within this text.

1.9 REFERENCES

[1] S.-T. Chin, G.T. Eyres, P.J. Marriott, Application of integrated comprehensive/multidimensional gas chromatography with mass spectrometry and olfactometry for aroma analysis in wine and coffee, Food Chem. 185 (2015) 355–361. doi:10.1016/j.foodchem.2015.04.003.

[2] R.B. Mastello, M. Capobiango, S.-T. Chin, M. Monteiro, P.J. Marriott, Identification of odour-active compounds of pasteurised orange juice using multidimensional gas chromatography techniques, Food Res. Int. 75 (2015) 281–288. doi:10.1016/j.foodres.2015.06.014.

[3] F. Magagna, A. Guglielmetti, E. Liberto, S.E. Reichenbach, E. Allegrucci, G. Gobino, C. Bicchi, C. Cordero, Comprehensive Chemical Fingerprinting of High-Quality Cocoa at Early Stages of Processing: Effectiveness of Combined Untargeted and Targeted Approaches for Classification and Discrimination, J. Agric. Food Chem. 65 (2017) 6329–6341. doi:10.1021/acs.jafc.7b02167.

[4] S. Samanipour, P. Dimitriou-Christidis, D. Nabi, J.S. Arey, Elevated Concentrations of 4-Bromobiphenyl and 1,3,5-Tribromobenzene Found in Deep Water of Lake Geneva Based on GC×GC-ENCI-TOFMS and GC×GC-μECD.pdf, ACS Omega. 2 (2017) 641–652.

[5] S.A. Mackintosh, N.G. Dodder, N.J. Shaul, L.I. Aluwihare, K.A. Maruya, S.J. Chivers, K. Danil, D.W. Weller, E. Hoh, Newly Identified DDT-Related Compounds Accumulating in Southern California Bottlenose Dolphins, Environ. Sci. Technol. 50 (2016) 12129–12137. doi:10.1021/acs.est.6b03150.

[6] P.S. Prata, G.L. Alexandrino, N.G.S. Mogollón, F. Augusto, Discriminating Brazilian crude oils using comprehensive two-dimensional gas chromatography–mass spectrometry and multiway principal component analysis, J. Chromatogr. A. 1472 (2016) 99–106. doi:10.1016/j.chroma.2016.10.044.

[7] N.G.S. Mogollón, F.A. de L. Ribeiro, R.J. Poppi, A. Quintana, J. Chávez, D. Agualongo, H. Aleme, F. Augusto, Exploratory Analysis of Biodiesel by Combining Comprehensive Two-Dimensional Gas Chromatography and Multiway Principal Component Analysis, J. Braz. Chem. Soc. (2016). doi:10.21577/0103-5053.20160222.

[8] K.D. Nizio, M. Ueland, B.H. Stuart, S.L. Forbes, The analysis of textiles associated with decomposing remains as a natural training aid for cadaver-detection dogs, Forensic Chem. 5 (2017) 33–45. doi:10.1016/j.forc.2017.06.002.

[9] T. Schwemer, T. Rössler, B. Ahrens, M. Schäffer, A. Hasselbach-Minor, M. Pütz, M. Sklorz, T. Gröger, R. Zimmermann, Characterization of a heroin manufacturing process based on acidic extracts by combining complementary information from two-dimensional gas chromatography and high resolution mass spectrometry, Forensic Chem. 4 (2017) 9–18. doi:10.1016/j.forc.2017.02.006.

[10] M.K. Das, S.C. Bishwal, A. Das, D. Dabral, A. Varshney, V.K. Badireddy, R. Nanda, Investigation of Gender-Specific Exhaled Breath Volatome in Humans by GCxGC-TOF-MS, Anal. Chem. 86 (2014) 1229–1237. doi:10.1021/ac403541a.

[11] C. Hurtado, H. Parastar, V. Matamoros, B. Piña, R. Tauler, J.M. Bayona, Linking the morphological and metabolomic response of Lactuca sativa L exposed to emerging contaminants using GC × GC-MS and chemometric tools, Sci. Rep. 7 (2017). doi:10.1038/s41598-017-06773-0.

[12] J.C. Giddings, Two-dimensional separations: concept and promise, Anal. Chem. 56 (1984) 1258A-1270A. doi:10.1021/ac00276a003.

[13] Z. Liu, J. B. Phillips, Comprehensive Two-Dimensional Gas Chromatography using an On-Column Thermal Modulator Interface, J. Chromatogr. Sci. 29 (1991) 227–231. doi:10.1093/chromsci/29.6.227.

[14] J.V. Seeley, S.K. Seeley, Multidimensional Gas Chromatography: Fundamental Advances and New Applications, Anal. Chem. 85 (2013) 557–578. doi:10.1021/ac303195u.

[15] P.J. Marriott, S.-T. Chin, B. Maikhunthod, H.-G. Schmarr, S. Bieri, Multidimensional gas chromatography, TrAC Trends Anal. Chem. 34 (2012) 1–21. doi:10.1016/j.trac.2011.10.013.

[16] P.Q. Tranchida, Comprehensive two-dimensional gas chromatography: A perspective on processes of modulation, J. Chromatogr. A. (2017). doi:10.1016/j.chroma.2017.04.039.
[17] P.Q. Tranchida, G. Purcaro, P. Dugo, L. Mondello, Modulators for comprehensive two-dimensional gas chromatography, TrAC Trends Anal. Chem. 30 (2011) 1437–1461. doi:10.1016/j.trac.2011.06.010.
[18] M. Edwards, A. Mostafa, T. Górecki, Modulation in comprehensive two-dimensional gas chromatography: 20 years of innovation, Anal. Bioanal. Chem. 401 (2011) 2335–2349. doi:10.1007/s00216-011-5100-6.
[19] J.V. Seeley, Recent advances in flow-controlled multidimensional gas chromatography, J. Chromatogr. A. 1255 (2012) 24–37. doi:10.1016/j.chroma.2012.01.027.
[20] D.R. Deans, A new technique for heart cutting in gas chromatography [1], Chromatographia. 1 (1968) 18–22. doi:10.1007/BF02259005.
[21] R.E. Murphy, M.R. Schure, J.P. Foley, Effect of Sampling Rate on Resolution in Comprehensive Two-Dimensional Liquid Chromatography, Anal. Chem. 70 (1998) 1585–1594. doi:10.1021/ac971184b.
[22] H.-J. de Geus, J. de Boer, U.A.T. Brinkman, Development of a thermal desorption modulator for gas chromatography, J. Chromatogr. A. 767 (1997) 137–151. doi:10.1016/S0021-9673(97)00038-1.
[23] B.V. Burger, T. Snyman, W.J.G. Burger, W.F. van Rooyen, Thermal modulator array for analyte modulation and comprehensive two-dimensional gas chromatography, J. Sep. Sci. 26 (2003) 123–128. doi:10.1002/jssc.200390002.
[24] P.J. Marriott, R.M. Kinghorn, Longitudinally Modulated Cryogenic System. A Generally Applicable Approach to Solute Trapping and Mobilization in Gas Chromatography, Anal. Chem. 69 (1997) 2582–2588. doi:10.1021/ac961310w.
[25] E.B. Ledford, C. Billesbach, Jet-Cooled Thermal Modulator for Comprehensive Multidimensional Gas Chromatography, J. High Resolut. Chromatogr. 23 (2000) 202–204. doi:10.1002/(SICI)1521-4168(20000301)23:3<202::AID-JHRC202>3.0.CO;2-5.
[26] J. Harynuk, T. Górecki, New liquid nitrogen cryogenic modulator for comprehensive two-dimensional gas chromatography, J. Chromatogr. A. 1019 (2003) 53–63. doi:10.1016/j.chroma.2003.08.097.
[27] C.A. Bruckner, B.J. Prazen, R.E. Synovec, Comprehensive Two-Dimensional High-Speed Gas Chromatography with Chemometric Analysis, Anal. Chem. 70 (1998) 2796–2804. doi:10.1021/ac980164m.
[28] J.V. Seeley, F. Kramp, C.J. Hicks, Comprehensive Two-Dimensional Gas Chromatography via Differential Flow Modulation, Anal. Chem. 72 (2000) 4346–4352. doi:10.1021/ac000249z.
[29] C.E. Freye, L. Mu, R.E. Synovec, High temperature diaphragm valve-based comprehensive two-dimensional gas chromatography, J. Chromatogr. A. 1424 (2015) 127–133. doi:10.1016/j.chroma.2015.10.098.
[30] A.E. Sinha, B.J. Prazen, C.G. Fraga, R.E. Synovec, Valve-based comprehensive two-dimensional gas chromatography with time-of-flight mass spectrometric detection: instrumentation and figures-of-merit, J. Chromatogr. A. 1019 (2003) 79–87. doi:10.1016/j.chroma.2003.08.047.
[31] J.V. Seeley, N.J. Micyus, S.V. Bandurski, S.K. Seeley, J.D. McCurry, Microfluidic Deans Switch for Comprehensive Two-Dimensional Gas Chromatography, Anal. Chem. 79 (2007) 1840–1847. doi:10.1021/ac061881g.
[32] C. Duhamel, P. Cardinael, V. Peulon-Agasse, R. Firor, L. Pascaud, G. Semard-Jousset, P. Giusti, V. Livadaris, Comparison of cryogenic and differential flow (forward and reverse fill/flush) modulators and applications to the analysis of heavy petroleum cuts by high-temperature comprehensive gas chromatography, J. Chromatogr. A. 1387 (2015) 95–103. doi:10.1016/j.chroma.2015.01.095.

[33] J.V. Seeley, N.E. Schimmel, S.K. Seeley, The multi-mode modulator: A versatile fluidic device for two-dimensional gas chromatography, J. Chromatogr. A. (2017). doi:10.1016/j.chroma.2017.06.030.
[34] C.E. Freye, H.D. Bahaghighat, R.E. Synovec, Comprehensive two-dimensional gas chromatography using partial modulation via a pulsed flow valve with a short modulation period, Talanta. 177 (2018) 142–149. doi:10.1016/j.talanta.2017.08.095.
[35] B. Xu, L. Zhang, F. Ma, W. Zhang, X. Wang, Q. Zhang, D. Luo, H. Ma, P. Li, Determination of free steroidal compounds in vegetable oils by comprehensive two-dimensional gas chromatography coupled to time-of-flight mass spectrometry, Food Chem. 245 (2018) 415–425. doi:10.1016/j.foodchem.2017.10.114.
[36] N.G.S. Mogollón, P.S. Prata, J.Z. dos Reis, E.V. dos S. Neto, F. Augusto, Characterization of crude oil biomarkers using comprehensive two-dimensional gas chromatography coupled to tandem mass spectrometry, J. Sep. Sci. 39 (2016) 3384–3391. doi:10.1002/jssc.201600418.
[37] M.A. Moreira, L.C. André, A.B. Ribeiro, M.D.R.G. da Silva, Z.L. Cardeal, Quantitative Analysis of Endocrine Disruptors by Comprehensive Two-Dimensional Gas Chromatography, J. Braz. Chem. Soc. 26 (2015) 531–536. doi:10.5935/0103-5053.20150006.
[38] J. Krupčík, R. Gorovenko, I. Špánik, P. Sandra, D.W. Armstrong, Enantioselective comprehensive two-dimensional gas chromatography. A route to elucidate the authenticity and origin of Rosa damascena Miller essential oils, J. Sep. Sci. 38 (2015) 3397–3403. doi:10.1002/jssc.201500744.
[39] Y.V. Patrushev, V.N. Sidelnikov, The use of high-speed multicapillary column in comprehensive two-dimensional gas chromatography with flow modulation, J. Chromatogr. A. 1426 (2015) 183–190. doi:10.1016/j.chroma.2015.11.064.
[40] P.-H. Stefanuto, K. Perrault, J.-F. Focant, S. Forbes, Fast Chromatographic Method for Explosive Profiling, Chromatography. 2 (2015) 213–224. doi:10.3390/chromatography2020213.
[41] L.M. Blumberg, Accumulating resampling (modulation) in comprehensive two-dimensional capillary GC (GC×GC), J. Sep. Sci. 31 (2008) 3358–3365. doi:10.1002/jssc.200800424.
[42] W. Khummueng, J. Harynuk, P.J. Marriott, Modulation Ratio in Comprehensive Two-dimensional Gas Chromatography, Anal. Chem. 78 (2006) 4578–4587. doi:10.1021/ac052270b.
[43] A.A.S. Sampat, M. Lopatka, G. Vivó-Truyols, P.J. Schoenmakers, A.C. van Asten, Towards chemical profiling of ignitable liquids with comprehensive two-dimensional gas chromatography: Exploring forensic application to neat white spirits, Forensic Sci. Int. 267 (2016) 183–195. doi:10.1016/j.forsciint.2016.08.006.
[44] J.M. Davis, D.R. Stoll, P.W. Carr, Effect of First-Dimension Undersampling on Effective Peak Capacity in Comprehensive Two-Dimensional Separations, Anal. Chem. 80 (2008) 461–473. doi:10.1021/ac071504j.
[45] R.E. Mohler, K.M. Dombek, J.C. Hoggard, E.T. Young, R.E. Synovec, Comprehensive Two-Dimensional Gas Chromatography Time-of-Flight Mass Spectrometry Analysis of Metabolites in Fermenting and Respiring Yeast Cells, Anal. Chem. 78 (2006) 2700–2709. doi:10.1021/ac052106o.
[46] H.D. Bean, J.-M.D. Dimandja, J.E. Hill, Bacterial volatile discovery using solid phase microextraction and comprehensive two-dimensional gas chromatography–time-of-flight mass spectrometry, J. Chromatogr. B. 901 (2012) 41–46. doi:10.1016/j.jchromb.2012.05.038.
[47] J.M. Davis, J.C. Giddings, Statistical theory of component overlap in multicomponent chromatograms, Anal. Chem. 55 (1983) 418–424. doi:10.1021/ac00254a003.
[48] J.M. Davis, J.C. Giddings, Statistical method for estimation of number of components from single complex chromatograms: theory, computer-based testing, and analysis of errors, Anal. Chem. 57 (1985) 2168–2177. doi:10.1021/ac00289a002.

[49] B.D. Fitz, R.B. Wilson, B.A. Parsons, J.C. Hoggard, R.E. Synovec, Fast, high peak capacity separations in comprehensive two-dimensional gas chromatography with time-of-flight mass spectrometry, J. Chromatogr. A. 1266 (2012) 116–123. doi:10.1016/j.chroma.2012.09.096.
[50] D.K. Pinkerton, B.A. Parsons, R.E. Synovec, Method to determine the true modulation ratio for comprehensive two-dimensional gas chromatography, J. Chromatogr. A. 1476 (2016) 114–123. doi:10.1016/j.chroma.2016.11.015.
[51] D.K. Pinkerton, B.A. Parsons, T.J. Anderson, R.E. Synovec, Trilinearity deviation ratio: A new metric for chemometric analysis of comprehensive two-dimensional gas chromatography time-of-flight mass spectrometry data, Anal. Chim. Acta. 871 (2015) 66–76. doi:10.1016/j.aca.2015.02.040.
[52] J.L. Adcock, M. Adams, B.S. Mitrevski, P.J. Marriott, Peak Modeling Approach to Accurate Assignment of First-Dimension Retention Times in Comprehensive Two-Dimensional Chromatography, Anal. Chem. 81 (2009) 6797–6804. doi:10.1021/ac900960n.
[53] M.S. Klee, J. Cochran, M. Merrick, L.M. Blumberg, Evaluation of conditions of comprehensive two-dimensional gas chromatography that yield a near-theoretical maximum in peak capacity gain, J. Chromatogr. A. 1383 (2015) 151–159. doi:10.1016/j.chroma.2015.01.031.
[54] L.M. Blumberg, Flow optimization in one-dimensional and comprehensive two-dimensional gas chromatography, J. Chromatogr. A. 1536 (2018) 27–38. doi:10.1016/j.chroma.2017.08.040.
[55] A. Giri, M. Coutriade, A. Racaud, K. Okuda, J. Dane, R.B. Cody, J.-F. Focant, Molecular Characterization of Volatiles and Petrochemical Base Oils by Photo-Ionization GC×GC-TOF-MS, Anal. Chem. 89 (2017) 5395–5403. doi:10.1021/acs.analchem.7b00124.
[56] M.S. Alam, C. Stark, R.M. Harrison, Using Variable Ionization Energy Time-of-Flight Mass Spectrometry with Comprehensive GC×GC To Identify Isomeric Species, Anal. Chem. 88 (2016) 4211–4220. doi:10.1021/acs.analchem.5b03122.
[57] W.J. Robson, P.A. Sutton, P. McCormack, N.P. Chilcott, S.J. Rowland, Class Type Separation of the Polar and Apolar Components of Petroleum, Anal. Chem. 89 (2017) 2919–2927. doi:10.1021/acs.analchem.6b04202.
[58] M.J. Wilde, S.J. Rowland, Structural Identification of Petroleum Acids by Conversion to Hydrocarbons and Multidimensional Gas Chromatography-Mass Spectrometry, Anal. Chem. 87 (2015) 8457–8465. doi:10.1021/acs.analchem.5b01865.
[59] J. Luong, X. Guan, S. Xu, R. Gras, R.A. Shellie, Thermal Independent Modulator for Comprehensive Two-Dimensional Gas Chromatography, Anal. Chem. 88 (2016) 8428–8432. doi:10.1021/acs.analchem.6b02525.
[60] A.M. Muscalu, M. Edwards, T. Górecki, E.J. Reiner, Evaluation of a single-stage consumable-free modulator for comprehensive two-dimensional gas chromatography: Analysis of polychlorinated biphenyls, organochlorine pesticides and chlorobenzenes, J. Chromatogr. A. 1391 (2015) 93–101. doi:10.1016/j.chroma.2015.02.074.
[61] M. Edwards, T. Górecki, Inlet backflushing device for the improvement of comprehensive two dimensional gas chromatographic separations, J. Chromatogr. A. 1402 (2015) 110–123. doi:10.1016/j.chroma.2015.05.014.
[62] G. Ntlhokwe, A.G.J. Tredoux, T. Górecki, M. Edwards, J. Vestner, M. Muller, L. Erasmus, E. Joubert, J.C. Cronje, A. de Villiers, Analysis of honeybush tea (Cyclopiaspp.) volatiles by comprehensive two-dimensional gas chromatography using a single-stage thermal modulator | SpringerLink, Anal. Bioanal. Chem. 409 (n.d.) 4127–4138.
[63] V. Mucédola, L.C.S. Vieira, D. Pierone, A.L. Gobbi, R.J. Poppi, L.W. Hantao, Thermal desorption modulation for comprehensive two-dimensional gas chromatography using a simple and inexpensive segmented-loop fluidic interface, Talanta. 164 (2017) 470–476. doi:10.1016/j.talanta.2016.12.005.

[64] S.-J. Kim, S.M. Reidy, B.P. Block, K.D. Wise, E.T. Zellers, K. Kurabayashi, Microfabricated thermal modulator for comprehensive two-dimensional micro gas chromatography: design, thermal modeling, and preliminary testing, Lab. Chip. 10 (2010) 1647–1654. doi:10.1039/C001390K.
[65] W.R. Collin, N. Nuñovero, D. Paul, K. Kurabayashi, E.T. Zellers, Comprehensive two-dimensional gas chromatographic separations with a temperature programmed microfabricated thermal modulator, J. Chromatogr. A. 1444 (2016) 114–122. doi:10.1016/j.chroma.2016.03.072.
[66] S.-J. Kim, K. Kurabayashi, Uniform-temperature, microscale thermal modulator with area-adjusted air-gap isolation for comprehensive two-dimensional gas chromatography, Sens. Actuators B Chem. 181 (2013) 518–522. doi:10.1016/j.snb.2013.01.077.
[67] A. Mostafa, T. Górecki, Development and Design of a Single-Stage Cryogenic Modulator for Comprehensive Two-Dimensional Gas Chromatography, Anal. Chem. 88 (2016) 5414–5423. doi:10.1021/acs.analchem.6b00767.
[68] P.Q. Tranchida, M. Zoccali, F.A. Franchina, P. Dugo, L. Mondello, Measurement of fundamental chromatography parameters in conventional and split-flow comprehensive two-dimensional gas chromatography-mass spectrometry: A focus on the importance of second-dimension injection efficiency, J. Sep. Sci. 36 (2013) 212–218. doi:10.1002/jssc.201200592.
[69] P.Q. Tranchida, F.A. Franchina, P. Dugo, L. Mondello, Use of greatly-reduced gas flows in flow-modulated comprehensive two-dimensional gas chromatography-mass spectrometry, J. Chromatogr. A. 1359 (2014) 271–276. doi:10.1016/j.chroma.2014.07.054.
[70] G. Purcaro, C. Cordero, E. Liberto, C. Bicchi, L.S. Conte, Toward a definition of blueprint of virgin olive oil by comprehensive two-dimensional gas chromatography, J. Chromatogr. A. 1334 (2014) 101–111. doi:10.1016/j.chroma.2014.01.067.
[71] G. Purcaro, L. Barp, M. Beccaria, L.S. Conte, Characterisation of minor components in vegetable oil by comprehensive gas chromatography with dual detection, Food Chem. 212 (2016) 730–738. doi:10.1016/j.foodchem.2016.06.048.
[72] B. Savareear, M.R. Jacobs, R.A. Shellie, Multiplexed dual first-dimension comprehensive two-dimensional gas chromatography–mass spectrometry with contra-directional thermal modulation, J. Chromatogr. A. 1365 (2014) 183–190. doi:10.1016/j.chroma.2014.09.014.
[73] G.L. Alexandrino, G.R. de Sousa, F. de A.M. Reis, F. Augusto, Optimizing loop-type cryogenic modulation in comprehensive two-dimensional gas chromatography using time-variable combination of the dual-stage jets for analysis of crude oil, J. Chromatogr. A. (2017). doi:10.1016/j.chroma.2017.10.054.
[74] D. Yan, L. Tedone, A. Koutoulis, S.P. Whittock, R.A. Shellie, Parallel comprehensive two-dimensional gas chromatography, J. Chromatogr. A. 1524 (2017) 202–209. doi:10.1016/j.chroma.2017.09.063.
[75] B.A. Parsons, D.K. Pinkerton, R.E. Synovec, Implications of phase ratio for maximizing peak capacity in comprehensive two-dimensional gas chromatography time-of-flight mass spectrometry, J. Chromatogr. A. 1536 (2018) 16–26. doi:10.1016/j.chroma.2017.07.018.
[76] G. Serrano, D. Paul, S.-J. Kim, K. Kurabayashi, E.T. Zellers, Comprehensive Two-Dimensional Gas Chromatographic Separations with a Microfabricated Thermal Modulator, Anal. Chem. 84 (2012) 6973–6980. doi:10.1021/ac300924b.
[77] P.Q. Tranchida, M. Zoccali, F.A. Franchina, A. Cotroneo, P. Dugo, L. Mondello, Gas velocity at the point of re-injection: An additional parameter in comprehensive two-dimensional gas chromatography optimization, J. Chromatogr. A. 1314 (2013) 216–223. doi:10.1016/j.chroma.2013.09.025.
[78] W.R. Collin, A. Bondy, D. Paul, K. Kurabayashi, E.T. Zellers, μGC × μGC: Comprehensive Two-Dimensional Gas Chromatographic Separations with Microfabricated Components, Anal. Chem. 87 (2015) 1630–1637. doi:10.1021/ac5032226.

[79] M.R. Jacobs, M. Edwards, T. Górecki, P.N. Nesterenko, R.A. Shellie, Evaluation of a miniaturised single-stage thermal modulator for comprehensive two-dimensional gas chromatography of petroleum contaminated soils, J. Chromatogr. A. 1463 (2016) 162–168. doi:10.1016/j.chroma.2016.08.009.
[80] W.R. Collin, N. Nuñovero, D. Paul, K. Kurabayashi, E.T. Zellers, Comprehensive two-dimensional gas chromatographic separations with a temperature programmed microfabricated thermal modulator, J. Chromatogr. A. 1444 (2016) 114–122. doi:10.1016/j.chroma.2016.03.072.
[81] D. Paul, K. Kurabayashi, First-principle modeling and characterization of thermal modulation in comprehensive two-dimensional gas chromatography using a microfabricated device, Sens. Actuators B Chem. 231 (2016) 135–146. doi:10.1016/j.snb.2016.02.132.
[82] C.E. Freye, R.E. Synovec, High temperature diaphragm valve-based comprehensive two-dimensional gas chromatography with time-of-flight mass spectrometry, Talanta. 161 (2016) 675–680. doi:10.1016/j.talanta.2016.09.002.
[83] N.E. Watson, H.D. Bahaghighat, K. Cui, R.E. Synovec, Comprehensive Three-Dimensional Gas Chromatography with Time-of-Flight Mass Spectrometry, Anal. Chem. 89 (2017) 1793–1800. doi:10.1021/acs.analchem.6b04112.
[84] J.V. Seeley, Micyus, Nicole J., McCurry, James D., S.K. Seeley, Comprehensive Two-Dimensional Gas Chromatography With a Simple Fluidic Modulator, Am. Lab. 38 (2006) 24–26.
[85] K.M. Sharif, S.-T. Chin, C. Kulsing, P.J. Marriott, The microfluidic Deans switch: 50 years of progress, innovation and application, TrAC Trends Anal. Chem. 82 (2016) 35–54. doi:10.1016/j.trac.2016.05.005.
[86] J. Krupčík, R. Gorovenko, I. Špánik, P. Sandra, D.W. Armstrong, Flow-modulated comprehensive two-dimensional gas chromatography with simultaneous flame ionization and quadrupole mass spectrometric detection, J. Chromatogr. A. 1280 (2013) 104–111. doi:10.1016/j.chroma.2013.01.015.
[87] J. Krupčík, P. Májek, R. Gorovenko, I. Špánik, P. Sandra, D.W. Armstrong, On the determination of a detector response enhancement factor for flow modulated comprehensive two-dimensional gas chromatography, J. Chromatogr. A. 1286 (2013) 235–240. doi:10.1016/j.chroma.2013.02.068.
[88] L.M. Dubois, K.A. Perrault, P.-H. Stefanuto, S. Koschinski, M. Edwards, L. McGregor, J.-F. Focant, Thermal desorption comprehensive two-dimensional gas chromatography coupled to variable-energy electron ionization time-of-flight mass spectrometry for monitoring subtle changes in volatile organic compound profiles of human blood, J. Chromatogr. A. 1501 (2017) 117–127. doi:10.1016/j.chroma.2017.04.026.
[89] C.E. Freye, N.R. Moore, R.E. Synovec, Enhancing the chemical selectivity in discovery-based analysis with tandem ionization time-of-flight mass spectrometry detection for comprehensive two-dimensional gas chromatography, J. Chromatogr. A. 1537 (2018) 99–108. doi:10.1016/j.chroma.2018.01.008.
[90] A. Ghosh, C.T. Bates, S.K. Seeley, J.V. Seeley, High speed Deans switch for low duty cycle comprehensive two-dimensional gas chromatography, J. Chromatogr. A. 1291 (2013) 146–154. doi:10.1016/j.chroma.2013.04.003.
[91] J.V. Seeley, S.K. Seeley, Comprehensive two-dimensional gas chromatography with pattern modulation, J. Chromatogr. A. 1421 (2015) 114–122. doi:10.1016/j.chroma.2015.07.117.
[92] P.Q. Tranchida, G. Purcaro, A. Visco, L. Conte, P. Dugo, P. Dawes, L. Mondello, A flexible loop-type flow modulator for comprehensive two-dimensional gas chromatography, J. Chromatogr. A. 1218 (2011) 3140–3145. doi:10.1016/j.chroma.2010.11.082.
[93] P.Q. Tranchida, S. Salivo, F.A. Franchina, L. Mondello, Flow-Modulated Comprehensive Two-Dimensional Gas Chromatography Combined with a High-Resolution Time-of-Flight Mass

Spectrometer: A Proof-of-Principle Study, Anal. Chem. 87 (2015) 2925–2930. doi:10.1021/ac5044175.
[94] F.A. Franchina, M. Maimone, P.Q. Tranchida, L. Mondello, Flow modulation comprehensive two-dimensional gas chromatography–mass spectrometry using ≈4mLmin−1 gas flows, J. Chromatogr. A. 1441 (2016) 134–139. doi:10.1016/j.chroma.2016.02.041.
[95] H. Cai, S.D. Stearns, Partial Modulation Method via Pulsed Flow Modulator for Comprehensive Two-Dimensional Gas Chromatography, Anal. Chem. 76 (2004) 6064–6076. doi:10.1021/ac0492463.
[96] R.B. Wilson, W.C. Siegler, J.C. Hoggard, B.D. Fitz, J.S. Nadeau, R.E. Synovec, Achieving high peak capacity production for gas chromatography and comprehensive two-dimensional gas chromatography by minimizing off-column peak broadening, J. Chromatogr. A. 1218 (2011) 3130–3139. doi:10.1016/j.chroma.2010.12.108.
[97] C.N. Reilley, G.P. Hildebrand, J.W. Ashley, Gas Chromatographic Response as a Function of Sample Input Profile., Anal. Chem. 34 (1962) 1198–1213. doi:10.1021/ac60190a008.
[98] M.I.H. Helaleh, K. Tanaka, M. Mori, Q. Xu, H. Taoda, M.-Y. Ding, W. Hu, K. Hasebe, P.R. Haddad, Vacancy ion-exclusion chromatography of haloacetic acids on a weakly acidic cation-exchange resin, J. Chromatogr. A. 997 (2003) 133–138. doi:10.1016/S0021-9673(03)00546-6.
[99] M. Mori, M.I.H. Helaleh, Q. Xu, W. Hu, M. Ikedo, M.-Y. Ding, H. Taoda, K. Tanaka, Vacancy ion-exclusion/adsorption chromatography of aliphatic amines on a polymethacrylate-based weakly basic anion-exchange column, J. Chromatogr. A. 1039 (2004) 129–133. doi:10.1016/j.chroma.2004.02.012.
[100] K. Kaczmarski, W. Zapała, W. Wanat, M. Mori, B.K. Głód, T. Kowalska, Modeling of Ion-Exclusion and Vacancy Ion-Exclusion Chromatography in Analytical and Concentration Overload Conditions, J. Chromatogr. Sci. 45 (2007) 6–15. doi:10.1093/chromsci/45.1.6.
[101] W. Zapała, J. Kostka, K. Kaczmarski, Comparison of different columns in analysis of C1–C5 aliphatic acids mixture in ion exclusion chromatography and vacancy ion exclusion chromatography modes, Acta Chromatogr. 23 (2011) 377–388. doi:10.1556/AChrom.23.2011.3.1.
[102] A. Gonciarz, K. Kus, M. Szafarz, M. Walczak, A. Zakrzewska, J. Szymura-Oleksiak, Capillary electrophoresis/frontal analysis versus equilibrium dialysis in dexamethasone sodium phosphate-serum albumin binding studies, ELECTROPHORESIS. 33 (2012) 3323–3330. doi:10.1002/elps.201200166.
[103] F. Gritti, A. Tarafder, G. Guiochon, Interpretation of dynamic frontal analysis data in solid/supercritical fluid adsorption systems. I: Theory, J. Chromatogr. A. 1290 (2013) 73–81. doi:10.1016/j.chroma.2013.02.049.
[104] Z. Tong, K.S. Joseph, D.S. Hage, Detection of heterogeneous drug–protein binding by frontal analysis and high-performance affinity chromatography, J. Chromatogr. A. 1218 (2011) 8915–8924. doi:10.1016/j.chroma.2011.04.078.
[105] P.Q. Tranchida, F.A. Franchina, P. Dugo, L. Mondello, Flow-modulation low-pressure comprehensive two-dimensional gas chromatography, J. Chromatogr. A. 1372 (2014) 236–244. doi:10.1016/j.chroma.2014.10.097.
[106] F.A. Franchina, M.E. Machado, P.Q. Tranchida, C.A. Zini, E.B. Caramão, L. Mondello, Determination of aromatic sulphur compounds in heavy gas oil by using (low-)flow modulated comprehensive two-dimensional gas chromatography–triple quadrupole mass spectrometry, J. Chromatogr. A. 1387 (2015) 86–94. doi:10.1016/j.chroma.2015.01.082.
[107] P.Q. Tranchida, M. Maimone, F.A. Franchina, T.R. Bjerk, C.A. Zini, G. Purcaro, L. Mondello, Four-stage (low-)flow modulation comprehensive gas chromatography⊠quadrupole mass

spectrometry for the determination of recently-highlighted cosmetic allergens, J. Chromatogr. A. 1439 (2016) 144–151. doi:10.1016/j.chroma.2015.12.002.
[108] F.A. Franchina, M. Maimone, D. Sciarrone, G. Purcaro, P.Q. Tranchida, L. Mondello, Evaluation of a novel helium ionization detector within the context of (low-)flow modulation comprehensive two-dimensional gas chromatography, J. Chromatogr. A. 1402 (2015) 102–109. doi:10.1016/j.chroma.2015.05.013.
[109] M. Zoccali, K.A. Schug, P. Walsh, J. Smuts, L. Mondello, Flow-modulated comprehensive two-dimensional gas chromatography combined with a vacuum ultraviolet detector for the analysis of complex mixtures, J. Chromatogr. A. 1497 (2017) 135–143. doi:10.1016/j.chroma.2017.03.073.
[110] A. Burel, M. Vaccaro, Y. Cartigny, S. Tisse, G. Coquerel, P. Cardinael, Retention modeling and retention time prediction in gas chromatography and flow-modulation comprehensive two-dimensional gas chromatography: The contribution of pressure on solute partition, J. Chromatogr. A. 1485 (2017) 101–119. doi:10.1016/j.chroma.2017.01.011.
[111] G. Semard, C. Gouin, J. Bourdet, N. Bord, V. Livadaris, Comparative study of differential flow and cryogenic modulators comprehensive two-dimensional gas chromatography systems for the detailed analysis of light cycle oil, J. Chromatogr. A. 1218 (2011) 3146–3152. doi:10.1016/j.chroma.2010.08.082.
[112] J. Krupčík, R. Gorovenko, I. Špánik, P. Sandra, M. Giardina, Comparison of the performance of forward fill/flush and reverse fill/flush flow modulation in comprehensive two-dimensional gas chromatography, J. Chromatogr. A. 1466 (2016) 113–128. doi:10.1016/j.chroma.2016.08.032.
[113] S.E. Prebihalo, K.L. Berrier, C.E. Freye, H.D. Bahaghighat, N.R. Moore, D.K. Pinkerton, R.E. Synovec, Multidimensional Gas Chromatography: Advances in Instrumentation, Chemometrics, and Applications, Anal. Chem. (2017). doi:10.1021/acs.analchem.7b04226.
[114] D.K. Pinkerton, K.M. Pierce, R.E. Synovec, Chemometric Resolution of Complex Higher Order Chromatographic Data with Spectral Detection. Resolving Spectral Mixtures With Applications from Ultrafast Time-Resolved Spectroscopy to Super-Resolution Imaging, 1st ed., Elsevier, 2016.
[115] C.G. Fraga, Chemometric approach for the resolution and quantification of unresolved peaks in gas chromatography–selected-ion mass spectrometry data, J. Chromatogr. A. 1019 (2003) 31–42. doi:10.1016/S0021-9673(03)01329-3.
[116] A.E. Sinha, C.G. Fraga, B.J. Prazen, R.E. Synovec, Trilinear chemometric analysis of two-dimensional comprehensive gas chromatography–time-of-flight mass spectrometry data, J. Chromatogr. A. 1027 (2004) 269–277. doi:10.1016/j.chroma.2003.08.081.
[117] M. He, Z.-Y. Yang, T. Yang, Y. Ye, J. Nie, Y. Hu, P. Yan, Chemometrics-enhanced one-dimensional/comprehensive two-dimensional gas chromatographic analysis for bioactive terpenoids and phthalides in Chaihu Shugan San essential oils, J. Chromatogr. B. 1052 (2017) 158–168. doi:10.1016/j.jchromb.2017.03.029.
[118] Y. Izadmanesh, E. Garreta-Lara, J.B. Ghasemi, S. Lacorte, V. Matamoros, R. Tauler, Chemometric analysis of comprehensive two dimensional gas chromatography–mass spectrometry metabolomics data, J. Chromatogr. A. 1488 (2017) 113–125. doi:10.1016/j.chroma.2017.01.052.
[119] A.C. Olivieri, H.-L. Wu, R.-Q. Yu, MVC3: A MATLAB graphical interface toolbox for third-order multivariate calibration, Chemom. Intell. Lab. Syst. 116 (2012) 9–16. doi:10.1016/j.chemolab.2012.03.018.
[120] A. Eftekhari, H. Parastar, Multivariate analytical figures of merit as a metric for evaluation of quantitative measurements using comprehensive two-dimensional gas chromatography–mass spectrometry, J. Chromatogr. A. 1466 (2016) 155–165. doi:10.1016/j.chroma.2016.09.016.
[121] N.G.S. Mogollón, F.A. de L. Ribeiro, M.M. Lopez, L.W. Hantao, R.J. Poppi, F. Augusto, Quantitative analysis of biodiesel in blends of biodiesel and conventional diesel by comprehensive two-

dimensional gas chromatography and multivariate curve resolution, Anal. Chim. Acta. 796 (2013) 130–136. doi:10.1016/j.aca.2013.07.071.
[122] J. Omar, M. Olivares, J.M. Amigo, N. Etxebarria, Resolution of co-eluting compounds of Cannabis Sativa in comprehensive two-dimensional gas chromatography/mass spectrometry detection with Multivariate Curve Resolution-Alternating Least Squares, Talanta. 121 (2014) 273–280. doi:10.1016/j.talanta.2013.12.044.
[123] N.E. Watson, W.C. Siegler, J.C. Hoggard, R.E. Synovec, Comprehensive Three-Dimensional Gas Chromatography with Parallel Factor Analysis, Anal. Chem. 79 (2007) 8270–8280. doi:10.1021/ac070829x.

Chapter 2. Investigation of Ultrafast Separations via a Pulse Flow Valve for MDGC (GC×GC, GC^3)

This chapter was reproduced from H.D. Bahaghighat[†], C.E. Freye[†], R.E. Synovec, "Investigation of Ultrafast Separations via a Pulse Flow Valve for MDGC (GC×GC, GC^3)" *prepared for submission in Journal of Chromatography A*

[†] These authors contributed equally to this work

2.1 INTRODUCTION

Comprehensive two-dimensional gas chromatography (GC×GC) was first conceptually introduced by Giddings [1] and established by Liu and Phillips in 1991 [2]. The transition from the initial instrumentation design to the modern GC×GC platform has yielded a highly efficient and effective instrument for the separation of complex samples [3–9]. In tandem with the development of GC×GC instrumentation, a large amount of effort has been dedicated into developing tools to analyze these information dense datasets [10–15]. There are many reviews written that cover GC×GC instrumental development [16–19] as well as improvements to data analysis techniques [16,17,20,21]. The goal of GC×GC as with any analytical technique is to provide the greatest amount of information within the shortest period of time. For any separation technique, this is normally quantified as the peak capacity or peak capacity production (e.g. peak capacity per unit time). When compared to one-dimensional (1D) GC, GC×GC has roughly a factor of 10 improvements in peak capacity due to addition of the second (^{2}D) dimension [22]. Furthermore, the addition of ^{2}D dimension results in increased chemical selectivity. Analytes that are overlapped on the first (^{1}D) dimension have the opportunity to be resolved on the ^{2}D dimension.

Despite the numerous benefits of GC×GC compared to 1D-GC (increased peak capacity and chemical selectivity), it is still possible to have unresolved analytes. This may be overcome by increasing the overall peak capacity of the instrument, but this may negatively impact the duty cycle (i.e. run time and cool down time) which may be of special concern when multiple samples are analyzed. In order to further enhance the chemical selectivity, it is intriguing to consider higher order instruments especially comprehensive separations. There have been a limited number of comprehensive three-dimensional gas chromatography (GC×GC×GC), herein referred to as GC^3, publications [23–26], but the work serves as an anchor for further refinements to the technique. In the second report [24], the addition of a third dimension (^3D) composed of an ionic liquid stationary phase was leveraged in order to fully resolve several phosphonated compounds (i.e. chemical warfare simulants). More recently, GC^3 was coupled to a TOFMS which allowed for another dimension of selectivity and peak identification [25,26].

While GC^3 is an attractive instrumental platform due to the increased selectivity provided by the three different dimensions, past work has traded peak capacity (or peak capacity production) for an increase in selectivity. In the first report, a peak capacity of 3,500 or peak capacity production of ~45 peaks/min was demonstrated [23]. This was improved by 4-fold in the second report, with approximately the same peak capacity obtained in a 20-minute time period resulting in a peak capacity production of ~180 peaks/min [24]. The third iteration resulted in a similar peak capacity production of ~140 peaks/min and a total peak capacity of 7,000 [25] which is very similar to state-of-the art GC×GC [5,22,27–30]. However, one would expect the peak capacity (and peak capacity production) of GC^3 to exceed that of GC×GC by a significant amount similar to how GC×GC has ~10 times more peak capacity compared to 1D-GC. In order to understand where GC^3 fails to produce the expected increase in peak capacity (and peak capacity production), the factors

that govern 3D peak capacity, $n_{c,3D}$, must be examined. For GC^3, the ideal peak capacity is given by

$$n_{c,3D} = {}^1n_c * {}^2n_c * {}^3n_c \quad (2.1)$$

where ${}^1n_c$, ${}^2n_c$, and ${}^3n_c$ are the ^{1}D, ^{2}D, and ^{3}D peak capacities, respectively. At unit resolution, R_s = 1, equation 1 can be expressed as

$$n_{c,3D} = \frac{{}^1t}{{}^1W_b} * \frac{{}^2t}{{}^2W_b} * \frac{{}^3t}{{}^3W_b} \quad (2.2)$$

where ${}^1t$ is the total run time, ${}^2t$ is equivalent to the modulation period, ${}^1P_M$, for the coupling of the ^{1}D to the ^{2}D separations, and ${}^3t$ is equivalent to the modulation period, ${}^2P_M$, for the coupling of the ^{2}D to the ^{3}D separations. The nominal peak width at base (4σ) for each dimension is given by ${}^1W$, ${}^2W$, and ${}^3W$, respectively. In terms of modulation periods, instead of separation run times equation 2 can be expressed as

$$n_{c,3D} = \frac{{}^1t}{{}^1W_b} * \frac{{}^1P_M}{{}^2W_b} * \frac{{}^2P_M}{{}^3W_b} \quad (2.3)$$

At the time of the publication of the previous GC^3 work, the fastest modulator published was a diaphragm valve with a P_M of 200 ms which produced peaks ~ 30 ms wide at base [24,31]. In order for GC×GC and GC^3 to be considered comprehensive, the sampling density, ρ_s, defined as the width at base divided by the modulation period, must be greater than 2 [32–34]. Thus peaks sampled by the diaphragm valve must be at a minimum of 400 ms wide. If a peak is 400 ms wide, ${}^2W$, an appropriate modulation period, ${}^1P_M$, might be 3 seconds and thus the peak being sampled must be 6 seconds wide at a minimum. Substituting these numbers in to equation 3, assuming a 30 minute (1800 s) run time

$$n_{c,3D} = \frac{1800\ s}{6} * \frac{3\ s}{400\ ms} * \frac{200\ ms}{30\ ms} = 15{,}000\ or\ 500\ \frac{peaks}{min} \quad (2.4)$$

results in a theoretical maximum peak capacity of 15,000 or 500 peaks/min. However, this equation assumes that peaks on the ^{2}D and ^{3}D separations have constant widths which is not a correct assumption since these separations are considered to be pseudo-isothermal. Thus more appropriate numbers to use would be the average widths for those dimension which might be 600 ms and 40 ms for ^2W and ^3W, respectively resulting in a peak capacity of 7,500 and peak capacity production of 250 peaks/min. The limiting factor for GC^3 is the ^2P_M which requires wider than optimum peaks on ^{2}D. Recently, work has been published using a pulse flow valve that can actuate as fast as 50 ms and create peaks as narrow as 15 ms [35]. It is intriguing to use this as a modulator linking the ^{2}D to ^{3}D allowing for optimal separations conditions to be used.

Herein we explore the feasibility of the pulse flow valve to serve as a modulator for GC^3 and continue to evaluate the pulse flow valve for GC×GC. For the GC×GC instrumentation, we continue to optimize the separations based on the previous work with the pulse flow valve with the overall goal to maximize peak capacity on ^{2}D without reducing the peak capacity of the ^{1}D separation. Additionally, we continue to assess the pulse flow valve as an ultra-fast modulator. The optimized conditions gained from GC×GC study were then applied to GC^3 instrumentation. We evaluate the GC^3 instrument using a two test mixtures and a "real world" sample of diesel fuel spiked with 8 compounds.

2.2 EXPERIMENTAL

2.2.1 *Instrumental Summary*

The GC×GC and GC^3 instruments were both evaluated using a flame ionization detector (FID). The instrumental platforms consisted of an Agilent 6890 GC (Agilent Technologies, Palo

Alto, CA, USA). The stock electrometer for the Agilent FID was replaced with a high-speed electrometer built in-house allowing the data to be collected at 100 kHz, with the data boxcar averaged to 10 kHz. The electrometer was interfaced to a National Instruments data acquisition board, and the resulting data was collected using an in-house written LabVIEW program (National Instruments, Austin, TX, USA). Post-run data processing was performed in MATLAB R2015b (The Mathworks, Inc., Natick, MA, USA). Data was imported into MATLAB and further binned to 1 kHz. Samples were introduced to the instrument via a 7683B auto-injector (Agilent Technologies). Prior to each sample injection, HPLC grade hexane and acetone obtained from Fisher Scientific were used as solvent rinses. Ultra-high purity hydrogen (Grade 5, 99.999%) was used as the carrier gas (Praxair, Seattle, WA, USA). For all instrumental setups an inlet and FID temperature of 250 °C was implemented. All columns were contained within the same oven thus all had the same temperature. Four distinct instrumental setups were implemented (two GC×GC and two GC^3) with each instrumental setup described below.

2.2.2 *GC×GC*

For the two GC×GC evaluations, the GC was fitted with a high-speed pulse valve model 009–1643-900 (Parker Hannifin, Hollis, NH, USA) mounted outside of the oven. The pulsed flow valve was controlled using the same program that was used to collect the FID data. A schematic of the GC×GC instrument is shown in Figure 2.1A. The ^{1}D and ^{2}D columns were linked using a 3-way T-union model MT.5CXS6 (Valco Instruments Company Inc., Houston, TX, USA). An in-house fitting was fabricated to mate the pulse flow valve to 7.24 cm × 1.65 mm copper tubing (Restek, Bellefonte, PA, USA) reduced to 3.81 cm × 0.635 mm steel tubing interfaced with a 2 µl sample loop model CSL2 (Valco Instruments Company Inc.) which was connected to the 3-way T-union.

For the first investigation, the ^{1}D column was a SPB-5 (5% diphenyl/95% dimethyl siloxane) stationary phase: 8 m length × 100 µm inner diameter (I.D.) × 0.1 µm film thickness (d.f.), and the ^{2}D column was a DB-WAX (polyethylene glycol) stationary phase: 1 m × 100 µm I.D. × 0.1 µm d.f. A test mixture containing a diverse set of 115-compounds was used to evaluate the instrumental platform. The test mixture contained a wide range of boiling points (36–372 °C) with nine chemical compound classes: alkanes, esters, halogenated alkanes, aromatics, alkenes, alkynes, ketones, alcohols, cycloalkanes [25,35]. A 0.5 µl volume of the 115-component test mixture was injected at a split of 100:1. A constant flow rate of 0.8 ml/min was applied. The oven was held at 40 °C for 1 min and ramped at 40 °C/min to 250 °C where it was held for 1 min. A modulation period, P_M, of 500 ms was applied with an injection pulse width of 2 ms (i.e. how long the pulse valve injects carrier gas). The head pressure on the pulse valve was held at 30.5 psig for 1 min and ramped at 1.08 psig/min to 36.2 psig and held for 1 min.

For the second investigation, the ^{1}D column was a SPB-5 stationary phase: 3 m length × 100 µm I.D. × 0.1 µm d.f., and the ^{2}D column was a DB-WAX stationary phase: 1 m × 100 µm I.D. × 0.1 µm d.f. A 0.5 µl volume of a test mixture containing 15 compounds (see Table A.1, Supporting Information) was injected at a split of 100:1. A constant flow rate of 5.3 ml/min was applied. The oven was held at 50 °C for 3 min. The P_M was 75 ms with a 2 ms injection pulse width, and the head pressure on the pulse valve was held at 91 psig.

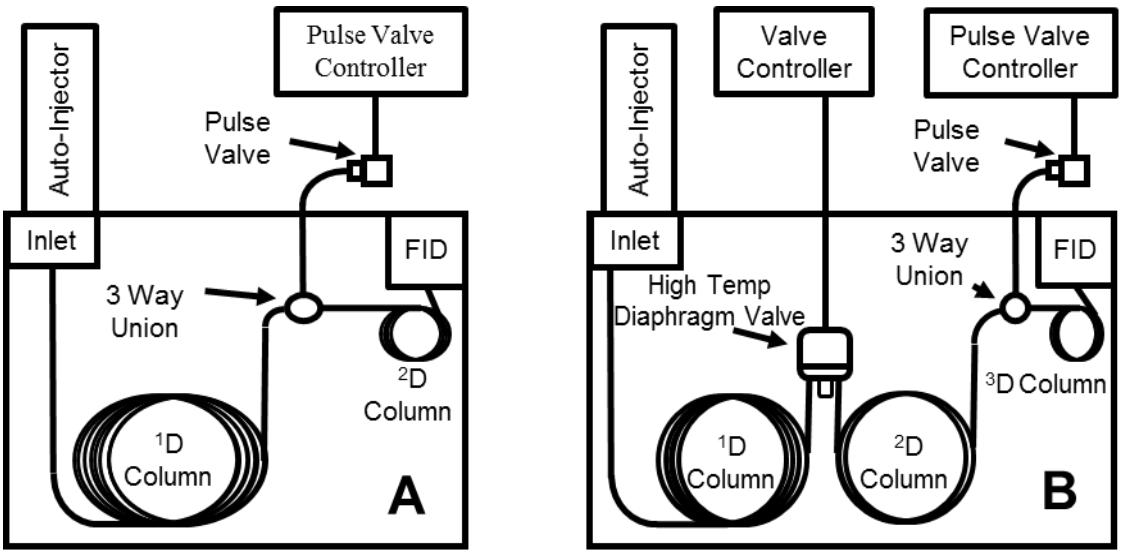

Figure 2.1. GC×GC and GC^3 Instrumental Schematics.

(A) Schematic of the major components of the GC×GC - FID instrument. A pulse flow valve was implemented to link the ^{1}D and ^{2}D columns. (B) Schematic of the major components of the GC^3 - FID instrument. A high-temperature diaphragm valve was utilized as a modulator to link the ^{1}D and ^{2}D columns, and a pulse flow valve was implemented to link the ^{2}D and ^{3}D columns.

2.2.3 *GC^3*

For the two GC^3 instrumental setups, the GC was fitted with a high-speed, six-port, high temperature diaphragm valve VICI model DV-12-1116 T (Valco Instruments Company Inc.) fitted with a 5 µl sample loop mounted inside the oven which was used to link ^{1}D and ^{2}D columns [25,27,36,37]. The pulse valve was used to link columns ^{2}D and ^{3}D in an identical manner as described in section 2.2.2. The diaphragm valve, pulse flow valve, and the FID data were all controlled/collected using a LabVIEW program. A schematic of the GC^3 instrument is shown in Figure 2.1B.

For the third investigation, the ^{1}D column was a RTX-17 Sil MS (50% phenyl/50% methylpolysiloxane) stationary phase: 20 m length × 180 µm I.D. × 0.18 µm d.f., the ^{2}D column

was a SPB-5 stationary phase: 6 m length × 100 µm I.D. × 0.1 µm d.f, and the ^{3}D column was a DB-WAX stationary phase: 1 m length × 100 µm I.D. × 0.1 µm d.f. A 0.5 µl volume of an 18 component test mixture (see Table A.2, Supporting Information) was injected at a split of 100:1. A constant flow rate of 0.8 ml/min was applied to ^{1}D. The ^{2}D and ^{3}D columns were controlled via the auxiliary pressure controller with a pressure of 100 psig which corresponds to a flow rate of ~6.3 ml/min. The oven was held at 50 °C for 3 min. A $^{1}P_{M}$ of 1 sec with an injection pulse width of 20 ms applied to the diaphragm valve and a $^{2}P_{M}$ of 50 ms with an injection pulse width of 2 ms was applied to the pulse valve. The head pressure on the pulse valve was held at 83 psig.

For the fourth investigation, the ^{1}D column was a RTX-17 Sil MS stationary phase: 20 m length × 180 µm I.D. × 0.18 µm d.f., the ^{2}D column was a SPB-5 stationary phase: 2 m length × 100 µm I.D. × 0.1 µm d.f, and the ^{3}D column was a DB-WAX stationary phase: 0.75 m length × 100 µm I.D. × 0.1 µm d.f. 1 µl of the 115-component mixture was injected at a split of 60:1. A constant flow rate of 0.7 ml/min was applied to ^{1}D. The ^{2}D and ^{3}D columns were controlled via the auxiliary pressure controller under a ramped pressure program held at 39.2 psig for 1.5 min, ramped at 2.55 psig/min to 65.9 psig, and held at the final pressure for 1 minute. This pressure ramp corresponds to a flow rate of ~3 ml/min. The oven was held at 40 °C for 1.5 min, ramped at 20 °C/min to 250 °C, and held for 1 min. A $^{1}P_{M}$ of 1.2 sec with an injection pulse width of 20 ms applied to the diaphragm valve and a $^{2}P_{M}$ of 60 ms with an injection pulse width of 2 ms was applied to the pulse valve. The head pressure on the pulse valve was held at 36.9 psig for 1.5 min, ramped at 2.55 psig/min to 63.7 psig and held for 1 min. Diesel fuel spiked with 8 compounds (see Table A.3, Supporting Information) was also evaluated using the same conditions as noted above except the split was reduced to 20:1.

2.3 RESULTS AND DISCUSSION

2.3.1 *GC×GC*

The GC×GC - FID chromatogram for the 115-component test mixture using a modulation period, P_M, of 500 ms in the raw vector form is shown in Fig 2.2A. Three representative analytes (Methyl Decanoate, Pentadecane, Dodecanol) are shown in Fig. 2.2B which range from relatively unretained on ^{2}D to moderately retained. In the raw vector format, the sharp decreases in signal is representative of the ^{2}D analyte response of interest, nominally in the form of an "error" function, followed by a slow decay of the analyte response back to the original ^{1}D concentration profile. This ^{2}D analyte response is created by rapid actuation of the pulse flow valve in combination with the three-way union and coupled with the tubing assembly (see Fig 2.1A). Reducing the tubing assembly from a large inner diameter to a smaller inner diameter results in a pressure wave in the form of an exponentially modified Gaussian with a very sharp leading edge. Using the same method as previously reported [35], a 3-step method involving differentiation, inversion, and baseline correction was implemented to convert the data from the raw form into the final processed form which appears analogous to a "traditional" vector GC×GC chromatogram. Figure A.1 (Supporting Information) demonstrates the data processing method. Figure 2.2C shows the processed vector chromatogram of the data shown in Figure 2.2B.

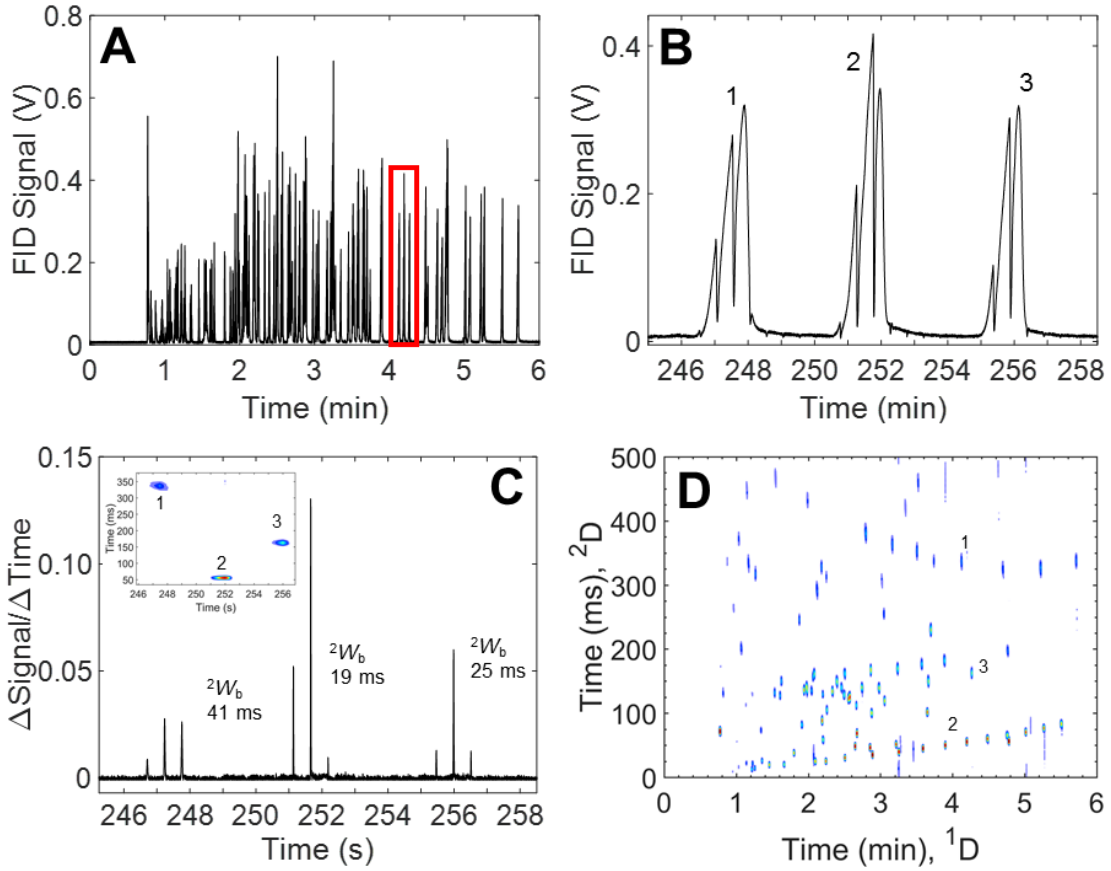

Figure 2.2. P_M 500 ms 115-Component Data

(A) Raw (preprocessed) chromatogram of the 115 component mixture collected using a modulation period P_M of 500 ms. The highlighted subset shown contains three non-overlapped analytes (1: Methyl Decanoate, 2: Pentadecane, 3: Dodecanol). (B) Enhanced view of three non-overlapped analytes is shown. (C) Processed vector chromatogram of the three analytes with width of base annotated. The insert shows the 2D chromatogram of the three analytes. (D) GC×GC - FID chromatogram of the 115 component mixture. Using the three step data processing method, the raw chromatogram shown in (A) has been

The ^2W_b is annotated for the three analytes. Since a polar column (DB-WAX) was implemented as the ^{2}D dimension, the most retained analyte should be methyl decanoate, an ester, which has an apparent ^2W_b of 41 ms. The next most retained analyte is dodecanol with an apparent ^2W_b of 25 ms,

and the least retained analyte is pentadecane which has an apparent ^2W_b of 19 ms. The ^2W_b of each analyte is dependent on the slope of the "error" function, and the ^{2}D retention time, ^2t_R, is defined by the inflection point of the "error" function. The insert in Figure 2.2C shows the GC×GC chromatogram of these three analytes which has been registered by 200 ms on the ^{2}D to remove the dead time. Figure 2.2D shows the GC×GC chromatogram of the data processed in Figure 2.2A. The data was registered on ^{2}D by 200 ms to remove the dead time.

In order to accurately measure the ^{2}D peak capacity (^2n_c), 12 representative analytes that spanned the entire ^{2}D separation were selected (see Figure A.2, Supporting Information). The ^2t_R and the ^2W_b for each analyte was measured and an equation was fitted to those values [34–36]. Compared to the previous report [35], the slope of the equation is ~40% less which is due to the use of micro-bore columns and optimization of the pulse flow valve. Using the following recursive equation, the ^2n_c was calculated.

$$R_s = \frac{t_{R,n} - t_{R,n-1}}{0.5(W_{b,n} - W_{b,n-1})} = 1 \qquad (2.5)$$

The equation obtained from Figure A.2 (Supporting Information) was substituted into equation 5.5 for both $W_{b,n}$ and $W_{b,n-1}$ and rearranging allows the calculation of the retention times of successive peaks (and R_s = 1) based on the measured dead time, $t_{R,(n=0)}$ on ^{2}D [35,38,39]. These retention times were used to calculate apparent ^2W_b from the experimentally observed linear relationship between ^2t_R and apparent ^2W_b. Individual Gaussian peaks of equivalent area were modeled based on these peak widths and retention times, then concatenated to give a continuous chromatogram (see Figure A.2, Supporting Information).

1542

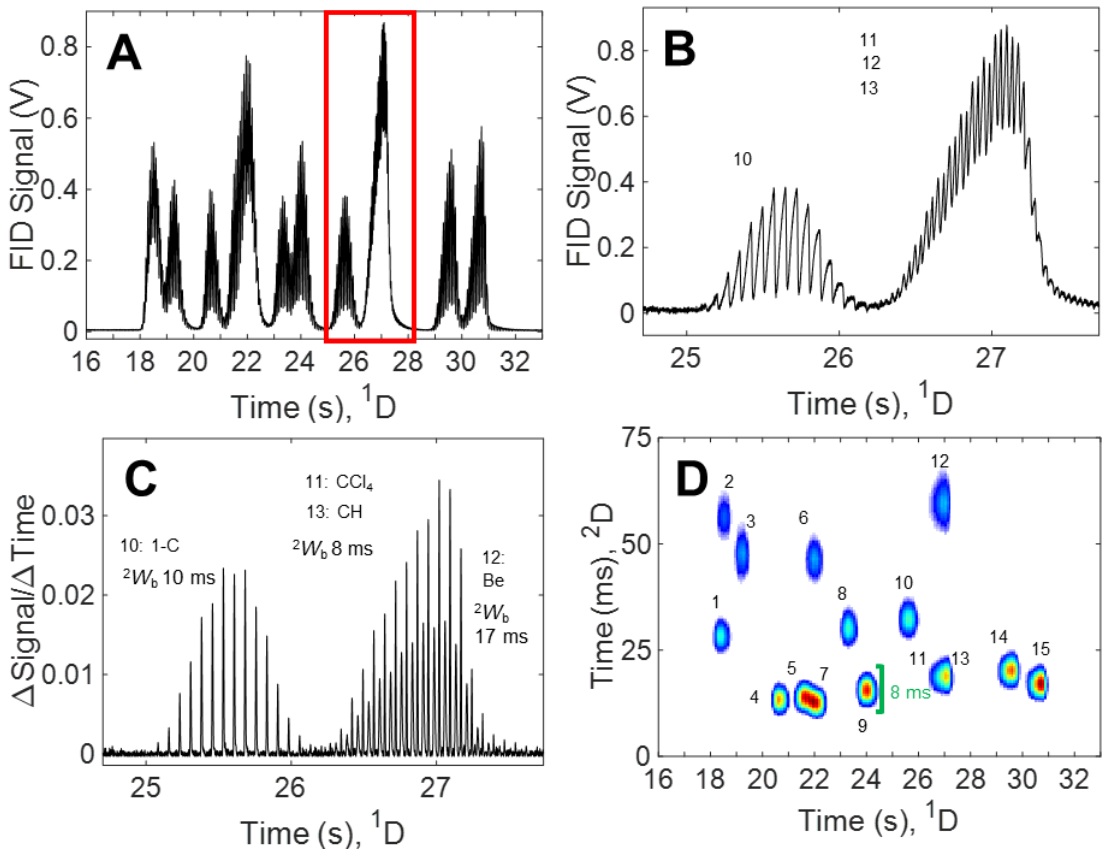

Figure 2.3. P_M 75 ms 18-Component Data

(A) Raw (preprocessed) chromatogram of a GC×GC - FID separation of a 15-component low boiling point mixture collected using a modulation period P_M of 75 ms. The highlighted subset is shown in figure (B). (B) Close up view of raw chromatogram containing four analytes numbered in elution order (10: 1-Chlorobutane, 11: Carbon Tetrachloride, 12: Benzene, 13: Cyclohexane). Analytes 11 and 13 are observed to be overlapped in both dimensions which can be seen in (D) (C) Processed vector chromatogram of the four analytes with width of base annotated. (D) GC×GC - FID chromatogram of the 15 component mixture. Using the three step Data processing method, the raw chromatogram shown in (A) has been converted into a "traditional" 2D plot. The names of the compounds can be found in Table A.1. The ^{2}D peaks are extremely narrow, with an average ^2W_b of 10 ms. However, the ^{1}D peaks have been oversampled with a ρ_S of ~12 as seen in (C).

The resulting ${}^{2}n_c$ was calculated to be 20. Using the same 12 analytes, the average ${}^{1}W_b$ was calculated to be ~1 s resulting in a ^{1}D peak capacity (${}^{1}n_c$) of 360 (t_{sep} = 6 min). Thus the 2D peak capacity, $n_{c,2D,}$ is ~7200 or a peak capacity production of ~1200 peaks/min for this separation.

While pulse flow valve using a P_M of 500 ms results in extremely high peak capacity production, investigation of its potential as a high speed modulator is warranted. Using a P_M of 75 ms, a 15 component mixture (see Table A.1, Supporting Information) was evaluated. Figure 2.3A shows the raw vector chromatogram of the separation with a t_{sep} of ~13 s. Figure 2.3B shows an enhanced view of Figure 2.3A where 4 analytes are present. One analyte (10: 1-chlorobutane) is totally resolved on ^{1}D while three analytes (11: carbon tetrachloride, 12: benzene, and 13: cyclohexane) are severely overlapped. The processed vector chromatogram is shown in Figure 2.3C with the ${}^{2}W_b$ annotated. Figure 2.4D shows the 2D chromatogram obtained from processing the data in Figure 2.4A. The narrowest peaks measured (analytes 4, 5, 7, and 9) had ${}^{2}W_b$ of 8 ms. The ${}^{2}n_c$ was calculated to be 7.5 and the ${}^{1}n_c$ was calculated to be ~14.5 (${}^{1}W_{b,avg}$ ~ 0.9 s and t_{sep} ~ 13 s) resulting in a $n_{c,2D}$ of ~110 or a peak capacity production of ~510 peaks/min. However, the ^{1}D peaks were significantly oversampled with a sampling density, ρ_s, of ~12. In order to reduce the ρ_s to an appropriate number (~2-4), one could use a modified injection source [38,40–43] or perhaps more interesting would be to sample analytes with pulse flow valve as the second modulator in a GC^3 instrument.

2.3.2 *GC^3*

Building from past research of high temperature diaphragm valve-based GC×GC [27,36] and GC^3 [25,26] it was considered ideal to combine the known attributes of the high temperature diaphragm valve modulator with pulse flow valve modulator. Figure 2.1B shows the instrumental schematic for the GC^3 separations.

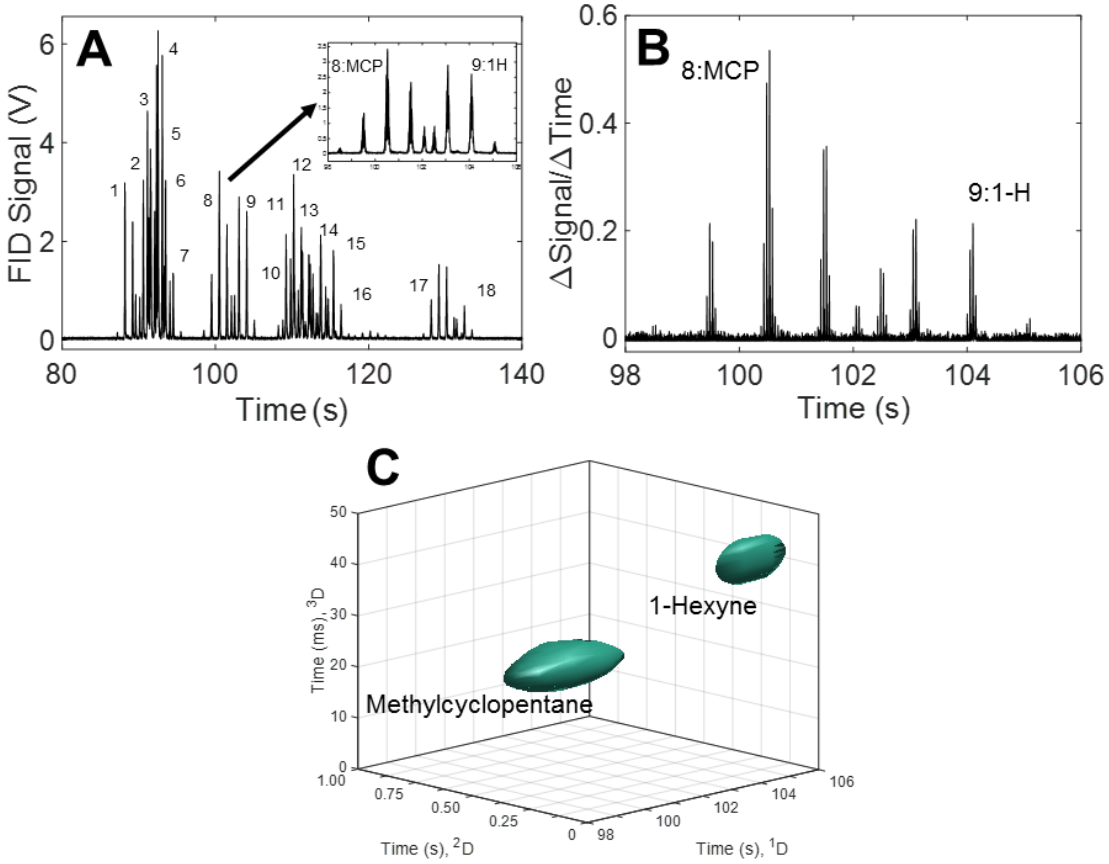

Figure 2.4. GC^3 18-Component Data

(A) The raw (pre-processed) vector chromatogram of a GC^3 - FID separation of the 18 component mixture. The ^1P_M was 1 sec and the ^2P_M was 50 ms. An insert of two analytes (8: methylcyclopentane and 9: 1-Hexyne) are shown which are slightly overlapped on the ^{1}D dimension. (B) An enhanced view of the processed vector chromatogram is shown for the two analytes highlighted in (A). (C) Isosurface plot of the region depicted in (B).

Figure 2.4A shows the raw vector chromatogram of an 18 component mixture (see Table A.2, Supporting Information) that was collected using a ^1P_M of 1.0 seconds and a ^2P_M of 50 ms. The elution order was determined by a series of individual injections of the analytes under the same separation conditions of the 18 analyte mixture. A processed vector chromatogram of the 18 individual analytes that are overlaid onto one chromatogram is shown in Figure A.3 (Supporting

Information). Figure 2.4B shows the processed vector chromatogram of two analytes (8: methylcyclopentane and 9: 1-hexyne) that exhibit a slight overlap on the ^{1}D dimension. In order to demonstrate the selectivity provided by the addition of two dimensions (^{2}D and ^{3}D), Figure 2.4C shows an isosurface plot of the same region shown in Figure 2.4B. The data was registered by 10 ms on the ^{3}D to remove the dead time.

To further explore the selectivity provided by the three separation dimensions, the data shown in Figure 5.4A has been plotted in Figure 2.5A and 2.5B which show the ^{1}D vs ^{2}D where the data has been summed along the ^{3}D and ^{1}D vs ^{3}D where the data has been summed along the ^{2}D, respectively. The chemical selectivity provided by the 3 dimensions can easily be seen when elution pattern of Figure 2.5A is compared to Figure 2.5B. Analytes that are not resolved or only partially resolved on ^{1}D are either separated on the ^{2}D or ^{3}D dimensions. To further explore the selectivity of the GC^{3} system, the ^{2}D vs ^{3}D chromatogram has been prepared in Figure 2.5C where the data was summed along the ^{1}D. Figure 2.5D is a 3-D isosurface plot of the entire separation. In order to calculate the peak capacity of the GC^{3} instrument, three representative analytes were selected (n-hexane, 1-hexyne, methylcyclopentane). These 3 analytes span a wide range of retention times on all three dimensions and thus deemed appropriate in calculate the peak capacity. The figures of merit for the 3 analytes are shown in Table 2.1. For the three representative analytes, the total peak capacity (1-minute total time), $n_{c,3D}$, ranged from 772 to 914 with an average of ~825 or a peak capacity production of 825 peaks/min, which is a 4.5 times improvement over previously published GC^{3} values [24,25]. These results were based on a simple mixture separated isothermally which in itself is impressive; however, further work on a more complex mixture that required temperature ramping is needed.

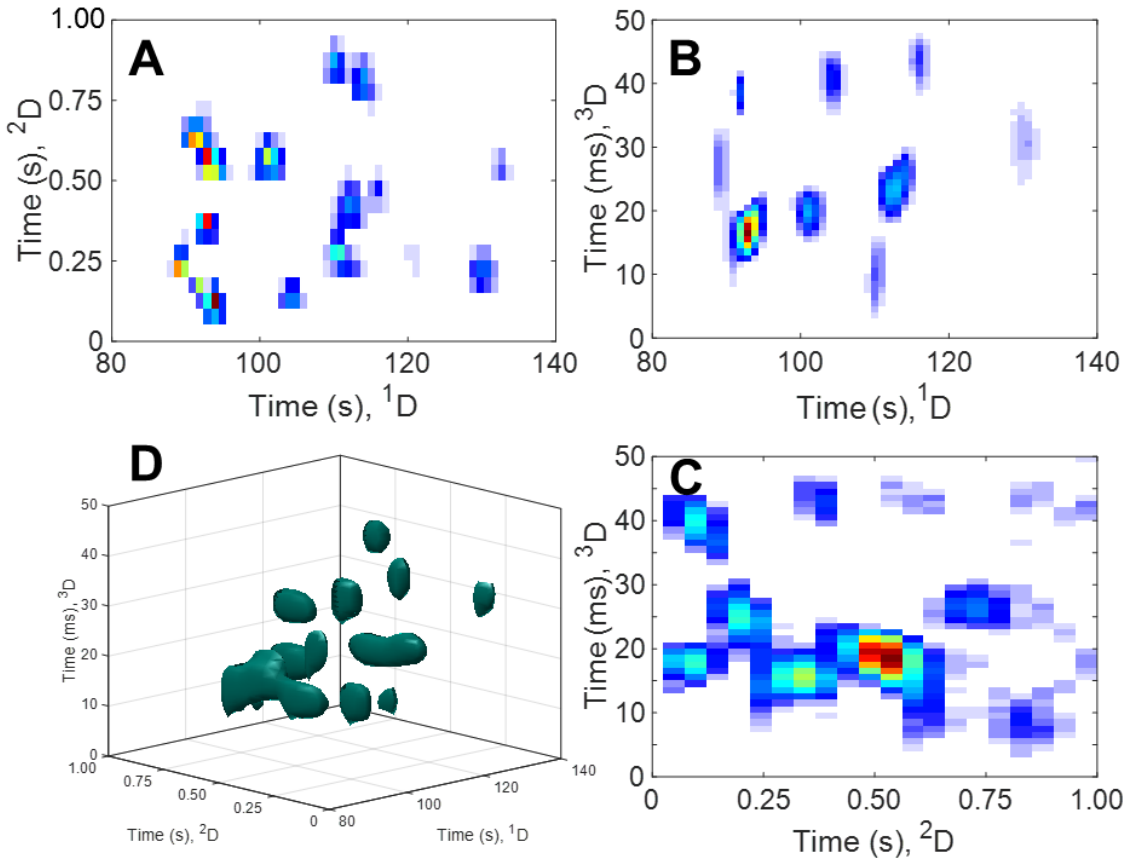

Figure 2.5. 2D and 3D Chromatograms of 18-Component Data

In order to show the benefits of the chemical selectivity of the GC^3 - FID system, three contour plots and an isosurface plot have been prepared for the separation of the 18 component mixture. (A) Contour plot of ^2D vs ^1D summed along the ^3D. (B) Contour plot of ^3D vs ^1D summed along the ^2D. (C) Contour plot of ^3D vs ^2D summed along the ^1D. (D) Isosurface plot. An example of the chemical selectivity provided by the three different columns can be seen in A and B. Analytes (8) methylcyclopentane and (9) 1-hexyne have a dramatic shift in retention of the non-polar ^2D and polar ^3D columns. This shift in affinity for ^2D and ^3D columns is highlighted in Figure (C).

1594

	n-Hexane	1-Hexyne	Methylcyclopentane
${}^1t_R$ (min)	1.54	1.68	1.64
${}^1W_b$ (sec)	2.26	2.28	2.41
${}^1\rho_s$	2.26	2.28	2.41
${}^1n_c$	26.50	26.36	24.89
${}^2t_R$ (sec)	0.19	0.47	0.35
${}^2W_b$ (msec)	177	128	171
${}^2\rho_s$	3.54	2.56	3.43
${}^2n_c$	5.65	7.83	5.84
${}^3t_R$ (msec)	27.5	3.2	31.8
${}^3W_b$ (msec)	8.2	13.1	9.4
${}^3n_c$	6.10	3.83	5.31
$n_{c,3D}$	914	790	772
Peaks/min	914	790	772

Table 2.1. Figures of Merit for GC^3 for 18-Component Separation.

Chromatographic peak measurements and figures of merit for three representative compounds in the 18 component mix.

To further evaluate the merits of the GC^3 system, the same 115 component mixture was assessed using optimized experimental conditions (see Section 2.3). Figure 2.6A shows the processed vector chromatogram that was collected using a ${}^1P_M$ of 1.2 seconds and a ${}^2P_M$ of 60 ms. In order to see the selectivity provided by three dimensions, Figure 2.6B and 2.6C show the ^{1}D vs ^{3}D chromatogram where the data has been summed along the ^{2}D and ^{1}D vs ^{2}D where the data has been summed along the ^{3}D, respectively. The chemical selectivity provided by the 3 dimensions can be especially seen at ~ 4 to 6 minute range on ^{1}D. Analytes that are not resolved or only partially resolved on ^{1}D are either separated on the ^{2}D or ^{3}D dimensions. To further explore the selectivity of the GC^3 system, the ^{2}D vs ^{3}D chromatogram has been prepared (see Fig A.5A, Supporting Information). When all the data along the ^{1}D dimension is summed, the chemical

selectivity that is provided by this view disappears. This is because the analyst is "looking down the tube" and thus it is difficult to extract useful information. Thus 3 ^{2}D vs ^{3}D chromatograms have also been prepared (see Fig A.5B-D, Supporting Information) that span a range of 60 seconds (same as GC^{3} separation of the 18 component mixture). Figure 2.6D shows the isosurface plot of the 115 component mixture. Four analytes listed in Table 2.2 (see Fig A.6, Supporting Information) have been selected to demonstrate the figures of merit for the GC^{3} system. While this is a small portion of the 115 component mixture, these 4 analytes span a wide range of times on all three dimensions and thus deemed appropriate to quote the figures of merit. The method for determining these values was the same as those used in the evaluation of the 18 component

	Analyte 1	**Analyte 2**	**Analyte 3**	**Analyte 4**
$^{1}t_R$ (min)	1.19	2.03	5.46	6.01
$^{1}W_b$ (sec)	2.45	2.47	2.86	4.98
$^{1}\rho_s$	2.04	2.06	2.38	4.15
$^{1}n_c$	267	263	229	130
$^{2}t_R$ (sec)	0.42	0.28	0.29	1.02
$^{2}W_b$ (msec)	131	136	125	122
$^{2}\rho_s$	2.18	2.26	2.09	2.03
$^{2}n_c$	9.7	8.8	9.7	9.9
$^{3}t_R$ (msec)	22.5	37.2	17.7	13.0
$^{3}W_b$ (msec)	7.9	17.2	14.2	13.8
$^{3}n_c$	7.58	3.50	4.23	4.35
$n_{c,3D}$	19622	8125	9328	5597
Peaks/min	1811	750	861	517

Table 2.2 Figures of Merit for GC^{3} for 115-Component Separation

Chromatographic peak measurements and figures of merit for the 115 component test mixture. See supporting information Fig A.6 for location of the analytes in the chromatograms.

mixture. For the 4 representative analytes, the total peak capacity, $n_{c,3D}$, ranged from 5600 to

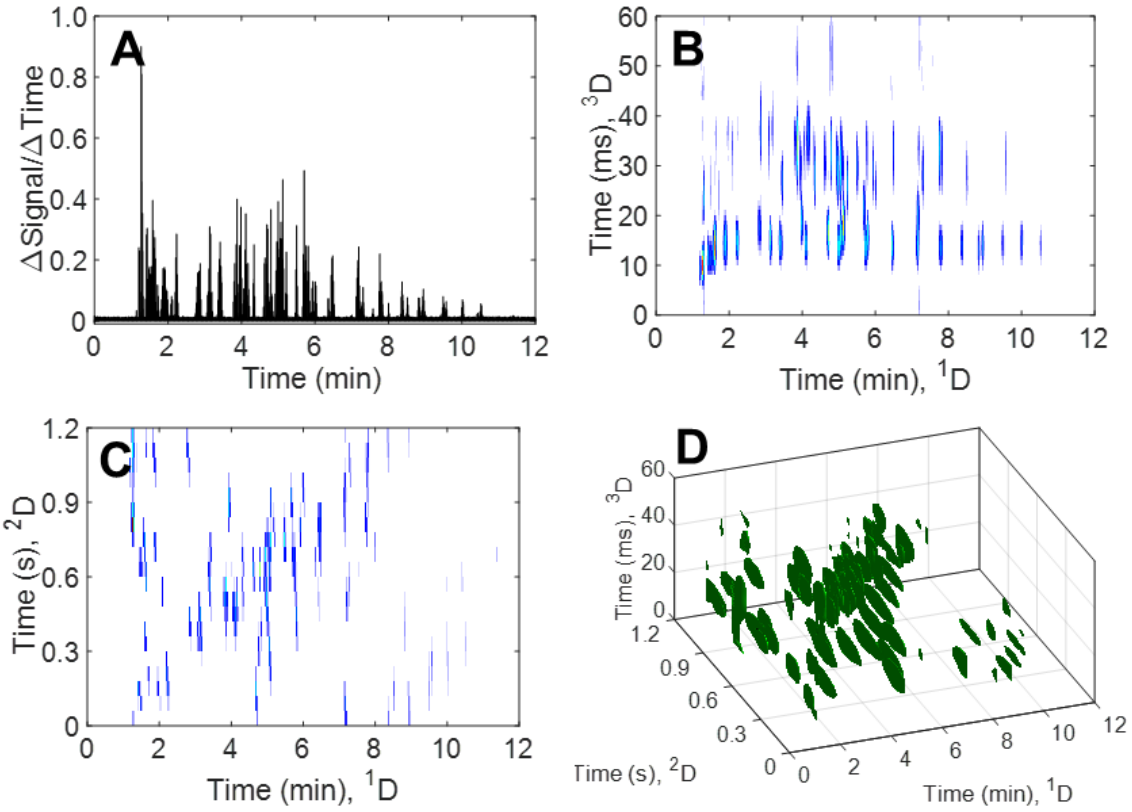

Figure 2.6. GC^3 115-Component Vector, 2D, 3D Chromatograms.

(A) Vector chromatogram (processed data) of the 115 component test mixture collected using a ^1P_M of 1.2 seconds and a ^2P_M of 60 ms. (B) Plot of ^{1}D vs ^{3}D summed along ^{2}D. (C) Plot of ^{1}D vs ^{2}D summed along ^{3}D. (D) Isosurface plot of the 115 component mix. For ^{2}D vs ^{3}D see supporting information Fig A.5.

19,000 with an average of ~10,700. Perhaps more importantly is the peak capacity production which ranges from 520 to 1,800 with an average of ~1000 peaks/min which is a significant improvement over previously published GC^3 values of 140 and 180 peaks/min [24,25].

To further show the selectivity provided by the GC^3 system, diesel fuel was spiked with 8 non-native analytes. Figure 2.7A shows the processed vector chromatogram of the diesel fuel. In this view, it is possible to see the characteristic “petroleum hump” which can be totally resolved using GC^3. For this analysis, the conditions were optimized to provide the most separation for the

8 spike analytes instead of attempting to totally resolve the matrix (diesel) background. An isosurface plot shown in Figure 2.7B, has been prepared to shows the selectivity for the 8 spiked analytes. In order to visual the data, analytes that have a ^{3}D retention times from 0 to 25 ms are colored blue, analytes that have a ^{3}D retention times from 25 to 40 ms are colored green, and analytes that have a ^{3}D retention times from 40 to 60 ms are colored red. The blue color roughly corresponds to the location of the alkanes and cycloalkanes and the green color roughly corresponds to the location of the aromatics present in diesel fuel. The 8 spiked analytes were highly retained on ^{3}D and have ^{3}D retention times >40 ms and thus are colored red. In order to visualize the diesel fuel in a planar fashion analogous to a GC×GC chromatogram, Figure A.7 (Supporting Information) has been prepared.

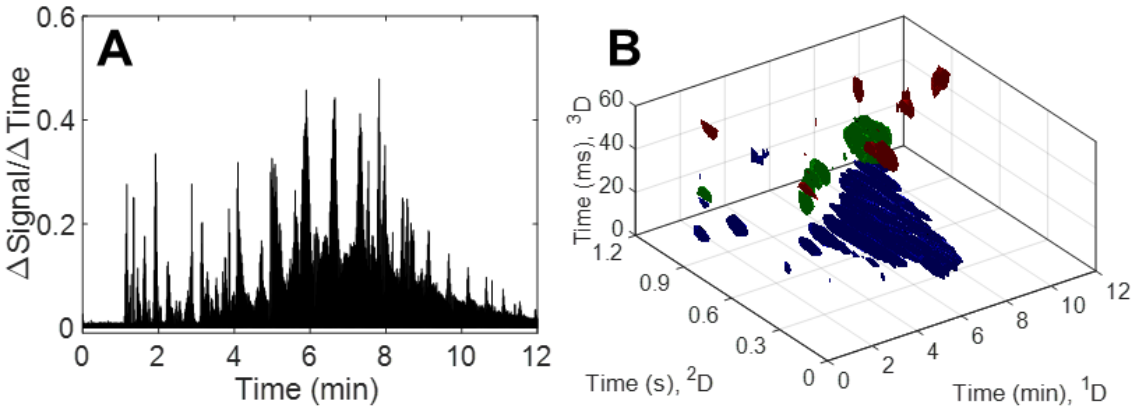

Figure 2.7. Diesel Vector and 3D Chromatogram with Spiked Analytes.

(A) Vector chromatogram (processed data) of the diesel that has been spiked with 8 components collected using a $^{1}P_{M}$ of 1.2 seconds and a $^{2}P_{M}$ of 60 ms. (B) Isosurface plot of diesel spiked with the 8 components. Analytes that have a ^{3}D retention time from 0 to 25 ms are colored blue, analytes that have ^{3}D retention time from 25 to 40 ms are colored green, and analytes that have ^{3}D retention times from 40 to 60 ms are colored red. All 8 spiked compounds have ^{3}D retention times greater than 40 ms and thus are colored red. For ^{1}D vs ^{2}D, ^{1}D vs ^{3}D, and ^{2}D vs ^{3}D chromatograms, see supporting information Fig A.7.

2.4 CONCLUSION

Past applications of GC^{3} instrumentation demonstrated great promise based on the increased selectivity provided for separations that was superior to GC×GC, but this increase in selectivity came at the cost of peak capacity and peak capacity production. It has been demonstrated that the use of a high temperature diaphragm valve in conjunction with a recently introduced pulse flow valve, it is now possible to take advantage of the increased selectivity of a GC^{3} instrument, while achieving a peak capacity production of ~1000 peaks/min. Future studies

will be focused on applying these instrumental improvements with spectral data, to create an ultra-fast 4D data structure to address complex separation mixtures.

2.5 Acknowledgements

We would like to thank Stan Stearns of Valco for providing the high temperature valves.

2.6 Supporting Information

Figures A.1 to A.7 and Table A.1 to A.3 can be found in Appendix A.

2.7 REFERENCES

[1] J.C. Giddings, Unified separation science, 1st ed., Wiley-Interscience, 1991.

[2] Z. Liu, J. B. Phillips, Comprehensive Two-Dimensional Gas Chromatography using an On-Column Thermal Modulator Interface, Journal of Chromatographic Science. 29 (1991) 227–231. doi:10.1093/chromsci/29.6.227.

[3] V. Abrahamsson, N. Ristic, K. Franz, K. Van Geem, Comprehensive two-dimensional gas chromatography in combination with pixel-based analysis for fouling tendency prediction, Journal of Chromatography A. 1501 (2017) 89–98. doi:10.1016/j.chroma.2017.04.021.

[4] H.D. Bean, J.-M.D. Dimandja, J.E. Hill, Bacterial volatile discovery using solid phase microextraction and comprehensive two-dimensional gas chromatography–time-of-flight mass spectrometry, Journal of Chromatography B. 901 (2012) 41–46. doi:10.1016/j.jchromb.2012.05.038.

[5] L.M. Dubois, K.A. Perrault, P.-H. Stefanuto, S. Koschinski, M. Edwards, L. McGregor, J.-F. Focant, Thermal desorption comprehensive two-dimensional gas chromatography coupled to variable-energy electron ionization time-of-flight mass spectrometry for monitoring subtle changes in volatile organic compound profiles of human blood, Journal of Chromatography A. 1501 (2017) 117–127. doi:10.1016/j.chroma.2017.04.026.

[6] A. Giri, M. Coutriade, A. Racaud, K. Okuda, J. Dane, R.B. Cody, J.-F. Focant, Molecular Characterization of Volatiles and Petrochemical Base Oils by Photo-Ionization GC×GC-TOF-MS, Analytical Chemistry. 89 (2017) 5395–5403. doi:10.1021/acs.analchem.7b00124.

[7] H. Potgieter, R. Bekker, J. Beigley, E. Rohwer, Analysis of oxidised heavy paraffininc products by high temperature comprehensive two-dimensional gas chromatography, Journal of Chromatography A. 1509 (2017) 123–131. doi:10.1016/j.chroma.2017.06.046.

[8] S. Prebihalo, A. Brockman, J. Cochran, F.L. Dorman, Determination of emerging contaminants in wastewater utilizing comprehensive two-dimensional gas-chromatography coupled with time-of-flight mass spectrometry, Journal of Chromatography A. 1419 (2015) 109–115. doi:10.1016/j.chroma.2015.09.080.

[9] P.-H. Stefanuto, K.A. Perrault, L.M. Dubois, B. L'Homme, C. Allen, C. Loughnane, N. Ochiai, J.-F. Focant, Advanced method optimization for volatile aroma profiling of beer using two-dimensional gas chromatography time-of-flight mass spectrometry, Journal of Chromatography A. 1507 (2017) 45–52. doi:10.1016/j.chroma.2017.05.064.

[10] S.L. Forbes, A.N. Troobnikoff, M. Ueland, K.D. Nizio, K.A. Perrault, Profiling the decomposition odour at the grave surface before and after probing, Forensic Science International. 259 (2016) 193–199. doi:10.1016/j.forsciint.2015.12.038.

[11] B. Kehimkar, J.C. Hoggard, L.C. Marney, M.C. Billingsley, C.G. Fraga, T.J. Bruno, R.E. Synovec, Correlation of rocket propulsion fuel properties with chemical composition using comprehensive two-dimensional gas chromatography with time-of-flight mass spectrometry followed by partial least squares regression analysis, Journal of Chromatography A. 1327 (2014) 132–140. doi:10.1016/j.chroma.2013.12.060.

[12] B.A. Weggler, T. Gröger, R. Zimmermann, Advanced scripting for the automated profiling of two-dimensional gas chromatography-time-of-flight mass spectrometry data from combustion

aerosol, Journal of Chromatography A. 1364 (2014) 241–248. doi:10.1016/j.chroma.2014.08.091.

[13] J. Omar, M. Olivares, J.M. Amigo, N. Etxebarria, Resolution of co-eluting compounds of Cannabis Sativa in comprehensive two-dimensional gas chromatography/mass spectrometry detection with Multivariate Curve Resolution-Alternating Least Squares, Talanta. 121 (2014) 273–280. doi:10.1016/j.talanta.2013.12.044.

[14] C. Hurtado, H. Parastar, V. Matamoros, B. Piña, R. Tauler, J.M. Bayona, Linking the morphological and metabolomic response of Lactuca sativa L exposed to emerging contaminants using GC×GC-MS and chemometric tools, Scientific Reports. 7 (2017). doi:10.1038/s41598-017-06773-0.

[15] C.E. Freye, N.R. Moore, R.E. Synovec, Enhancing the chemical selectivity in discovery-based analysis with tandem ionization time-of-flight mass spectrometry detection for comprehensive two-dimensional gas chromatography, Journal of Chromatography A. 1537 (2018) 99–108. doi:10.1016/j.chroma.2018.01.008.

[16] S.E. Prebihalo, K.L. Berrier, C.E. Freye, H.D. Bahaghighat, N.R. Moore, D.K. Pinkerton, R.E. Synovec, Multidimensional Gas Chromatography: Advances in Instrumentation, Chemometrics, and Applications, Anal. Chem. 90 (2018) 505–532. doi:10.1021/acs.analchem.7b04226.

[17] J.V. Seeley, S.K. Seeley, Multidimensional Gas Chromatography: Fundamental Advances and New Applications, Anal. Chem. 85 (2013) 557–578. doi:10.1021/ac303195u.

[18] P.J. Marriott, S.-T. Chin, B. Maikhunthod, H.-G. Schmarr, S. Bieri, Multidimensional gas chromatography, TrAC, Trends Anal. Chem. 34 (2012) 1–21. doi:10.1016/j.trac.2011.10.013.

[19] M. Edwards, H. Boswell, T. Górecki, Comprehensive Multidimensional Chromatography, Current Chromatography. 2 (2015) 80–109. doi:10.2174/2213240602666150722232236.

[20] K.M. Pierce, B. Kehimkar, L.C. Marney, J.C. Hoggard, R.E. Synovec, Review of chemometric analysis techniques for comprehensive two dimensional separations data, Journal of Chromatography A. 1255 (2012) 3–11. doi:10.1016/j.chroma.2012.05.050.

[21] Z. Zeng, J. Li, H.M. Hugel, G. Xu, P.J. Marriott, Interpretation of comprehensive two-dimensional gas chromatography data using advanced chemometrics, TrAC Trends in Analytical Chemistry. 53 (2014) 150–166. doi:10.1016/j.trac.2013.08.009.

[22] M.S. Klee, J. Cochran, M. Merrick, L.M. Blumberg, Evaluation of conditions of comprehensive two-dimensional gas chromatography that yield a near-theoretical maximum in peak capacity gain, Journal of Chromatography A. 1383 (2015) 151–159. doi:10.1016/j.chroma.2015.01.031.

[23] N.E. Watson, W.C. Siegler, J.C. Hoggard, R.E. Synovec, Comprehensive Three-Dimensional Gas Chromatography with Parallel Factor Analysis, Anal. Chem. 79 (2007) 8270–8280. doi:10.1021/ac070829x.

[24] W.C. Siegler, J.A. Crank, D.W. Armstrong, R.E. Synovec, Increasing selectivity in comprehensive three-dimensional gas chromatography via an ionic liquid stationary phase column in one dimension, Journal of Chromatography A. 1217 (2010) 3144–3149. doi:10.1016/j.chroma.2010.02.082.

[25] N.E. Watson, H.D. Bahaghighat, K. Cui, R.E. Synovec, Comprehensive Three-Dimensional Gas Chromatography with Time-of-Flight Mass Spectrometry, Anal. Chem. 89 (2017) 1793–1800. doi:10.1021/acs.analchem.6b04112.

[26] N.E. Watson, S.E. Prebihalo, R.E. Synovec, Targeted analyte deconvolution and identification by four-way parallel factor analysis using three-dimensional gas chromatography with mass spectrometry data, Analytica Chimica Acta. 983 (2017) 67–75. doi:10.1016/j.aca.2017.06.017.
[27] C.E. Freye, R.E. Synovec, High temperature diaphragm valve-based comprehensive two-dimensional gas chromatography with time-of-flight mass spectrometry, Talanta. 161 (2016) 675–680. doi:10.1016/j.talanta.2016.09.002.
[28] A.M. Muscalu, M. Edwards, T. Górecki, E.J. Reiner, Evaluation of a single-stage consumable-free modulator for comprehensive two-dimensional gas chromatography: Analysis of polychlorinated biphenyls, organochlorine pesticides and chlorobenzenes, Journal of Chromatography A. 1391 (2015) 93–101. doi:10.1016/j.chroma.2015.02.074.
[29] J. Luong, X. Guan, S. Xu, R. Gras, R.A. Shellie, Thermal Independent Modulator for Comprehensive Two-Dimensional Gas Chromatography, Anal. Chem. 88 (2016) 8428–8432. doi:10.1021/acs.analchem.6b02525.
[30] J.V. Seeley, N.E. Schimmel, S.K. Seeley, The multi-mode modulator: A versatile fluidic device for two-dimensional gas chromatography, Journal of Chromatography A. in press (2017). doi:10.1016/j.chroma.2017.06.030.
[31] R.B. Wilson, W.C. Siegler, J.C. Hoggard, B.D. Fitz, J.S. Nadeau, R.E. Synovec, Achieving high peak capacity production for gas chromatography and comprehensive two-dimensional gas chromatography by minimizing off-column peak broadening, Journal of Chromatography A. 1218 (2011) 3130–3139. doi:10.1016/j.chroma.2010.12.108.
[32] L.M. Blumberg, Accumulating resampling (modulation) in comprehensive two-dimensional capillary GC (GC×GC), J. Sep. Science. 31 (2008) 3358–3365. doi:10.1002/jssc.200800424.
[33] W. Khummueng, J. Harynuk, P.J. Marriott, Modulation Ratio in Comprehensive Two-dimensional Gas Chromatography, Anal. Chem. 78 (2006) 4578–4587. doi:10.1021/ac052270b.
[34] W.C. Siegler, B.D. Fitz, J.C. Hoggard, R.E. Synovec, Experimental Study of the Quantitative Precision for Valve-Based Comprehensive Two-Dimensional Gas Chromatography, Anal. Chem. 83 (2011) 5190–5196. doi:10.1021/ac200302b.
[35] C.E. Freye, H.D. Bahaghighat, R.E. Synovec, Comprehensive two-dimensional gas chromatography using partial modulation via a pulsed flow valve with a short modulation period, Talanta. 177 (2018) 142–149. doi:10.1016/j.talanta.2017.08.095.
[36] C.E. Freye, L. Mu, R.E. Synovec, High temperature diaphragm valve-based comprehensive two-dimensional gas chromatography, Journal of Chromatography A. 1424 (2015) 127–133. doi:10.1016/j.chroma.2015.10.098.
[37] C.E. Freye, B.D. Fitz, M.C. Billingsley, R.E. Synovec, Partial least squares analysis of rocket propulsion fuel data using diaphragm valve-based comprehensive two-dimensional gas chromatography coupled with flame ionization detection, Talanta. 153 (2016) 203–210. doi:10.1016/j.talanta.2016.03.016.
[38] R.B. Wilson, J.C. Hoggard, R.E. Synovec, High throughput analysis of atmospheric volatile organic compounds by thermal injection – isothermal gas chromatography – time-of-flight mass spectrometry, Talanta. 103 (2013) 95–102. doi:10.1016/j.talanta.2012.10.013.
[39] D.K. Pinkerton, B.A. Parsons, T.J. Anderson, R.E. Synovec, Trilinearity deviation ratio: A new metric for chemometric analysis of comprehensive two-dimensional gas chromatography time-of-flight mass spectrometry data, Analytica Chimica Acta. 871 (2015) 66–76. doi:10.1016/j.aca.2015.02.040.

[40] J.L. Hope, K.J. Johnson, M.A. Cavelti, B.J. Prazen, J.W. Grate, R.E. Synovec, High-speed gas chromatographic separations with diaphragm valve-based injection and chemometric analysis as a gas chromatographic "sensor," Analytica Chimica Acta. 490 (2003) 223–230. doi:10.1016/S0003-2670(03)00670-6.

[41] G.M. Gross, B.J. Prazen, J.W. Grate, R.E. Synovec, High-Speed Gas Chromatography Using Synchronized Dual-Valve Injection, Anal. Chem. 76 (2004) 3517–3524. doi:10.1021/ac049909g.

[42] H. Smith, R.D. Sacks, Column Selectivity Programming and Fast Temperature Programming for High-Speed GC Analysis of Purgeable Organic Compounds, Anal. Chem. 70 (1998) 4960–4966. doi:10.1021/ac980463b.

[43] T.-Y. Chen, M.-J. Li, J.-L. Wang, Sub-second thermal desorption of a micro-sorbent trap for the analysis of ambient volatile organic compounds, Journal of Chromatography A. 976 (2002) 39–45. doi:10.1016/S0021-9673(02)01073-7.

Chapter 3. A Study of Ultra-Fast Modulation for Comprehensive (GC×GC-TOFMS) Gas Chromatography with Multivariate Curve Resolution-Alternating Least Squares

This chapter was reproduced from H.D. Bahaghighat, C.E. Freye, R.E. Synovec, "A Study of Ultra-Fast Modulation for Comprehensive (GC×GC-TOFMS) Gas Chromatography with Multivariate Curve Resolution-Alternating Least Squares" *prepared for submission in Analytical Chemistry*

3.1 INTRODUCTION

Twenty-seven years ago, the advent of comprehensive two-dimensional (2D) gas chromatography (GC×GC) was established by Liu and Phillips in 1991.[1] This form of gas chromatography is a powerful technique tailored for the analysis of complex samples composed of analytes that are amenable to gas chromatography. The addition of a second separation dimension, 2D, provides typically a 10-fold increase in total peak capacity when compared to one-dimensional (1D) separation (1D-GC).[2,3] Liu and Phillips's work is acknowledged as the first to successfully trap analytes eluting from ^{1}D column and then reinjecting them onto ^{2}D column for the entire duration of a separation, thus opening the door to comprehensive 2D-GC. The critical component for GC×GC to perform properly is the modulator, the term used for the device or process used to transfer analytes from the ^{1}D column to the ^{2}D column.

The modulator has been called the 'heart' of GC×GC separations because it is the component of the instrument responsible for transferring analytes from ^{1}D column to the ^{2}D column with a user defined period, termed the modulation period (P_M). Current comprehensive GC×GC modulators are subdivided into three classes, thermal,[1,4–8] diaphragm valve,[9–12] and flow

modulators.[13–17] Each class of modulators functions on the basis that the modulator has the ability to trap or isolate a portion of the ^{1}D eluate, and reinject that portion on the ^{2}D column for the duration of the separation.

Thermal modulators use temperature control to trap and focus analytes as the elute from the ^{1}D column and then introduce them in a narrow pulse on the head of the ^{2}D column via rapid heating. The Liu and Phillips design was a thermal modulator that used a separation column with a thick stationary phase that was then gold plated that was routed external to the GC oven to allow trapping of the analytes at ambient room temperatures. Desorption was then accomplished with an application of DC voltage to the gold plated region, that region of column was rapidly heated to release the trapped analytes.[1] Thermal modulators are now divided into three types: resistively heated trap, heated sweeper, and cryogenic focus. The most widely used in literature is the cryogenic focus, that uses jets of cold cryogen gas (LN_2 or CO_2) to trap and heated jets of gas to release and inject onto the ^{2}D separation column. A significant research investment has been devoted recently to development of thermal modulators with the performance of cryogen jet traps without the need for large quantities of costly liquid cryogens.[18–21]

Valve-based modulators make use of a diaphragm valve to control and divert aliquots of collected ^{1}D eluate to accomplish the transfer of eluate from the ^{1}D and ^{2}D column.[10,12] Initial work with the diaphragm was plagued with two key issues, a temperature limit of 175 °C and only ~10% of the eluate from the 1D column was transferred to the 2D column.[9] Improvements via the employment of a sample loop to collect a fraction of the eluate by Seeley increased detection sensitivity and improved overall transfer to nearly 100% [10], which addressed the first concern of poor a duty cycle. The solution to the temperature limitations first came by face mounting the valve which allowed for a separation maximum temperature of 265 °C.[12] A new diaphragm valve

was recently introduced that replaced the temperature sensitive O-rings with Karez O-rings made from a perfluoroelastormer, which allows for operational temperature of 325 °C [11]. A key attribute to the operation of the diaphragm valve is the independent flow rates of the separation columns because the diaphragm valve decouples the two flows.

Flow modulation originated with Deans switching[13] originally used for another gas chromatography technique that predates 2D-GC, termed heart-cutting GC-GC, which only select portion/s of the eluate from the ^{1}D column is transferred onto a ^{2}D column. Numerous [14,22–25] research groups have devoted time exploring multiple approaches as the technique has gained popularity due to simplicity, low operational cost, lack of cryogens, and capability to modulate a wide volatility range (C_1-C_{40}+). One underlying issue associated with many methods of flow modulations relates to elevated flow rates on the ^{2}D dimension. These elevated flow rates preclude many to be used with mass spectral detectors due to exceeding the vacuum capacities of the detector, which has led to research into how to overcome this issue.[23,26,27] Seeley, in particular with two of his groups recent advances has advanced this field, first was his technique of using a pattern to transfer eluate to the ^{2}D column, instead of the normal single pulses.[17] The generated signal requires extra processing to deconvolute and transform into a GC×GC chromatogram, the resultant data had the advantage of increased signal-to-noise (S/N) and narrower width-at-base (W_b) peaks when compared to traditional flow modulation. The second advance was the introduction of the multi-mode modulator[22], that allow the user to select three different transfer duty cycles, either low duty cycle (<0.5), high duty cycle(>0.5), or full duty cycle with minimal instrumental adjustments.

Each modulator category has distinct advantages and disadvantages, but have a common function of isolating and transferring eluate from the ^{1}D column to the ^{2}D column as quickly and

efficiently as possible. Modulators have four parameters by which their performance may be evaluated; 1) duty cycle: the quantity of injected analyte on the ^{1}D column transferred to the ^{2}D separation column, 2) modulation period (P_M): speed which eluate from ^{1}D column can be modulated and placed onto the ^{2}D column, 3) injection pulse width: width of injected analyte onto the head of the ^{2}D column, and 4) resulting peak capacity ($n_{c,2D}$): total peak capacity of both 1D and 2D separation column driven in large part by the width-at-base (W_b) of peaks on both dimension.

Critical to any modulator discussed is its ability to repeatedly and precisely trap or collect eluent before reinjecting it onto the ^{2}D column while still preserving the ^{1}D separation. There are many articles written specifically discussing the evolution of modulators for the GC×GC field.[15,28–31] Normally, modulators are discussed in context of the method used for trapping/collecting the analyte and transfer to the head of the ^{2}D column. The pulse plow valve modulator, modulates the eluate in a different manner than any other currently known modulator. The form of modulation which has been termed 'partial modulation'[32] is only known to have been employed in a similar manner twice once prior in literature.[32,33] In the first, Cai and Stearns, in 2004,[32] performed a method similar to the one presented here, in which a discrete amount of carrier gas was periodically injected into the flow of the separation column. The method was referred to as 'partial modulation' that employed a custom built flow modulator to inject small pulses of carrier gas repetitively at the connection of the ^{1}D and ^{2}D columns.

Building off this method, Freye et. al., recently introduced a similar method of 'partial modulation' capable of producing peaks less than 10 ms wide with a minimum modulation period of 50 ms.[33] Using a flame ionization detector, the partial modulation method was applied to a 115-componenet test mixture with a boiling point range of (36-372 °C) using modulation periods of

50, 100, 250, and 500 ms. The modulator was developed using a Parker Hannifan Corp©; Miniature High Speed High Vacuum Dispense Valve Series 9 mounted outside the GC oven that was connected to a T-union with the ^{1}D and ^{2}D separation columns located inside the GC oven. This partial modulation technique of injecting pure carrier gas at the ^{1}D and ^{2}D union created data in which negative peaks appear in the Gaussian peaks of the ^{1}D peak profile. This method is very similar to performing vacancy chromatography on ^{1}D eluate. The technique required a three step process to convert the data into traditional 2D GC×GC chromatograms with resultant 'apparent' 2D peaks created by differentiation of the negative front created by the pulse of carrier gas.[33] This method of modulation is best suited as being considered part of the flow modulation family of techniques. The method has the advantage ultra-fast modulation, narrow injection pulse, no need for cryogens, sampling loops, trapping or desorption which has the advantage of lending the method toward generation of narrow ^{2}D peaks.

Utilizing the new ultra-fast pulse flow modulator first introduced by Freye et.al., the Parker Hannifan Corp©; Miniature High Speed High Vacuum Dispense Valve, Series 9 will be demonstrated for GC×GC-TOFMS application. Applying the pulse valve flow modulator to a GC×GC-TOFMS system was deemed important for evolution of the technique for two reasons; captability with a system at vacuum (1×10^{-7} Torr), and modulation performance with helium as the carrier gas.

During testing and development of the pulse valve flow modulator, it had been determined that a P_M of 50 ms was the shortest duty cycle the Parker Hannifin Series 9 valve would support. For the TOFMS study it was decided to use 50 ms to demonstrate the valve's maximum performance and their effects on the vacuum system. The extremely short modulation period, P_M of 50 ms will be examined, which is fourfold faster than the shortest previously reported PM of

200 ms.[34] Another important performance parameter using the pulse flow valve modulator is the injection pulse of a mere 2 ms, which contributes to extremely narrow ^2W_b peaks previously reported. This type of modulation is similar to vacancy chromatography, discussed later, which is an old method that has been used with some success in liquid chromatography.[35–38] For this study, a separation of a 18-component test mixture of low boilers at seven different concentrations will be examined using P_M of 50 ms.

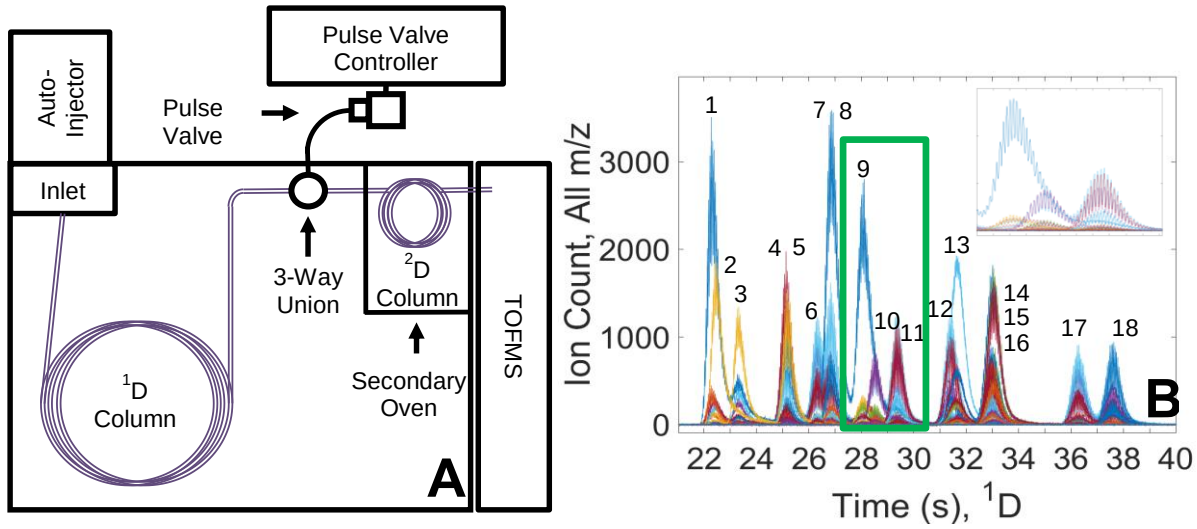

Figure 3.1. Instrumental Schematic GC×GC-TOFMS, 18-Component Data.

(**A**) Schematic of the major components of the GC×GC-TOFMS instrument. A pulse flow valve and three-way union was implemented to serially link the ^{1}D and ^{2}D columns. Modulation occurs via the pulse flow valve at the three-way union linking the ^{1}D and ^{2}D columns. (**B**) Raw (preprocessed) chromatogram (mass channels 35-225) of the 18 component mixture collected using a modulation period, P_M of 50 ms. The highlighted region contains analytes (9: ethyl acetate, 10: 1-hexyne, 11: methylcyclopentane) is shown in the inset to better represent the modulation of the pulse flow valve. These three analytes will be studied in detail as part of the demonstration of pulse valve modulation along with data deconvolution. Injected concentration shown is 14 ng per analyte.

3.1.1 *Pulse Flow Valve Modulation Theory*

The pulsed flow valve modulator (Figure 3.1A), modulates the analytes as they exit the ^{1}D column by injecting a narrow pulse of carrier gas perpendicular to the flow separation gas at the T-union that joins the ^{1}D and ^{2}D separation columns. This injection of carrier gas has two effects on the signal, it first creates a vacancy in the signal of the analyte, and secondly that vacancy is manifest as an error function that mimics frontal analysis of signal.

Vacancy chromatography is not a commonly used technique despite it having characteristics that lend it applicable to process monitoring. In process monitoring a mobile phase would contain a solute at a concentration that is continually passed through a column till equilibrium is achieved at both the inlet and outlet. If a pulse of pure carrier gas were to be injected a negative peak profile would be created and pass through the column the same way a positive peak would be expected to pass through. In a similar manner the pulse flow valve modulator injects carrier gas at a user defined time period creating vacancies in the signal. The key difference from traditional vacancy chromatograph and the pulse flow valve is it is not performed on analytes at equilibrium along the length of the column, but rather on Gaussian ^{1}D peaks resulting from the elution of analytes from the ^{1}D separation column.

The results of partial modulation by carrier gas created by the pulse flow valve are displayed as error functions as seen in Figure 3.1B. In this technique the error functions contain the critical chromatographic information that are analyzed using a modified frontal analysis technique. Frontal analysis is a form of chromatography where a continuous flow of analytes passes through a column, each component elutes at a different time depending on its affinity for the stationary phase of the column.[39–41] This type of analysis traditionally is used for liquid chromatography and the resulting appearance of analytes would only happen once for a separation

as the solution elutes from the column. In the current application, the combination of the principles of vacancy chromatography and frontal analysis occurs with each pulse of the valve, with the production of an error functions encoded with the critical chromatographic information. The concept is shown in Figure 1.4 showing the modulation of a single analyte using pulse flow valve with the conversion of raw data into a typical 2D GC×GC chromatogram. The process for conversion of the data will be discussed in more detail in the results and discussion section.

3.1.2 *Data Analysis/Chemometrics*

Data generated by the pulse flow valve modulator, Figure 3.1B, is processed in a similar process[33] first developed by Freye et. al. for processing the univariate data generated by the flame ionization detector. The process was adapted to incorporate MCR-ALS loadings used to deconvolute the data generated using the TOFMS which replaces the univariate data generated in the previous work. Peak deconvolution methods are important to addressing the challenges of analyte identification, quantification, and peak purity. Two deconvolution techniques are commonly used to separate and help identify analytes are parallel factor analysis (PARAFAC) and multivariate curve resolution alternating least squares (MCR-ALS). Both PARAFAC and MCR-ALS are based on alternating least squares decomposition requiring at least three-way trilinear data. MCR-ALS is an iterative method that initially estimates the pure chromatographic profiles and pure spectra and repetitively alternates and tests these values for convergence.[42,43] MCR-ALS operates essentially the same as PARAFAC, but is more forgiving to data that is not as well aligned as PARAFAC requires. For that reason, MCR-ALS was chosen to deconvolute the data generated by the GC×GC –TOFMS and identify the analytes. The results of MCR-ALS will be discussed in detail in the discussion section of the paper.

Applying the previously developed technique, the MCR-ALS loadings will be processed to generate Gaussian peaks (Figure 3.3B) in the second dimension as the result of differentiation of the error function now found in the MCR-ALS loading Figure 2B. These peaks widths will hence forth be referred to as 'apparent' width-of-base due to the fact that the peaks are not the result of traditional Gaussian peaks, but rather the mathematical results of the differentiation of the negative slope of the MCR-ALS loadings error function. Once these steps are complete the final 1-D chromatogram (Figure 3.3B) is complete. A standard cut and fold technique, whereby the data is divided and stacked by the P_M to produced 2D chromatograms (Figure 3.3C,D).

3.2 EXPERIMENTAL

A Pegasus 4D GC × GC/TOFMS (LECO Corporation, St. Joseph, MI) with an integrated Agilent 6890N gas chromatograph (Agilent Technologies, Santa Clara, CA, U.S.A.) was modified to evaluate the pulse flow valve modulator as shown in Figure 3.1A. A high-speed pulse valve, series 9, model 009–1643-900 (Parker Hannifin, Hollis, NH, USA), was mounted outside the oven. An in-house connection was used to connect the valve to a 3-way T-union inside the GC oven. The pulse flow valve was controlled using LabVIEW 8.2 (National Instruments, Austin, TX, USA) interfaced to a National Instruments data acquisition board. The high-speed pulse valve was utilized as the modulator at the T-union connection of the ^{1}D and ^{2}D separation columns. The stock thermal modulator and secondary oven were not used for this experiment. Detection was accomplished with a LECO Pegasus 4D TOFMS. Effluent was passed through a 0.33 m, 280 °C transfer line into the TOFMS where is was analyzed at a scan rate 500 Hz, between 35 and 225 Da. Samples were introduced to the GC×GC via a 7683B auto-injector (Agilent Technologies, Palo Alto, CA, USA). The inlet was set to 250 °C. The ^{1}D column was a SPB-5 (5% diphenyl / 95% dimethyl siloxane) stationary phase: 3 m length, 100 μm inner diameter (i.d.), and 0.1 μm

film thickness. The ^{2}D column was a DB-Wax (polyethylene glycol) stationary phase: 1.0 m length, 100 µm i.d., and 0.100 µm film thickness. Prior to each sample injection, HPLC grade dichloromethane obtained from EMB Chemicals was used as a solvent rinse. Ultra-high purity helium (Grade 5, 99.999%) was used as the carrier gas (Praxair, Seattle, WA, USA) at a constant flow of 90.0 psig (4.2 ml/min) and the pulse valve flow modulator pressure was held at 90.0 psig.

A test mixture of 18 analytes (v/v) was used to evaluate analytical performance. The samples were diluted by a factor of two from neat to 64:1. The test mixture (Table 3.1) contained a narrow range of boiling points that was intentionally developed to produce several areas of overlap on the ^{1}D (Resolution (R_s) < 0.5).

Elution	Name	Boiling Point (°C)	Supplier	Purity (%)	*m/z*
1	acetone	56	Sigma-Aldrich	99.9	**43**, 58
2	isopropyl alcohol	83	Sigma-Aldrich	99.7	**45**
3	2-methyl-2-propanol	82	Sigma-Aldrich	99.5	**59**, 57, 60
4	t-butyl methyl ether	55	Sigma-Aldrich	99.8	**73**, 57, 74
5	cyclopentane	49	Sigma-Aldrich	99.0	**42**, 70, 55
6	1-hexene	63	Sigma-Aldrich	97.0	56, **41**, 84, 69, 55
7	hexane	68	Sigma-Aldrich	97.0	57, **86**, 42, 71
8	2-butanone	80	Sigma-Aldrich	99.0	43, **72**, 57
9	ethyl acetate	77	J.T. Baker	99.9	**43**, 61, 70, 88
10	1-hexyne	71	Sigma-Aldrich	97.0	**67**, 41, 54, 81
11	methylcyclopentane	72	Honeywell	97.0	56, **69**, 55, 84
12	1-chlorobutane	79	Sigma-Aldrich	99.5	**56**, 41, 91, 94
13	1,2-dichloroethane	83	Sigma-Aldrich	99.8	**62**, 64, 49, 98, 100
14	cyclohexane	81	Sigma-Aldrich	99.0	**56**, 84, 55, 69, 41
15	benzene	80	Fisher Chemical	99.0	**78**, 77, 51, 50, 52
16	carbon tetrachloride	77	Sigma-Aldrich	99.9	**117**, 119, 121, 82
17	1-heptene	94	Sigma-Aldrich	97.0	56, 70, **98**
18	heptane	98	Fisher Chemical	99.4	43, **71**, 85, 100

Table 3.1. 18-Component Test Mixture.
The 18 compounds were combined by volume at approximately equal proportions with a neat mixture concentration of 56 ng per analyte injected (56 parts per thousand). A serial dilution in Toluene (neat – 64:1) (56 ng – 0.087 ng per analyte injected) was used for performance evaluation of the system. Selection mass channels are listed, the first is the dominant, bold is the selective ion.

A 0.1 µl volume of the test mixture was injected at a split of 80:1. Based on injection conditions, the on-column quantity of each analyte ranged (56 ng, neat - 0.88 ng, 64:1). The oven was held isothermal at 50 ˚C for the duration of the separation with no secondary oven temperature offset. Various modulation periods were studied: P_M of 50, 75, 250, 500 all using an injection pulse width of 2 ms, P_M 50 ms will be shown and discussed in the results section.

All data were collected using ChromaTOF 3.32 and transferred to MATLAB 2016b (The Mathworks, Natick, MA, U.S.A.) using in-house software (peg2mat3p8).37 All chromatograms were baseline-corrected in a 1D fashion prior to any other processing. Compounds were identified in two manners, first through a library search utilizing MS Search 2.0 (NIST, Gaithersburg, MD, U.S.A.) using ChromaTOF 3.32. Second, the compounds were identified and matched to an in-house created library of compound spectra using MATLAB 2016b software (wdotmatch4_new). All chemometrics and multidimensional visualization was achieved using functions and utilities included with MATLAB 2016b. The peak widths (W_b) and retention times (t_R) of the 18 representative compounds were measured by Gaussian curve fitting utilizing the Curve Fitting toolbox available as an add-on application for MATLAB 2016b.

3.3 Results and Discussion

Data collected from the 18-component test mixture (Table 3.1) using the GC×GC-TOFMS with partial modulation from the pulse valve flow modulator is presented in Figure 3.1B. Prior to data processing with MCR-ALS the spectral data was only baseline corrected. No further processing prior to MCR-ALS was performed nor was needed. In this example all mass channels (34-225) are shown with a P_M of 50 ms. Six regions of overlap (R_s < 1.0) are observed (analytes 1-3, 4-5, 6-8, 9-11, 12, 14-16), the overlapped region containing analytes 9: ethyl acetate, 10: 1-hexyne, 11: methylcyclopentane are highlighted in the insert. This chromatogram is a result of

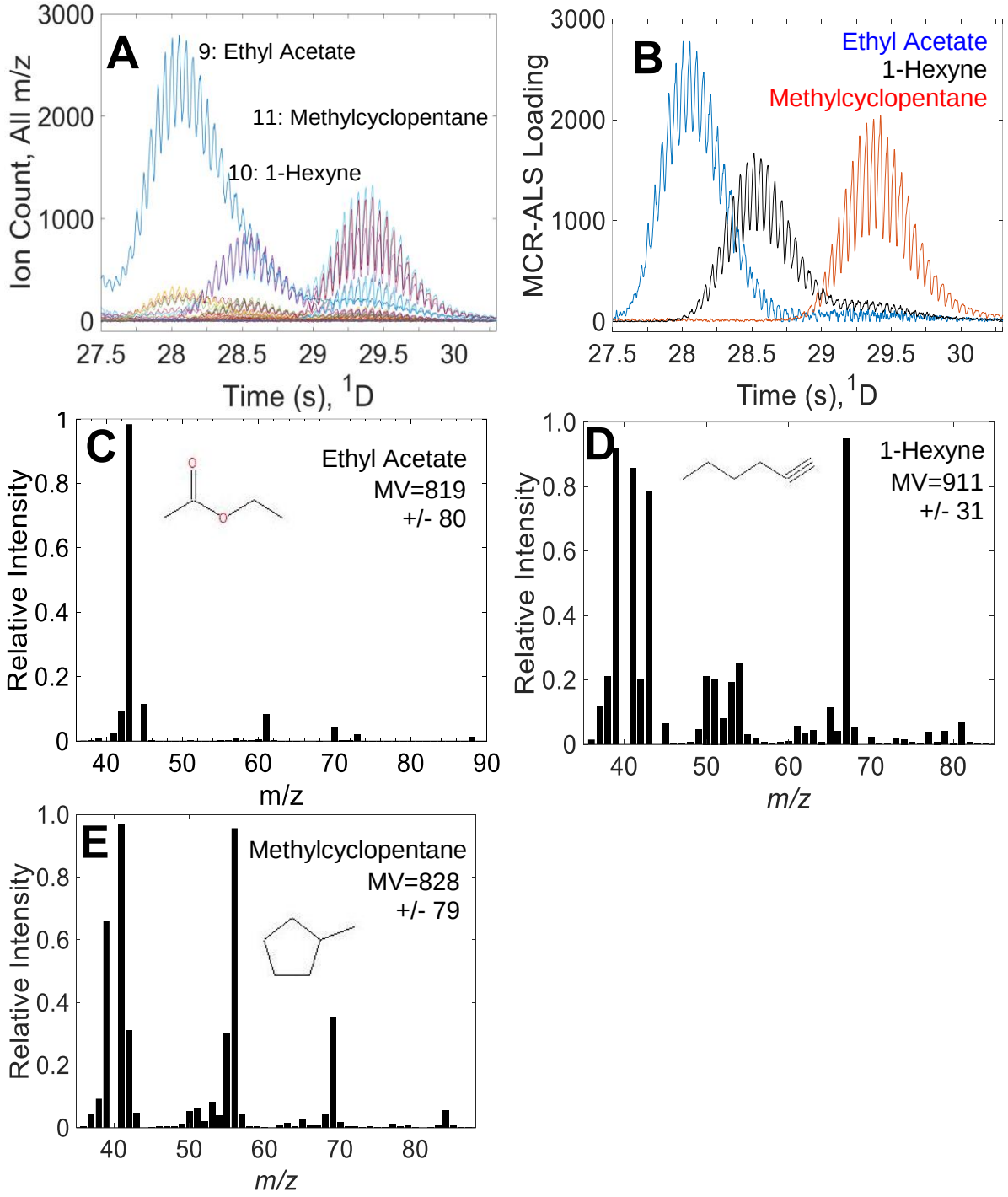

Figure 3.2. MCR-ALS Loadings and Match Values for Three Select Analytes.
(**A**) Raw data of analytes (9-11) is from a separation at an approximate concentration of 14 ng injected, (14 parts per thousand) is shown. (**B**) Unconstrained MCR-ALS loadings of analytes, 9-11. The pulse valve modulation is retained in the loadings. (**C-E**) The mass spectral data from each MCR-ALS loading is compared to pure in-house spectra of the respective analytes. Analyte structure, match value and standard deviation across four separations list shown for each analyte.

2014

analysis of a 4:1 dilution injection, each analyte is at an approximate concentration of 14 ng injected. This region will be studied in detail for performance of the modulator and application of MCR-ALS for data deconvolution. For detailed information concerning the chromatographic performance of all analytes, resolution and match values, please see supplemental Tables 3.1 and 3.2 respectively. Seen in the insert of Figure 3.1B, is the pattern of modulations produced by the partial modulation of pulse valve flow modulator. Each modulation in this example are 50 ms apart and are caused by the 2 ms pulse of carrier gas at the union of the ^{1}D and ^{2}D columns.

Deconvolution and analyte identification were accomplished using MCR-ALS with a combination of in-house written script and toolbox add-on. The method of MCR-ALS application was a non-targeted, unconstrained application that used no form of filters or thresholds to deconvolute and identify the analytes. Detailed results of MCR-ALS analysis including MCR-ALS loadings (Figure 3.2B) and spectral match values (Figures 3.2C-E) on analytes 9-11 can be seen in Figure 3.2. Figure 3.2A, shown are the mass channels in the region containing analytes 9: ethyl acetate, 10: 1-hexyne, 11: methylcyclopentane. The resulting MCR-ALS loadings of the three analytes are shown in Figure 3.2B, with the position of each analyte easily noted. Each of the loadings are comprised of their respective mass channels assigned to each analyte. The mass channels associated with each loading are shown in Figs 3.2C-D, with relative intensity, with reported average match values and standard deviation for all four separations of the analytes at the 4:1 dilution. Reported match values were generated by comparison of the loading spectra (Fig 3.2C-E) to pure spectra of the analytes generated on the LECO Pegasus 4D TOFMS, at the same time of the study without modulation. The resolution (R_S) between 9: ethyl acetate and 10: 1-hexyne was determined to be 0.53, and between 10: 1-hexyne and 11-methylcyclopentane of 0.91.

Resolution, match value, and relative standard deviation for all 18 analytes at the 4:1 dilution concentration are summarized in Table B.1.

For one to fully appreciate the unique form of partial modulation, it is needed to develop a simple and straightforward method to convert the resultant data (Figure 3.2A) into a vector chromatogram that is composed of 'apparent' ^{2}D peaks. Following previous work using the pulse valve modulator,[33] the loadings (Figure 3.3A) generated by MCR-ALS are converted from loadings to the 'apparent' ^{2}D peaks in a three-step process. First the loadings are differentiated, converting the sharp leading edge of the vacancy pulse, which creates the resulting ^{2}D peak. In the second step the differentiated data is inverted to finish the process of inversion. The return portion (decay) of the signal results in mild baseline sag that is easily removed in the third step by which an in-house low frequency filter is applied to remove baseline sag. For a detailed figure of merit addressing this process please refer to figure 1 of the 2018 partial modulation paper.[33] The resultant final vector chromatogram composed of ^{2}D peaks is shown in Figure 3.3B. The differentiated peaks shown do exhibit a high sampling density due to an average $^{1}W_{b}$ 0.95 for the three analytes shown. Ethyl acetate exhibited a $^{2}W_{b}$ of 29 ms with a standard deviation of 0.8 ms, 1-hexyne exhibited a $^{2}W_{b}$ 27 ms with a standard deviation of 1.1 ms and methylcyclopentane exhibited a $^{2}W_{b}$ of 22 ms with a standard deviation of 0.8 ms. The data is now folded at the modulations, in this case 50 ms which with the collection frequency of 500 Hz is 25 data points,

to create the traditional 2D contour chromatogram of data as shown in Figure 3.3C, the data was registered 10 ms to remove wrap around in the image. A more traditional 2D chromatogram is shown in Figure of 3.3D. The 2D chromatogram in Figure 3.3D highlights the oversampling caused by the P_M of 50 ms.

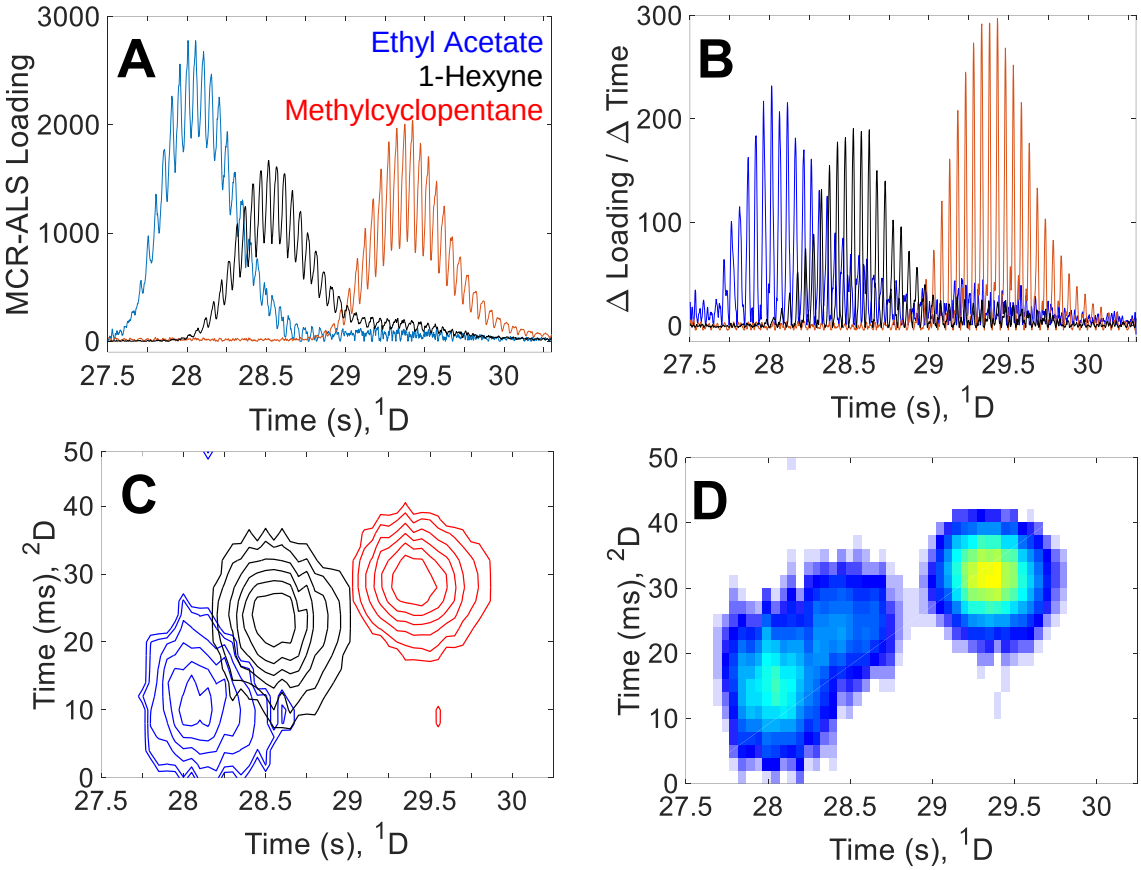

Figure 3.3. MCR-ALS Loadings and Final 1D and 2D Chromatograms.

(**A**) Loadings of analytes 9-11, as seen in figure 2B. (**B**) Processed differentiated loadings in the 1D vector form. The colors of analytes corresponded to names in Figure 3A. (**C**) 2D contour chromatogram generated from the processed data in Figure 3B. (**D**) 2D chromatogram shown in the more traditional form. Processing data in this manner is useful to visualize retention times on ^{2}D dimension. Data was adjusted 10 ms for visualization purposes for both Figure 3C and 3D.

To quantify the performance of the GC×GC-TOFMS utilizing the pulse flow modulator, the MCR-ALS loading areas were utilized. Shown in Figure 3.4A are the average MCR-ALS

loading areas with error bars of four separations at each of the seven concentrations injected of analytes 9, 10, and 11. Of note, one of the separation runs for the 16:1 dilution (3.5 ng mass injected) was compromised and resultant data was not used for this study. To remove injector variance, all data was normalized using compound 17: heptane as the internal standard. All three analytes exhibited R^2 values of 0.999. Inset in Figure 3.4A shows details at the lower concentrations. This data which is taken from analytes (9-11) all of which have resolutions higher than 0.3 to determine the quantitative performance of the GC×GC-TOFMS separation combined with MCR-ALS used for deconvolution. Positive performance such as these is expected for analytes with resolution values above 0.3, as noted by recent research into probability of achieving a successful quantitative analysis for GC-MS data.[44]

Match values along with an average standard deviation across the span of concentrations is show in Figure 3.4B. Match values has a notable decrease in performance as the injected concentration decreases. This trend correlates with the decrease in signal-to-noise and again is supported by past research.[44] Despite the decreased match values at lower concentrations, analytes were readily identified by MCR-ALS with an overall separation (at concentration of 14 ng/analyte) average match value of all analytes at 822, with an average RSD of 7%. All match values were determined by comparison of results with spectra generated by injection of lone analytes.

During the study of performance of MCR-ALS for the 18-componenet data set it was shown to deteriorate at reduced resolutions (below 0.3) in regards to loading area error, and in decreased match values as the signal-to-noise decreased below ~10. The general trend of deconvolution performance for MCR-ALS loading area, and reduced match values agrees with previous work[44] that showed that as analytes S/N decreased, match values decreased rapidly.

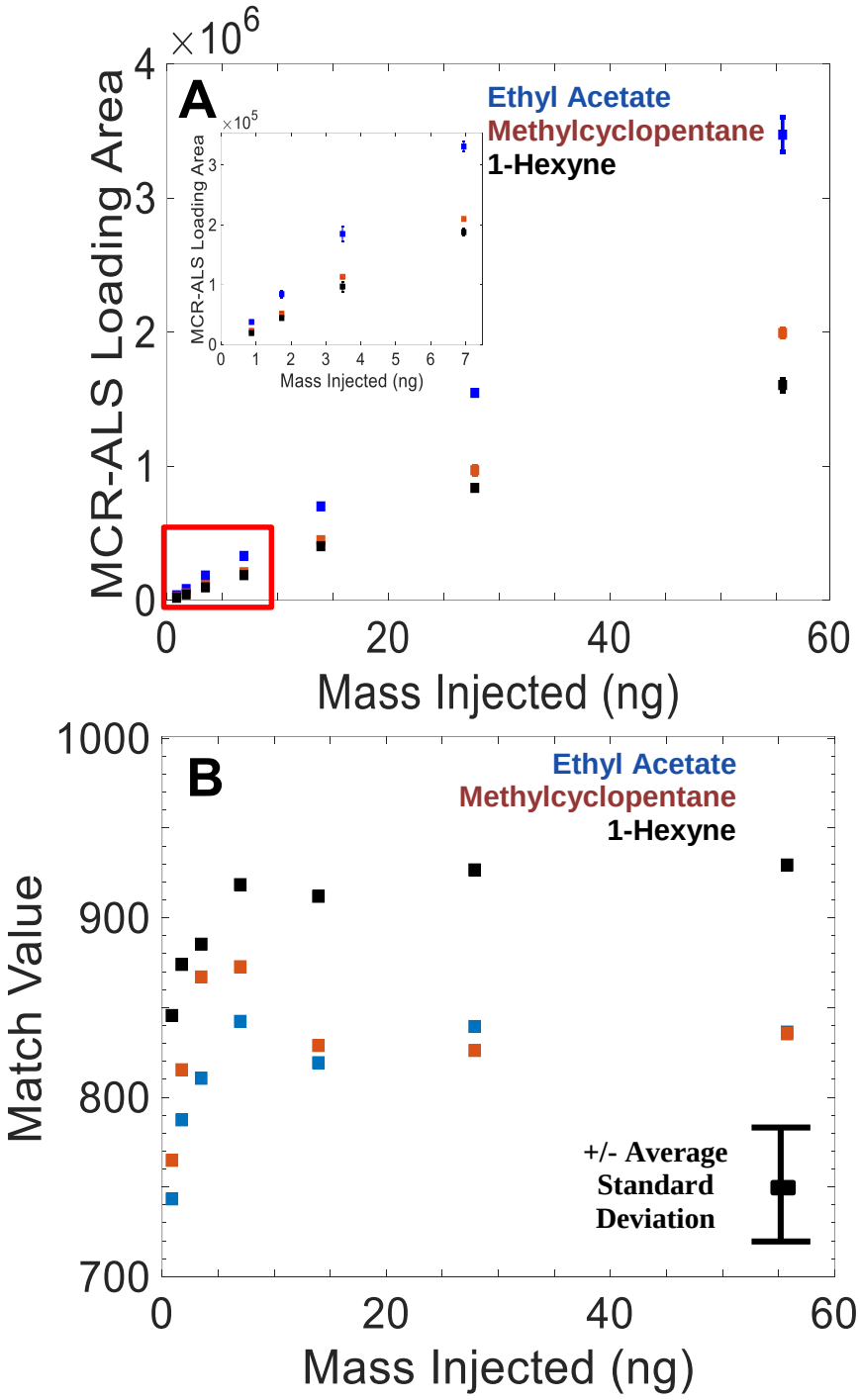

Figure 3.4. Loadings and Match Values vs. Mass Injected.

(**A**) MCR-ALS Loading area results based on mass injected for analytes 9-11 are shown. Inset shown for detail of lower inject concentrations. R2 values of 0.999 were achieved for the three analytes in question. (**B**) Match values for all concentrations are shown with average error bar shown for the three analytes. The decrease in match values is evident at lower

2083

That study also showed a similar trend-as resolution fell below 0.3, the percent error of loading area increased rapidly. The current data gathered supports the estimated performance of MCR-ALS and shows trends in both poor performances in loading area error at low resolution and decreased match values at lower signal-to-noise. Figures of merit are shown for analytes 4: t-butyl methyl ether and 5: cyclopentane with a resolution of 0.06 that demonstrates MCR-ALS struggles to properly assign the correct loading to the respective analyte as shown in Figure B.3. These results, especially the calibration curve data, is a further example of the limits of MCR-ALS to properly deconvolute analytes with a resolution less than 0.3.

Following the same approach of data processing as shown in Figure 3.3, the raw data was converted to MCR-ALS loadings for the entire 18 analyte separation (Figure 3.5A) then differentiated, and finally cut and folded to generate the 2D chromatogram shown in Figure 3.5B. Analyte 13: 1,2-dichloroethane that elutes at $^{1}t_{R}$ of 32 seconds exhibits an unusual behavior of minimal partial modulation, this behavior results in the analyte generating extremely low intensity of 'apparent' ^{2}D peaks during the differentiation phase of data processing. For that reason, the analyte that is seen in Figure 3.5A at $^{1}t_{R}$ 32 second fails to show up in the 2D chromatogram in Figure 3.5B. This behavior is attributed to the analyte being highly retained on the ^{2}D wax stationary phase, which causes the vacancy and resulting front form generated by the pulse valve flow modulator to be dramatically reduced. However, despite such an unfortunate behavior, the analyte was still easily separated and identified with a match value of 855 and an RSD of 2.18%.

Chromatographic performance of the separation measured using the 4:1 dilution (14 ng/analyte injected) was deemed to be a good representative concentration to examine performance. Data collection rate of 500 Hz for the TOFMS limits the

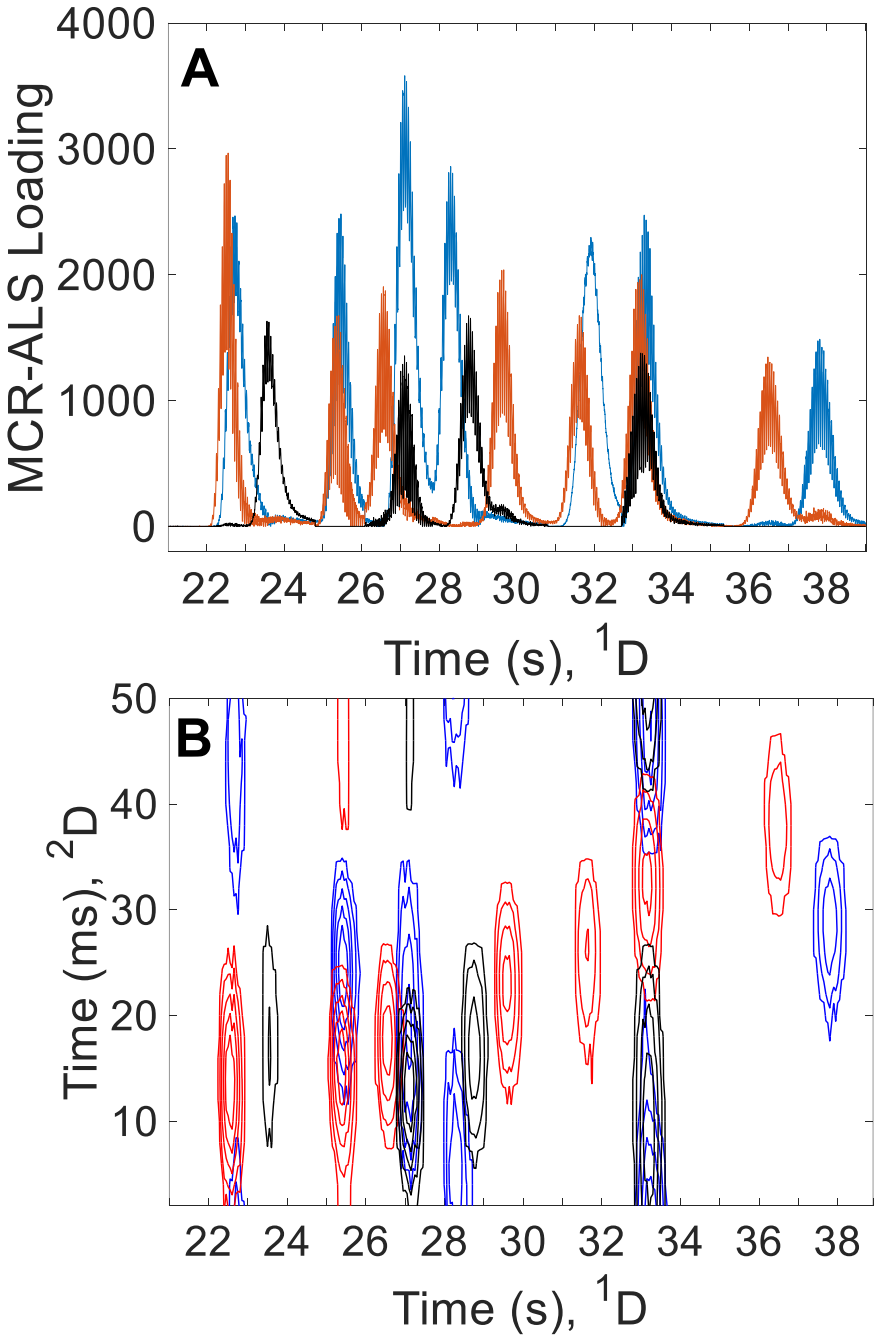

2106

Figure 3.5. MCR-ALS Loadings and 2D Chromatogram, 18-Component Mixture

(**A**) MCR-ALS loadings for all 18 analytes is shown at an injected 14 ng (14 parts per thousand) concentration. Various colors were used to help the reader distinguish the overlapped regions. Analyte (13: 1,2-dichloroethane) was highly retained on the ^{2}D DB-Wax column resulting in loss of the pulse valve flow modulator's pattern of partial modulation. (**B**) 2D Chromatogram generated from the differentiated loadings as demonstrated in Figure 3B and 3D. Analyte 1,2-dichloroethane is not shown in the 2D chromatogram due to lack of pulse valve modulations which results in data that is not readily differentiated to produce apparent ^{2}D peaks

measuring performance of the pulse flow valve modulator, as each data point takes 2 ms, thus only 25 data points can be acquired for the entire modulation period. Higher collection rate at 10,000 Hz has been used before, which affords a significant improvement in precision when measuring ^{2}D performance. All data are shown in Table B.2 in the supplemental figures. For the ^{2}D performance, the average standard deviation for ^2t_R was 0.54 ms, the average relative standard deviation percentage was 3.50%. For the ^2W_b performance the average standard deviation was 0.92 ms, and the average relative standard deviation was 3.75%.

3.4 CONCLUSIONS

A novel pulse flow valve modulator for GC×GC-TOFMS has been demonstrated, which is capable ultra-fast modulations while being compatible with a time-of-flight mass spectrometry. Also, an innovative method of unrestricted deconvolution and data processing was developed that allows for analyte identification and creation of traditional 2D chromatograms. Herein, we presented data which supports this assertion. The addition of this type of flow modulator to a mass spectral detector is a further step in exploration of the benefits of an ultra-fast, low cost, high duty cycle modulator. If one were able to create sufficiently narrow peaks on the ^{1}D to support the pulse valve flow modulators minimum modulation time of 50 ms, one could imagine that 2D peak capacity production of 1000 peaks per minute is a reasonable expectation. Further studies targeted towards creating high peak capacities along with novel data interpretation will help leverage the potential of the pulse valve modulator. The pulse flow valve modulator has shown to be a very interesting new modulator, not suffering from common modulator issues like breakthrough, desorption, or loss of analyte signal concerns.

3.5 REFERENCES

(1) Liu, Z.; B. Phillips, J. Comprehensive Two-Dimensional Gas Chromatography Using an On-Column Thermal Modulator Interface. *J. Chromatogr. Sci.* **1991**, *29*, 227–231.

(2) Klee, M. S.; Cochran, J.; Merrick, M.; Blumberg, L. M. Evaluation of Conditions of Comprehensive Two-Dimensional Gas Chromatography That Yield a near-Theoretical Maximum in Peak Capacity Gain. *J. Chromatogr. A* **2015**, *1383*, 151–159.

(3) Blumberg, L. M. Flow Optimization in One-Dimensional and Comprehensive Two-Dimensional Gas Chromatography. *J. Chromatogr. A* **2018**, *1536*, 27–38.

(4) de Geus, H.-J.; de Boer, J.; Brinkman, U. A. T. Development of a Thermal Desorption Modulator for Gas Chromatography. *J. Chromatogr. A* **1997**, *767* (1), 137–151.

(5) Burger, B. V.; Snyman, T.; Burger, W. J. G.; van Rooyen, W. F. Thermal Modulator Array for Analyte Modulation and Comprehensive Two-Dimensional Gas Chromatography. *J. Sep. Sci.* **2003**, *26* (1–2), 123–128.

(6) Marriott, P. J.; Kinghorn, R. M. Longitudinally Modulated Cryogenic System. A Generally Applicable Approach to Solute Trapping and Mobilization in Gas Chromatography. *Anal. Chem.* **1997**, *69* (13), 2582–2588.

(7) Ledford, E. B.; Billesbach, C. Jet-Cooled Thermal Modulator for Comprehensive Multidimensional Gas Chromatography. *J. High Resolut. Chromatogr.* **2000**, *23* (3), 202–204.

(8) Harynuk, J.; Górecki, T. New Liquid Nitrogen Cryogenic Modulator for Comprehensive Two-Dimensional Gas Chromatography. *J. Chromatogr. A* **2003**, *1019* (1), 53–63.

(9) Bruckner, C. A.; Prazen, B. J.; Synovec, R. E. Comprehensive Two-Dimensional High-Speed Gas Chromatography with Chemometric Analysis. *Anal. Chem.* **1998**, *70* (14), 2796–2804.

(10) Seeley, J. V.; Kramp, F.; Hicks, C. J. Comprehensive Two-Dimensional Gas Chromatography via Differential Flow Modulation. *Anal. Chem.* **2000**, *72* (18), 4346–4352.

(11) Freye, C. E.; Mu, L.; Synovec, R. E. High Temperature Diaphragm Valve-Based Comprehensive Two-Dimensional Gas Chromatography. *J. Chromatogr. A* **2015**, *1424*, 127–133.

(12) Sinha, A. E.; Prazen, B. J.; Fraga, C. G.; Synovec, R. E. Valve-Based Comprehensive Two-Dimensional Gas Chromatography with Time-of-Flight Mass Spectrometric Detection: Instrumentation and Figures-of-Merit. *J. Chromatogr. A* **2003**, *1019* (1), 79–87.

(13) Deans, D. R. A New Technique for Heart Cutting in Gas Chromatography [1]. *Chromatographia* **1968**, *1* (1–2), 18–22.

(14) Seeley, J. V.; Micyus, N. J.; Bandurski, S. V.; Seeley, S. K.; McCurry, J. D. Microfluidic Deans Switch for Comprehensive Two-Dimensional Gas Chromatography. *Anal. Chem.* **2007**, *79* (5), 1840–1847.

(15) Edwards, M.; Mostafa, A.; Górecki, T. Modulation in Comprehensive Two-Dimensional Gas Chromatography: 20 Years of Innovation. *Anal. Bioanal. Chem.* **2011**, *401* (8), 2335–2349.

(16) Duhamel, C.; Cardinael, P.; Peulon-Agasse, V.; Firor, R.; Pascaud, L.; Semard-Jousset, G.; Giusti, P.; Livadaris, V. Comparison of Cryogenic and Differential Flow (Forward and Reverse Fill/Flush) Modulators and Applications to the Analysis of Heavy Petroleum Cuts by High-Temperature Comprehensive Gas Chromatography. *J. Chromatogr. A* **2015**, *1387*, 95–103.

(17) Seeley, J. V.; Seeley, S. K. Comprehensive Two-Dimensional Gas Chromatography with Pattern Modulation. *J. Chromatogr. A* **2015**, *1421*, 114–122.

(18) Robson, W. J.; Sutton, P. A.; McCormack, P.; Chilcott, N. P.; Rowland, S. J. Class Type Separation of the Polar and Apolar Components of Petroleum. *Anal. Chem.* **2017**, *89* (5), 2919–2927.

(19) Luong, J.; Guan, X.; Xu, S.; Gras, R.; Shellie, R. A. Thermal Independent Modulator for Comprehensive Two-Dimensional Gas Chromatography. *Anal. Chem.* **2016**, *88* (17), 8428–8432.
(20) Jacobs, M. R.; Edwards, M.; Górecki, T.; Nesterenko, P. N.; Shellie, R. A. Evaluation of a Miniaturised Single-Stage Thermal Modulator for Comprehensive Two-Dimensional Gas Chromatography of Petroleum Contaminated Soils. *J. Chromatogr. A* **2016**, *1463*, 162–168.
(21) Muscalu, A. M.; Edwards, M.; Górecki, T.; Reiner, E. J. Evaluation of a Single-Stage Consumable-Free Modulator for Comprehensive Two-Dimensional Gas Chromatography: Analysis of Polychlorinated Biphenyls, Organochlorine Pesticides and Chlorobenzenes. *J. Chromatogr. A* **2015**, *1391*, 93–101.
(22) Seeley, J. V.; Schimmel, N. E.; Seeley, S. K. The Multi-Mode Modulator: A Versatile Fluidic Device for Two-Dimensional Gas Chromatography. *J. Chromatogr. A* **2017**, *in press*.
(23) Franchina, F. A.; Maimone, M.; Tranchida, P. Q.; Mondello, L. Flow Modulation Comprehensive Two-Dimensional Gas Chromatography–mass Spectrometry Using ≈4mLmin−1 Gas Flows. *J. Chromatogr. A* **2016**, *1441*, 134–139.
(24) Gorovenko, R.; Krupčík, J.; Špánik, I.; Bočková, I.; Sandra, P.; Armstrong, D. W. On the Use of Quadrupole Mass Spectrometric Detection for Flow Modulated Comprehensive Two-Dimensional Gas Chromatography. *J. Chromatogr. A* **2014**, *1330* (Supplement C), 51–60.
(25) Freye, C. E.; Moore, N. R.; Synovec, R. E. Enhancing the Chemical Selectivity in Discovery-Based Analysis with Tandem Ionization Time-of-Flight Mass Spectrometry Detection for Comprehensive Two-Dimensional Gas Chromatography. *J. Chromatogr. A* **2018**, *1537*, 99–108.
(26) Gorovenko, R.; Krupčík, J.; Špánik, I.; Bočková, I.; Sandra, P.; Armstrong, D. W. On the Use of Quadrupole Mass Spectrometric Detection for Flow Modulated Comprehensive Two-Dimensional Gas Chromatography. *J. Chromatogr. A* **2014**, *1330*, 51–60.
(27) Krupčík, J.; Gorovenko, R.; Špánik, I.; Sandra, P.; Armstrong, D. W. Flow-Modulated Comprehensive Two-Dimensional Gas Chromatography with Simultaneous Flame Ionization and Quadrupole Mass Spectrometric Detection. *J. Chromatogr. A* **2013**, *1280*, 104–111.
(28) Marriott, P. J.; Chin, S.-T.; Maikhunthod, B.; Schmarr, H.-G.; Bieri, S. Multidimensional Gas Chromatography. *TrAC Trends Anal. Chem.* **2012**, *34*, 1–21.
(29) Kulsing, C.; Nolvachai, Y.; Rawson, P.; Evans, D. J.; Marriott, P. J. Continuum in MDGC Technology: From Classical Multidimensional to Comprehensive Two-Dimensional Gas Chromatography. *Anal. Chem.* **2016**, *88* (7), 3529–3538.
(30) Seeley, J. V. Recent Advances in Flow-Controlled Multidimensional Gas Chromatography. *J. Chromatogr. A* **2012**, *1255*, 24–37.
(31) Tranchida, P. Q.; Purcaro, G.; Dugo, P.; Mondello, L. Modulators for Comprehensive Two-Dimensional Gas Chromatography. *TrAC Trends Anal. Chem.* **2011**, *30* (9), 1437–1461.
(32) Cai, H.; Stearns, S. D. Partial Modulation Method via Pulsed Flow Modulator for Comprehensive Two-Dimensional Gas Chromatography. *Anal. Chem.* **2004**, *76* (20), 6064–6076.
(33) Freye, C. E.; Bahaghighat, H. D.; Synovec, R. E. Comprehensive Two-Dimensional Gas Chromatography Using Partial Modulation via a Pulsed Flow Valve with a Short Modulation Period. *Talanta* **2018**, *177*, 142–149.
(34) Wilson, R. B.; Siegler, W. C.; Hoggard, J. C.; Fitz, B. D.; Nadeau, J. S.; Synovec, R. E. Achieving High Peak Capacity Production for Gas Chromatography and Comprehensive Two-Dimensional Gas Chromatography by Minimizing off-Column Peak Broadening. *J. Chromatogr. A* **2011**, *1218* (21), 3130–3139.
(35) Mori, M.; Itabashi, H.; Helaleh, M. I. H.; Kaczmarski, K.; Głód, B.; Kowalska, T.; Xu, Q.; Ikedo, M.; Hu, W.; Tanaka, K. Vacancy Ion-Exclusion Chromatography of Inorganic Acids on a Weakly Acidic Cation-Exchange Resin Column. *J. Chromatogr. A* **2006**, *1118* (1), 41–45.

(36) Phillips, C. S. G.; McIlwrick, C. R. Sample Vacancy Chromatography and Catalysis. *Anal. Chem.* **1973**, *45* (4), 782–786.
(37) Scott, R. P. W.; Scott, C. G.; Kucera, P. Liquid-Solid Vacancy Chromatography. *Anal. Chem.* **1972**, *44* (1), 100–104.
(38) Ye, M.; Ding, Y.; Mao, J.; Shi, L. High-Performance Vacancy Gel Permeation Chromatography. *J. Chromatogr. A* **1990**, *518* (Supplement C), 238–241.
(39) Gonciarz, A.; Kus, K.; Szafarz, M.; Walczak, M.; Zakrzewska, A.; Szymura-Oleksiak, J. Capillary Electrophoresis/Frontal Analysis versus Equilibrium Dialysis in Dexamethasone Sodium Phosphate-Serum Albumin Binding Studies. *ELECTROPHORESIS* **2012**, *33* (22), 3323–3330.
(40) Gritti, F.; Tarafder, A.; Guiochon, G. Interpretation of Dynamic Frontal Analysis Data in Solid/Supercritical Fluid Adsorption Systems. I: Theory. *J. Chromatogr. A* **2013**, *1290* (Supplement C), 73–81.
(41) Tong, Z.; Joseph, K. S.; Hage, D. S. Detection of Heterogeneous Drug–protein Binding by Frontal Analysis and High-Performance Affinity Chromatography. *J. Chromatogr. A* **2011**, *1218* (49), 8915–8924.
(42) Parastar, H.; Radović, J. R.; Jalali-Heravi, M.; Diez, S.; Bayona, J. M.; Tauler, R. Resolution and Quantification of Complex Mixtures of Polycyclic Aromatic Hydrocarbons in Heavy Fuel Oil Sample by Means of GC × GC-TOFMS Combined to Multivariate Curve Resolution. *Anal. Chem.* **2011**, *83* (24), 9289–9297.
(43) Izadmanesh, Y.; Garreta-Lara, E.; Ghasemi, J. B.; Lacorte, S.; Matamoros, V.; Tauler, R. Chemometric Analysis of Comprehensive Two Dimensional Gas Chromatography–mass Spectrometry Metabolomics Data. *J. Chromatogr. A* **2017**, *1488*, 113–125.
(44) Pinkerton, D. K.; Reaser, B. C.; Berrier, K. L.; Synovec, R. E. Determining the Probability of Achieving a Successful Quantitative Analysis for Gas Chromatography–Mass Spectrometry. *Anal. Chem.* **2017**, *89* (18), 9926–9933.

Chapter 4. Continuous Monitoring with One-Dimensional Gas Chromatography (1D-GC) via Injection by Pulse Flow Valve.

4.1 INTRODUCTION

The analytical chemist employs a diverse range of techniques to investigate the reaction mechanisms of a system. Most techniques focus on the analysis of either the precursors or the analysis of the final products. In many fields of work, from industrial to environmental, monitoring efforts are devoted to observing a system for changes in the concentration of reactants, intermediates and products as a reaction or process progresses. Recently, in the field of gas chromatography, a new form of flow modulation for comprehensive two-dimensional gas chromatography (GC×GC) was introduced [1] that makes use of rapid pulses of carrier gas as the source of modulation - dubbed 'partial' modulation due to the resultant data shown later. This form of modulation is a hybrid of two chromatographic techniques; vacancy chromatography and frontal analysis. It will be shown that this modulator has the ability to be used for continuous sampling of volatile analytes present in a chemical system by the same process used for GC×GC based on the principles of vacancy chromatography and frontal analysis discussed in chapter 1 of this text.

In previous work, [1] it was shown that the pulse flow valve modulator modulates the analytes as they exit the 1D column by injecting a narrow pulse of carrier gas perpendicular to the flow of the column at the union with the 2D column. This injection of carrier gas has two effects on the signal, it first creates a vacancy in the signal of the analyte, and secondly that vacancy is manifest as an error function encoded with the critical separation data that mimics frontal analysis separation. This same phenomenon will be shown to work as a continuous sampling/injection system for analytes flowing off the headspace of a system. Thus, the researcher can easily and inexpensively monitor a system with gas chromatography and a detector of choice.

Vacancy chromatography is an older chromatographic technique first demonstrated by Reilley and co-worker in 1962 [2]. Termed at the time as 'inverse chromatography', it was demonstrated that in a separation with a steady state concentration of analytes, the removal of an analyte would give the equal but inverted response as an injection of the analyte. In the traditional application of vacancy gas chromatography, the mobile phase contains a small fraction of analyte contained in the carrier gas. An injection of pure carrier gas into the region that contains the analyte causes a region of negative concentration of analyte. This negative concentration of carrier gas will have the same retention time as positive injection of the analyte. This behavior lends vacancy gas chromatography applicable to process monitoring, however is not a commonly used technique as most analytical chemist opt to take periodic samples to be tested. Currently, most literature written on vacancy chromatography is related to liquid chromatography, specifically vacancy ion-exclusion chromatography [3–6]. In process monitoring, a mobile phase would contain analytes that are continually passed through a separation column. If a pulse of pure carrier gas were to be injected, a negative peak profile would be created and pass through the column the same way a positive peak would be expected to pass through. In a similar manner, the pulse flow valve modulator injects carrier gas at a user defined time period creating vacancies in the signal (Fig 1.7, Ch 1). The key difference from traditional vacancy chromatograph and the pulse flow valve modulator applied to (GC×GC) separation is it is not performed on analytes at equilibrium along the length of the column, but rather on Gaussian peaks resulting from the injection of analytes.

The results of partial modulation by carrier gas created by the pulse flow valve are displayed as error functions. In this technique, the error functions contain the critical chromatographic information that is analyzed using a modified frontal analysis technique. Frontal analysis is a form of chromatography where a continuous flow of analytes passes through a column, each

analyte elutes at a different time depending on its affinity for the stationary phase of the column [7–9]. This type of analysis traditionally is used for liquid chromatography and the resulting appearance of analytes would only happen once for a separation as the solution elutes from the column. In the current application, the combination of the principles of vacancy chromatography and frontal analysis occurs with each pulse of the valve, with the production of an error function encoded with the critical chromatographic information. The concept of vacancy chromatography and frontal analysis was previously shown in Fig 1.7 of chapter 1.

4.2 EXPERIMENTAL

4.2.1 *Instrumental Summary*

The 1D-GC continuous monitoring of headspace instrument was evaluated using a flame ionization detector (FID). The instrumental platforms consisted of an Agilent 6890 GC (Agilent Technologies, Palo Alto, CA, USA). The stock electrometer for the Agilent FID was replaced with a high-speed electrometer built in-house allowing the data to be collected at 2 kHz. The electrometer was interfaced to a National Instruments data acquisition board, and the resulting data was collected using an in-house written LabVIEW program (National Instruments, Austin, TX, USA). Post-run data processing was performed in MATLAB R2015b (The Mathworks, Inc., Natick, MA, USA). Samples were manually placed into an in-house made sample vial contained within the GC oven. Ultra-high purity hydrogen (Grade 5, 99.999%) was used as the carrier gas (Praxair, Seattle, WA, USA). For all instrumental setups an inlet and FID temperature of 175 °C was implemented. All columns were contained within the same oven thus all had the same temperature.

4.2.2 1D-GC

For the 1D-GC evaluation, the GC was fitted with a high-speed pulse valve model 009–1643-900 (Parker Hannifin, Hollis, NH, USA) mounted outside of the oven. The pulsed flow valve was controlled using the same program that was used to collect the FID data. A schematic of the 1D-GC instrument is shown in Fig. 4.1A. The guard column and separation column were linked using a 3-way T-union model MT.5CXS6 (Valco Instruments Company Inc., Houston, TX, USA). An in-house fitting was fabricated to mate the pulse flow valve to 7.24 cm × 1.65 mm copper tubing (Restek, Bellefonte, PA, USA) reduced to 3.81 cm × 0.635 mm steel tubing interfaced with a 2 µl sample loop model CSL2 (Valco Instruments Company Inc.) which was connected to the 3-way T-union.

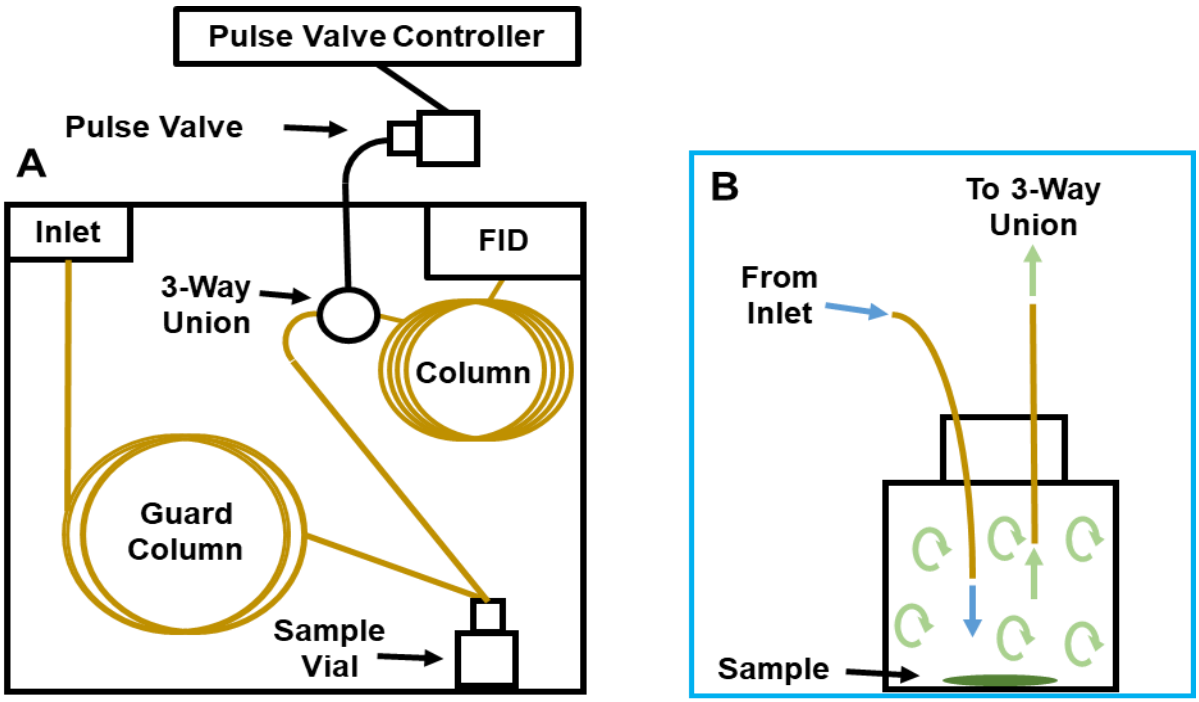

Figure 4.1. 1D-GC Instrumental Schematic.
(A) Instrumental schematic perform gas chromatography of headspace sampling through an injection of carrier gas via the pulse flow valve. Guard column is used to direct carrier gas from the inlet, through the sample vial and to the 3-way union. Continuous sample injection occurs at the 3-way union via pulses of pure carrier gas from the pulse flow valve. (B) Close up view of sample vial to show detail of carrier gas flow through the vial headspace.

The guard column was a Restek IP Deactivated: 3 m length × 100 µm inner diameter (I.D.) × 0.1 µm film thickness (d.f.). This column was cut to allow approximately 2.75 m of the column to connect the GC inlet to the sample vial, the remain 0.25 m connected the sample vial to the T-union. The separation column was a DB-Wax (polyethylene glycol) stationary phase :1 m × 100 µm (I.D.) × 0.1 µm (d.f.), this column connected the T-union to the detector. These dimensions of columns were chosen due to past work where the flow performance of a system made from these dimensions was well known. A test mixture containing four low boiling analytes (Table C.1) was used to evaluate the instrumental platform. A 40 µL volume of the four-component test mixture was manually placed into the sample vial prior to each separation. A constant flow rate of 2.0 mL/min was applied to the system for all separations. Three experimental separations with the four-component mixture were conducted isothermal at 50 °C in which continuous sampling was conducted at three different rates, 75, 100, 150 ms with an injection of carrier gas pulse width of 2 ms (i.e. how long the pulse valve injects carrier gas). The head pressure on the pulse valve began at 25 psi for each separation and was increased incrementally by 0.5 psi approximately every 20 seconds until a maximum pressure for the conditions was reached on the pulse valve that caused the flow from the sample vial to be stopped, which was typically 36-38 psi. These three experiments were conducted to monitor performance changes due to two variables, sampling rate, and pulse flow valve sampling pressure. Two experiments applied oven ramping: 1) 50-100 °C at 3 °C/min, 2) 30-100 °C at 1 °C/min. The 50-100 °C oven ramp was applied to a separation of the four-component mixture with the modulation pressure (32 psi) and flow (2 mL/min) held constant in order to observe the change in separation due to temperature changes. The 30-100 °C oven ramp was used to separate a 0.2 µL volume of unleaded gasoline with the pulse flow valve pressure (32 psi) and flow rate (2.0 mL/min) held constant during the sampling. Prior to all

experiments, the system (i.e. the sample vial) was allowed to come to equilibrium, this was confirmed by ensuring a steady analyte signal was observed, this typically took 1-2 minutes.

4.3 Results and Discussion

4.3.1 *Sample vessel.*

The first challenge presented was the development of the sample vessel that would provide a continuous sample to test the hypothesis that the pulse flow valve modulator could be converted into a continuous sampling 1D-GC system (Fig. 4.1A). After some trial and error, it was found that the simplest design that facilitated the test requirements was a 2 mL standard sample vial (Fig. 4.1B). Insertion of the guard column shown in Fig. 4.1B required the lid to be installed on the vial before attempting to puncture the septum using the guard column. After both sections of the column were inserted, it was found to be best practice to insert the column from the inlet deeper than the column leading to the T-union. This allowed the inlet column to be close to the sample located at the bottom of the vial, and the T-union column to be closer to the top, with the intent to help with smooth flow through the vessel and attempt to reduce the turbulent flow within the vessel. Elmer's Rubber Cement to the outside of the vial covering the two insertion holes. With this addition the sample vial was able to be heated to 100 °C repeatedly without suffering from leaks.

4.3.2 *1D-GC Isothermal.*

Three sampling rates (75, 100, 150 ms) were employed during the isothermal sampling of the four-component mixture. With the signal of the four analytes at equilibrium the pulse flow valve would be turned on, beginning at 25 psi. Each pressure increase (0.5 psi) was held for

approximately 20 seconds to allow the signal to once again come to a steady state. The resultant raw data from the 75 ms sampling rate can be seen in Fig. 4.2A. With each resultant increase in pulse

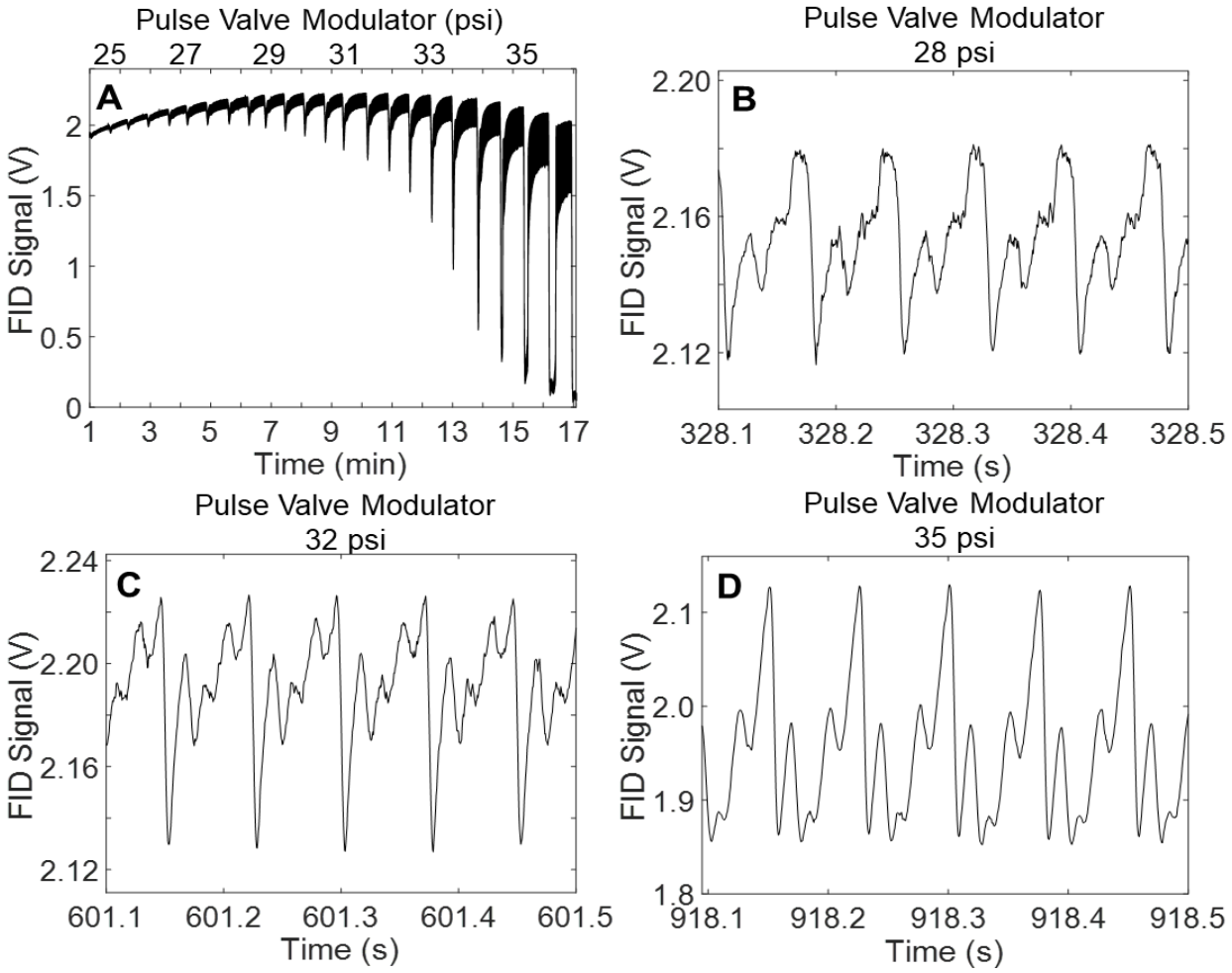

Figure 4.2. 75 ms Sampling Rate Raw Data

(A) Raw data from continuous sampling at 75 ms of four test analytes (1: hexane, 2: cyclohexane, 3: methylcyclohexane, 4: 1-hexyne). The pulse flow valve was turned on at 1 minute at an initial pressure of 25 psi, approximately every 20 seconds the pressure on the pulse flow valve was increased by 0.5 psi. The increase in pressure results in an initial decrease in signal as the flow of the carrier gas containing the test analytes momentarily decreases. This process was continued till the flow of carrier gas from the sample vial was complete stopped by the flow of gas from the pulse flow valve. (B-D) Shown are close up views of five injections at various pressures from the pulse flow valve.

flow valve pressures a slight decrease in signal is noted, this is assumed to be caused by the sudden added interruption in the flow from the sample vial resulting in a temporary reduction in analyte signal. At higher pressures, in the case of the 75 ms sampling rate, at 37 psi the flow from the vial is assumed to have gone to zero as the signal decreased to zero and failed to return, which was intentionally not displayed in Fig. 4.2A. Figure 4.2B-D shows a close up view of the raw data at three different pulse flow valve pressures (28, 32, and 35 psi). It is interesting to note that under these conditions the meaningful data that is normally only observed in the front created during the partial modulation is now found in the return portion of the signal. Figures 4.2B and 4.2C have a very similar analyte elution pattern, while the pattern in Fig. 4.2D at 35 psi takes on a different analyte pattern similar to that of traditional Gaussian peaks. The final processed data for the 75 ms data sampling rate is shown in Fig. 4.3A-D. As can be seen as the pulse valve pressure increased, the partial modulation increased, and the resultant processed data improved in regard to signal-to-noise (S/N). The order of elution of the analytes shown in Fig. 4.3D was determined by individual runs of single analytes, which is not shown. The order of elution was also confirmed by accessing Kovats retention indices online. The order of elution for the analytes did not change during any of the testing as would be expected. The resultant 2D chromatogram of the processed data in Fig. 4.3A is shown in Fig. 4.4. As can be seen hexane is detectable even at the lowest pulse valve pressure, which is assumed to be attributed to higher vapor pressure resulting in more analyte in the gas phase. The remaining three analytes, all with lower vapor pressures, do not become detectable till pressure on the pulse valve approaches ~28psi.

Data for the 100 and 150 ms sampling rates are extremely similar in performance and will be discussed together. The key difference with the 75 ms sampling rate data when compared to the

100 and 150 ms sampling rate data is the location of the chromatographic information. As shown with the 75 ms data, the chromatographic data was found in following the partial modulation in

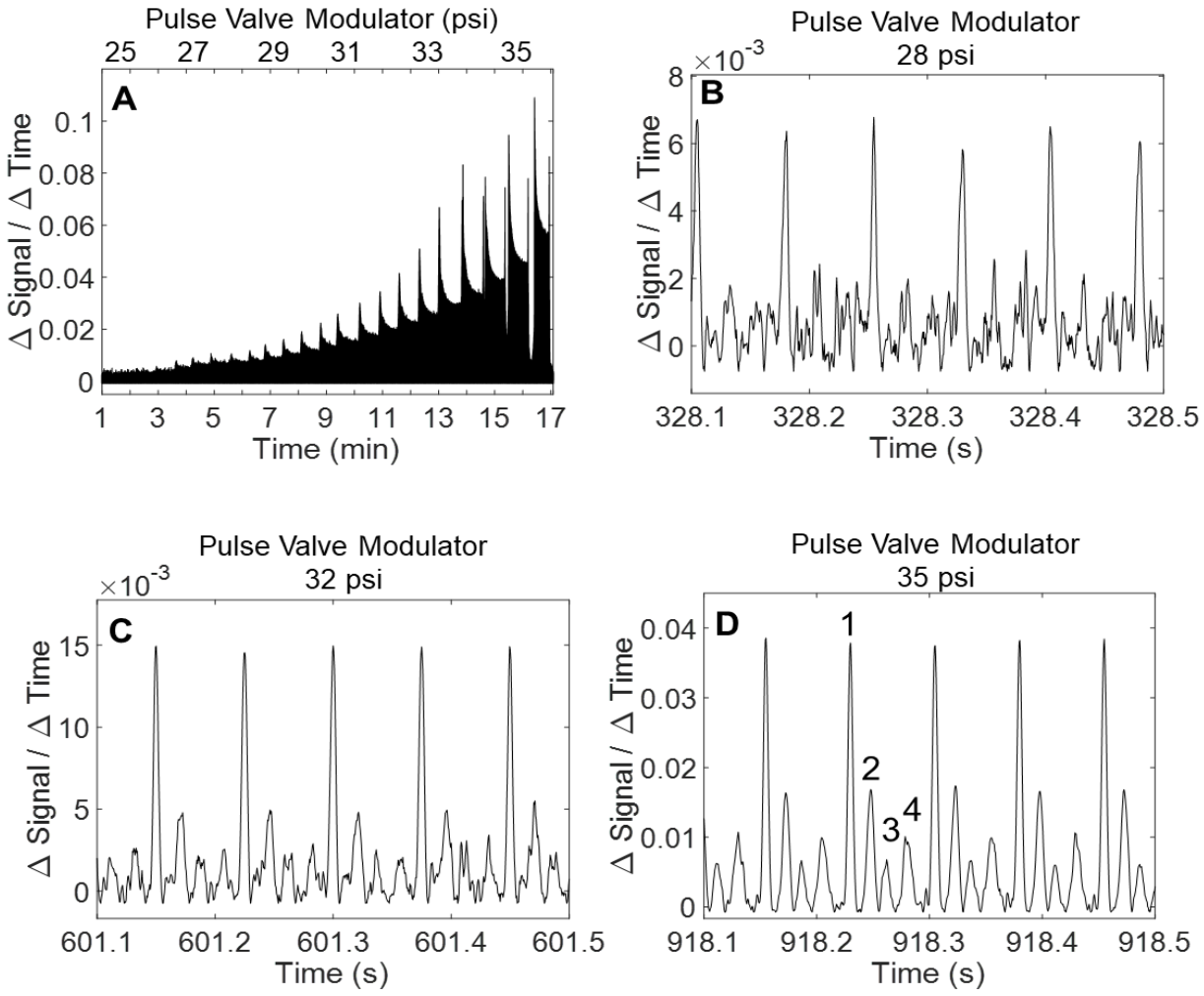

Figure 4.3. 75 ms Sampling Rate Final Processed Data

(A) Processed data of four test analytes (1: hexane, 2: cyclohexane, 3: methylcyclohexane, 4: 1-hexyne) from Fig 4.2A after the three step data conversion process that converts raw data into apparent Gaussian peaks. The increase in intensity with the increase in pulse flow valve pressure is direct related to the increase in peak intensity in the final data. Each increase in pulse flow valve pressure is apparent by the spike in signal. (B-D) Shown are close up views of five injections at various pressures from the pulse flow valve. A clear increase in *S/N* occurs at the higher pulse flow valve pressures.

the return portion of the signal. For 100 and 150 ms the important chromatographic information is found in the frontal portion of the vacancy front. This location of chromatographic information encoded in the data front is consistent with past GC×GC[10] and GC3 data. It is observed for both

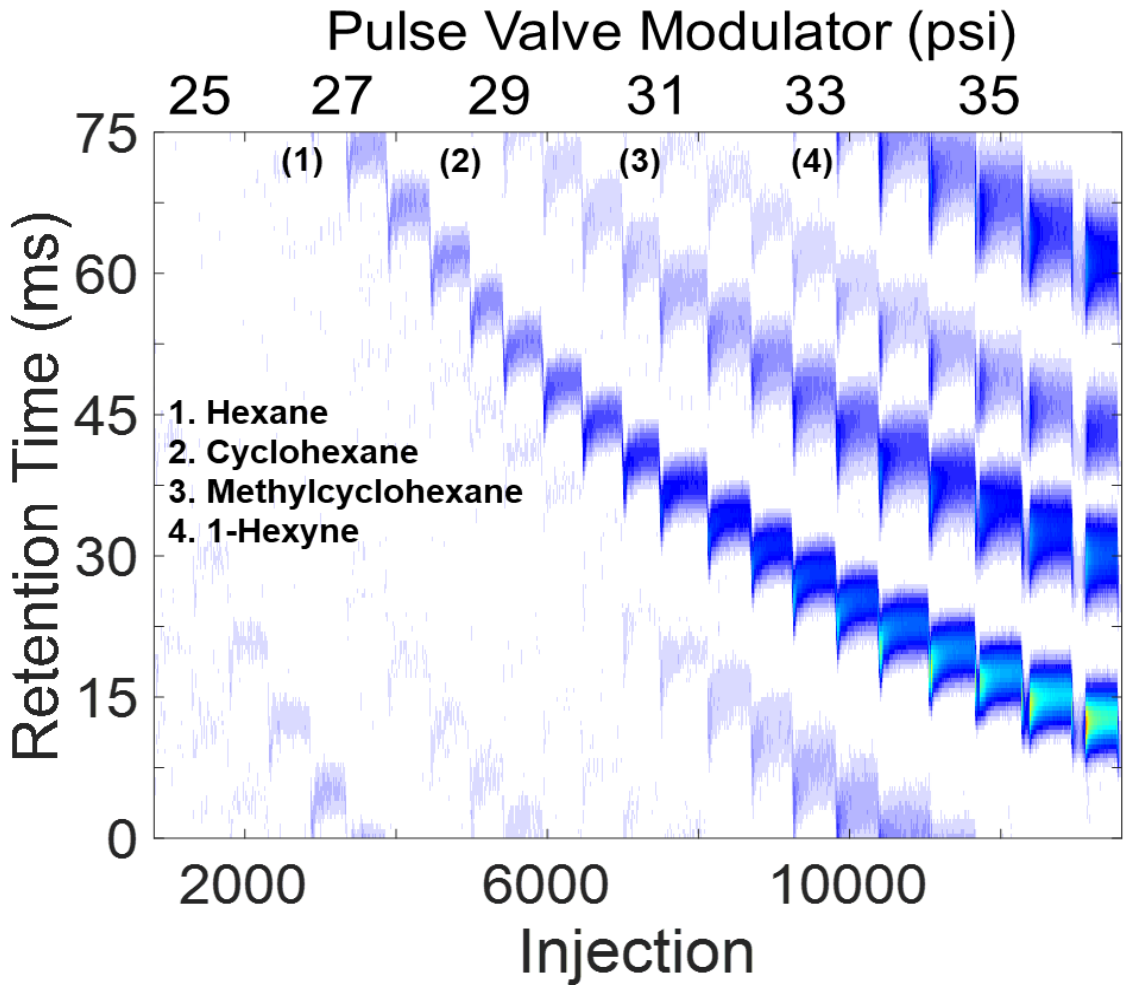

Figure 4.4. 2D Chromatogram of 75 ms Sampling Rate Data.

A 2D chromatogram of continuous sampling rate of 75 ms is shown where the retention time of the analyte on the DB-Wax column is shown compared to the pressure of the gas injected from the pulse flow valve. The shift in retention time is related to the change in overall flow of carrier gas with the increase in carrier gas injected by the pulse flow valve. The total number of injections during this separation is shown on the horizontal axis.

the 100 and 150 ms sampling rate the separation profile changed very little as the pulse valve pressure increased. The key change in the 100 ms data from Fig. 4.5B to Fig. 4.5D with the increased pressure is the increase in the partial modulation which would be expected, which results in increased S/N in the processed data for both 100 ms and 150 ms seen in Figs. 4.6 and 4.8 respectively. One can see that when the data is viewed in a traditional 2D chromatogram plot,

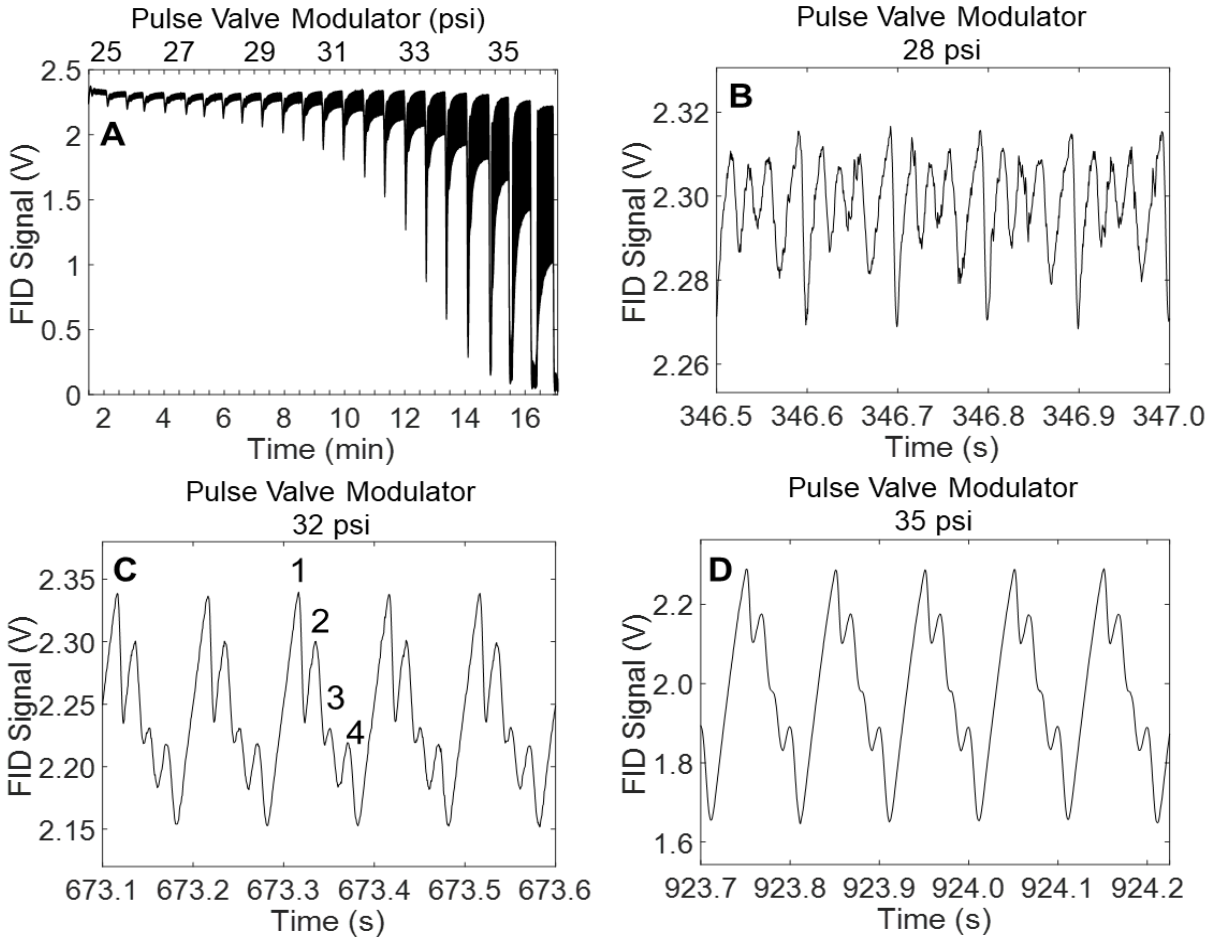

Figure 4.5. 100 ms Sampling Rate Raw Data

(A) Raw data from continuous sampling at 100 ms of four test analytes (1: hexane, 2: cyclohexane, 3: methylcyclohexane, 4: 1-hexyne). The pulse flow valve was turned on at 1 minute at an initial pressure of 25 psi, approximately every 20 seconds the pressure on the pulse flow valve was increased by 0.5 psi. The increase in pressure results in an initial decrease in signal as the flow of the carrier gas containing the test analytes momentarily decreases. This process was continued till the flow of carrier gas from the sample vial was complete stopped by the flow of gas from the pulse flow valve. (B-D) Shown are close up views of five injections at various pressures from the pulse flow valve

that as the sampling rate increases from 75 ms (Fig. 4.4) to 100 ms (Fig. 4.7) and 150 ms (Fig. 4.10), the separation time of the four analytes remained consistent at approximately 65-70 ms.

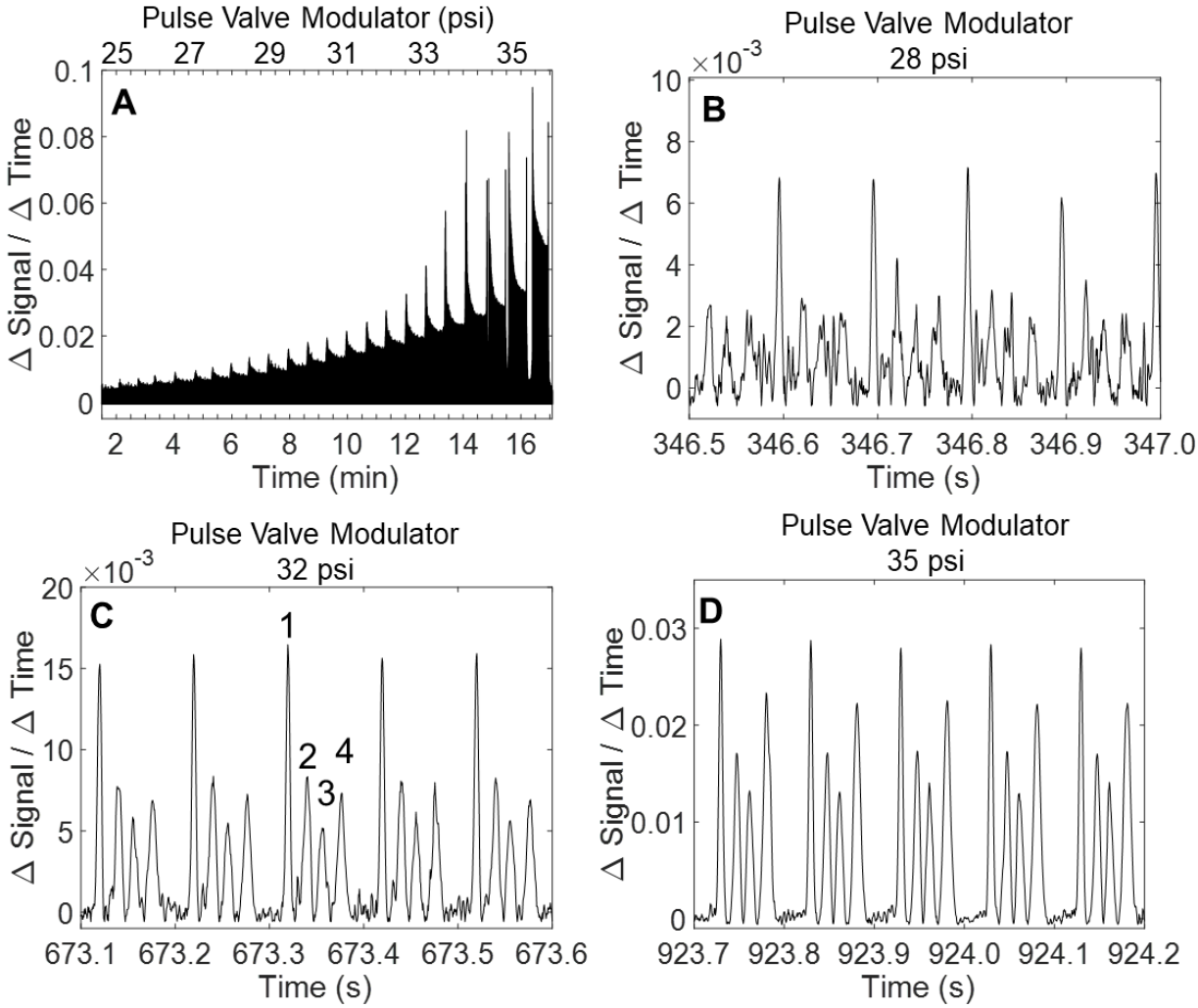

Figure 4.6. 100 ms Sampling Rate Final Processed Data

(A) Processed data of four test analytes (1: hexane, 2: cyclohexane, 3: methylcyclohexane, 4: 1-hexyne) from Fig 4.5A after the three step data conversion process that converts raw data into apparent Gaussian peaks. The increase in intensity with the increase in pulse flow valve pressure is direct related to the increase in peak intensity in the final data. Each increase in pulse flow valve pressure is apparent by the spike in signal. (B-D) Shown are close up views of five injections at various pressures from the pulse flow valve. A clear increase in *S/N* occurs at the higher pulse flow valve pressures.

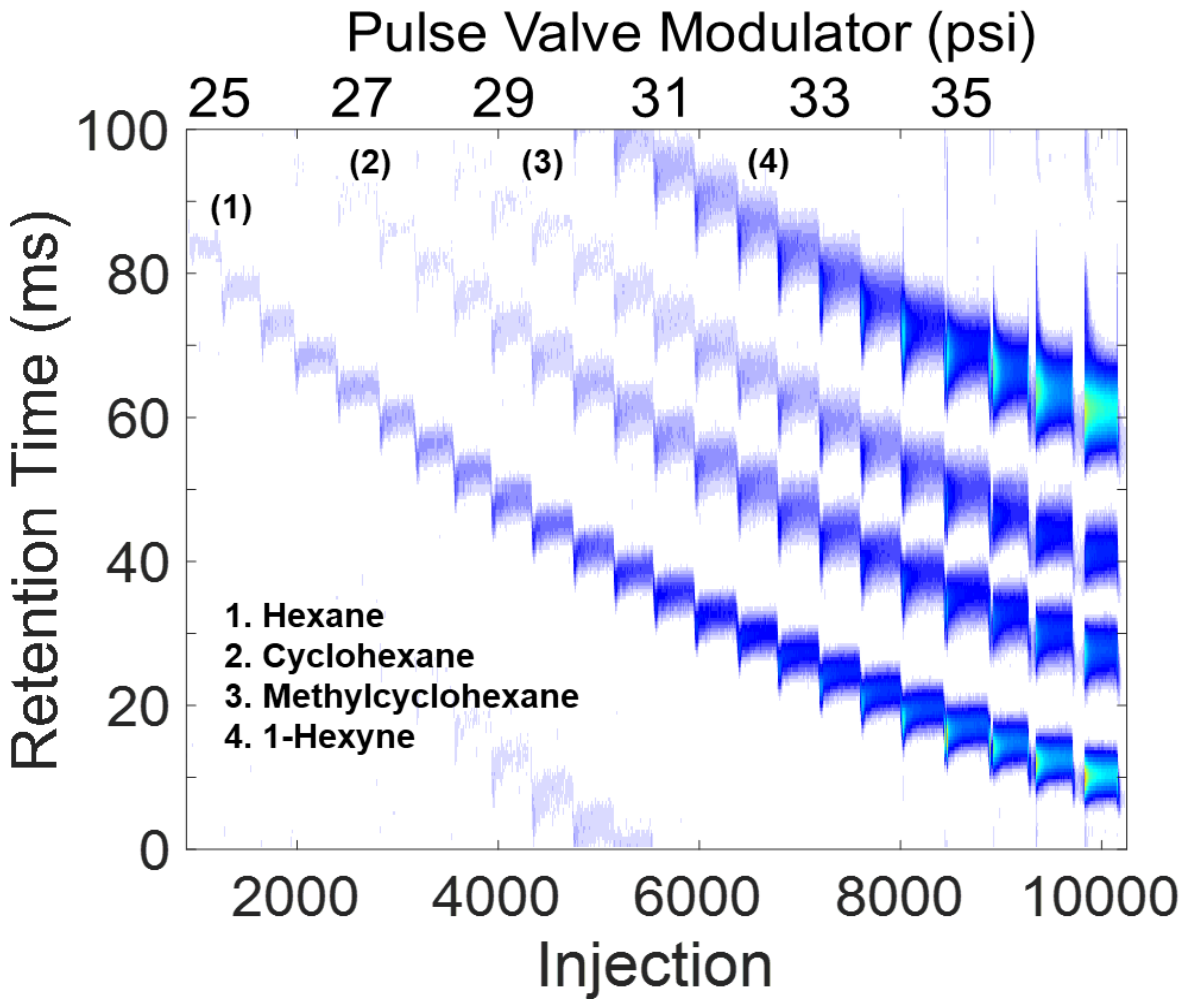

Figure 4.7. 2D Chromatogram of 100 ms Sampling Rate Data.

A 2D chromatogram of continuous sampling rate of 100 ms is shown where the retention time of the analyte on the DB-Wax column is shown compared to the pressure of the gas injected from the pulse flow valve. The shift in retention time is related to the change in overall flow of carrier gas with the increase in carrier gas injected by the pulse flow valve. The total number of injections during this separation is shown on the horizontal axis.

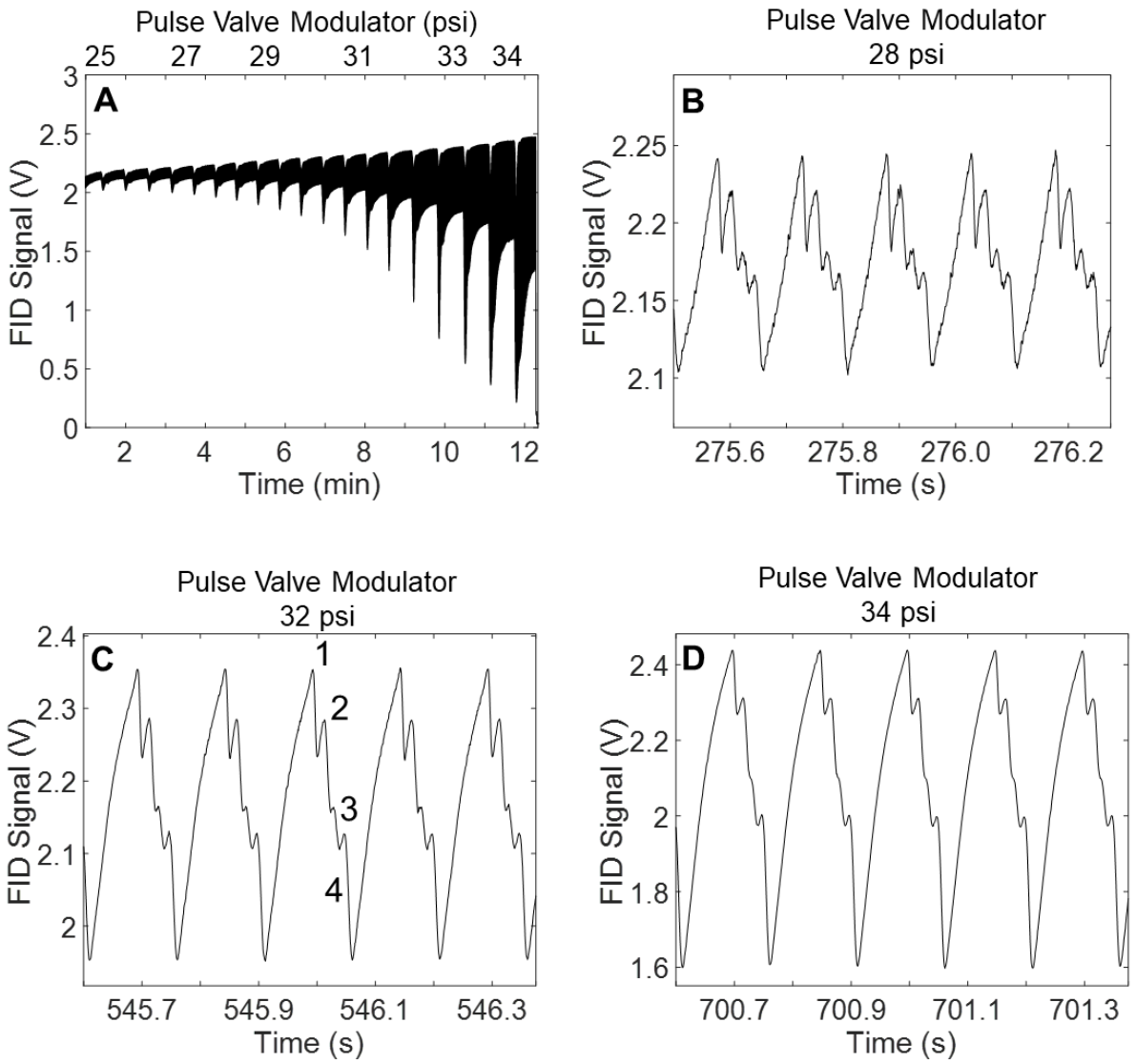

Figure 4.8. 150 ms Sampling Rate Raw Data

(A) Raw data from continuous sampling at 150 ms of four test analytes (1: hexane, 2: cyclohexane, 3: methylcyclohexane, 4: 1-hexyne). The pulse flow valve was turned on at 1 minute at an initial pressure of 25 psi, approximately every 20 seconds the pressure on the pulse flow valve was increased by 0.5 psi. The increase in pressure results in an initial decrease in signal as the flow of the carrier gas containing the test analytes momentarily decreases. This process was continued till the flow of carrier gas from the sample vial was complete stopped by the flow of gas from the pulse flow valve. (B-D) Shown are close up views of five injections at various pressures from the pulse flow valve.

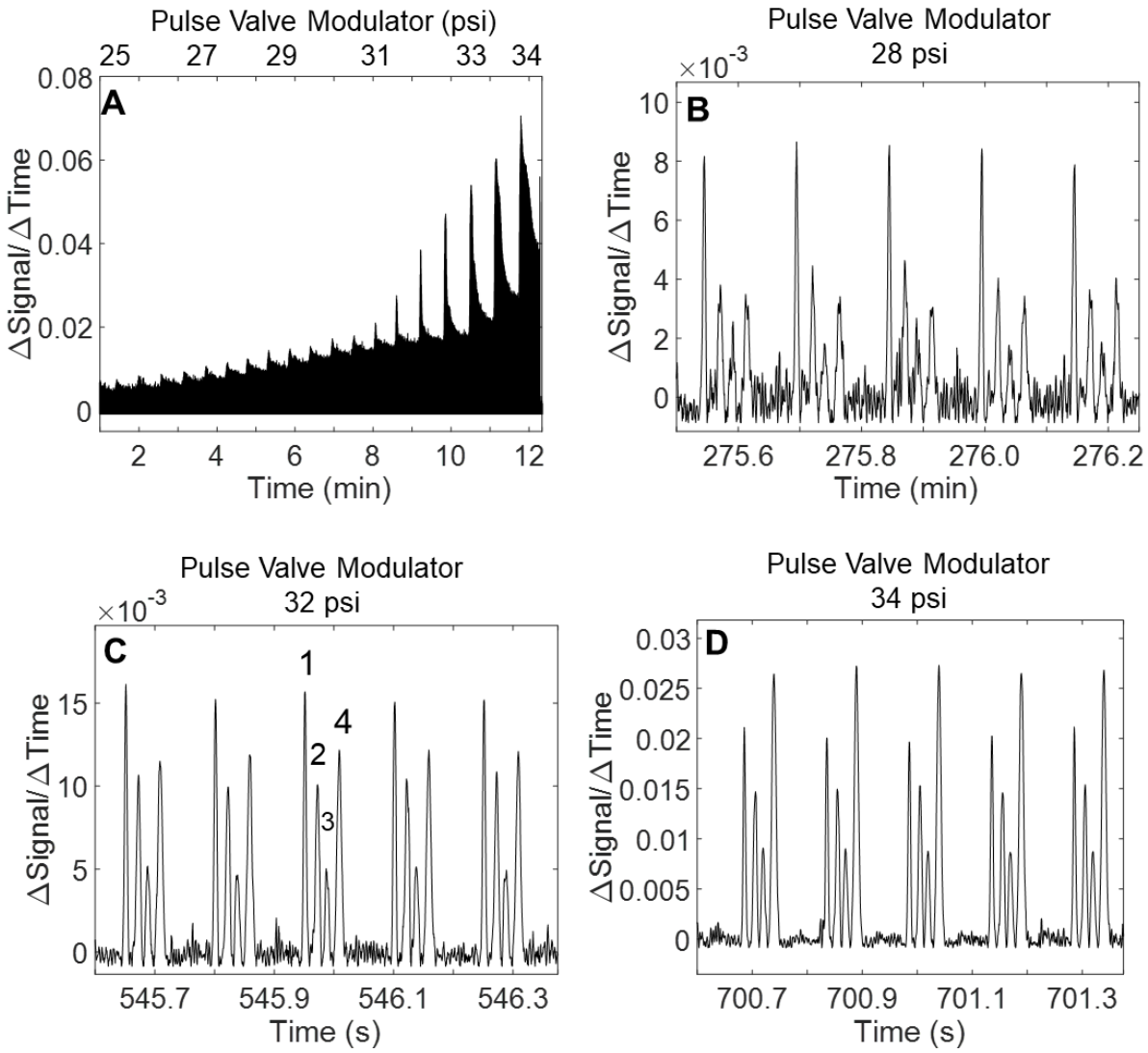

Figure 4.9. 150 ms Sampling Rate Final Processed Data

(A) Processed data of four test analytes (1: hexane, 2: cyclohexane, 3: methylcyclohexane, 4: 1-hexyne) from Fig 4.8A after the three step data conversion process that converts raw data into apparent Gaussian peaks. The increase in intensity with the increase in pulse flow valve pressure is direct related to the increase in peak intensity in the final data. Each increase in pulse flow valve pressure is apparent by the spike in signal. (B-D) Shown are close up views of five injections at various pressures from the pulse flow valve. A clear increase in *S/N* occurs at the higher pulse flow valve pressures.

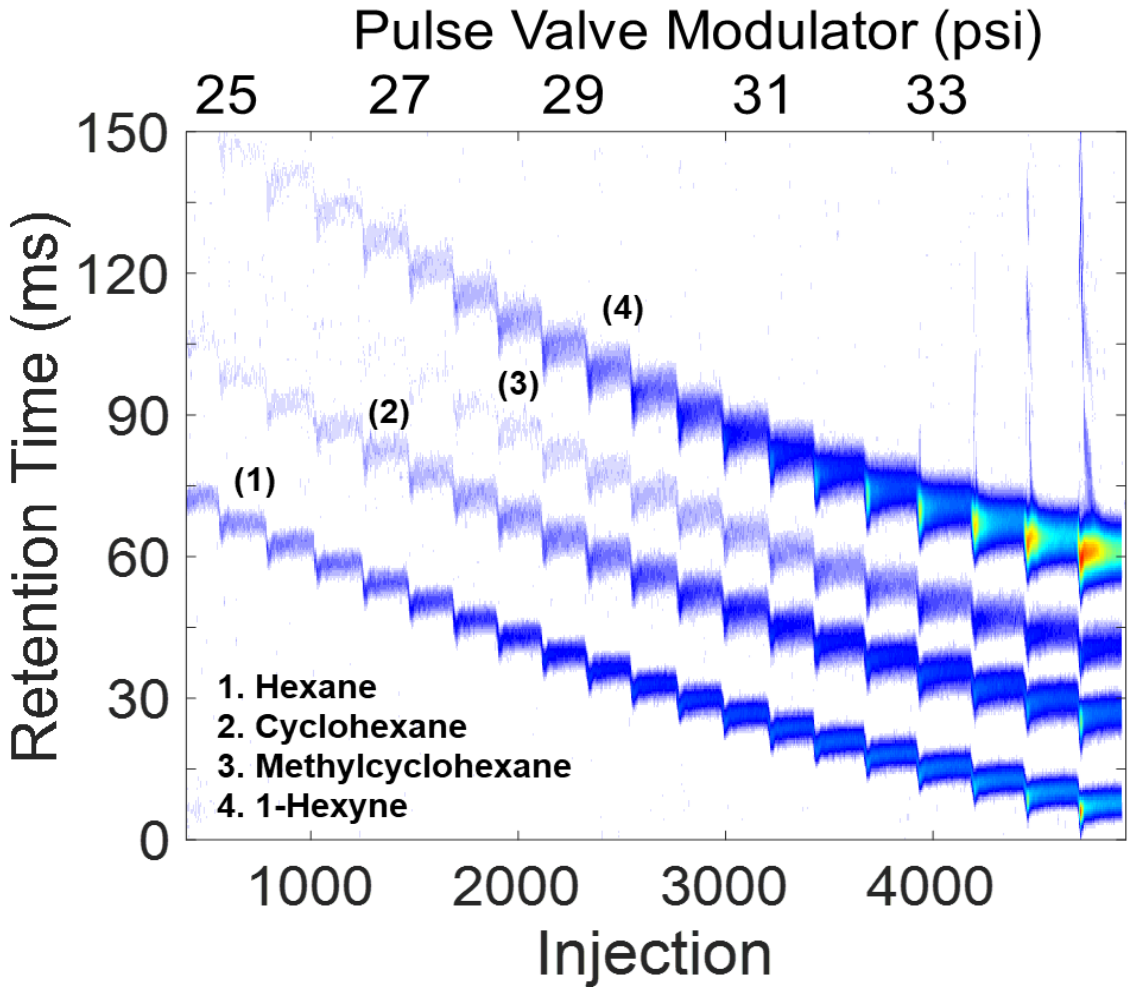

Figure 4.10. 2D Chromatogram of 150 ms Sampling Rate Data.

A 2D chromatogram of continuous sampling rate of 150 ms is shown where the retention time of the analyte on the DB-Wax column is shown compared to the pressure of the gas injected from the pulse flow valve. The shift in retention time is related to the change in overall flow of carrier gas with the increase in carrier gas injected by the pulse flow valve. The total number of injections during this separation is shown on the horizontal axis.

Based on that observation it can be assumed that peak capacity on the separation column is directly influenced by the rate of sampling, i.e. slower the sampling rate, the higher the peak capacity. There should be a limit to this observation, however a large enough span of sampling rate was not tested.

4.3.3 *1D-GC Temperature Ramped Separation of Four Analytes*.

Flow rate (2.0 mL/min) and pulse valve flow (32 psi) conditions were selected for the temperature ramped separations that are based upon the data generated during the isothermal work. One key issue that was not properly addressed during the separation is the adjustment of the flow and pulse valve pressure to account for increased pressure of the separation column as the temperature increases. Based on a commercially available pressure flow calculator, at 50 °C and a constant flow of 2.0 mL/min the separation column inlet pressure would be ~36 psi, with an average velocity of 188 cm/s. At 100 °C and with the same constant flow of 2.0 mL/min, the separation column inlet pressure would increase to ~42 psi, with an average velocity of 197 cm/s. These changes in flow, and more importantly in pressure, should have been matched with a similar increase in pulse valve pressure throughout the experiment. This oversight undoubtedly had some influence over the data shown in Fig. 4.11 of the separation of the four-component mixture. Figures 4.11B-F, show that the data took some unusual forms in the raw format as the temperature began to rise. It can be seen in the raw data (Figs. 4.11B-E) covering 50-80 °C that all four analytes were resolved with a resolution of at least R_s = (1) which was shown by the observation of four individual fronts corresponding to each analyte. That pattern is changed to three fronts at 90-100 °C (Figs. 4.11F-G) when 1-hexyne and methylcyclohexane become overlapped at higher temperatures. Seen in the processed data (Fig. 4.12) is the results of the raw data from Fig. 4.11, where one can observe the Gaussian peaks of the four analytes until the temperature approaches 80 °C (Fig. 4.12E) as the two analytes begin to overlap. This behavior is most evident in the 2D chromatogram in Fig. 4.13 that shows that the resolution of all analytes decreased as the temperature rose, with 1-hexyne and methycyclohexane becoming overlapped. A 2D chromatogram of a

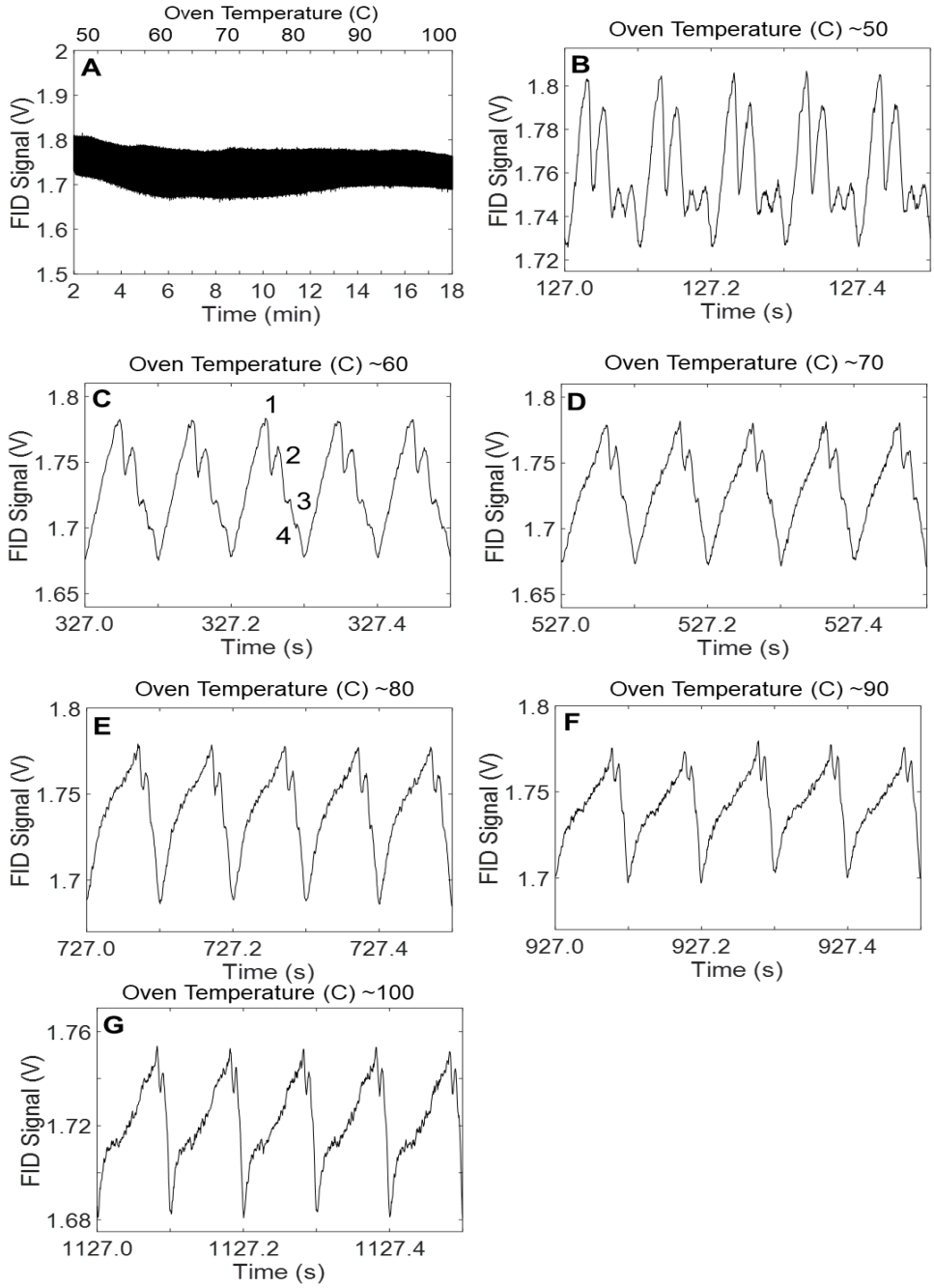

Figure 4.11. Temperature Ramp Separation of 4 Analytes Raw Data.

(A) Raw data from continuous sampling at 100 ms of four test analytes (1: hexane, 2: cyclohexane, 3: methylcyclohexane, 4: 1-hexyne). The pulse flow valve was turned on at 1 minute at a pressure of 32 psi. The flow (2.0 mL/min) and pulse valve flow were held constant while the oven was

ramped from 50 ˚C to 100 ˚C at 3 ˚C/min. The oven was held constant for the initial two minutes. (B-G) Shown are close up views of five injections at five different temperatures.

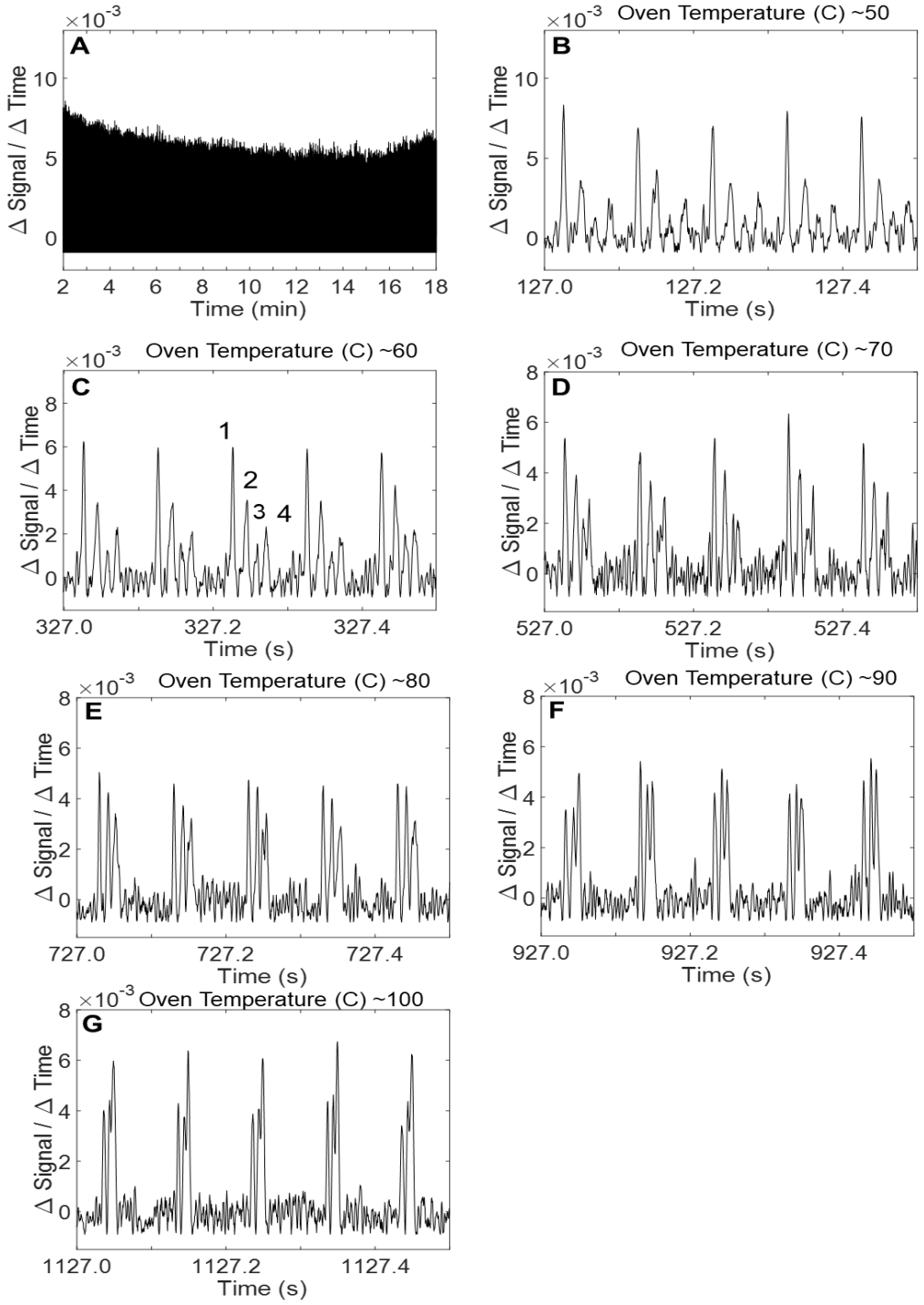

Figure 4.12. Temperature Ramp Separation of 4 Analytes Final Processed Data.

(A) Processed data of four test analytes (1: hexane, 2: cyclohexane, 3: methylcyclohexane, 4: 1-hexyne) from Fig 4.11A after the three step data conversion process that converts raw data into

apparent Gaussian peaks. (B-G) Shown are close up views of five injections at five different temperatures.

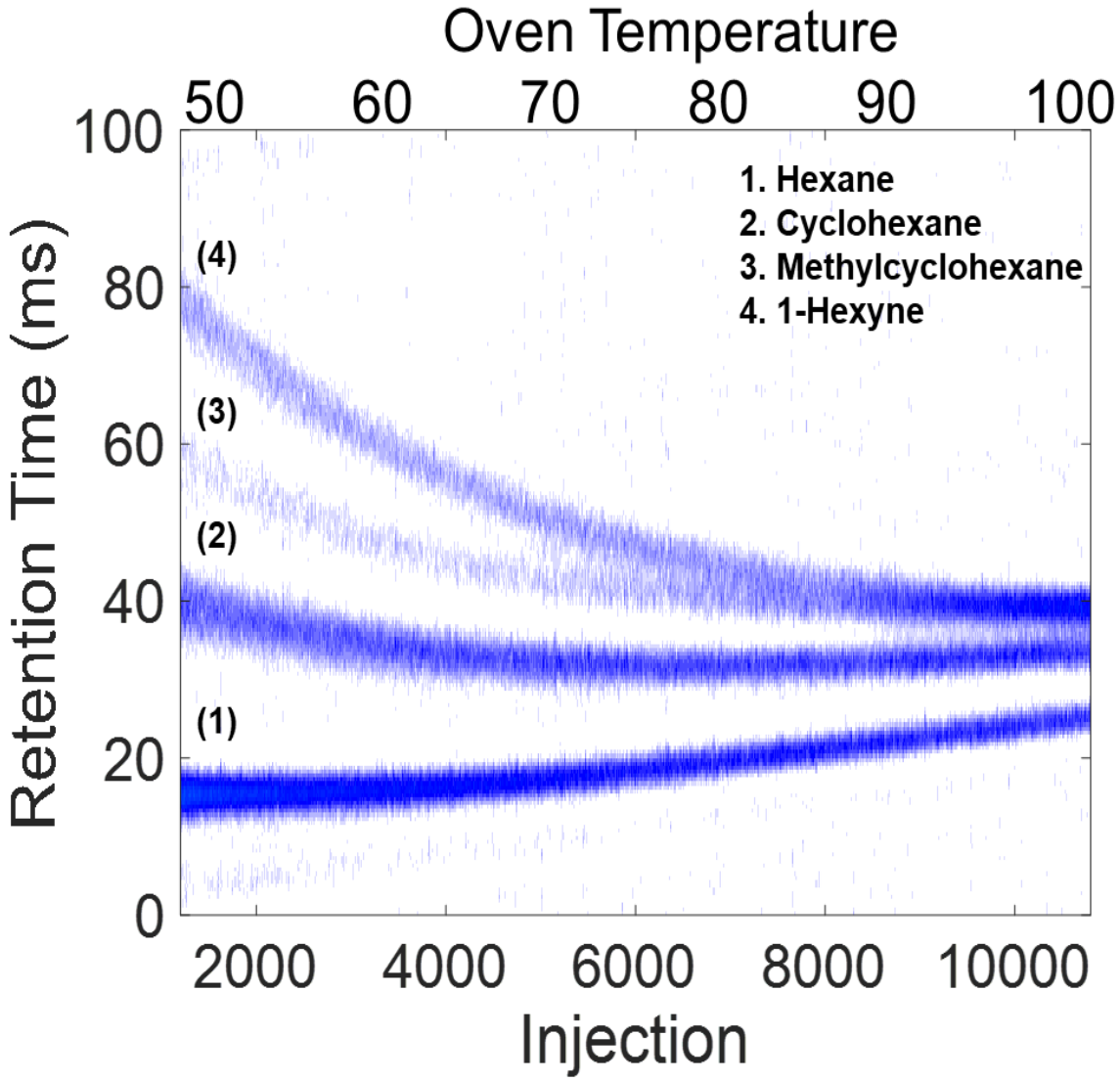

Figure 4.13. 2D Chromatogram of 100 ms Temperature Ramp Data

A 2D chromatogram of continuous sampling rate of 100 ms at 32 psi from the pulse flow valve is shown where the retention time of the analyte on the DB-Wax column is shown during oven ramp (50-100 ˚C) at 3 ˚C/min. The shift in retention time is related to the increase in temperature which reduces the k' of the retained peaks. Note hexane experiences very little shift as it was an unretained peak on the DB-Wax column. The slight increase in retention time as the temperature increases is due to instrument set to constant flow (2.0 mL/min) which resulted in a decrease in linear flow velocity of the carrier gas as increased temperatures.

ramped temperature gasoline separation using similar conditions is shown in Fig. C1. This work clearly shows separation of alkanes, saturated hydrocarbons, and cyclic hydrocarbons.

4.4 Conclusions

It has been shown that the pulse flow valve used for multidimensional gas chromatography can be potentially used in a 1D-GC fashion as a sample injection platform for continuous monitoring of a chemical system comprised of volatile analytes. Herein, data was presented that support this assertion. The pulse flow valve combined with 1D-GC demonstrates the ability to rapidly ($\geq$ 50 ms) sample the volatile chemicals associated with any form of a chemical system. Further work is warranted to develop a sample vessel that allows for monitoring of a chemical reaction in-situ. Other potential exists to use the pulse flow valve combined with mass spectrometry to allow for on-line sampling of atmospheric environment conditions that provide near real time detection of compounds.

4.5 REFERENCES.

[1] C.E. Freye, H.D. Bahaghighat, R.E. Synovec, Comprehensive two-dimensional gas chromatography using partial modulation via a pulsed flow valve with a short modulation period, Talanta. 177 (2018) 142–149. doi:10.1016/j.talanta.2017.08.095.

[2] C.N. Reilley, G.P. Hildebrand, J.W. Ashley, Gas Chromatographic Response as a Function of Sample Input Profile., Anal. Chem. 34 (1962) 1198–1213. doi:10.1021/ac60190a008.

[3] M.I.H. Helaleh, K. Tanaka, M. Mori, Q. Xu, H. Taoda, M.-Y. Ding, W. Hu, K. Hasebe, P.R. Haddad, Vacancy ion-exclusion chromatography of haloacetic acids on a weakly acidic cation-exchange resin, J. Chromatogr. A. 997 (2003) 133–138. doi:10.1016/S0021-9673(03)00546-6.

[4] M. Mori, M.I.H. Helaleh, Q. Xu, W. Hu, M. Ikedo, M.-Y. Ding, H. Taoda, K. Tanaka, Vacancy ion-exclusion/adsorption chromatography of aliphatic amines on a polymethacrylate-based weakly basic anion-exchange column, J. Chromatogr. A. 1039 (2004) 129–133. doi:10.1016/j.chroma.2004.02.012.

[5] K. Kaczmarski, W. Zapała, W. Wanat, M. Mori, B.K. Głód, T. Kowalska, Modeling of Ion-Exclusion and Vacancy Ion-Exclusion Chromatography in Analytical and Concentration Overload Conditions, J. Chromatogr. Sci. 45 (2007) 6–15. doi:10.1093/chromsci/45.1.6.

[6] W. Zapała, J. Kostka, K. Kaczmarski, Comparison of different columns in analysis of C1–C5 aliphatic acids mixture in ion exclusion chromatography and vacancy ion exclusion chromatography modes, Acta Chromatogr. 23 (2011) 377–388. doi:10.1556/AChrom.23.2011.3.1.

[7] A. Gonciarz, K. Kus, M. Szafarz, M. Walczak, A. Zakrzewska, J. Szymura-Oleksiak, Capillary electrophoresis/frontal analysis versus equilibrium dialysis in dexamethasone sodium phosphate-serum albumin binding studies, ELECTROPHORESIS. 33 (2012) 3323–3330. doi:10.1002/elps.201200166.

[8] F. Gritti, A. Tarafder, G. Guiochon, Interpretation of dynamic frontal analysis data in solid/supercritical fluid adsorption systems. I: Theory, J. Chromatogr. A. 1290 (2013) 73–81. doi:10.1016/j.chroma.2013.02.049.

[9] Z. Tong, K.S. Joseph, D.S. Hage, Detection of heterogeneous drug–protein binding by frontal analysis and high-performance affinity chromatography, J. Chromatogr. A. 1218 (2011) 8915–8924. doi:10.1016/j.chroma.2011.04.078.

Chapter 5. Conclusion

5.1 SUMMARY OF WORK

The separation, identification, and quantification of analytes contained within complex mixtures are often addressed with chromatographic methods. The goal of analytical separations, such as gas chromatography (GC), is to provide the desired chemical information to meet the goals of the analysis, often with analysis speed being an important factor. This type of situation commonly occurs in the analysis of complex mixtures frequently experienced in the following areas: food, flavors, fragrance, environmental, petroleum sciences, forensic, biological, metabolomics, and volatile organic compounds. While the GC field is dominated by traditional one-dimensional gas chromatography (1D-GC), two-dimensional gas chromatography (2D-GC) has rapidly emerged from a niche technique into a widely used method in industrial, national laboratories and academic research sectors. The progression from traditional one-dimensional gas chromatography (GC) to comprehensive multi-dimensional gas chromatography (MDGC), namely two-dimensional gas chromatography (GC×GC), has been one of the more significant advancements in the field of gas chromatography. Numerous advancements in instrumentation, optimization, data processing and analysis have been of utmost importance. A multitude of researchers have applied numerous approaches to improve the various components of GC×GC separation and data analysis techniques, resulting in significant improvements in the past 27 years. Central to development of GC×GC separation science is evolution of modulators and modulation techniques, which the presented work has focused on, and that further expand the chemical information that can be gathered in minimal time.

Chapter 1 focused on the principles that govern the science of gas chromatography separations. Within this chapter fundamentals and thermodynamic properties are reviewed that

governs key separation performance parameters such as resolution, peak capacity, sampling density, and modulation period. Discussed in detail is the evolution of three classes of modulators, various modulations techniques and their respective advantages and limits.

Chapters 2 and 3 focus on application of two new modulators for MDGC that are reliable, cost-effective, able to modulate a wide range of compounds (C_1-C_{40}+) and while producing high peak capacity, with ultra-fast modulation period of 50 ms, a four-fold reduction in modulation period over previous work. Chapter 2 applies a pulse flow valve modulator, that through an unconventional form of modulation designated 'partial modulation' was studied in combination with a time-of-flight mass spectrometer. Operating with P_M of 50 ms, the modulator enables use for high-speed separations. The data produced was deconvoluted and quantified by use of MCR-ALS chemometric technique. The critical parameter of this study was the ability of this form of modulation to be compatible with a detector at vacuum, and that the results show the form of modulation does not interfere with quantification of detection limits. Chapter 3 explored the use of the pulse valve flow modulator as both an ultra-fast modulator for GC×GC-FID, and a modulator in a GC^3 instrumental platform was designed allowing for both increased selectivity provided by the three dimensions. In the GC×GC-FID study a high peak capacity production of 1,200 peaks/min was achieved with a peak capacity on the ^{2}D dimensional ($^2n_c = 20$), in the GC^3 segment of the study high peak capacity production of 1,000 peaks/min, a 4-fold improvement from previous GC^3 platforms.

Chapter 4 presented a concept of continuous sampling 1D chromatography utilizing the pulse flow valve modulator dubbed a "GC sensor." During this study select low boiling analytes were separated by use of the pulse flow valve that produced separation fronts onto a separation column. Various temperatures and modulation pulse flow pressures were studied to determine the

response of the system. While this study was very preliminary, further research with this pulse flow valve is warranted for its merits as a continuous monitor of a dynamic chemical system.

5.2 Future Direction

5.2.1 Instrumentation

Rarely does instrument with so much potential as that of the pulse flow valve modulator come along that has such a large untapped reservoir. This feeling must have been what others within the field of comprehensive gas chromatography felt when they first realized the potential of their discovery. Two proposals have already been made for research into application of the pulse flow valve, first is extended research into the concept of continuous monitoring of a chemical reaction process, and second is use of the GC^3 instrumental platform presented with a TOF detector. In the first proposal the pulse valve would be used to continuously monitor a reaction in real time. A continuous stream of gas from the headspace of a reaction vessel would be routed into a GC oven containing a separation column and the pulse valve. The pulse valve could be actuated at a user defined rate (≥50 ms) to create the miniature 'injection fronts' on the separation column. The resulting data from the separation would be "cut" at each modulation resulting in a series of 1D separations that are representative of the reaction headspace changes. A form of chemometrics such as PCA could be used in the analysis of the data, with the resulting scores plots serving as a function of the time at which the sampling took place. From this data, one would gain insight into the reaction mechanisms, reaction rates, and possible reaction intermediate products.

In the second proposal the GC^3 instrumental platform would be applied to spectral data collected with a TOF mass spectrometer. The resulting data combined with multivariate curve resolution alternating least squares (MCR-ALS) could be used to deconvolute GC×GC×GC – TOFMS in order to extract the chemical information without processing the data. Along with these

two proposals there are literally countless other research opportunities associated with use of the pulse valve modulator, that take advantage of the simple design, robust behavior and lack of associated costs and other concerns with using cryogens accompanying many thermal modulators or high flow rate concerns related most other flow modulators.

5.2.2 Data Analysis

Multivariate curve resolution alternating least squares (MCR-ALS) analysis has been shown to be an effective tool in relating chemical information obtained from GC×GC – TOFMS. The effectiveness however has shown to be limited to approximately a resolution of (≥0.3) which for high speed separation of complex mixtures has shown to be a problem in chapter 2 of the text. Currently within the Synovec group research continues attempting to develop a feature selection system that would be used with MCR-ALS in a constrained manner for regions of overlap with a resolution less than 0.3. This breakthrough when achieved for MCR-ALS will further expand the usefulness of MDGC with all forms of modulation.

APPENDIX

Appendix A

Table A.1. 15-Component Mixture

Table of the 15-component mixture ordered by elution time on ^{1}D. The supplier and purity are included. The 15 compounds were combined equally by volume by adding 25 µl each for a total volume of 375 µl.

Elution	Name	Boiling Point (°C)	Supplier	Purity (%)
1	Acetone	56	Sigma-Aldrich	99.9
2	Isopropyl Alcohol	83	Sigma-Aldrich	99.7
3	2-Methyl-2-propanol	82	Sigma-Aldrich	99.5
4	Cyclopentane	49	Sigma-Aldrich	99.0
5	1-Hexene	63	Sigma-Aldrich	97.0
6	2-Butanone	80	Sigma-Aldrich	99.0
7	Hexane	68	Sigma-Aldrich	97.0
8	1-Hexyne	71	Sigma-Aldrich	97.0
9	Methylcyclopentane	72	Honeywell	97.0
10	1-Chlorobutane	79	Sigma-Aldrich	99.5
11	Carbon Tetrachloride	77	Sigma-Aldrich	99.9
12	Benzene	80	Fisher Chemical	99.0
13	Cyclohexane	81	Sigma-Aldrich	99.0
14	Heptane	98	Fisher Chemical	99.4
15	1-Heptene	94	Sigma-Aldrich	97.0

Table A.2. 18-Component Mixture

Table of the 18-component mixture ordered by elution time on ^{1}D. The supplier and purity are included. The 18 compounds were combined equally by volume by adding 25 µl each for a total volume of 450 µl.

Elution	Name	Boiling Point (°C)	Supplier	Purity (%)
1	Isopropyl Alcohol	83	Sigma-Aldrich	99.7
2	Acetone	56	Sigma-Aldrich	99.9
3	Hexane	68	Sigma-Aldrich	97.0
4	1-Hexene	63	Sigma-Aldrich	97.0
5	t-butyl methyl ether	55	Sigma-Aldrich	99.8
6	2-Methyl-2-propanol	82	Sigma-Aldrich	99.5
7	Cyclopentane	49	Sigma-Aldrich	99.0
8	Methylcyclopentane	72	Honeywell	97.0
9	1-Hexyne	71	Sigma-Aldrich	97.0
10	Carbon Tetrachloride	77	Sigma-Aldrich	99.9
11	Heptane	98	Fisher Chemical	99.4
12	Ethyl acetate	77	J.T.Baker	99.9
13	Cyclohexane	81	Sigma-Aldrich	99.0
14	1-Heptene	94	Sigma-Aldrich	97.0
15	2-Butanone	80	Sigma-Aldrich	99.0
16	1-Chlorobutane	79	Sigma-Aldrich	99.5
17	Benzene	80	Fisher Chemical	99.0
18	1,2-Dichloroethane	83	Sigma-Aldrich	99.8

Table A.3. Diesel Spiked Compounds.

List of 8 compounds that were spiked into diesel fuel in order of elution time on ^{1}D. 100 µl of each compound was mixed to create a 800 µl stock solution. Then 10 µl of the stock solution was added to 190 µl of diesel fuel to create a 200 µl solution.

Elution	Name	Boiling Point (°C)	Supplier	Purity (%)
1	1,1,1-Trichloroethane	74	Sigma-Aldrich	99.5
2	Butylamine	78	Sigma-Aldrich	99.8
3	1,2-Dichloroethane	83	Sigma-Aldrich	99.8
4	1,6-Dichlorohexane	90	Sigma-Aldrich	98.0
5	N-Cyclohexylaniline	192	Sigma-Aldrich	99.0
6	N,N-Dimethylaniline	194	Sigma-Aldrich	99.0
7	m-Toluidine	203	Sigma-Aldrich	99.0
8	Dibenzylamine	300	Sigma-Aldrich	97.0

Figure A.1. Three Step Data Conversion from Frontal to ^{2}D Gaussian Peaks.

Modulation of ^{1}D signal with pulse flow valve and processing steps (3 steps) to convert signal to ^{2}D format with the appearance of a GC × GC chromatogram. (A) The unmodulated peak of a non-overlapped single analyte. (B) The same analyte after partial modulation with the pulse flow valve. (C) Differentiation of the partially modulated peak in (B). The minima represents the inflection point of the error function produced by the pulse valve flow modulator. (D) Inversion of the differentiated data. This is performed by multiplying the differentiated by -1. (E) The baseline sag produced by the differentiation step is removed by an in-house low frequency noise filter. (F) A 2D chromatogram produced by cutting and folding the data by the modulation period (P_M) time.

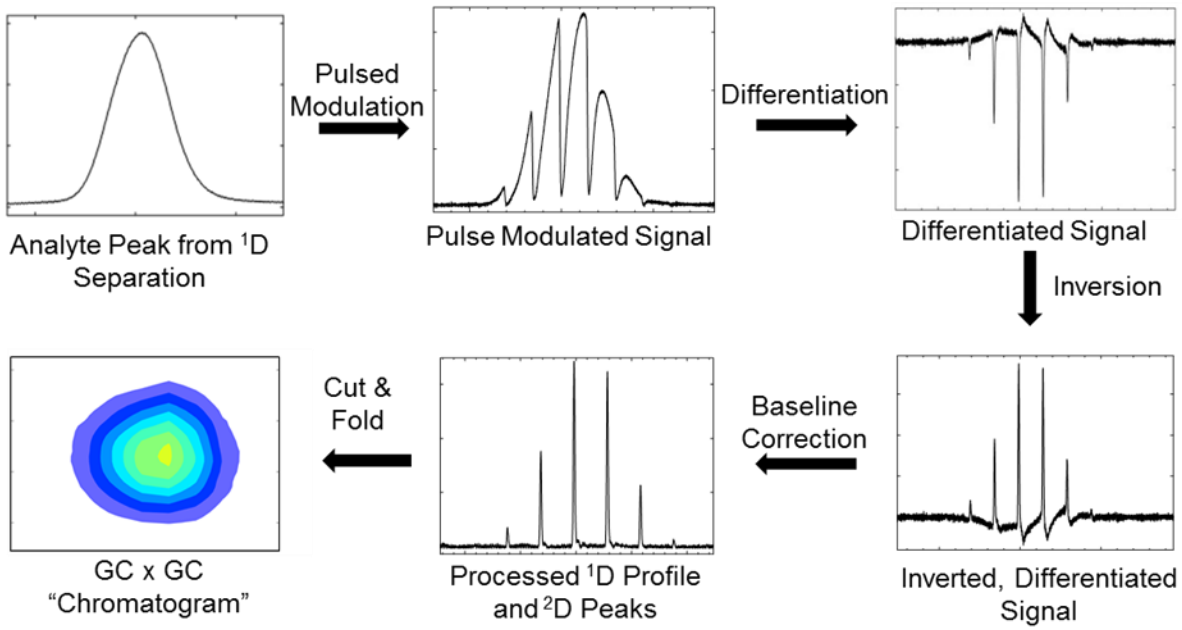

Figure A.2. PM 500 GC×GC-FID Data with ^2n_c Determination.

(A) Shown is a 2D Chromatogram of the 115 mixture separation shown in Figure 2.2. Twelve analytes were used to evaluate the peak capacity on the second dimension (^2n_c). (B) The twelve analytes were cut out of the 2D chromatogram, concatenated, and are plotted in a single chromatogram to measure their respective ^{2}D retention time and peak width (^2W_b). Retention times verses peak width is shown in the subset along with the fitted equation. (C) A model based on the equation from (B) is used to calculate the ^2n_c. A resulting second dimension peak capacity of 20 was calculated at a resolution of 1, for a total peak capacity $n_{c,2D}$ of ~7200 or a peak capacity production of ~1200 peaks/min for this separation.

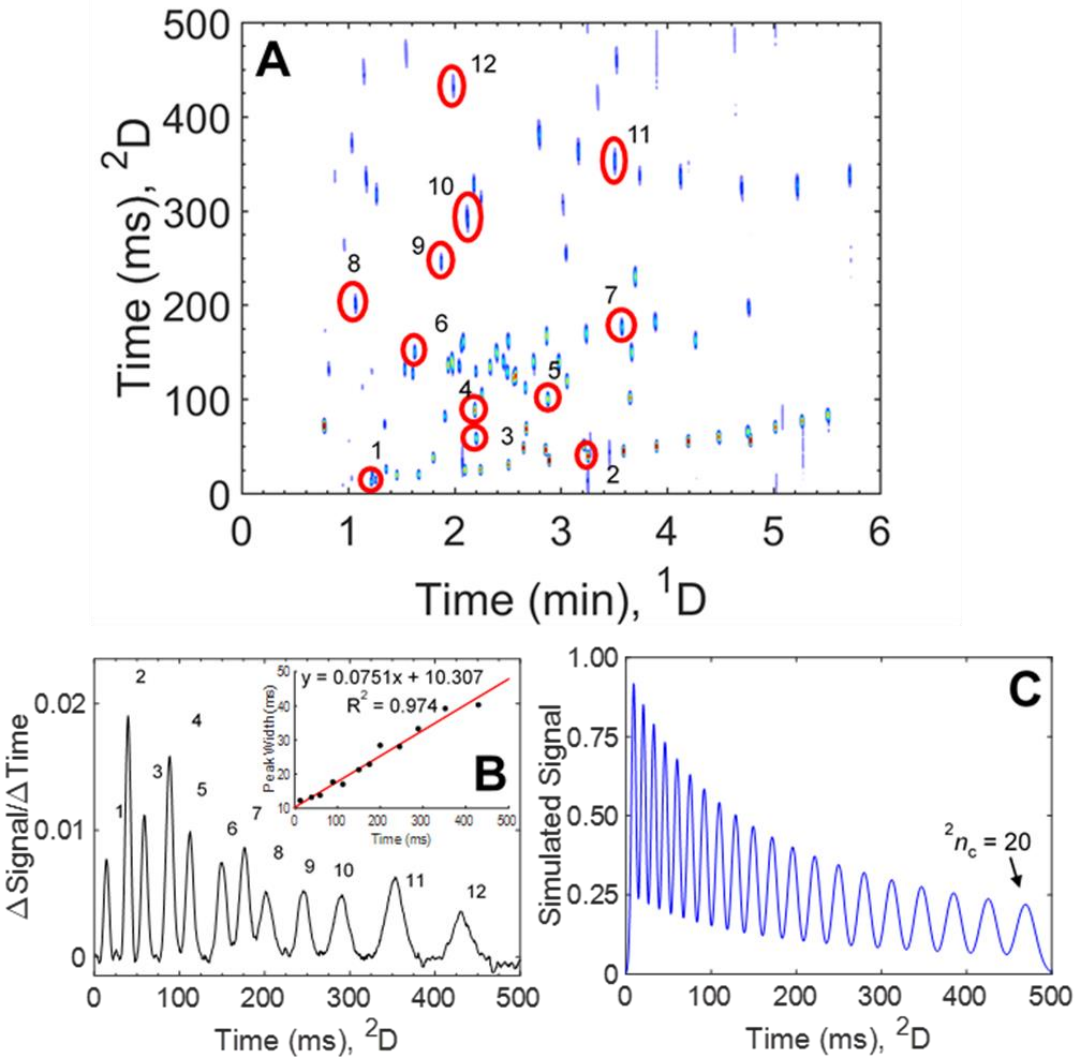

Figure A.3. Overlapped GC^3 – FID 18-Component Vector Data.

(A) The combined processed vector chromatogram of a GC^3 - FID separation of the 18 component mixture. Each analyte was injected individually to identify the analyte based on retention times. The ^1P_M was 1 sec and the ^2P_M was 50 ms. (**B**) An enhanced view of the processed vector chromatogram of is shown for n-Hexane. The width of based data is listed for all three separation dimensions. (**C**) An enhanced view of the processed vector chromatogram of is shown for Methylcyclopentane (red), and 1-Hexyne (yellow). The width of based data is listed for all three separation dimensions.

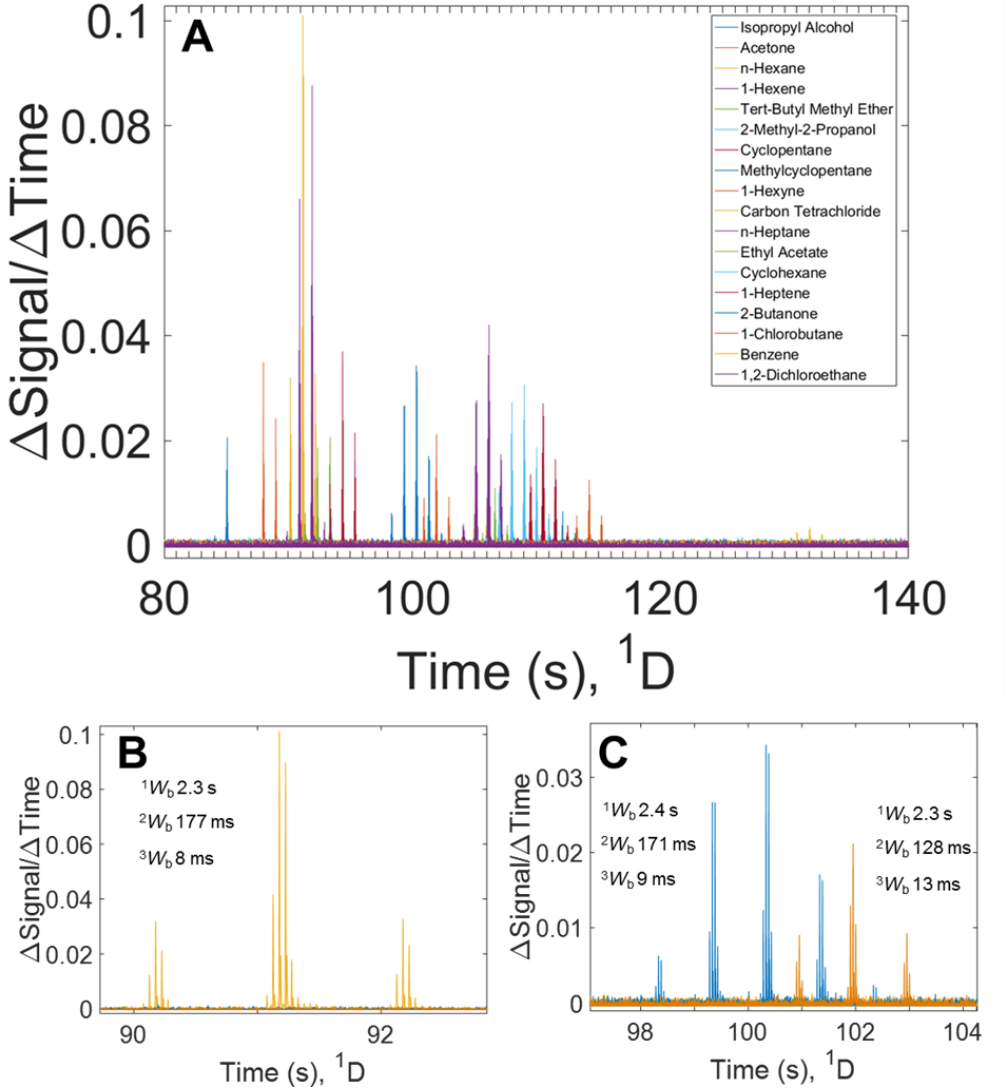

Figure A.4. 2D Chromatograms of 3 Analytes used for Figures of Merit.

(A) ^{1}D vs ^{2}D chromatogram of the 18 component test mixture collected using a $^{1}P_{M}$ of 1.0 seconds and a $^{2}P_{M}$ of 50 ms that has been summed on the ^{3}D. The analytes from Table 2.1 have been circled. (B) ^{1}D vs ^{3}D chromatogram of the 18 component test mixture collected using a $^{1}P_{M}$ of 1.0 seconds and a $^{2}P_{M}$ of 50 ms that has been summed on the ^{2}D. The analytes from Table 2.1 have been circled.

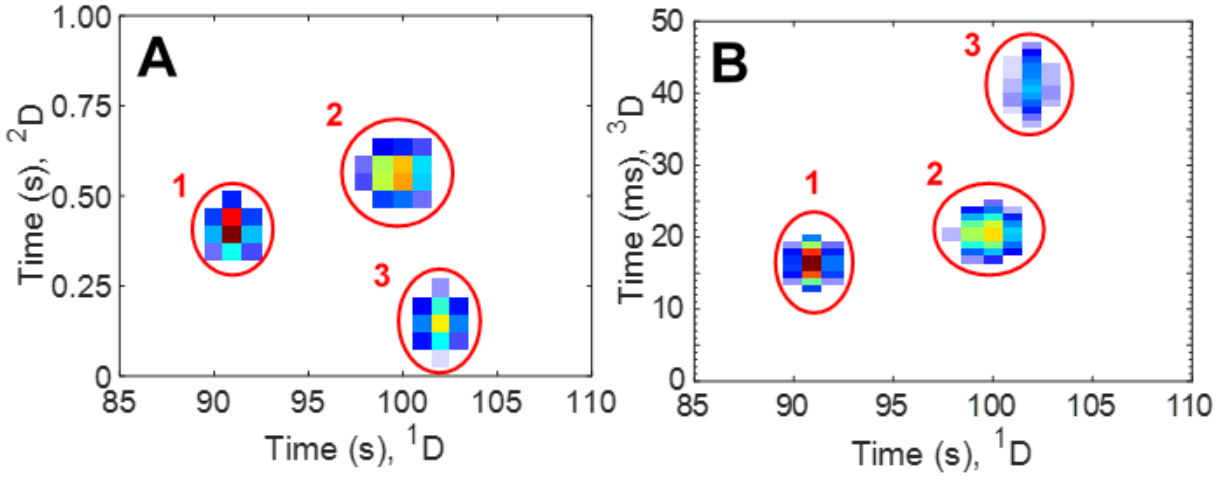

Figure A.5. 2D Chromatograms of 115-Component Test Mixture

(A) ^{2}D vs ^{3}D chromatogram of the 115 component test mixture collected using a $^{1}P_{M}$ of 1.2 seconds and a $^{2}P_{M}$ of 60 ms that has been summed on the ^{1}D. Because this is the summation of all the ^{1}D modulations, it is difficult to extract meaningful information. Thus (B), (C), and (D) have been prepared to show the benefit of visualizing the data in this manner. (B) Plot of ^{2}D vs ^{3}D chromatogram of the 115 component test mixture summed on ^{1}D between 3 to 4 minutes. (C) Plot of ^{2}D vs ^{3}D chromatogram of the 115 component test mixture summed on ^{1}D between 5 to 6 minutes. (D) Plot of ^{2}D vs ^{3}D chromatogram of the 115 component test mixture summed on ^{1}D between 7 to 8 minutes.

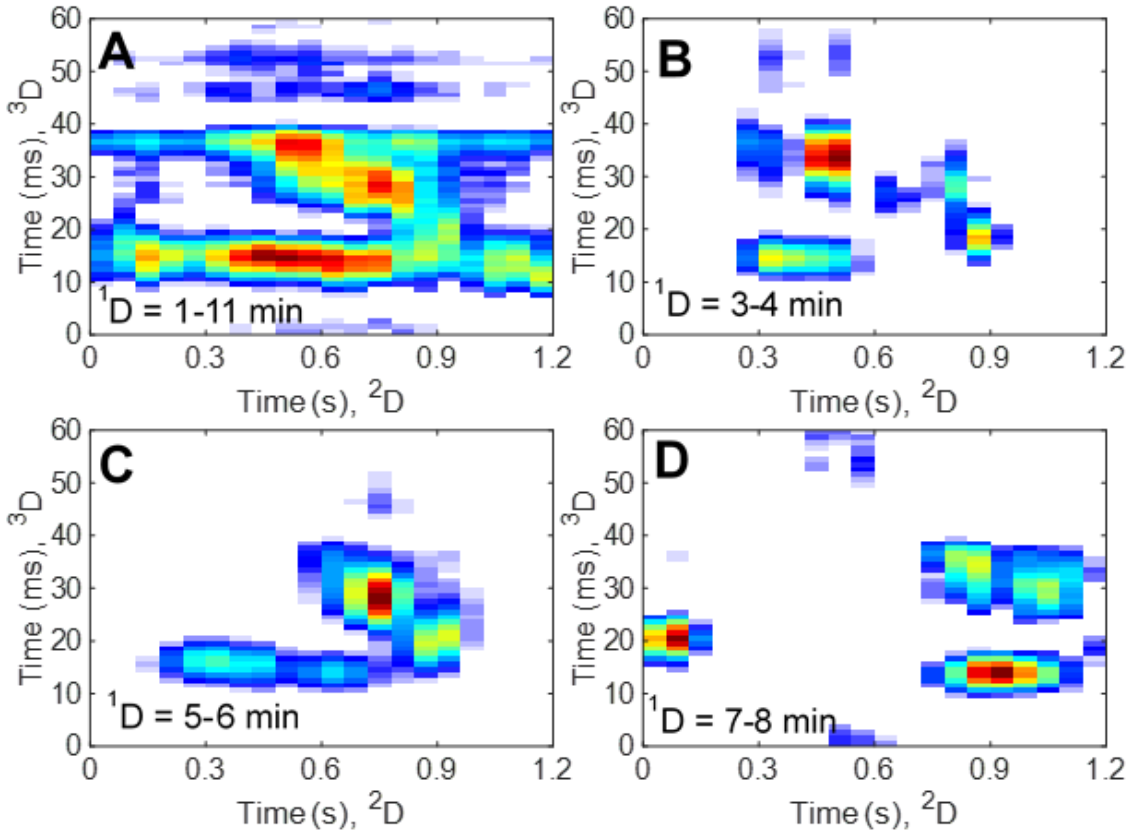

Figure A.6. 2D Chromatograms of 115-Component Test Mixture

(A) ^{1}D vs ^{2}D chromatogram of the 115 component test mixture collected using a $^{1}P_{M}$ of 1.2 seconds and a $^{2}P_{M}$ of 60 ms that has been summed on the ^{3}D. The analytes from Table 2.2 have been circled. (B) ^{1}D vs ^{3}D chromatogram of the 115 component test mixture collected using a $^{1}P_{M}$ of 1.2 seconds and a $^{2}P_{M}$ of 60 ms that has been summed on the ^{2}D. The analytes from Table 2.2 have been circled.

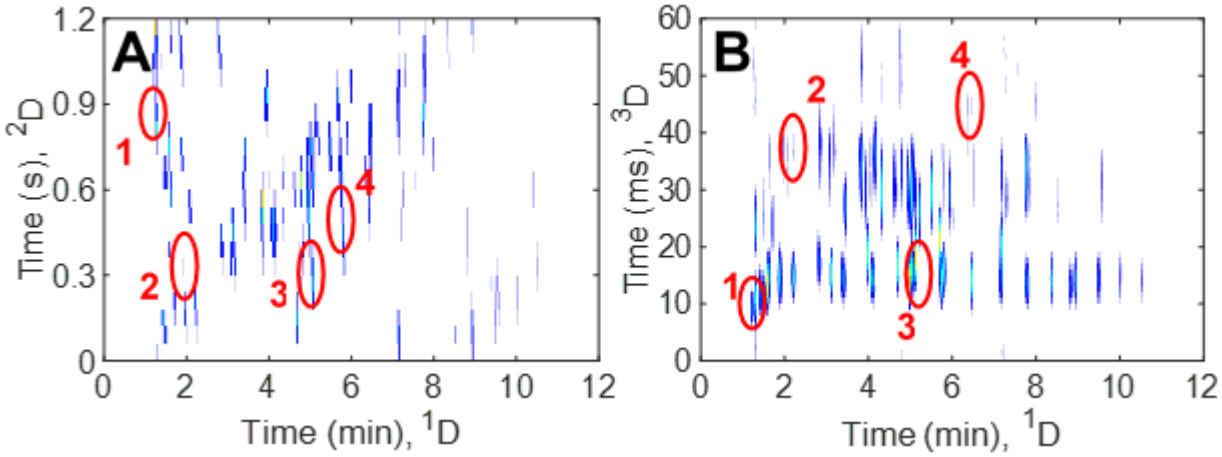

Figure A.7. 2D Chromatograms of Diesel with Spiked Analytes.

(A) ^{1}D vs ^{2}D chromatogram of diesel fuel spiked with 8 compounds collected using a $^{1}P_{M}$ of 1.2 seconds and a $^{2}P_{M}$ of 60 ms that has been summed on the ^{3}D. (B) ^{1}D vs ^{3}D chromatogram of diesel fuel spiked with 8 compounds collected using a $^{1}P_{M}$ of 1.2 seconds and a $^{2}P_{M}$ of 60 ms that has been summed on the ^{2}D. (C) ^{2}D vs ^{3}D chromatogram of diesel fuel spiked with 8 compounds collected using a $^{1}P_{M}$ of 1.2 seconds and a $^{2}P_{M}$ of 60 ms that has been summed on the ^{1}D. Diesel fuel is even more complicated than the 115 and 18 component mixtures and because there are thousands of compounds, viewing the data in this manner does not yield much information. Thus (D), (E), and (F) have been prepared where only portions of the ^{1}D chromatogram are shown. In order to improve the visualization, only 3 modulations (3.6 seconds) are shown. (D) ^{2}D vs ^{3}D chromatogram of diesel fuel spiked with 8 compounds collected using a $^{1}P_{M}$ of 1.2 seconds and a $^{2}P_{M}$ of 60 ms that has been summed on the ^{1}D from 6.4 to 6.44 minutes. The analyte at a ^{2}D retention time of ~0.45 s and ^{3}D retention time of ~45 ms is butylamine 1 of the 8 spiked analytes. (E) ^{2}D vs ^{3}D chromatogram of diesel fuel spiked with 8 compounds collected using a $^{1}P_{M}$ of 1.2 seconds and a $^{2}P_{M}$ of 60 ms that has been summed on the ^{1}D from 7.82 to 7.86 minutes. The analyte at a ^{2}D retention time of ~0.90 s and ^{3}D retention time of ~55 ms is 1,2-dichloroethane 1 of the 8 spiked analytes. (F) ^{2}D vs ^{3}D chromatogram of diesel fuel spiked with 8 compounds collected using a $^{1}P_{M}$ of 1.2 seconds and a $^{2}P_{M}$ of 60 ms that has been summed on the ^{1}D from 9.42 to 9.46 minutes. The analyte at a ^{2}D retention time of ~0.90 s and ^{3}D retention time of ~50 ms is N,N-dimethylaniline 1 of the 8 spiked analytes.

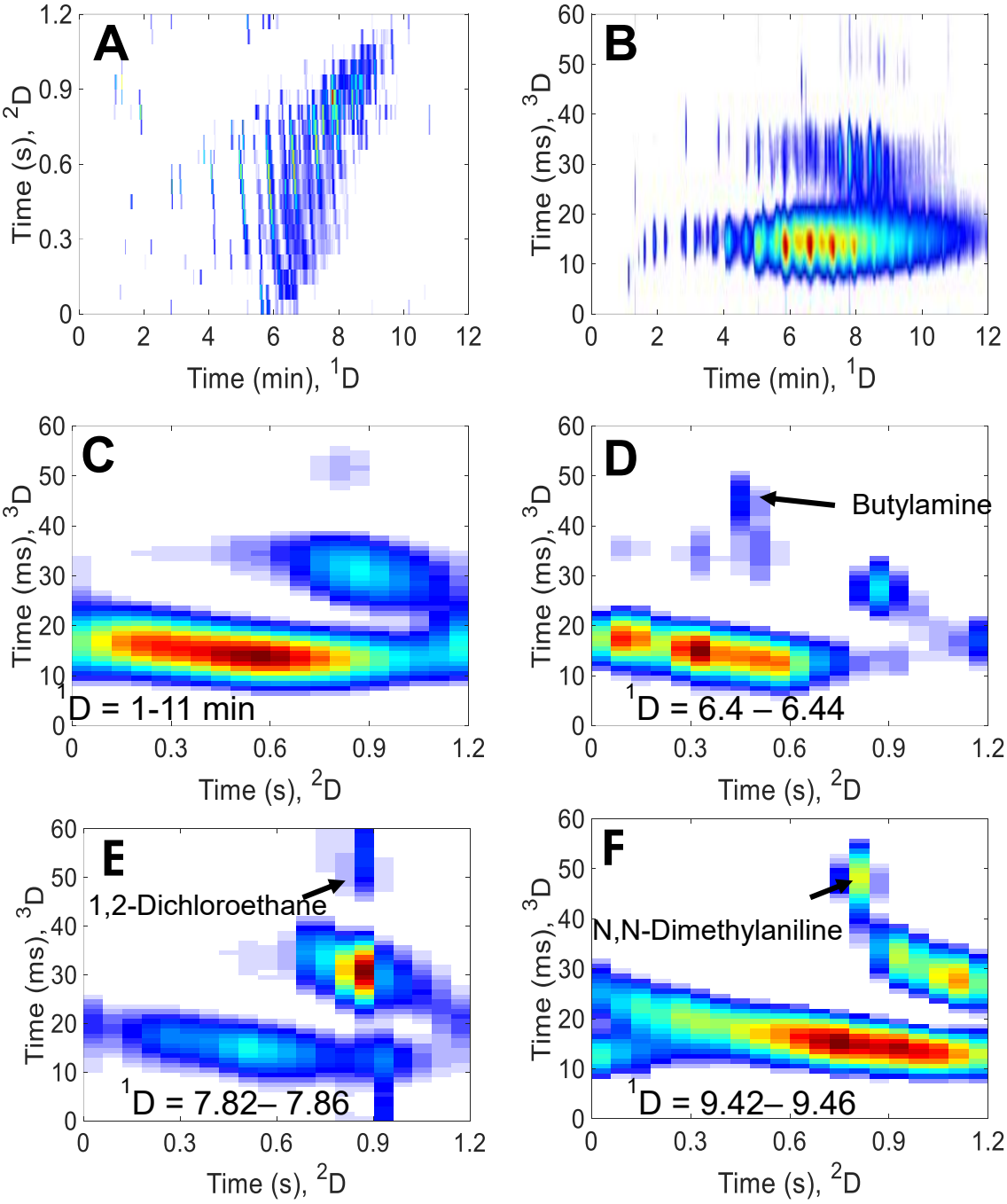

2874

2875

2876

Appendix B

Table B.1. 18-Component Mixture with Resolution and Match Values.

All data taken from four separations of the 4:1 concentration (14 ng per Analyte) injected. Resolution is reported to the nearest neighbor, some analytes have to resolutions listed as they have two neighbors

Elution	Name	R_s(s)	Match Value	MV RSD %
1	acetone	0.17	794	0.6
2	isopropyl alcohol	0.17, 1.09	858	5.6
3	2-methyl-2-propanol	1.09	871	13.6
4	t-butyl methyl ether	0.06	845	3.7
5	cyclopentane	0.06	820	14.5
6	1-hexene	0.53	914	3.1
7	hexane	0.53, 0.13	856	5.9
8	2-butanone	0.13	674	4.1
9	ethyl acetate	0.53	819	9.8
10	1-hexyne	0.53, 0.91	912	3.8
11	methylcyclopentane	0.91	829	10.2
12	1-chlorobutane	0.53	842	9.3
13	1,2-dichloroethane	0.53	855	2.2
14	cyclohexane	0.06	546	10.6
15	benzene	0.06, 0.03	838	3.1
16	carbon tetrachloride	0.03	756	15.4
17	1-heptene	1.19	913	3.8
18	heptane	1.19	855	8.9

Table B.2. Chromatographic Figures of Merit 18-Component Mixture.

All data ^{1}D data reported herein is the mean with standard deviation and relative standard deviation percentage given for four (4) separations at the 4:1 concentration (14 ng per analyte injected). ^{2}D data reported is taken from one (1) separation of the 4:1 concentration.

Order	Name	$^{1}t_R$ (s) ($\bar{x}$)	$^{1}t_R$ RSD%	$^{1}W_b$ (s) ($\bar{x}$)	$^{1}W_b$ RSD%	$^{2}t_R$ (ms) ($\bar{x}$)	$^{2}t_R$ RSD%	$^{2}W_b$ (ms) ($\bar{x}$)	$^{2}W_b$ RSD%
1	acetone	22.32 (0.20)	0.89	0.83 (0.010)	1.23	14 (0.9)	4.02	26 (0.8)	3.19
2	isopropyl alcohol	22.46 (0.21)	0.94	0.84 (0.010)	1.13	44 (0.5)	7.90	36 (1.1)	3.17
3	2-methyl-2-propanol	23.33 (0.17)	0.73	0.76 (0.008)	1.04	16 (0.6)	5.02	32 (0.8)	2.60
4	t-butyl methyl ether	25.15 (0.19)	0.77	0.77 (0.008)	1.10	14 (0.5)	4.06	16 (0.6)	3.90
5	cyclopentane	25.20 (0.19)	0.77	0.84 (0.012)	1.28	24 (0)	0	23 (1.0)	4.53
6	1-hexene	26.34 (0.10)	0.65	0.81 (0.009)	1.07	18 (0.9)	5.48	21 (1.0)	4.51
7	hexane	26.78 (0.10)	0.63	0.83 (0.007)	0.89	18 (0.3)	1.90	18 (0.6)	3.55
8	2-butanone	26.89 (0.17)	0.37	0.93 (0.008)	0.92	12 (0.5)	3.11	36 (1.3)	3.55
9	ethyl acetate	28.07 (0.17)	0.61	1.05 (0.017)	1.63	2 (0.8)	4.87	29 (0.8)	3.63
10	1-hexyne	28.57 (0.17)	0.60	0.89 (0.014)	1.53	24 (0.5)	1.93	27 (1.1)	5.24
11	methylcyclopentane	29.39 (0.17)	0.59	0.91 (0.011)	1.16	30 (0.6)	2.84	22 (0.8)	3.90
12	1-chlorobutane	31.42 (0.19)	0.60	1.01 (0.008)	0.76	26 (0.5)	3.69	27 (1.0)	3.53
13	1,2-dichloroethane	31.69 (0.17)	0.53	1.02 (0.013)	1.30	N/A	N/A	N/A	N/A
14	cyclohexane	32.99 (0.17)	0.46	1.01 (0.011)	1.65	32 (0.4)	3.88	31 (1.1)	3.46
15	benzene	33.05 (0.15)	0.53	1.01 (0.017)	1.13	50 (0.5)	2.95	24 (0.8)	3.40
16	carbon tetrachloride	33.08 (0.17)	0.51	1.01 (0.012)	1.18	48 (0.8)	3.29	35 (1.0)	2.73
17	1-heptene	36.31 (0.15)	0.42	1.09 (0.017)	1.54	38 (0.5)	2.70	22 (0.8)	3.76
18	heptane	37.61 (0.17)	0.45	1.10 (0.017)	1.52	28 (0.4)	1.94	21 (1.1)	5.02

Figure B.1. Total Ion and Selection Ion Chromatograms.

A total ion count 1D chromatogram of all injected concentrations shown. (**B**) Select ions 1D chromatogram at an injected concentration of 14 ng (4:1 dilution).

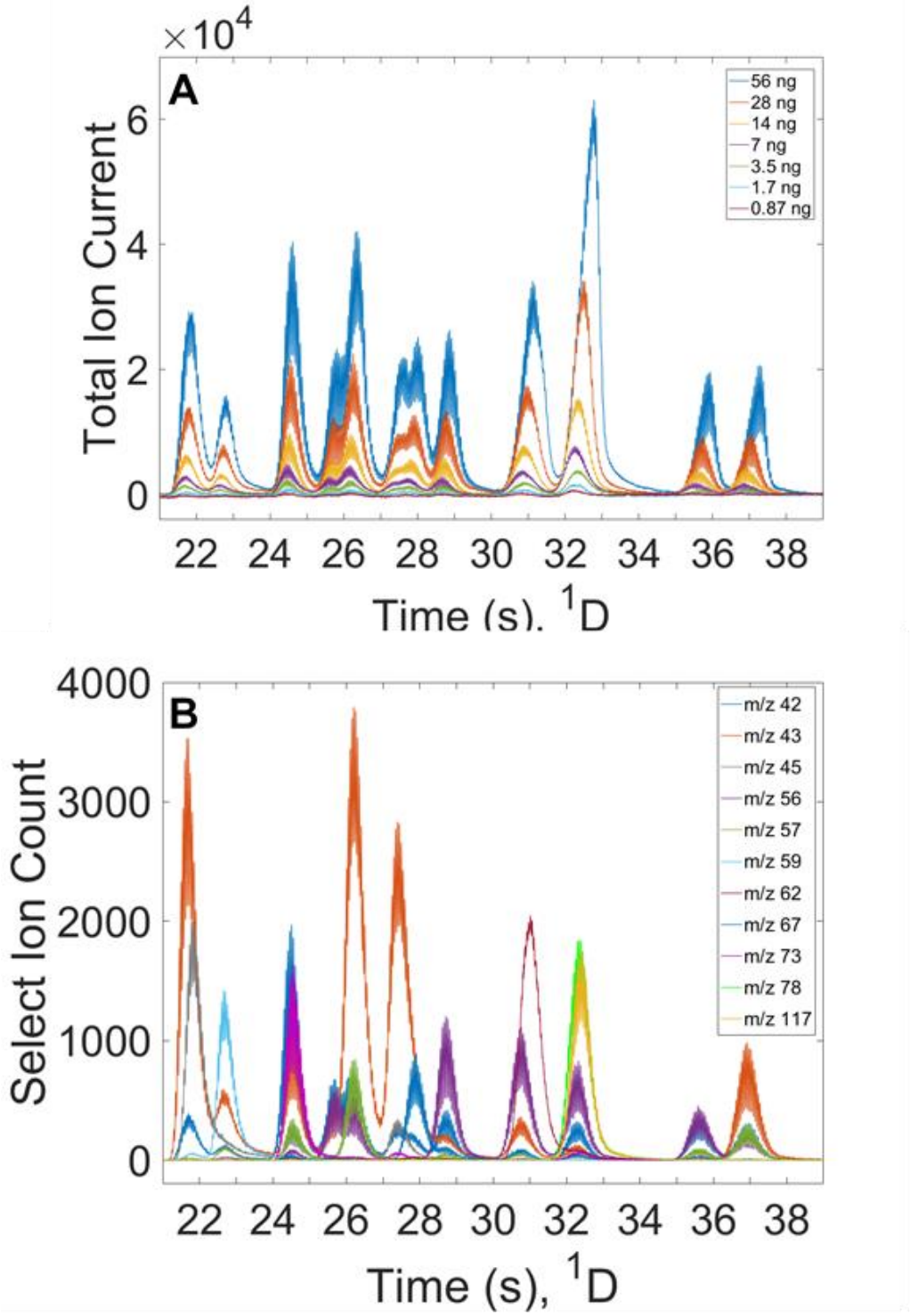

Figure B.2. Raw Data, MCR-ALS Loadings, 2D Chromatograms for Overlapped Regions.

The following series of figures show a close up of all analytes. The raw data (i.), MCR-ALS loadings (ii.) and 2D contour chromatogram (iii.) are shown. (**A**) Analytes 1: acetone, 2: isopropyl alcohol, 3: 2-methyl-2-propanol. (**B**) Analytes 4: T-butyl methyl ether, 5: cyclopentane. (**C**) Analytes 6: 1-hexene, 7: hexane, 8: 2-butanone. (**D**) Analytes 12: 1-chlorobutane, 13: 1,2-dichloroethane. Note that 1,2-dichloroethane is missing from 2D contour chromatogram due to excessive retention on the ^{2}D polar column. (**E**) Analytes 14: cyclohexane, 15: benzene, 16: carbon tetrachloride. (**F**) Analytes 17: 1-heptene, 18: heptene.

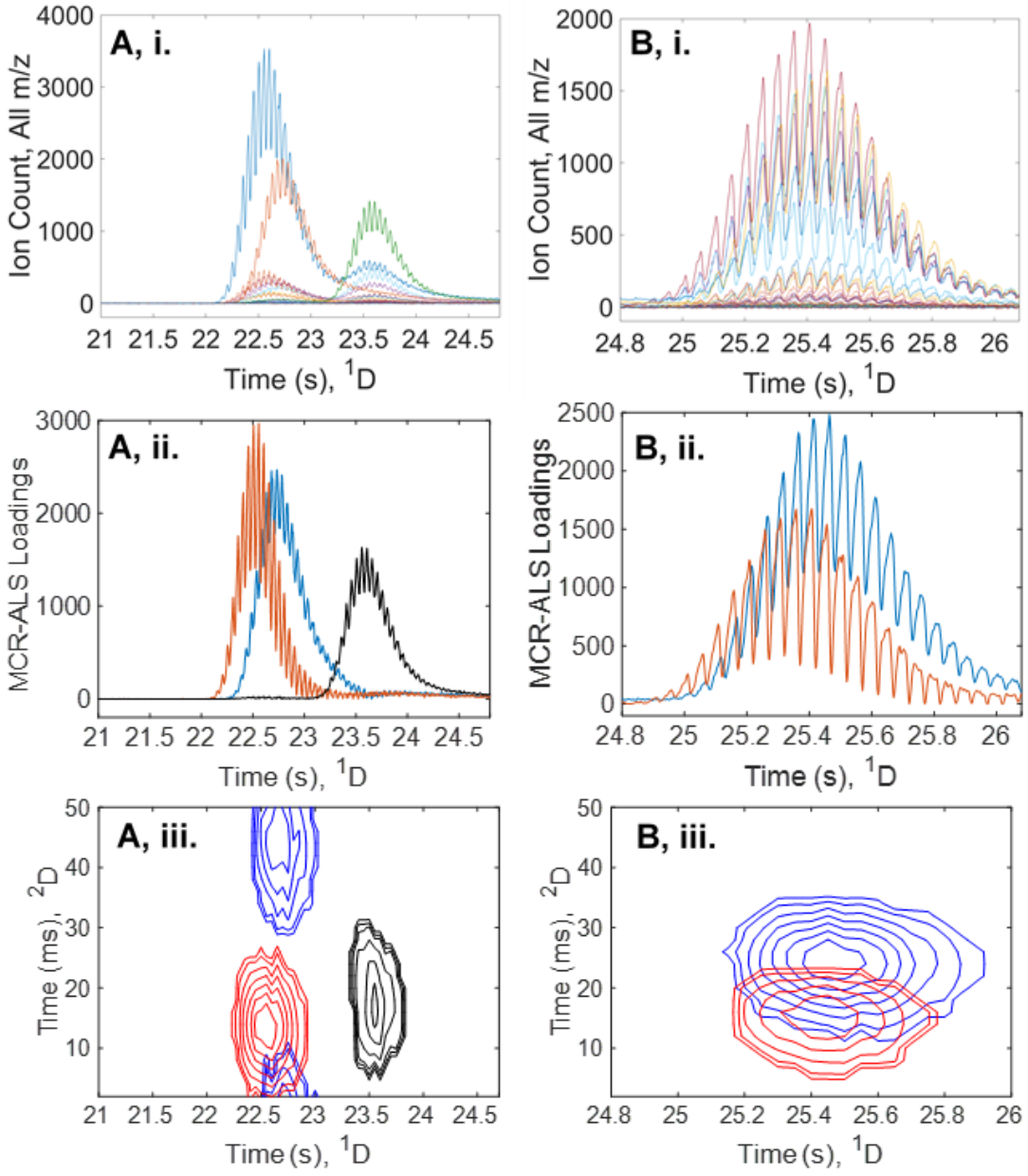

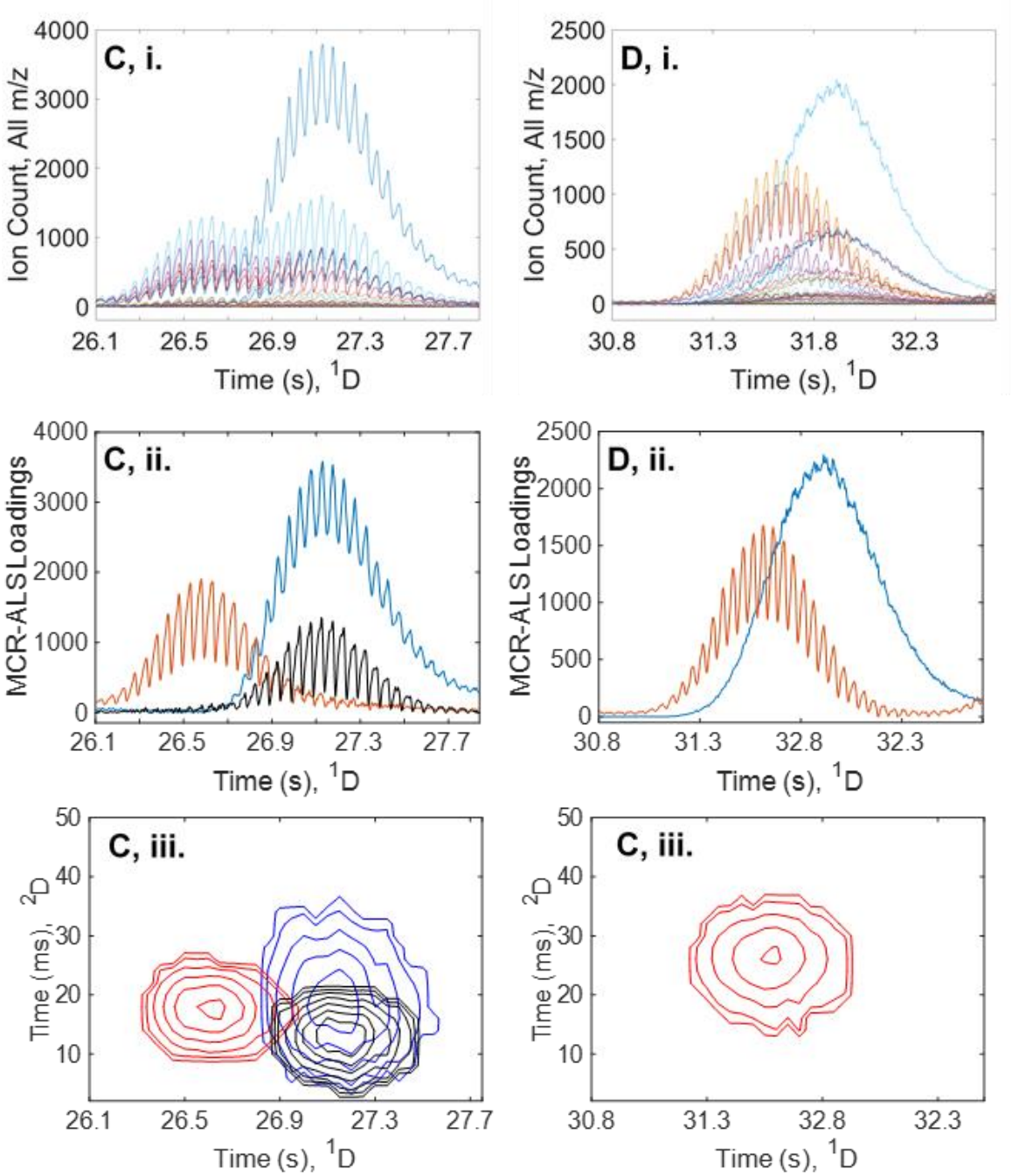

2918
2919
2920
2921

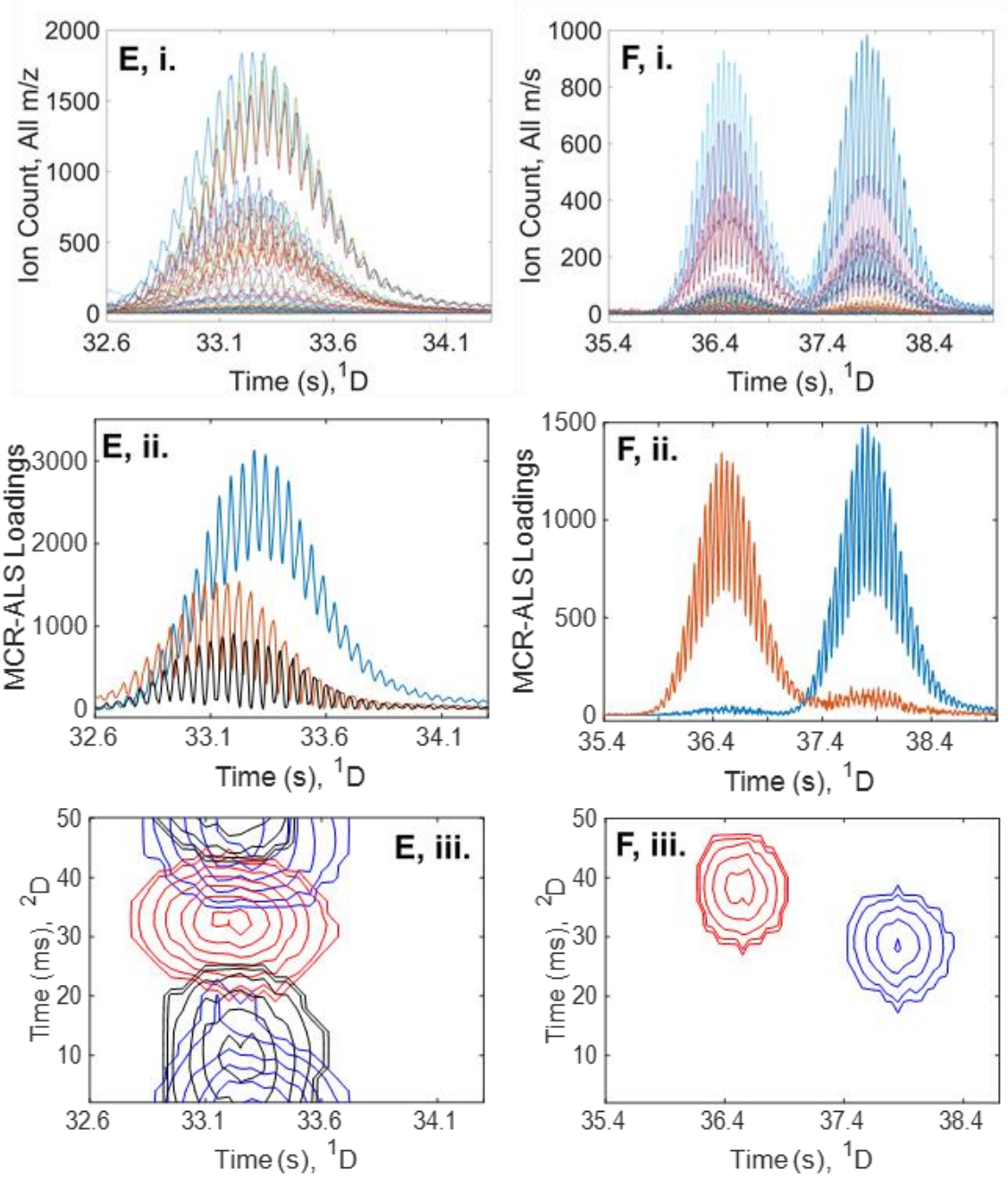
E, i.
Ion Count, All m/z
Time (s), 1D
F, i.
Ion Count, All m/s
Time (s), 1D
E, ii.
MCR-ALS Loadings
Time (s), 1D
F, ii.
MCR-ALS Loadings
Time (s), 1D
E, iii.
Time (ms), 2D
Time (s), 1D
F, iii.
Time (ms), 2D
Time (s), 1D

Figure B.3. MCR-ALS Loading vs Mass Injected.

(A) MCR-ALS Loading area results based on mass injected for analytes 4: T-butyl methyl ether 5: cyclopentane are shown. Inset shown for detail of lower inject concentrations. (B) Match values for all concentrations. The resolution (R_S) of the two analytes was calculated at (0.06).

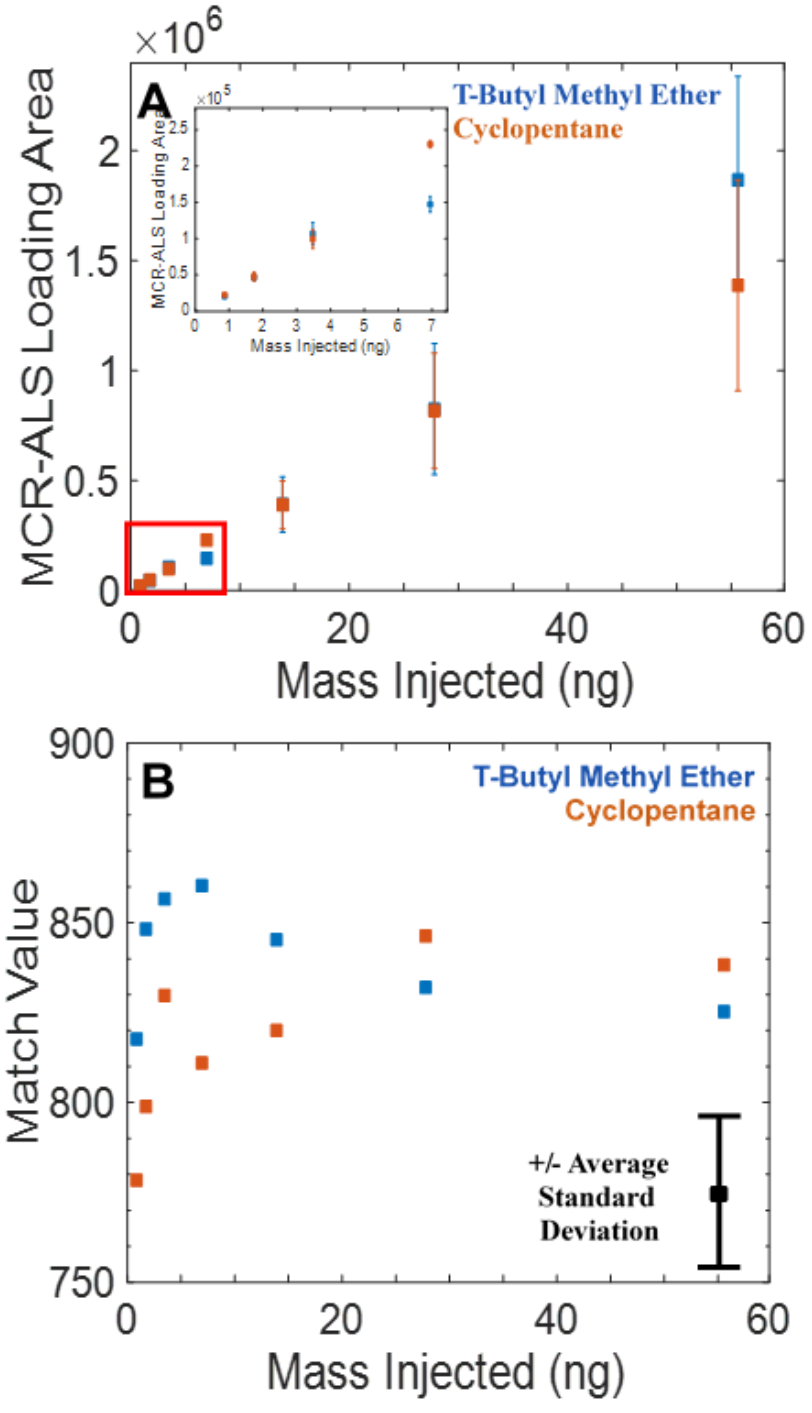

Figure B.4. Figures of Merit ^{1}D and ^{2}D Peaks.

(A) MCR-ALS loading of the internal standard, 1-Heptene. (B) Differentiated MCR-ALS loading in Figure S2A. (C) 1D chromatogram of 1-Hexane generated from the 2D peak maximum shown in Figure S2B, $^{1}w_{b}$ of 1.09 s was determined. (D) Close up view of three ^{2}D peaks from Figure S2B, $^{2}w_{b}$ of 22 ms was determined.

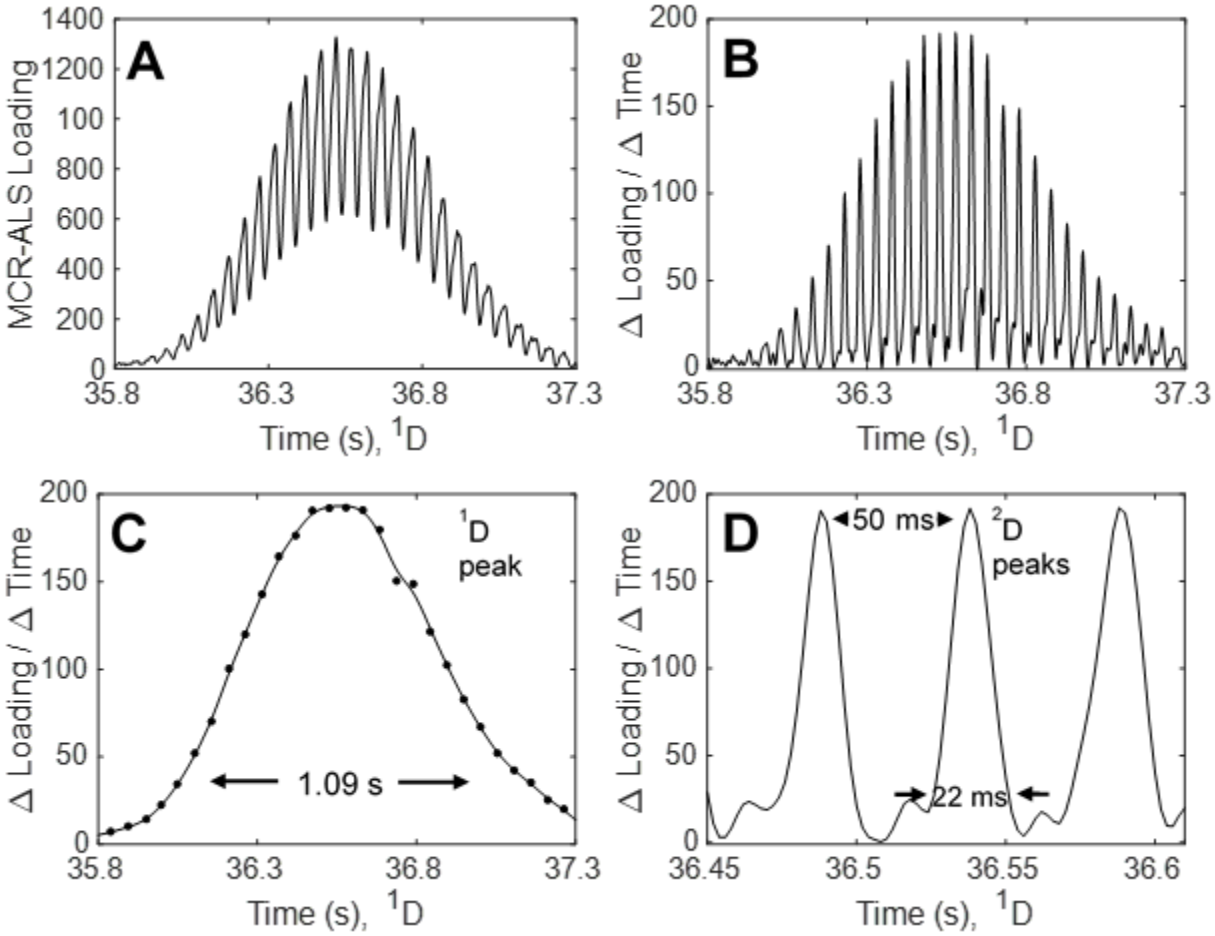

Appendix C

Table C.1. 4-Component Mixture.

Table of the 4-component mixture ordered by elution order. The supplier and purity are included. The 4 compounds were combined equally by volume by adding 10 µL each for a total volume of 40 µL contained in the sample vial prior to each separation.

Elution	Name	Boiling Point (°C)	Supplier	Purity (%)
1	Hexane	68	Sigma-Aldrich	97.0
2	Cyclohexane	81	Sigma-Aldrich	99.0
3	Methylcyclopentane	72	Honeywell	97.0
4	1-Hexyne	71	Sigma-Aldrich	97.0

Figure C.1 2D Chromatogram of Gasoline Separated via 1D-GC Sampling.

A 2D chromatogram of gasoline is shown with a continuous sampling rate of 75 ms at 32 psi from the pulse flow valve where the retention time of the compounds on the DB-Wax column is shown compared to the oven temperature ramped (30-100 ˚C) at 1 ˚C/min. The slight increase in retention time as the temperature increases is due to instrument set to constant flow (2.0 mL/min) which resulted in a decrease in linear flow velocity of the carrier gas as increased temperatures. Data was registered 5 ms to align the alkane band close to 0 ms.

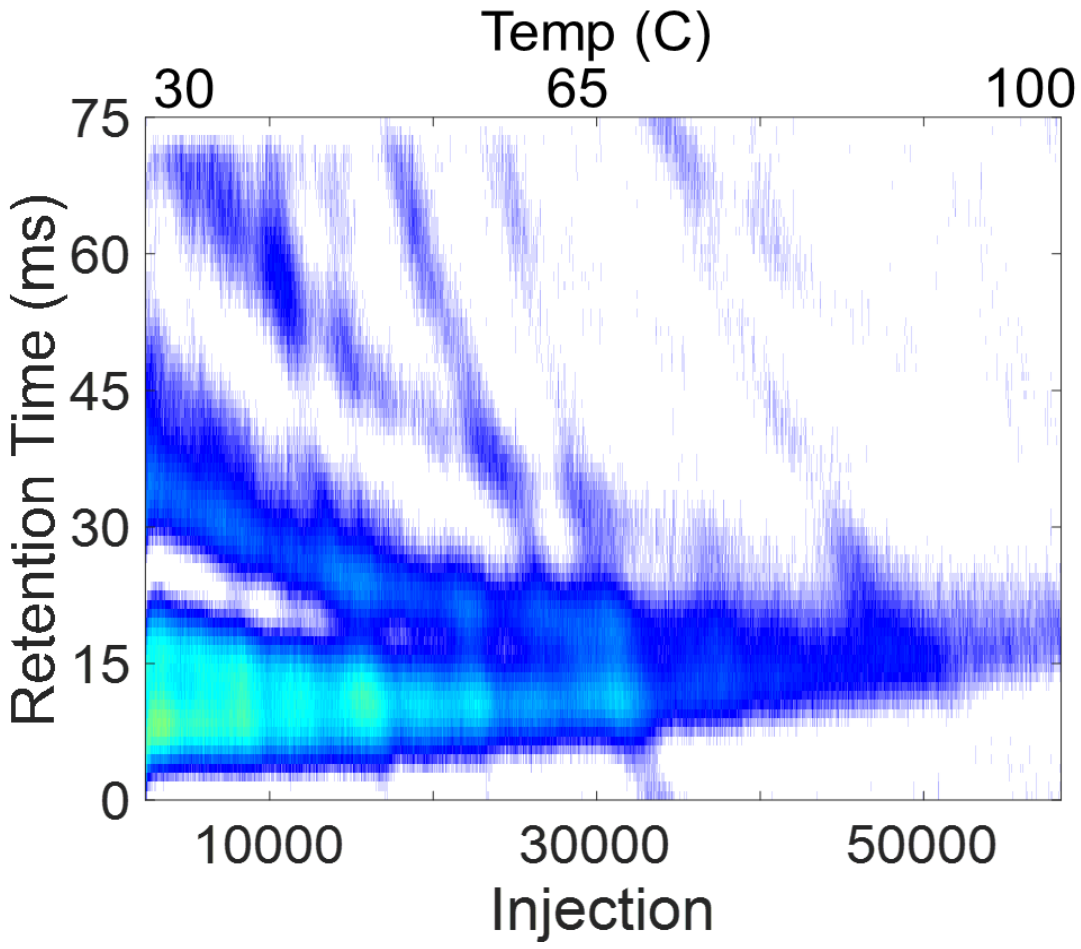

BIBLIOGRAPHY

V. Abrahamsson, N. Ristic, K. Franz, K. Van Geem, Comprehensive two-dimensional gas chromatography in combination with pixel-based analysis for fouling tendency prediction, Journal of Chromatography A. 1501 (2017) 89–98.

J.L. Adcock, M. Adams, B.S. Mitrevski, P.J. Marriott, Peak Modeling Approach to Accurate Assignment of First-Dimension Retention Times in Comprehensive Two-Dimensional Chromatography, Anal. Chem. 81 (2009) 6797–6804.

M.S. Alam, C. Stark, R.M. Harrison, Using Variable Ionization Energy Time-of-Flight Mass Spectrometry with Comprehensive GC×GC To Identify Isomeric Species, Anal. Chem. 88 (2016) 4211–4220.

G.L. Alexandrino, G.R. de Sousa, F. de A.M. Reis, F. Augusto, Optimizing loop-type cryogenic modulation in comprehensive two-dimensional gas chromatography using time-variable combination of the dual-stage jets for analysis of crude oil, Journal of Chromatography A. (2017).

H.D. Bean, J.-M.D. Dimandja, J.E. Hill, Bacterial volatile discovery using solid phase microextraction and comprehensive two-dimensional gas chromatography–time-of-flight mass spectrometry, Journal of Chromatography B. 901 (2012) 41–46.

L.M. Blumberg, Accumulating resampling (modulation) in comprehensive two-dimensional capillary GC (GC×GC), J. Sep. Science. 31 (2008) 3358–3365.

L.M. Blumberg, Flow optimization in one-dimensional and comprehensive two-dimensional gas chromatography, Journal of Chromatography A. 1536 (2018) 27–38.

C.A. Bruckner, B.J. Prazen, R.E. Synovec, Comprehensive Two-Dimensional High-Speed Gas Chromatography with Chemometric Analysis, Anal. Chem. 70 (1998) 2796–2804.

A. Burel, M. Vaccaro, Y. Cartigny, S. Tisse, G. Coquerel, P. Cardinael, Retention modeling and retention time prediction in gas chromatography and flow-modulation comprehensive two-dimensional gas chromatography: The contribution of pressure on solute partition, Journal of Chromatography A. 1485 (2017) 101–119.

B.V. Burger, T. Snyman, W.J.G. Burger, W.F. van Rooyen, Thermal modulator array for analyte modulation and comprehensive two-dimensional gas chromatography, J. Sep. Science. 26 (2003) 123–128.

H. Cai, S.D. Stearns, Partial Modulation Method via Pulsed Flow Modulator for Comprehensive Two-Dimensional Gas Chromatography, Anal. Chem. 76 (2004) 6064–6076.

T.-Y. Chen, M.-J. Li, J.-L. Wang, Sub-second thermal desorption of a micro-sorbent trap for the analysis of ambient volatile organic compounds, Journal of Chromatography A. 976 (2002) 39–45.

S.-T. Chin, G.T. Eyres, P.J. Marriott, Application of integrated comprehensive/multidimensional gas chromatography with mass spectrometry and olfactometry for aroma analysis in wine and coffee, Food Chemistry. 185 (2015) 355–361.

W.R. Collin, A. Bondy, D. Paul, K. Kurabayashi, E.T. Zellers, μGC × μGC: Comprehensive Two-Dimensional Gas Chromatographic Separations with Microfabricated Components, Anal. Chem. 87 (2015) 1630–1637.

W.R. Collin, N. Nuñovero, D. Paul, K. Kurabayashi, E.T. Zellers, Comprehensive two-dimensional gas chromatographic separations with a temperature programmed microfabricated thermal modulator, Journal of Chromatography A. 1444 (2016) 114–122.

M.K. Das, S.C. Bishwal, A. Das, D. Dabral, A. Varshney, V.K. Badireddy, R. Nanda, Investigation of Gender-Specific Exhaled Breath Volatome in Humans by GCxGC-TOF-MS, Analytical Chemistry. 86 (2014) 1229–1237.
J.M. Davis, J.C. Giddings, Statistical theory of component overlap in multicomponent chromatograms, Anal. Chem. 55 (1983) 418–424.
J.M. Davis, J.C. Giddings, Statistical method for estimation of number of components from single complex chromatograms: theory, computer-based testing, and analysis of errors, Anal. Chem. 57 (1985) 2168–2177.
J.M. Davis, D.R. Stoll, P.W. Carr, Effect of First-Dimension Undersampling on Effective Peak Capacity in Comprehensive Two-Dimensional Separations, Anal. Chem. 80 (2008) 461–473.
D.R. Deans, A new technique for heart cutting in gas chromatography [1], Chromatographia. 1 (1968) 18–22.
L.M. Dubois, K.A. Perrault, P.-H. Stefanuto, S. Koschinski, M. Edwards, L. McGregor, J.-F. Focant, Thermal desorption comprehensive two-dimensional gas chromatography coupled to variable-energy electron ionization time-of-flight mass spectrometry for monitoring subtle changes in volatile organic compound profiles of human blood, Journal of Chromatography A. 1501 (2017) 117–127.
C. Duhamel, P. Cardinael, V. Peulon-Agasse, R. Firor, L. Pascaud, G. Semard-Jousset, P. Giusti, V. Livadaris, Comparison of cryogenic and differential flow (forward and reverse fill/flush) modulators and applications to the analysis of heavy petroleum cuts by high-temperature comprehensive gas chromatography, Journal of Chromatography A. 1387 (2015) 95–103.
M. Edwards, H. Boswell, T. Górecki, Comprehensive Multidimensional Chromatography, Current Chromatography. 2 (2015) 80–109.
M. Edwards, T. Górecki, Inlet backflushing device for the improvement of comprehensive two dimensional gas chromatographic separations, Journal of Chromatography A. 1402 (2015) 110–123.
M. Edwards, A. Mostafa, T. Górecki, Modulation in comprehensive two-dimensional gas chromatography: 20 years of innovation, Anal Bioanal Chem. 401 (2011) 2335–2349.
A. Eftekhari, H. Parastar, Multivariate analytical figures of merit as a metric for evaluation of quantitative measurements using comprehensive two-dimensional gas chromatography–mass spectrometry, Journal of Chromatography A. 1466 (2016) 155–165.
B.D. Fitz, R.B. Wilson, B.A. Parsons, J.C. Hoggard, R.E. Synovec, Fast, high peak capacity separations in comprehensive two-dimensional gas chromatography with time-of-flight mass spectrometry, Journal of Chromatography A. 1266 (2012) 116–123.
S.L. Forbes, A.N. Troobnikoff, M. Ueland, K.D. Nizio, K.A. Perrault, Profiling the decomposition odour at the grave surface before and after probing, Forensic Science International. 259 (2016) 193–199.
C.G. Fraga, Chemometric approach for the resolution and quantification of unresolved peaks in gas chromatography–selected-ion mass spectrometry data, Journal of Chromatography A. 1019 (2003) 31–42.
F.A. Franchina, M.E. Machado, P.Q. Tranchida, C.A. Zini, E.B. Caramão, L. Mondello, Determination of aromatic sulphur compounds in heavy gas oil by using (low-)flow modulated comprehensive two-dimensional gas chromatography–triple quadrupole mass spectrometry, Journal of Chromatography A. 1387 (2015) 86–94.

F.A. Franchina, M. Maimone, D. Sciarrone, G. Purcaro, P.Q. Tranchida, L. Mondello, Evaluation of a novel helium ionization detector within the context of (low-)flow modulation comprehensive two-dimensional gas chromatography, Journal of Chromatography A. 1402 (2015) 102–109.

F.A. Franchina, M. Maimone, P.Q. Tranchida, L. Mondello, Flow modulation comprehensive two-dimensional gas chromatography–mass spectrometry using ≈4mLmin−1 gas flows, Journal of Chromatography A. 1441 (2016) 134–139.

C.E. Freye, H.D. Bahaghighat, R.E. Synovec, Comprehensive two-dimensional gas chromatography using partial modulation via a pulsed flow valve with a short modulation period, Talanta. 177 (2018) 142–149.

C.E. Freye, B.D. Fitz, M.C. Billingsley, R.E. Synovec, Partial least squares analysis of rocket propulsion fuel data using diaphragm valve-based comprehensive two-dimensional gas chromatography coupled with flame ionization detection, Talanta. 153 (2016) 203–210.

C.E. Freye, N.R. Moore, R.E. Synovec, Enhancing the chemical selectivity in discovery-based analysis with tandem ionization time-of-flight mass spectrometry detection for comprehensive two-dimensional gas chromatography, Journal of Chromatography A. (2018).

C.E. Freye, L. Mu, R.E. Synovec, High temperature diaphragm valve-based comprehensive two-dimensional gas chromatography, Journal of Chromatography A. 1424 (2015) 127–133.

C.E. Freye, R.E. Synovec, High temperature diaphragm valve-based comprehensive two-dimensional gas chromatography with time-of-flight mass spectrometry, Talanta. 161 (2016) 675–680.

H.-J. de Geus, J. de Boer, U.A.T. Brinkman, Development of a thermal desorption modulator for gas chromatography, Journal of Chromatography A. 767 (1997) 137–151.

A. Ghosh, C.T. Bates, S.K. Seeley, J.V. Seeley, High speed Deans switch for low duty cycle comprehensive two-dimensional gas chromatography, Journal of Chromatography A. 1291 (2013) 146–154.

J.C. Giddings, Two-dimensional separations: concept and promise, Anal. Chem. 56 (1984) 1258A-1270A.

A. Giri, M. Coutriade, A. Racaud, K. Okuda, J. Dane, R.B. Cody, J.-F. Focant, Molecular Characterization of Volatiles and Petrochemical Base Oils by Photo-Ionization GC×GC-TOF-MS, Analytical Chemistry. 89 (2017) 5395–5403.

A. Gonciarz, K. Kus, M. Szafarz, M. Walczak, A. Zakrzewska, J. Szymura-Oleksiak, Capillary electrophoresis/frontal analysis versus equilibrium dialysis in dexamethasone sodium phosphate-serum albumin binding studies, ELECTROPHORESIS. 33 (2012) 3323–3330.

R. Gorovenko, J. Krupčík, I. Špánik, I. Bočková, P. Sandra, D.W. Armstrong, On the use of quadrupole mass spectrometric detection for flow modulated comprehensive two-dimensional gas chromatography, Journal of Chromatography A. 1330 (2014) 51–60.

F. Gritti, A. Tarafder, G. Guiochon, Interpretation of dynamic frontal analysis data in solid/supercritical fluid adsorption systems. I: Theory, Journal of Chromatography A. 1290 (2013) 73–81.

G.M. Gross, B.J. Prazen, J.W. Grate, R.E. Synovec, High-Speed Gas Chromatography Using Synchronized Dual-Valve Injection, Anal. Chem. 76 (2004) 3517–3524.

J. Harynuk, T. Górecki, New liquid nitrogen cryogenic modulator for comprehensive two-dimensional gas chromatography, Journal of Chromatography A. 1019 (2003) 53–63.

M. He, Z.-Y. Yang, T. Yang, Y. Ye, J. Nie, Y. Hu, P. Yan, Chemometrics-enhanced one-dimensional/comprehensive two-dimensional gas chromatographic analysis for bioactive terpenoids and phthalides in Chaihu Shugan San essential oils, Journal of Chromatography B. 1052 (2017) 158–168.
M.I.H. Helaleh, K. Tanaka, M. Mori, Q. Xu, H. Taoda, M.-Y. Ding, W. Hu, K. Hasebe, P.R. Haddad, Vacancy ion-exclusion chromatography of haloacetic acids on a weakly acidic cation-exchange resin, Journal of Chromatography A. 997 (2003) 133–138.
J.L. Hope, K.J. Johnson, M.A. Cavelti, B.J. Prazen, J.W. Grate, R.E. Synovec, High-speed gas chromatographic separations with diaphragm valve-based injection and chemometric analysis as a gas chromatographic "sensor," Analytica Chimica Acta. 490 (2003) 223–230.
C. Hurtado, H. Parastar, V. Matamoros, B. Piña, R. Tauler, J.M. Bayona, Linking the morphological and metabolomic response of Lactuca sativa L exposed to emerging contaminants using GC × GC-MS and chemometric tools, Scientific Reports. 7 (2017).
Y. Izadmanesh, E. Garreta-Lara, J.B. Ghasemi, S. Lacorte, V. Matamoros, R. Tauler, Chemometric analysis of comprehensive two dimensional gas chromatography–mass spectrometry metabolomics data, Journal of Chromatography A. 1488 (2017) 113–125.
M.R. Jacobs, M. Edwards, T. Górecki, P.N. Nesterenko, R.A. Shellie, Evaluation of a miniaturised single-stage thermal modulator for comprehensive two-dimensional gas chromatography of petroleum contaminated soils, Journal of Chromatography A. 1463 (2016) 162–168.
K. Kaczmarski, W. Zapała, W. Wanat, M. Mori, B.K. Głód, T. Kowalska, Modeling of Ion-Exclusion and Vacancy Ion-Exclusion Chromatography in Analytical and Concentration Overload Conditions, J Chromatogr Sci. 45 (2007) 6–15.
B. Kehimkar, J.C. Hoggard, L.C. Marney, M.C. Billingsley, C.G. Fraga, T.J. Bruno, R.E. Synovec, Correlation of rocket propulsion fuel properties with chemical composition using comprehensive two-dimensional gas chromatography with time-of-flight mass spectrometry followed by partial least squares regression analysis, Journal of Chromatography A. 1327 (2014) 132–140.
W. Khummueng, J. Harynuk, P.J. Marriott, Modulation Ratio in Comprehensive Two-dimensional Gas Chromatography, Anal. Chem. 78 (2006) 4578–4587.
S.-J. Kim, K. Kurabayashi, Uniform-temperature, microscale thermal modulator with area-adjusted air-gap isolation for comprehensive two-dimensional gas chromatography, Sens. Actuators, B. 181 (2013) 518–522.
S.-J. Kim, S.M. Reidy, B.P. Block, K.D. Wise, E.T. Zellers, K. Kurabayashi, Microfabricated thermal modulator for comprehensive two-dimensional micro gas chromatography: design, thermal modeling, and preliminary testing, Lab Chip. 10 (2010) 1647–1654.
M.S. Klee, J. Cochran, M. Merrick, L.M. Blumberg, Evaluation of conditions of comprehensive two-dimensional gas chromatography that yield a near-theoretical maximum in peak capacity gain, Journal of Chromatography A. 1383 (2015) 151–159.
J. Krupčík, R. Gorovenko, I. Špánik, P. Sandra, D.W. Armstrong, Flow-modulated comprehensive two-dimensional gas chromatography with simultaneous flame ionization and quadrupole mass spectrometric detection, Journal of Chromatography A. 1280 (2013) 104–111.
J. Krupčík, R. Gorovenko, I. Špánik, P. Sandra, D.W. Armstrong, Enantioselective comprehensive two-dimensional gas chromatography. A route to elucidate the authenticity and origin of Rosa damascena Miller essential oils, J. Sep. Science. 38 (2015) 3397–3403.

J. Krupčík, R. Gorovenko, I. Špánik, P. Sandra, M. Giardina, Comparison of the performance of forward fill/flush and reverse fill/flush flow modulation in comprehensive two-dimensional gas chromatography, Journal of Chromatography A. 1466 (2016) 113–128.
J. Krupčík, P. Májek, R. Gorovenko, I. Špánik, P. Sandra, D.W. Armstrong, On the determination of a detector response enhancement factor for flow modulated comprehensive two-dimensional gas chromatography, Journal of Chromatography A. 1286 (2013) 235–240.
C. Kulsing, Y. Nolvachai, P. Rawson, D.J. Evans, P.J. Marriott, Continuum in MDGC Technology: From Classical Multidimensional to Comprehensive Two-Dimensional Gas Chromatography, Anal. Chem. 88 (2016) 3529–3538.
E.B. Ledford, C. Billesbach, Jet-Cooled Thermal Modulator for Comprehensive Multidimensional Gas Chromatography, J. High Resol. Chromatogr. 23 (2000) 202–204.
Z. Liu, J. B. Phillips, Comprehensive Two-Dimensional Gas Chromatography using an On-Column Thermal Modulator Interface, Journal of Chromatographic Science. 29 (1991) 227–231.
J. Luong, X. Guan, S. Xu, R. Gras, R.A. Shellie, Thermal Independent Modulator for Comprehensive Two-Dimensional Gas Chromatography, Anal. Chem. 88 (2016) 8428–8432.
S.A. Mackintosh, N.G. Dodder, N.J. Shaul, L.I. Aluwihare, K.A. Maruya, S.J. Chivers, K. Danil, D.W. Weller, E. Hoh, Newly Identified DDT-Related Compounds Accumulating in Southern California Bottlenose Dolphins, Environmental Science & Technology. 50 (2016) 12129–12137.

F. Magagna, A. Guglielmetti, E. Liberto, S.E. Reichenbach, E. Allegrucci, G. Gobino, C. Bicchi, C. Cordero, Comprehensive Chemical Fingerprinting of High-Quality Cocoa at Early Stages of Processing: Effectiveness of Combined Untargeted and Targeted Approaches for Classification and Discrimination, Journal of Agricultural and Food Chemistry. 65 (2017) 6329–6341.
P.J. Marriott, S.-T. Chin, B. Maikhunthod, H.-G. Schmarr, S. Bieri, Multidimensional gas chromatography, TrAC, Trends Anal. Chem. 34 (2012) 1–21.
P.J. Marriott, R.M. Kinghorn, Longitudinally Modulated Cryogenic System. A Generally Applicable Approach to Solute Trapping and Mobilization in Gas Chromatography, Anal. Chem. 69 (1997) 2582–2588.
R.B. Mastello, M. Capobiango, S.-T. Chin, M. Monteiro, P.J. Marriott, Identification of odour-active compounds of pasteurised orange juice using multidimensional gas chromatography techniques, Food Research International. 75 (2015) 281–288.
N.G.S. Mogollón, P.S. Prata, J.Z. dos Reis, E.V. dos S. Neto, F. Augusto, Characterization of crude oil biomarkers using comprehensive two-dimensional gas chromatography coupled to tandem mass spectrometry, J. Sep. Science. 39 (2016) 3384–3391.
N.G.S. Mogollón, F.A. de L. Ribeiro, M.M. Lopez, L.W. Hantao, R.J. Poppi, F. Augusto, Quantitative analysis of biodiesel in blends of biodiesel and conventional diesel by comprehensive two-dimensional gas chromatography and multivariate curve resolution, Analytica Chimica Acta. 796 (2013) 130–136.
N.G.S. Mogollón, F.A. de L. Ribeiro, R.J. Poppi, A. Quintana, J. Chávez, D. Agualongo, H. Aleme, F. Augusto, Exploratory Analysis of Biodiesel by Combining Comprehensive

Two-Dimensional Gas Chromatography and Multiway Principal Component Analysis, Journal of the Brazilian Chemical Society. (2016).
R.E. Mohler, K.M. Dombek, J.C. Hoggard, E.T. Young, R.E. Synovec, Comprehensive Two-Dimensional Gas Chromatography Time-of-Flight Mass Spectrometry Analysis of Metabolites in Fermenting and Respiring Yeast Cells, Analytical Chemistry. 78 (2006) 2700–2709.
M.A. Moreira, L.C. André, A.B. Ribeiro, M.D.R.G. da Silva, Z.L. Cardeal, Quantitative Analysis of Endocrine Disruptors by Comprehensive Two-Dimensional Gas Chromatography, Journal of the Brazilian Chemical Society. 26 (2015) 531–536.
M. Mori, M.I.H. Helaleh, Q. Xu, W. Hu, M. Ikedo, M.-Y. Ding, H. Taoda, K. Tanaka, Vacancy ion-exclusion/adsorption chromatography of aliphatic amines on a polymethacrylate-based weakly basic anion-exchange column, Journal of Chromatography A. 1039 (2004) 129–133.
M. Mori, H. Itabashi, M.I.H. Helaleh, K. Kaczmarski, B. Głód, T. Kowalska, Q. Xu, M. Ikedo, W. Hu, K. Tanaka, Vacancy ion-exclusion chromatography of inorganic acids on a weakly acidic cation-exchange resin column, Journal of Chromatography A. 1118 (2006) 41–45.
A. Mostafa, T. Górecki, Development and Design of a Single-Stage Cryogenic Modulator for Comprehensive Two-Dimensional Gas Chromatography, Anal. Chem. 88 (2016) 5414–5423.
V. Mucédola, L.C.S. Vieira, D. Pierone, A.L. Gobbi, R.J. Poppi, L.W. Hantao, Thermal desorption modulation for comprehensive two-dimensional gas chromatography using a simple and inexpensive segmented-loop fluidic interface, Talanta. 164 (2017) 470–476.
R.E. Murphy, M.R. Schure, J.P. Foley, Effect of Sampling Rate on Resolution in Comprehensive Two-Dimensional Liquid Chromatography, Anal. Chem. 70 (1998) 1585–1594.
A.M. Muscalu, M. Edwards, T. Górecki, E.J. Reiner, Evaluation of a single-stage consumable-free modulator for comprehensive two-dimensional gas chromatography: Analysis of polychlorinated biphenyls, organochlorine pesticides and chlorobenzenes, Journal of Chromatography A. 1391 (2015) 93–101.
K.D. Nizio, M. Ueland, B.H. Stuart, S.L. Forbes, The analysis of textiles associated with decomposing remains as a natural training aid for cadaver-detection dogs, Forensic Chemistry. 5 (2017) 33–45.
G. Ntlhokwe, A.G.J. Tredoux, T. Górecki, M. Edwards, J. Vestner, M. Muller, L. Erasmus, E. Joubert, J.C. Cronje, A. de Villiers, Analysis of honeybush tea (Cyclopiaspp.) volatiles by comprehensive two-dimensional gas chromatography using a single-stage thermal modulator | SpringerLink, Analytical and Bioanalytical Chemistry. 409 (n.d.) 4127–4138.
A.C. Olivieri, H.-L. Wu, R.-Q. Yu, MVC3: A MATLAB graphical interface toolbox for third-order multivariate calibration, Chemometrics and Intelligent Laboratory Systems. 116 (2012) 9–16.
J. Omar, M. Olivares, J.M. Amigo, N. Etxebarria, Resolution of co-eluting compounds of Cannabis Sativa in comprehensive two-dimensional gas chromatography/mass spectrometry detection with Multivariate Curve Resolution-Alternating Least Squares, Talanta. 121 (2014) 273–280.
H. Parastar, J.R. Radović, M. Jalali-Heravi, S. Diez, J.M. Bayona, R. Tauler, Resolution and Quantification of Complex Mixtures of Polycyclic Aromatic Hydrocarbons in Heavy Fuel Oil Sample by Means of GC × GC-TOFMS Combined to Multivariate Curve Resolution, Analytical Chemistry. 83 (2011) 9289–9297.

B.A. Parsons, D.K. Pinkerton, R.E. Synovec, Implications of phase ratio for maximizing peak capacity in comprehensive two-dimensional gas chromatography time-of-flight mass spectrometry, Journal of Chromatography A. (2017).
Y.V. Patrushev, V.N. Sidelnikov, The use of high-speed multicapillary column in comprehensive two-dimensional gas chromatography with flow modulation, Journal of Chromatography A. 1426 (2015) 183–190.
D. Paul, K. Kurabayashi, First-principle modeling and characterization of thermal modulation in comprehensive two-dimensional gas chromatography using a microfabricated device, Sensors and Actuators B: Chemical. 231 (2016) 135–146.
C.S.G. Phillips, C.R. McIlwrick, Sample vacancy chromatography and catalysis, Anal. Chem. 45 (1973) 782–786.
K.M. Pierce, B. Kehimkar, L.C. Marney, J.C. Hoggard, R.E. Synovec, Review of chemometric analysis techniques for comprehensive two dimensional separations data, Journal of Chromatography A. 1255 (2012) 3–11.
D.K. Pinkerton, B.A. Parsons, T.J. Anderson, R.E. Synovec, Trilinearity deviation ratio: A new metric for chemometric analysis of comprehensive two-dimensional gas chromatography time-of-flight mass spectrometry data, Analytica Chimica Acta. 871 (2015) 66–76.
D.K. Pinkerton, B.A. Parsons, R.E. Synovec, Method to determine the true modulation ratio for comprehensive two-dimensional gas chromatography, Journal of Chromatography A. 1476 (2016) 114–123.
D.K. Pinkerton, K.M. Pierce, R.E. Synovec, Chemometric Resolution of Complex Higher Order Chromatographic Data with Spectral Detection. Resolving Spectral Mixtures With Applications from Ultrafast Time-Resolved Spectroscopy to Super-Resolution Imaging, 1st ed., Elsevier, 2016.
D.K. Pinkerton, B.C. Reaser, K.L. Berrier, R.E. Synovec, Determining the Probability of Achieving a Successful Quantitative Analysis for Gas Chromatography–Mass Spectrometry, Anal. Chem. 89 (2017) 9926–9933.
H. Potgieter, R. Bekker, J. Beigley, E. Rohwer, Analysis of oxidised heavy paraffininc products by high temperature comprehensive two-dimensional gas chromatography, Journal of Chromatography A. 1509 (2017) 123–131.
P.S. Prata, G.L. Alexandrino, N.G.S. Mogollón, F. Augusto, Discriminating Brazilian crude oils using comprehensive two-dimensional gas chromatography–mass spectrometry and multiway principal component analysis, Journal of Chromatography A. 1472 (2016) 99–106.
S. Prebihalo, A. Brockman, J. Cochran, F.L. Dorman, Determination of emerging contaminants in wastewater utilizing comprehensive two-dimensional gas-chromatography coupled with time-of-flight mass spectrometry, Journal of Chromatography A. 1419 (2015) 109–115.
S.E. Prebihalo, K.L. Berrier, C.E. Freye, H.D. Bahaghighat, N.R. Moore, D.K. Pinkerton, R.E. Synovec, Multidimensional Gas Chromatography: Advances in Instrumentation, Chemometrics, and Applications, Analytical Chemistry. (2017).
G. Purcaro, L. Barp, M. Beccaria, L.S. Conte, Characterisation of minor components in vegetable oil by comprehensive gas chromatography with dual detection, Food Chemistry. 212 (2016) 730–738.
G. Purcaro, C. Cordero, E. Liberto, C. Bicchi, L.S. Conte, Toward a definition of blueprint of virgin olive oil by comprehensive two-dimensional gas chromatography, Journal of Chromatography A. 1334 (2014) 101–111.

C.N. Reilley, G.P. Hildebrand, J.W. Ashley, Gas Chromatographic Response as a Function of Sample Input Profile., Anal. Chem. 34 (1962) 1198–1213.
W.J. Robson, P.A. Sutton, P. McCormack, N.P. Chilcott, S.J. Rowland, Class Type Separation of the Polar and Apolar Components of Petroleum, Anal. Chem. 89 (2017) 2919–2927.
S. Samanipour, P. Dimitriou-Christidis, D. Nabi, J.S. Arey, Elevated Concentrations of 4-Bromobiphenyl and 1,3,5-Tribromobenzene Found in Deep Water of Lake Geneva Based on GC×GC-ENCI-TOFMS and GC×GC-μECD.pdf, ACS Omega. 2 (2017) 641–652.
A.A.S. Sampat, M. Lopatka, G. Vivó-Truyols, P.J. Schoenmakers, A.C. van Asten, Towards chemical profiling of ignitable liquids with comprehensive two-dimensional gas chromatography: Exploring forensic application to neat white spirits, Forensic Science International. 267 (2016) 183–195.
B. Savareear, M.R. Jacobs, R.A. Shellie, Multiplexed dual first-dimension comprehensive two-dimensional gas chromatography–mass spectrometry with contra-directional thermal modulation, Journal of Chromatography A. 1365 (2014) 183–190.
T. Schwemer, T. Rössler, B. Ahrens, M. Schäffer, A. Hasselbach-Minor, M. Pütz, M. Sklorz, T. Gröger, R. Zimmermann, Characterization of a heroin manufacturing process based on acidic extracts by combining complementary information from two-dimensional gas chromatography and high resolution mass spectrometry, Forensic Chemistry. 4 (2017) 9–18.
R.P.W. Scott, C.G. Scott, P. Kucera, Liquid-solid vacancy chromatography, Anal. Chem. 44 (1972) 100–104.
J.V. Seeley, Recent advances in flow-controlled multidimensional gas chromatography, Journal of Chromatography A. 1255 (2012) 24–37.
J.V. Seeley, F. Kramp, C.J. Hicks, Comprehensive Two-Dimensional Gas Chromatography via Differential Flow Modulation, Anal. Chem. 72 (2000) 4346–4352.
J.V. Seeley, Micyus, Nicole J., McCurry, James D., S.K. Seeley, Comprehensive Two-Dimensional Gas Chromatography With a Simple Fluidic Modulator, American Laboratory. 38 (2006) 24–26.
J.V. Seeley, N.J. Micyus, S.V. Bandurski, S.K. Seeley, J.D. McCurry, Microfluidic Deans Switch for Comprehensive Two-Dimensional Gas Chromatography, Anal. Chem. 79 (2007) 1840–1847.
J.V. Seeley, N.E. Schimmel, S.K. Seeley, The multi-mode modulator: A versatile fluidic device for two-dimensional gas chromatography, Journal of Chromatography A. 1536 (2018) 6–15.
J.V. Seeley, S.K. Seeley, Multidimensional Gas Chromatography: Fundamental Advances and New Applications, Anal. Chem. 85 (2013) 557–578.
J.V. Seeley, S.K. Seeley, Comprehensive two-dimensional gas chromatography with pattern modulation, Journal of Chromatography A. 1421 (2015) 114–122.
G. Semard, C. Gouin, J. Bourdet, N. Bord, V. Livadaris, Comparative study of differential flow and cryogenic modulators comprehensive two-dimensional gas chromatography systems for the detailed analysis of light cycle oil, Journal of Chromatography A. 1218 (2011) 3146–3152.
G. Serrano, D. Paul, S.-J. Kim, K. Kurabayashi, E.T. Zellers, Comprehensive Two-Dimensional Gas Chromatographic Separations with a Microfabricated Thermal Modulator, Anal. Chem. 84 (2012) 6973–6980.

K.M. Sharif, S.-T. Chin, C. Kulsing, P.J. Marriott, The microfluidic Deans switch: 50 years of progress, innovation and application, TrAC Trends in Analytical Chemistry. 82 (2016) 35–54.
W.C. Siegler, J.A. Crank, D.W. Armstrong, R.E. Synovec, Increasing selectivity in comprehensive three-dimensional gas chromatography via an ionic liquid stationary phase column in one dimension, Journal of Chromatography A. 1217 (2010) 3144–3149.
W.C. Siegler, B.D. Fitz, J.C. Hoggard, R.E. Synovec, Experimental Study of the Quantitative Precision for Valve-Based Comprehensive Two-Dimensional Gas Chromatography, Anal. Chem. 83 (2011) 5190–5196.
A.E. Sinha, C.G. Fraga, B.J. Prazen, R.E. Synovec, Trilinear chemometric analysis of two-dimensional comprehensive gas chromatography–time-of-flight mass spectrometry data, Journal of Chromatography A. 1027 (2004) 269–277.
A.E. Sinha, B.J. Prazen, C.G. Fraga, R.E. Synovec, Valve-based comprehensive two-dimensional gas chromatography with time-of-flight mass spectrometric detection: instrumentation and figures-of-merit, Journal of Chromatography A. 1019 (2003) 79–87.
H. Smith, R.D. Sacks, Column Selectivity Programming and Fast Temperature Programming for High-Speed GC Analysis of Purgeable Organic Compounds, Anal. Chem. 70 (1998) 4960–4966.
P.-H. Stefanuto, K. Perrault, J.-F. Focant, S. Forbes, Fast Chromatographic Method for Explosive Profiling, Chromatography. 2 (2015) 213–224.
P.-H. Stefanuto, K.A. Perrault, L.M. Dubois, B. L'Homme, C. Allen, C. Loughnane, N. Ochiai, J.-F. Focant, Advanced method optimization for volatile aroma profiling of beer using two-dimensional gas chromatography time-of-flight mass spectrometry, Journal of Chromatography A. 1507 (2017) 45–52.
Z. Tong, K.S. Joseph, D.S. Hage, Detection of heterogeneous drug–protein binding by frontal analysis and high-performance affinity chromatography, Journal of Chromatography A. 1218 (2011) 8915–8924.
P.Q. Tranchida, Comprehensive two-dimensional gas chromatography: A perspective on processes of modulation, Journal of Chromatography A. (2017).
P.Q. Tranchida, F.A. Franchina, P. Dugo, L. Mondello, Use of greatly-reduced gas flows in flow-modulated comprehensive two-dimensional gas chromatography-mass spectrometry, Journal of Chromatography A. 1359 (2014) 271–276.
P.Q. Tranchida, F.A. Franchina, P. Dugo, L. Mondello, Flow-modulation low-pressure comprehensive two-dimensional gas chromatography, Journal of Chromatography A. 1372 (2014) 236–244.
P.Q. Tranchida, M. Maimone, F.A. Franchina, T.R. Bjerk, C.A. Zini, G. Purcaro, L. Mondello, Four-stage (low-)flow modulation comprehensive gas chromatography⊠quadrupole mass spectrometry for the determination of recently-highlighted cosmetic allergens, Journal of Chromatography A. 1439 (2016) 144–151.
[P.Q. Tranchida, G. Purcaro, P. Dugo, L. Mondello, Modulators for comprehensive two-dimensional gas chromatography, TrAC, Trends Anal. Chem. 30 (2011) 1437–1461.
P.Q. Tranchida, G. Purcaro, A. Visco, L. Conte, P. Dugo, P. Dawes, L. Mondello, A flexible loop-type flow modulator for comprehensive two-dimensional gas chromatography, Journal of Chromatography A. 1218 (2011) 3140–3145.

P.Q. Tranchida, S. Salivo, F.A. Franchina, L. Mondello, Flow-Modulated Comprehensive Two-Dimensional Gas Chromatography Combined with a High-Resolution Time-of-Flight Mass Spectrometer: A Proof-of-Principle Study, Anal. Chem. 87 (2015) 2925–2930.
P.Q. Tranchida, M. Zoccali, F.A. Franchina, A. Cotroneo, P. Dugo, L. Mondello, Gas velocity at the point of re-injection: An additional parameter in comprehensive two-dimensional gas chromatography optimization, Journal of Chromatography A. 1314 (2013) 216–223.
P.Q. Tranchida, M. Zoccali, F.A. Franchina, P. Dugo, L. Mondello, Measurement of fundamental chromatography parameters in conventional and split-flow comprehensive two-dimensional gas chromatography-mass spectrometry: A focus on the importance of second-dimension injection efficiency, J. Sep. Science. 36 (2013) 212–218.
N.E. Watson, H.D. Bahaghighat, K. Cui, R.E. Synovec, Comprehensive Three-Dimensional Gas Chromatography with Time-of-Flight Mass Spectrometry, Anal. Chem. 89 (2017) 1793–1800.
N.E. Watson, S.E. Prebihalo, R.E. Synovec, Targeted analyte deconvolution and identification by four-way parallel factor analysis using three-dimensional gas chromatography with mass spectrometry data, Analytica Chimica Acta. 983 (2017) 67–75.
N.E. Watson, W.C. Siegler, J.C. Hoggard, R.E. Synovec, Comprehensive Three-Dimensional Gas Chromatography with Parallel Factor Analysis, Anal. Chem. 79 (2007) 8270–8280.
B.A. Weggler, T. Gröger, R. Zimmermann, Advanced scripting for the automated profiling of two-dimensional gas chromatography-time-of-flight mass spectrometry data from combustion aerosol, Journal of Chromatography A. 1364 (2014) 241–248.
M.J. Wilde, S.J. Rowland, Structural Identification of Petroleum Acids by Conversion to Hydrocarbons and Multidimensional Gas Chromatography-Mass Spectrometry, Anal. Chem. 87 (2015) 8457–8465.
R.B. Wilson, J.C. Hoggard, R.E. Synovec, High throughput analysis of atmospheric volatile organic compounds by thermal injection – isothermal gas chromatography – time-of-flight mass spectrometry, Talanta. 103 (2013) 95–102.
R.B. Wilson, W.C. Siegler, J.C. Hoggard, B.D. Fitz, J.S. Nadeau, R.E. Synovec, Achieving high peak capacity production for gas chromatography and comprehensive two-dimensional gas chromatography by minimizing off-column peak broadening, Journal of Chromatography A. 1218 (2011) 3130–3139.
B. Xu, L. Zhang, F. Ma, W. Zhang, X. Wang, Q. Zhang, D. Luo, H. Ma, P. Li, Determination of free steroidal compounds in vegetable oils by comprehensive two-dimensional gas chromatography coupled to time-of-flight mass spectrometry, Food Chemistry. 245 (2018) 415–425.
D. Yan, L. Tedone, A. Koutoulis, S.P. Whittock, R.A. Shellie, Parallel comprehensive two-dimensional gas chromatography, Journal of Chromatography A. 1524 (2017) 202–209.
M. Ye, Y. Ding, J. Mao, L. Shi, High-performance vacancy gel permeation chromatography, Journal of Chromatography A. 518 (1990) 238–241.
W. Zapała, J. Kostka, K. Kaczmarski, Comparison of different columns in analysis of C1–C5 aliphatic acids mixture in ion exclusion chromatography and vacancy ion exclusion chromatography modes, Acta Chromatographica. 23 (2011) 377–388.
Z. Zeng, J. Li, H.M. Hugel, G. Xu, P.J. Marriott, Interpretation of comprehensive two-dimensional gas chromatography data using advanced chemometrics, TrAC Trends in Analytical Chemistry. 53 (2014) 150–166.

M. Zoccali, K.A. Schug, P. Walsh, J. Smuts, L. Mondello, Flow-modulated comprehensive two-dimensional gas chromatography combined with a vacuum ultraviolet detector for the analysis of complex mixtures, Journal of Chromatography A. 1497 (2017) 135–143.
Wiley: Unified Separation Science - J. Calvin Giddings, (n.d.).

VITA

H. Daniel Bahaghighat ‘Baha’ is an 18-year veteran of the Army currently holding the rank of Lieutenant Colonel. He was born in Wise, Virginia in 1977 and grew up as an Army brat in multiple locations. After graduation form Clintwood High School, Clintwood, Virginia in 1995, he attended Carson-Newman University, Jefferson City, Tennessee, where he earned his Bachelor of Science in chemistry. In 2008 he earned is Master of Science in chemistry from Missouri University of Science and Technology. During his career he served in key roles such as; platoon leader, company commander, battalion operations officer (deployed), assistant professor (United States Military Academy), and guest scientist (Los Alamos National Laboratory), with one deployment to Iraq in support of operation New Dawn. He came to the University of Washington in 2015 to pursue a Ph.D. in analytical chemistry. Upon completion of his Ph.D. requirements he will return to the United States Military Academy and assume the role as Course Director for analytical chemistry.